

# OCTA IN OPHTHALMOLOGY

RETINA MANUAL

Angela Carneiro

Rita Flores

Antonio Campos



**GER**  
GRUPO DE  
ESTUDOS  
DA RETINA  
PORTUGAL

 **Théa**  
let's open our eyes





# OCTA IN OPHTHALMOLOGY

RETINA MANUAL

Angela Carneiro

Rita Flores

Antonio Campos



**GER**  
GRUPO DE  
ESTUDOS  
DA RETINA  
PORTUGAL

 **Théa**  
let's open our eyes

OCTA in Ophthalmology

Editors: Ângela Carneiro, Rita Flores and António Campos

1<sup>st</sup> Edition - December 2021

ISBN: 978-989-33-2449-3

Legal deposit: 491884/21

Design and layout: Ricardo Correia

Circulation: 1200 copies

Published by:

GER - Grupo de Estudos da Retina Portugal and SPO - Sociedade Portuguesa de Oftalmologia

All rights reserved. No part of this book shall be reproduced, stored in a retrieval system, or transmitted by any means – electronic, mechanical, photocopying, recording, or otherwise – without written permission from the publisher and the author.

All texts, diagrams and images in this book are responsibility of their authors.

All the content of this book was published without any interference from Théa Portugal S.A.

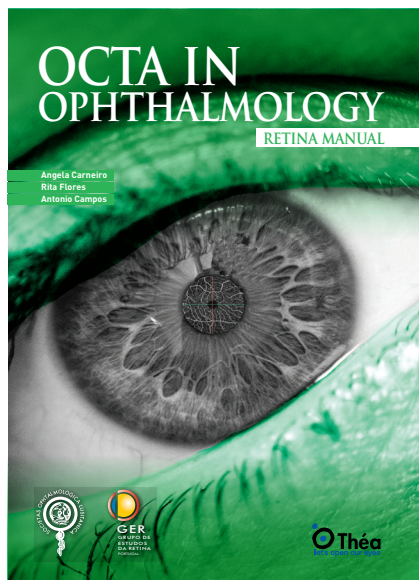
# OCTA IN OPHTHALMOLOGY

## RETINA MANUAL

EDITORS

Ângela Carneiro  
Rita Flores  
António Campos





Dear readers,

This book presents the viewpoints of the authors and does not necessarily reflect the opinions of Laboratoires Théa.

All rights of translation, adaptation and reproduction by any means are reserved for all countries.

Any reproduction in whole or in part—by any means—of the pages of this book, without prior, written approval from the publisher, is prohibited, illegal and constitutes an infringement. Reproduction is allowed only where the copied material is strictly reserved for the private use of the copier and not for collective use, and in the case of brief analysis and quotations the use of which is justified by the scientific or educational nature of the work in which they are included (French Law of 11 March 1957 Art. 40 and 41 and French Criminal Code Art. 425).







# FOREWORD

We are pleased to share with you this book, fruit of the collaboration of the Portuguese Retina and Vitreous Group (GPRV) of the Portuguese Society of Ophthalmology (SPO) and the Retina Study Group of Portugal (GER).

The rapid growth of scientific knowledge in recent years has led to a pressing need for constant scientific updates in the field of Ophthalmology.

From our perspective the current innovation in the field of OCT, and particularly OCT-A, justified the creation of a work that aggregates, synthesizes and clarifies its role in the study and monitoring of retinal diseases.

Portuguese Ophthalmology possesses great technical and scientific expertise, combined with a vigorous dynamism that allows for the elaboration of works of this kind without neglecting important international collaborations.

The sharing of knowledge among peers, its actualization in light of the most recent and reliable scientific evidence and the quest for continuous improvement in clinical practice are the main drivers of this joint initiative.

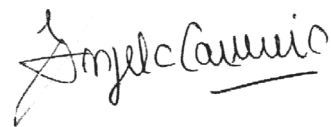
We are grateful to Laboratoires Théa who supported this initiative and permitted the free distribution of this book.

We hope that it will help to refresh your knowledge, and that quenches your need for answers and positively influences your daily clinical practice.

Together, we can achieve more and better!



Rufino Silva  
SPO. President



Ângela Carneiro  
GER. President

# INDEX

Foreword	07
1 Basics and Technical Aspects	09
2 Devices	13
3 Artifacts	19
4 The Retina	23
4.1 The Angio-architecture of the Capillary Plexuses	25
4.2 Vascular Autoregulatory Function of the Retina	33
5 The Choroid	39
5.1 Middle and Outer Choroid	41
5.2 The Choriocapillaris	45
6 Optic Nerve Head	49
7 Occlusive Diseases and The Ischemic Cascade	53
7.1 Paracentral Acute Middle Maculopathy	55
7.2 Acute Macular Outer Retinopathy	59
7.3 Central Retinal Vein Occlusion	63
7.4 Branch Retinal Vein Occlusion	67
7.5 Arterial Occlusions	71
8 Diabetic Retinopathy	75
8.1 Non-proliferative Diabetic Retinopathy	77
8.2 Diabetic Macular Edema	81
8.3 Proliferative Diabetic Retinopathy	89
9 Juxtafoveal Idiopathic Telangiectasia	93
10 Inflammatory Retinal Diseases	99
11 Age-related macular Degeneration (AMD)	103
11.1 Early and Intermediate AMD	105
11.2 Neovascular AMD	109
11.2.1 Type 1 Neovascularization	111
11.2.2 Type 2 Neovascularization	115
11.2.3 Type 3 Neovascularization	119
11.2.4 Mixed Neovascularization	125
11.2.5 Nonexudative Neovascularization	127
11.2.6 Fibrotic Neovascularization	131
11.2.7 Anti-VEGF Treatment and Follow up	135
11.3 Geographic Atrophy	139
12 Pachychoroid Related Diseases	145
12 Pachychoroid Diseases Of The Macula	147
12.1 Central Serous Chorioretinopathy	151
12.2 Polypoidal Choroidal Vasculopathy	157

<b>13 High Myopia</b>	163
<b>14 Other Diseases Associated with Choroidal Neovascularization</b>	167
<b>15 Macular Dystrophies</b>	171
<b>16 Vitelliform Dystrophies</b>	175
<b>17 Choroiditis</b>	179
<b>18 Ocular Tumors</b>	185
<b>19 Daily Practice</b>	191
<b>20 Unmet Needs</b>	195



# 1. BASICS AND TECHNICAL ASPECTS

Carla Teixeira  
Hospital Pedro Hispano, Matosinhos

The first demonstration of Optical Coherence Tomography Angiography (OCTA) was proposed by Wang et al, in 2007<sup>1</sup>. This new technique has rapidly progressed in recent years. Optical Coherence Tomography (OCT) measures the depth of a structure within the tissue as well as how much it reflects or scatters light. This measurement is known as an axial scan (A-scan) delay. A cross-sectional scan (B-scan) is generated by sequentially acquiring many A-scans as the light beam is scanned in the transverse direction. Volumetric information is generated by sequentially acquiring multiple B-scans which are displaced perpendicular to the B-scan image, covering a region of the retina using raster scan. The retina is a stationary object for the most part, so if successive B-scans at the same position are acquired, they will be largely similar, except for the motion of blood within the tissue. The reflectivity or scattering changes from one scan to the next, comparing repeated OCT B-scans, make possible to image blood flow by looking for differences among the scans on a pixel-by-pixel basis<sup>2</sup>.

The basic concept of OCTA is to use the moving particles, such as red blood cells (RBCs), in the biological tissues, as an intrinsic contrast agent to image blood flow. Observing two OCT signals over time (one is backscattered from the surrounding biological tissue and the other one is backscattered from a flowing vessel), only the signal backscattered from tissue components remains steady, while the signal backscattered from the vessels changes, as the RBCs are tumbling and moving while flowing through the vessel. By calculating the differences in OCT signals acquired at the same location at different time points, OCTA distinguishes the moving particles from the static tissue and is able to generate flow signals, allowing the visualization of microvascular networks in biological tissues without intravenous dye injection<sup>3-6</sup>.

There are several algorithms used to produce OCTA angiograms of perfused tissues, such as OCT amplitude signal (e.g., speckle variance), phase signal (e.g., phase variance) and complex signal (i.e., combined use of the OCT amplitude and phase information, e.g., optical microangiography or OMAG). All these algorithms are developed to detect the signal variations of moving RBCs, with the assumptions that OCT signals of static tissues remain static. One approach to OCTA signal is

to evaluate the various correlations of speckles between scans - speckle variation. Several different degrees of speckles occur with OCT based on interference and reflections of light within the tissues of interest. These changes are then compared in consecutive B-scans at identical pixel locations and the amount of correlation or similarity between these pixels is evaluated. Whenever a significant change in the speckle is present, decorrelation is present. Conversely, there is minimum change of these speckles in static tissues over time (i.e., minimal decorrelation). In areas with motion (RBCs), significant changes in speckle occur (i.e., decorrelation). A second approach to OCTA signal is with phase variance, using alterations that occur in the phase of the light waves from scan to scan: small variations are noted in static tissue and larger variations in phase will be noted in areas of active motion. Multiple research groups have optimized and developed unique versions of these OCTA algorithms which are now commercially available, including split-spectrum amplitude decorrelation angiography (SSADA), full-spectrum amplitude decorrelation angiography (FSADA), optical microangiography (OMAG) and OCTA ratio analysis (OCTARA)<sup>7</sup>.

OCTA devices execute repeated B-scans at the same location and the structural data are compared to identify signal modifications due to the one-by-one (single file) RBCs flow in the vessels (motion contrast). Each B-scan comprises different A-scans which are captured at following locations. The A-scan rate differs among instruments: 70000 A-scans in spectral devices (SD-OCT) and 100000 A-scans in swept source (SS-OCT) devices. Using dense volume scans, it is possible to obtain OCTA images that are similar to fluorescein angiography (FA) without using any dye injection. While FA provides only two-dimensional images of the fundus, OCTA enables the visualization of the structure and blood flow within the vitreous, the retina and the choroid, separately. This technology allows the in situ, high-resolution visualization of the individual vascular layers and using adjusted segmentation, it is possible to examine the distinct capillary networks of the retina. In contrast to FA, which displays only the superficial capillary network, OCTA visualizes the superficial, the deep and the choroidal vascular network; even the middle capillary plexus can be identified. With FA

and indocyanine green angiography (ICGA), dynamic phenomena, such as dye leakage, pooling and staining, can be observed. Conversely, these cannot be observed with OCTA because no motion of RBCs is involved. Retinal pathology may be obscured by leakage or haemorrhage in FA, while OCTA generates high contrast, well-defined images of the microvasculature below the areas of leakage or haemorrhage<sup>8,9</sup>. OCTA data may be viewed using two-dimensional (2D) B-scans and *en face* images. To obtain 2D *en face* images, the volumetric OCTA is segmented at specific depths and the flow data within any slab are projected into a 2D *en face* image that can be visualized. The generation of 2D OCTA *en face* images may be obtained using different methods: the “maximal intensity projection” approach works by projecting the maximum intensity pixel within each column and the “average intensity projection” that works by projecting the average intensity pixel within each column. The first algorithm may be more sensible in detecting smaller vessels, but may have more noise, while the second algorithm is less susceptible to noise but may be less sensitive for small vessels.

Current OCTA versions are developed based on Fourier Domain analysis (FD-OCT), either using either SD-OCT or SS-OCT. The scanning protocol of the OCTA image is determined by the acquisition time a subject can tolerate without blinking or moving, which is typically around 3-6 seconds. To strike a balance between sampling density and number of B-scan repetition, 300 and 500 A-scans are acquired in one B-scan with 4 repeats and 2 repeats for 3×3 mm<sup>2</sup> or 6×6 mm<sup>2</sup> scanning area, respectively. An OCTA system with faster acquisition speed is needed in order to be able to scan over a wider area, while keeping a similar sampling density and B-scan repetition. Alternatively, it may retain the same sampling density but increase the B-scan repetition – which allows a longer time interval between B-scan pairs so that the detection of slower flow signal becomes feasible. There are several OCTA devices available on routine practice: AngioPlex™ (Carl Zeiss Meditec) and AngioVue™ (Optovue), Spectralis OCTA™ (Heidelberg Engineering) and Angioscan™ (Nidek), based on SD-OCT technology; and PlexElite™ (Carl Zeiss Meditec) and Triton™ DRI SS-OCT (Topcon Corporation), based on SS-OCT technology<sup>10</sup>.

Image artifacts in OCTA are similar to artifacts that occur in OCT. In general, artifacts in OCTA occur as a result of: (1) scanning methodology used to generate the motion contrast signal, (2) data processing, (3) movement of the eye and (4) intrinsic properties and pathology of the eye<sup>11-13</sup>. With the complexities involved with OCTA image acquisition and image processing, OCTA images have unique artifact challenges. Several key artifact categories have been described and should be considered when reviewing OCTA images, including projection, motion, segmentation and signal attenuation artifacts. While some artifacts are innocuous or easily detectable, others can be severe.

Projection artifacts are recognized as the appearance of retinal vascular structures in layers deeper to where they actually reside. This artifact occurs due to the transmission and reflection of the OCT signal through the vasculature to the tissues below, resulting in a decorrelation signal that is interpreted (incorrectly) as vascular flow. These artifacts can be easily recognized through successive review of *en face* images and recent significant advances in software techniques have the potential to dramatically reduce these artifacts. OCTA is also susceptible to motion artifacts because false OCTA signals may be generated by patient movements. Even subtle changes and small movements can result in false positives and incorrect representation of the decorrelation signals. However, eye tracking systems have significantly decreased the impact of these motion artifacts in OCTA images. *En face* OCT images are susceptible to segmentation artifacts, especially in eyes with retinal and choroidal disorders, such as artefactual flow signals when the segmentation boundaries intersect a hyperreflective boundary (e.g., retinal pigment epithelium (RPE) over drusen).

OCTA flow information may be visualized on B-scan images with cross-sectional OCT data and pseudocolour overlay on the grayscale structural OCT image. Also, three-dimensional (3D) analysis may permit a more reliable visualization and quantification of the retinal vessels. Shadowing artifacts affect the visualization of the vascular layers and occur when the OCT beam is attenuated or blocked, thereby impeding its passage to the deeper layers. Loss of signal across an entire image is often caused by defocus. Beyond defocus, other common sources of global signal attenuation are cataracts and tear film break up. Local signal loss also occurs in OCTA imaging, such as signal attenuation beneath hyperreflective material along the beam path (e.g., hyperreflective material in the retina or in the vitreous). Modern deep-learning-based algorithms have the capability to distinguish shadowing artifacts from real pathology.

In clinical applications, the main limitation of OCTA is the restricted field-of-view, but almost all available devices are developing larger scan patterns. Another OCTA limitation is the fact that OCTA metrics and imaging methods are displayed and interpreted in a 2D manner encompassing the macula only.

Advances in 3D and wide-field metrics methods may provide more accurate information about retinal vascular changes in various diseases. A limitation of SD-OCTA devices is the low resolution of lesions underneath the RPE, but SS-OCTA devices, with longer wavelengths of coherent light, overcome this limitation.

## REFERENCES

1. Wang Y, Bower BA, Izatt JA, Tan O, Huang D. In vivo total retinal blood flow measurement by Fourier domain Doppler optical coherence tomography. *J Biomed Opt.* 2007;12(4):041215.
2. Wang RK, Zhang Q, Li Y, Song S. Optical coherence

- tomography angiography-based capillary velocimetry. *J Biomed Opt.* 2017;22(6):66008.
3. Hagag AM, Gao SS, Jia Y, Huang D. Optical coherence tomography angiography: Technical principles and clinical applications in ophthalmology. *Taiwan J Ophthalmol.* 2017;7(3):115-29.
  4. Kashani AH, Chen CL, Gahm JK, Zheng F, Richter GM, Rosenfeld PJ, et al. Optical coherence tomography angiography: A comprehensive review of current methods and clinical applications. *Prog Retin Eye Res.* 2017;60:66-100.
  5. Spaide RF, Fujimoto JG, Waheed NK. Optical Coherence Tomography Angiography. *Retina.* 2015;35(11):2161-2.
  6. Spaide RF, Fujimoto JG, Waheed NK, Sadda SR, Staurengi G. Optical coherence tomography angiography. *Prog Retin Eye Res.* 2018;64:1-55.
  7. Zhang A, Zhang Q, Chen CL, Wang RK. Methods and algorithms for optical coherence tomography-based angiography: a review and comparison. *J Biomed Opt.* 2015;20(10):100901.
  8. Borrelli E, Parravano M, Sacconi R, Costanzo E, Querques L, Vella G, et al. Guidelines on Optical Coherence Tomography Angiography Imaging: 2020 Focused Update. *Ophthalmol Ther.* 2020;9(4):697-707.
  9. Rocholz R, Corvi F, Weichsel J, Schmidt S, Staurengi G. OCT Angiography (OCTA) in Retinal Diagnostics. In: Bille JF, editor. *High Resolution Imaging in Microscopy and Ophthalmology: New Frontiers in Biomedical Optics.* Cham (CH)2019. p. 135-60.
  10. Munk MR, Giannakaki-Zimmermann H, Berger L, Huf W, Ebnetter A, Wolf S, et al. OCT-angiography: A qualitative and quantitative comparison of 4 OCT-A devices. *PLoS One.* 2017;12(5):e0177059.
  11. Ehlers JP. The OCT Angiography Revolution: Five Emerging Themes. *Ophthalmol Retina.* 2017;1(6):457-60.
  12. Hormel TT, Huang D, Jia Y. Artifacts and artifact removal in optical coherence tomographic angiography. *Quant Imaging Med Surg.* 2021;11(3):1120-33.
  13. Spaide RF, Fujimoto JG, Waheed NK. Image Artifacts in Optical Coherence Tomography Angiography. *Retina.* 2015;35(11):2163-80.





## 2. DEVICES

Carlos Neves Cruz, Nuno Gomes  
Hospital de Braga

OCT-A technology is recent and was commercially available in 2014<sup>1</sup>. In this chapter we present the OCT-A devices available, their specifications, and the advantages and disadvantages of each device. We begin with a description and explanation of different technologies incorporated in OCT-A, in order to better understand the differences between devices.

### WAVELENGTH:

OCT-A devices use either Spectral-Domain (SD) or Swept-Source (SS) technology, which are distinguished by the light source and the light detector. SD technology uses a superluminescent diode ( $\lambda \approx 840$  nm) as a source and a spectrometer as a detector, while SS uses a tunable scanning laser ( $\lambda \approx 1050$  nm) as a source and a photodiode as a detector<sup>2</sup>.

Clinically, the difference between the two technologies will depend mainly on the wavelength. The longer wavelength of the SS, together with other features, allows for greater axial resolution and greater penetration through the retinal pigment epithelium, with consequent better visualization of the choroid<sup>3, 4</sup>. Another advantage of SS is that the longer wavelength, the lower the propensity for shadow effect (light beam is blocked and does not reach the outer layers of the retina)<sup>5</sup>. Despite the aforementioned advantages, the higher price of SS results in the wider use of SD technology, as shown in Table 1<sup>1</sup>.

### ACQUISITION ALGORITHMS:

Each device is programmed with an algorithm to detect erythrocyte movement. Clinicians should be aware that there are differences between devices which can affect the results. Thus, whenever possible, the same patient should be evaluated with the same device. The five main algorithms used are: SSADA, CODAA, FSADA, and OCTARA.

OMAG (optical microangiography): incorporates intensity and phase changes between multiple B-scans acquired at the same location, in order to transform the complex signal into the contrast image that represents the vasculature;  
SSADA: divides a B-scan into multiple spectra in order to increase the signal/noise ratio, intensity, and contrast, obtaining better quality OCT-A images without the need for several repetitions or an increase in scanning time<sup>6</sup>;

CODAA (Complex OCT signal Difference Analysis Angiography): detects blood flow by calculating the amplitude and phase of the OCT signal variation over time, allowing high-detail images to be generated<sup>7</sup>;

FSADA: in contrast to SSADA, FSADA algorithm does not segregate each B-scan, and the decorrelation is obtained between “full spectrum” sequential B-scans<sup>8</sup>;  
OCTARA (OCT Angiography Ratio Analysis): it is based on the repetition of B-scans at the same location and calculation of differences in the signal amplitude of the images obtained, allowing for greater sensitivity when identifying slow blood flows, without compromising the axial resolution<sup>9</sup>.

### SCAN VOLUME:

Scan volume (density of acquired A-scans) differ between devices and vary depending on the size of the intended acquisition, affecting the visualization of small vessels. Vessels that are clearly visible on a 3x3 mm acquisition may not be evident on a 6x6 mm acquisition. Therefore, obtaining acquisitions of the same size is important for the patient’s follow-up without acquisition bias.

### Scanning speed:

The scanning speed is an important feature because it determines the capacity of each device in detecting slow blood flows, and it also influences the lateral resolution (capillary network detail). With a higher speed, it is possible to acquire more B-scans, thus increasing the area of the retina to be analyzed without compromising the resolution of the vascular network. On the other hand, it also allows a greater number of repetitions of each B-scan without increasing acquisition time, making it possible to visualize structures with slower flows (microaneurysms, IRMA or other vascular changes).

### Scanning area:

Most devices allow the acquisition of areas between 3x3 mm and 8x8 mm. The increase in scanning areas is directly related to the loss of lateral resolution and consequent lesser detail of the vascular network. By increasing the scanning area, the B-scans are spaced further apart and

the number of repetitions of equally located B-scans will decrease in order to maintain a feasible acquisition time (this compromises the resolution of the vascular network and the detection of blood flows at different speeds).

The montage option is available on some devices and allows the automatic combination of multiple scans in order to generate a larger single image, with more peripheral retina and choroid visualization.

### ARTIFACT REMOVAL TECHNOLOGIES:

- Motion artifacts: nowadays most devices combine two types of technology to correct motion artifacts: Eye Tracking (mechanical method) and motion correction software. Eye Tracking measures eye position and corrects for every eye movement that exceeds a predetermined threshold. Motion correction software calculates the offset between two acquisitions (one horizontal and one vertical) and corrects it into a final image.

- Projection artifacts: these are perhaps the most important artifacts in OCT-A due to the misinterpretation they can condition. Initially, the technology used to avoid these artifacts consisted of subtracting superficial vascular pattern from the acquisitions of the outer retina, with the disadvantage of leading to signal losses in the outer layers of the retina. In 2016, Zhang et al. published an algorithm that uses intensity-normalized decorrelation values (voxel-to-voxel) in order to distinguish in situ blood flow from projection artifacts, without causing signal loss in the outer retina<sup>10</sup>. More recently, a similar three-dimensional algorithm has emerged, which includes Z-axis information<sup>11</sup>.

- Segmentation artifacts: available OCT-A softwares allow the division of the retina and choroid into segments by selecting an upper horizontal boundary and a lower horizontal boundary to produce an image facing vessels falling between the two boundaries. Because the algorithms that calculate these limits are based on characteristics (eg. reflectivity and texture of retinal or choroid layers) of healthy eyes, pathologies that cause anatomical retinochoroid distortion (DME, drusen in AMD, myopia, among others) result in poorly calculated segmentations<sup>12</sup>. There are two methods to avoid segmentation errors: segment selection (simple method that involves repositioning the predefined limits up or down on the Z axis) and manual segmentation (very time-consuming process that consists of retracing the segments – only used for research purpose).

Currently available OCT-A devices and their specificities are described in Table 1. Next, we highlight some of the advantages and disadvantages of each device.

#### AngioPlex®<sup>13</sup>

##### Advantages:

- Quantitative analysis software available, allowing the quantification and monitoring of vascular density and perfusion, and foveal avascular zone;

- The automatic segmentation of the retina and choroid layers is adapted to the detection of neovascular membranes;
- EyeTracker with FastTrac technology, allowing to compensate for motion artifacts in real time.

##### Disadvantages:

- Quantitative analysis software not available in montage mode.

#### AngioVue®<sup>3,6</sup>

##### Advantages:

- Quantitative analysis software available, allowing to isolate areas of interest in order to obtain quantitative information on the blood flow, vascular density, and foveal avascular zone;
- Allows the edition of retinal and choroidal segmentation, contributing to a good visualization of neovascular membranes, even in patients with pathologies that alter the anatomy of the retina or the choroid.

##### Disadvantages:

- Does not allow to delimit flow and non-flow areas in the superficial retinal plexuses;
- Orthogonal scanning gives greater propensity for motion artifacts, cropped scans and vessels doubling, and the fact that each B-scan only repeats twice limits the detection of slower blood flows;
- Slower scan and longer acquisition time compared to other devices.

#### AngioScan®<sup>7</sup>

##### Advantages:

- Multiple integrated software, with quantitative analysis available;
- Allows a multimodal assessment, with correlation between structure and function through the use of combined images between OCT and microperimetry;
- Long Axial Length Normative Base: database of healthy eyes with long axial length (possibly useful for studying some pathologies);
- Tracing HD Plus tracks involuntary eye movements in real time, allowing for more accurate image acquisition while keeping the scan in the same location. It can also be defined for high contrast and definition or for fast image acquisition, depending on the clinical need.

#### PLEX® Elite<sup>14,15</sup>

##### Advantages:

- Available technologies:
- Swept-Source: allows better acquisition of structures located below the retinal pigment epithelium;
- Ultra-high definition: acquisition of cubes with high resolution images, good visualization of the vasculature, and allows the visualization of ocular structures with depths from the vitreous to the sclera;
- FastTrack: tracks real-time eye movements to minimize motion artifacts;
- HD spotlight: acquisition of high quality B-scans up

- to 16 mm;
- On-the-fly B-scan: allows to define an acquisition line at any angle.

Disadvantages:

- Quantitative analysis software not available;
- Only commercially approved by the U.S. Food and Drug Administration (FDA) for scientific research.

Spectralis OCTA®<sup>16</sup>

Advantages:

- Editable acquisition areas and number of B-scans, allowing to improve the resolution of the area to be analyzed. This allows to adapt the number of B-scan repetitions to patients with poor collaboration and to detect slower blood flows through a higher number of B-scan repetitions;
- Noise Reduction Technology, which uses multiple superimposed B-scans in order to differentiate structural information from noise, removing the latter;
- TruTrack (Eye Tracking technology): uses several real-time reference points in the background image in order to minimize motion artifacts;
- AutoRescan technology: positions tracking scans at the same location, making it easier to detect small structural changes, detecting retinal thickness changes of up to 1 micron;

- Allows multimodal assessment.

Disadvantages:

- Quantitative analysis software not available;
- The higher number of B-scan repetitions and the Eye Tracking technology result in a longer acquisition time.

SS OCT Angio®<sup>17</sup>

Advantages:

- The 1050 nm wavelength (the longest among the devices described in this chapter) allows for greater tissue penetration of the light beam, resulting in a higher quality of deeper acquisitions, even through cataract, hemorrhages or vessels;
- Invisible scan lines, helping the patient to fix on the target, consequently decreasing involuntary eye movements;
- Integrated IMAGEnet 6 system, enabling a multimodal assessment with direct access and comparison between OCT, retinography, red-free, auto-fluorescence and fluorescein angiography images;
- Integrated SMARTTrack system, ensuring that multiple tracking scans traverse exactly the same location. This system also compensates for involuntary eye movements.

Disadvantages:

- Quantitative analysis software not available.

Specifications	AngioPlex	AngioVue	AngioScan	PLEX Elite	Spectralis OCTA	SS OCT Angio
<b>OCT platform</b>	CIRRUS HD-OCT Model 6000	AngioVue Avanti XR	RS-3000 Advance 2	PLEX Elite 9000	Spectralis OCT-2	DRI-OCT Triton swept-source OCT
<b>Company (head-quarters)</b>	Carl Zeiss Meditec (Dublin, CA, USA)	Optovue (Fremont, CA, USA)	Nidek (Gamagori, Aichi, Japan)	Carl Zeiss Meditec (Dublin, CA, USA)	Heidelberg Engineering (Heidelberg, Germany)	Topcon Corporation (Tokyo, Japan)
<b>OCT methodology (wavelength, nm)</b>	Spectral Domain (840)	Spectral Domain (840)	Spectral Domain (880)	Swept Source (1000)	Spectral Domain (880)	Swept Source (1050)
<b>Acquisition algorithm</b>	OMAG	SSADA	CODAA	OMAG	FSADA	OCTARA
<b>Scan volume (A-scans)</b>	245 x 245 350 x 350	304 x 304 400 x 400 (orthogonal scan, acquiring only 2 B-scan repetitions in each position – 1 horizontal and 1 vertical)	256 x 256	300 x 300 500 x 500	Max. 512 x 512	320 x 320 512 x 512
<b>Scanning speed (scans/s)</b>	100000	70000	85000	100000	85000	100000
<b>Scanning area (mm), including montage mode</b>	3 x 3 4.5 x 4.5 6 x 6 8 x 8 14 x 10 14 x 14	3 x 3 4.5 x 4.5 6 x 6 8 x 8 10 x 6	3 x 3 4.5 x 4.5 6 x 6 9 x 9 12 x 9 12 x 12	3 x 3 6 x 6 12 x 12 15 x 9	10 x 10° (≈3 x 3) 20 x 20° (≈6 x 6) 30 x 15° (≈9 x 5)	3 x 3 4.5 x 4.5 6 x 6
<b>Optical resolution axial/lateral (µm)</b>	5/15	5/15	7/12	6.3/20	3.9/5.7	8/20
<b>Axial A-scan depth (mm)</b>	2	2-3 (depending on scan protocol)	2.1	3	1.9	2.6
<b>Eye Tracking and motion correction software</b>	✓	✓	✓	✓	✓	✓
<b>Motion artifacts removal</b>	✓	✓	✓	✓	✓	✓
<b>Anterior segment OCT-A</b>	Under development	Prototype	✓	✓	✓	✗
<b>Optic nerve OCT-A</b>	✓	✓	✓	✓	✓	✓

Table 1 – Specifications of commercially available OCT-A devices.

## REFERENCES

1. Greig EC, Duker JS, Waheed NK. A practical guide to optical coherence tomography angiography interpretation. *International Journal of Retina and Vitreous*. 2020;6(1):1-17.
2. Spaide RF, Fujimoto JG, Waheed NK, Sadda SR, Staurengi G. Optical coherence tomography angiography. *Prog Retin Eye Res*. 2018;64:1-55.
3. Turgut B. Optical coherence tomography angiography—a general view. *Journal-Optical Coherence Tomography Angiography—A General View*. 2016.
4. Novais EA, Adhi M, Moulton EM, Louzada RN, Cole ED, Husvagt L, et al. Choroidal Neovascularization Analyzed on Ultrahigh-Speed Swept-Source Optical Coherence Tomography Angiography Compared to Spectral-Domain Optical Coherence Tomography Angiography. *Am J Ophthalmol*. 2016;164:80-8.
5. Zhang Q, Zheng F, Motulsky EH, Gregori G, Chu Z, Chen CL, et al. A Novel Strategy for Quantifying Choriocapillaris Flow Voids Using Swept-Source OCT Angiography. *Invest Ophthalmol Vis Sci*. 2018;59(1):203-11.
6. Jia Y, Tan O, Tokayer J, Potsaid B, Wang Y, Liu JJ, et al. Split-spectrum amplitude-decorrelation angiography with optical coherence tomography. *Opt Express*. 2012;20(4):4710-25.
7. Rizzo S BD, Sodi A. OCT-Angiography Clinical Cases. *AngioScan*. Nidek CO, LTD.
8. Lindner M, Fang PP, Steinberg JS, Domdei N, Pfau M, Krohne TU, et al. OCT Angiography-Based Detection and Quantification of the Neovascular Network in Exudative AMD. *Invest Ophthalmol Vis Sci*. 2016;57(14):6342-8.
9. Li XX, Wu W, Zhou H, Deng JJ, Zhao MY, Qian TW, et al. A quantitative comparison of five optical coherence tomography angiography systems in clinical performance. *Int J Ophthalmol*. 2018;11(11):1784-95.
10. Zhang M, Hwang TS, Campbell JP, Bailey ST, Wilson DJ, Huang D, et al. Projection-resolved optical coherence tomographic angiography. *Biomedical optics express*. 2016;7(3):816-28.
11. Garrity ST, Iafe NA, Phasukkijwatana N, Chen X, Sarraf D. Quantitative Analysis of Three Distinct Retinal Capillary Plexuses in Healthy Eyes Using Optical Coherence Tomography Angiography. *Invest Ophthalmol Vis Sci*. 2017;58(12):5548-55.
12. Spaide RF, Fujimoto JG, Waheed NK. Image artifacts in optical coherence tomography angiography. *Retina*. 2015;35(11):2163-80.
13. Carl Zeiss Meditec. CIRRUS HD-OCT User Manual - Models 500, 5000. Available from: <https://www.zeiss.com/meditec>. 2017.
14. Carl Zeiss Meditec. PLEX® Elite 9000 Version 1.7 - Instructions for use. Available from: <https://www.zeiss.com/meditec/> 2018. .
15. Carl Zeiss Meditec. ARI Network Brochure. Available from: <https://www.zeiss.com/meditec> 2018.
16. Sacconi R, Corbelli E, Carnevali A, Querques L, Bandello F, Querques G. Optical coherence tomography angiography in geographic atrophy. *Retina*. 2018;38(12):2350-5.
17. Stanga PE, Tsamis E, Papayannis A, Stringa F, Cole T, Jalil A. Swept-Source Optical Coherence Tomography Angio™ (Topcon Corp, Japan): Technology Review. *Dev Ophthalmol*. 2016;56:13-7.



# 3. ARTIFACTS

Belmira Beltrán

Centro de Responsabilidad Integrada de Oftalmología (CRIO) Hospital Garcia de Orta, E.P.E.  
Hospital CUF Tejo, Clínica CUF Almada

Optical coherence tomography angiography (OCTA) is a functional extension of optical coherence tomography (OCT), that provides visualization of the microvasculature by detecting motion from blood flow in the retina and the choriocapillaris<sup>1,2,3</sup>. Understanding signal processing, displaying techniques, and image generation, is important in order to analyze OCTA images as well as how image defects or artifacts arise.

## PROJECTION ARTIFACTS

Projection artifacts or decorrelation tails, are one of the most important artifacts appearing on OCTA. To image deeper structures such as the photoreceptors or the retinal pigment epithelium (RPE), the light beam passes through the superficial retinal blood vessels where it may be reflected, absorbed, refracted or scattered<sup>3-5</sup>.

A fraction of the emitted light beam is reflected from the superficial capillary plexus and analyzed, while the unreflected fraction reaches the RPE. The RPE reflects light back towards the OCTA device. The light reflected from the moving cells within vessels changes over time, and this reflection generates a decorrelation signal that delineates the vascular lumen<sup>3,4</sup>. The mixture of these two beams results in the erroneous appearance of overlying retinal blood vessels while imaging the RPE.

OCTA projection artifacts occur when the superficial retinal vessels are seen in the deeper retinal layers, the deep capillary plexus projected on the choriocapillaris, but also when choroidal vessels appear in the scleral slab. Projection artifacts limit the ability of OCTA to resolve the depth of detected vessels<sup>5-7</sup>. Besides innovation methods for projection artifact removal, compensation methods are not perfect, nor uniformly available in OCTA devices. Projection artifacts may be detected by comparing *en face* flow image with the corresponding B scan. On cross-sectional angiograms, projection artifacts appear as axial tails that blur the vascular layers together. On *en face* angiograms, these artifacts appear to be above other layers (Figure 1).

Understanding OCTA projection artifacts is important to detect macular neovascularization (MNV) and to follow up diseases, avoiding unneeded invasive procedures as fluorescein angiography. In MNV, projection artifacts limit the visualization and quantitative analyzing is

difficult, since MNV is so close to the RPE, a naturally highly reflective surface<sup>4,7-9</sup>. Likewise, the correct follow up after anti-VEGF treatment by OCTA is difficult. Zhang et al, proposed an algorithm where the overlying retinal microvasculature and OCT structural information were included for artifact removal from images of MNV<sup>4</sup>.

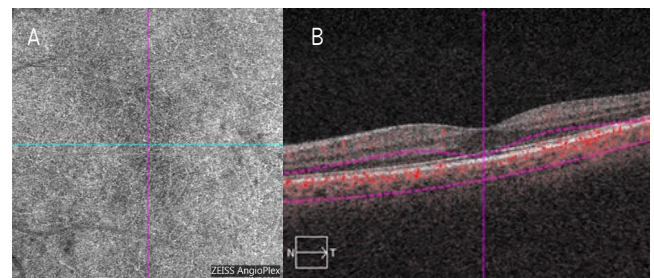


**Figure 1.** Segmentation artifacts. A. The superficial vascular plexus is seen in the deeper layers. B. The section taken in the B-scan is below the large vessels. There is a projected image due to a segmentation error.

## MOTION ARTIFACTS

Motion artifacts are relevant on sequential acquisition of OCT-B images of flow. Eye movements (movement from the head or body, loss of fixation or eye movement) may cause artifacts of movement. OCTA images are viewed *en face* and have much more contrast than the OCT images. Eye motion produces horizontal lines through the scans or gaps in the *en face* images<sup>1-3</sup> since movement has prevented data collection in that area (Figure 2).

Two types of technology can correct motion artifact: the eye tracking technology and the software motion correction. The eye tracking technology measures the position of the eye and corrects the eye movement when there is a change of a predetermined threshold position. The software motion correction obtains a horizontal and a vertical raster scan, used to calculate displacement between A-scans and corrects for motion in the final images<sup>1-3</sup>.

## SHADOWING ARTIFACTS

Shadowing artifacts occur when the OCT beam is



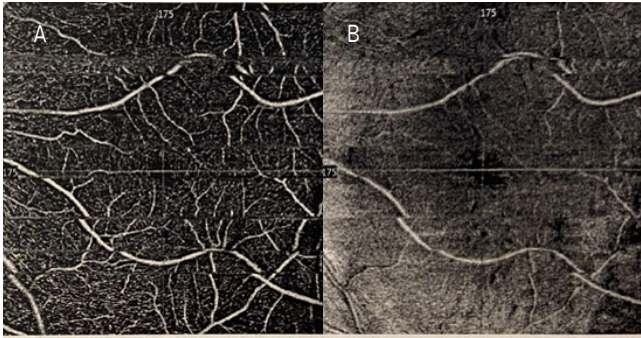


**Figure 2.** Motion artifacts. A and B. Displacement artifact which there is a displacement of the retinal vessels.

blocked and cannot reach the outer retinal layers. Vitreous floaters or drusen may cause local loss of signal behind the opacities, causing a false negative flow, while the flow actually exists (Figure 3). The shadowed areas are darkened where the flow is not visible<sup>1-3</sup>. A similar situation occurs with detachment of the RPE that decreases visualization of blood flow in the choroid<sup>1</sup>.

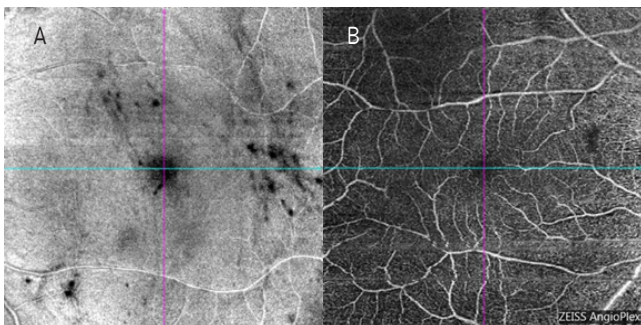


**Figure 3.** Shadowing Effect. A and B. A defect in the angiographic image correspond to a vitreous condensation.

## ARTIFACTS DUE TO SIGNAL STRENGTH

Dense cataracts or diffuse vitreous hemorrhages cause a global loss of signal. Image quality drops if the signal level is low or if noise levels are high. Noise is the unwanted information generated through image acquisition and processing<sup>1,2</sup>. The dry-eye syndrome reduces the image signal as well, being corrected by proper lubrication. The software reports a signal strength score for each acquisition and provides tools to decide whether that is a valid acquisition or there is a need to reacquire new images.

## DETECTION AND CORRECTION OF SEGMENTATION ARTIFACTS

The retinal slabs are automatically generated for analyses of the retinal vascularization of the superficial, middle, deep retinal capillary plexuses, and the choriocapillaris<sup>6,12-14</sup>. Each slab is generated by selecting an upper and lower

boundary through the three-dimensional OCTA cube. The vessels within these two boundaries are summed into a two-dimensional *en face* image. Algorithms detect predetermined retinal boundaries based on reflectivity and texture. However, in the presence of disease, such as drusen in age-related macular degeneration, fluid in diabetic macular edema, epiretinal membrane and myopia, the retinal anatomy may be changed and cause segmentation errors<sup>14, 15</sup>. In diabetic retinopathy (DR) the presence of segmentation errors was 11% in non-proliferative DR peaking to 50% in patients with proliferative DR<sup>13</sup>.

Manual correction of segmentation errors enables the user to retrace the mislabeled retinal layer. This process is time-consuming, because proper retracing must be completed for multiple B-scans<sup>3</sup>. Slab selection is another way to manipulate segmentation boundaries and involves dragging a preset boundary up and down the z-axis, generating a larger or smaller slab to better assess the structure of interest<sup>3</sup>.

## REFERENCES

1. Spaide RF, Fujimoto JG, Waheed NK. Image Artifacts in Optical coherence tomography angiography. *Retina*. 2015; 35:2163-80.
2. Spaide RF, Fujimoto JG, Waheed NK, Sadda SR, Staurengi G. Optical coherence tomography angiography. *Prog Retin Eye Res*. 2018; 64:1-55.
3. Greig EG, Duker JS, Waheed NK. A practical guide to optical coherence tomography angiography interpretation. *Int J Retin Vitre*. 2020; 6:1-17.
4. Zhang QM, Zhang A, Lee CS, et al. Projection artifact removal improves visualization and quantification of macula neovascularization imaged by optical coherence tomography angiography. *Ophthalmol Retina*. 2017;1(2):124-136.
5. Borrelli E, Sadda SR, Uji A, Qureques G. Pearl and pitfalls of optical coherence tomography angiography imaging: A review. *Ophthalmol Ther*. 2019; 8(2):2015-226.
6. Borrelli E, Parravano MC, Sacconi R, et al. Guidelines on Optical Coherence Tomography Imaging: 2020 Focused update. *Ophthalmol Ther*. Dec;9 (4): 697-707.
7. Sambhav K, Grover S, Chalam KV. The application of optical coherence tomography angiography in retinal diseases. *Surv Ophthalmol*. 2017; 62(6):838-866.
8. Kuehlewein L, Bansal M, Lenis TL, et al. Optical coherence tomography angiography of Type 1 neovascularization in age-related macular degeneration. *Am J Ophthalmol*. 2015; 160 (4):739-48.
9. Scharf J, Corradetti G, Corvi F, Sadda S, Sarraf D. Optical coherence tomography angiography of the choriocapillaris in age-related macular degeneration. *J Clin Med*. 2021; 10(4): 751.
10. Chalam KV, Sambhav K. Optical coherence tomography angiography in retinal diseases. *J Ophthalmic Vis Res*. 2016; 11(1):84-92.
11. Chua J, Sim R, Tan B, et al. Optical Coherence Tomography Angiography in Diabetes and diabetic Retinopathy. *J Clin Med*. 2020; 9(6):1723.
12. Hwang TS, Zhan M, Bhavsar K, et al. Visualization of 3 distinct

- retinal plexuses by projection-resolved optical coherence tomography angiography in diabetic retinopathy. *JAMA Ophthalmol.* 2016; 134(12): 1411-1419.
13. Cui Y, Zhu Y, Wang JC, et al. Imaging artifacts and segmentation errors with wide-field swept-source optical coherence tomography angiography in diabetic retinopathy. *Transl Vis Technol.* 2019; 15; 8(6):18.
  14. LI M, Yang Y, Jiang H, et al. Retinal Microvascular Network and microcirculation assessments in high Myopia. *Am J Ophthalmol.* 2017; 174:56-67.
  15. Bruyère E, Miere A, Cohen SY, et al. Neovascularization secondary to high myopia imaged by optical coherence tomography angiography. *Retina.* 2017; 37(11): 2095-2101.



4.

# THE RETINA



## 4.1.

# THE ANGIO-ARCHITECTURE OF THE CAPILLARY PLEXUSES

Alain Gaudric<sup>1</sup>, Carlo Lavia<sup>2</sup>

1 - Service d'Ophthalmologie, Université de Paris, Hôpital Lariboisière, APHP, Paris, France

2 - Surgical Department, Ophthalmology Service, Azienda Sanitaria Locale T05, Chieri, Italy

## INTRODUCTION

One of the oldest representations of the retinal capillary architecture is probably that provided by Wilhelm His in 1880<sup>1</sup>. He has precisely described 3 capillary levels in the inner macula including the direct drainage of the deep capillary plexus (DCP) in the superficial retinal veins. However, this work remains unknown as it has only been cited once in the book “The Retinal Circulation” by Wise, Dollery and Henkind in 1972<sup>2</sup>.

D. Toussaint<sup>3</sup>, who has detailed the three-dimensional (3D) organization of the retinal capillaries after trypsin digestion but failed to identify its multilaminar pattern, was another precursor of the study of the retinal circulation. However, he has assumed that “the capillary plexus (was) suspended like a hammock between its feeding arterioles and draining venule”. Jose Cunha-Vaz in his Thesis (personal communication) has described the organization of the retinal capillaries in 3 layers and the drainage of the DCP directly into the superficial retinal veins, while Paul Henkind in 1969 has only noted the presence of 2 layers of capillaries (except the radial peripapillary capillaries) in a drawing that has often been reproduced<sup>4</sup>. A remarkable histological work in monkeys of internal casts of the retinal capillary architecture by Koichi Shimizu in 1978<sup>5</sup> has clearly shown the 3 levels of capillaries, including the presence of venules draining the deep capillary layer into the superficial veins. But the most systematic and detailed analysis of the retinal capillary network has been performed by D Max Snodderly in 1992<sup>6</sup>. Indeed, he has not only described the complexity of the 3 levels of capillaries in the macular region but also emphasized the relationship between the neuronal density and the capillary density. He has also observed retinal venules linking directly the deep capillaries to the superficial veins. The topic has not evolved much until the availability of OCTA. Indeed, fluorescein angiography did not allow distinguishing the capillaries beyond the perifoveal area and provided only a 2D image of the capillary bed. However, in 2003, M. Paques in an experimental study in mice<sup>7</sup> has stated that “most microvessel connections on the arteriolar side direct the flow from the superficial to the deep layer, and vice versa on the venular side” in a three-layer model of retinal capillaries. This finding would become relevant again

only 12 years later with the first publications on OCTA. At the same time, new modern histological studies on the retinal capillary anatomy have been published, in particular by DT Yu and colleagues<sup>8-10</sup>.

## RETINAL VASCULAR ANATOMY IN HUMAN EYES

In human eyes, most of the knowledge about the anatomy of retinal capillaries *in vivo* has been acquired, for many years, through fluorescein angiography. Fluorescein angiography has the advantage of being dynamic and showing the blood-retinal barrier (BRB) breakdown in pathological cases. However, the retinal capillaries are often indistinguishable from the background fluorescence and only the superficial vascular plexus (SVP) may be seen inconsistently around the fovea and in the periphery.

The advent of OCTA, that allows detecting the movement of red blood cells in the capillaries, has improved their detection compared to fluorescein angiography and has allowed for the first time imaging *in vivo* the different layers of the retinal capillary plexuses, with a depth-resolved analysis directly related to the retinal structure on transverse and en face OCT scans. It is noteworthy that, while the lateral resolution between two OCT/OCTA A-scans is about 15  $\mu\text{m}$ , the retinal capillaries being 5-7  $\mu\text{m}$  in diameter, are better resolved on OCTA through the detection of any motion transiting on an A-scan. This results in an apparent capillary diameter that seems larger than the actual one (about 15  $\mu\text{m}$ ) and a capillary density that cannot be directly compared to histological data<sup>11</sup>.

The introduction of the projection artifacts removal software<sup>12</sup>, that removes the projection artifacts on a per voxel basis, has allowed segmenting separately the various levels of the capillary networks in the inner retina, and analyzing any abnormal subretinal capillary proliferation without the interference of the retinal capillary projection. Motion tracking systems, that significantly reduce motion and blinking artifacts, also represent a major improvement in OCTA imaging. Finally, the possibility to acquire OCTA scans with a follow-up mode, allows performing direct point-by-point comparisons over time.

The analysis of the retinal capillary architecture, that

was based on histological studies of a few animal or human specimens, has thus become easy to perform in a large number of normal subjects and has given rise to various interpretations. If an appropriate segmentation is applied on structural OCT, 4 levels of capillaries are distinguishable in the posterior pole, with respect to the neuronal structures of the inner retina: a layer located around the optic disc and the temporal arcades in the thick optic nerve fiber layer (ONFL), and 3 other layers in the ganglion cell layer (GCL), and in the inner and outer plexiform layers (IPL and OPL, respectively). Based on OCTA and histological findings, the nomenclature of the capillary layers proposed by Campbell et al<sup>13</sup> has been widely used.

The authors have proposed the following nomenclature:

1. A radial peripapillary capillary plexus (RPCP), located within the ONFL,
2. A SVP, located within the GCL and the superficial part of the IPL, *The RPCP and the SVP form the superficial vascular complex (SVC).*
3. An intermediate capillary plexus (ICP), located within the deeper part of the IPL and in the more superficial part of the inner nuclear layer (INL),
4. A DCP, located within the deeper part of the INL and the OPL.

*The ICP and the DCP form the deep vascular complex (DVC).*

Below the DCP, an avascular outer retinal slab is comprised between the outer nuclear layer (ONL) and the retinal pigment epithelium (RPE). This slab is particularly useful to detect the presence of abnormal macular neovascularization.

## PRACTICAL DETERMINATION OF THE RETINAL CAPILLARY PLEXUSES IN THE MACULA

The OCTA boundaries proposed to isolate each plexus are based on histological studies and findings from other imaging techniques. However, due to the intrinsic features of the OCTA devices, the flow signal of each capillary plexus within the OCT B-scan is located a little deeper in the retina than indicated by histology, so that a correct segmentation of each plexus results in a posterior shift of the segmentation boundaries (Figure 1).

In most devices, the boundaries of the SVC and DVC are proposed by default while the segmentation of the ICP and DCP is obtained manually by looking at the B- and C-scans with flow overlay. Due to the poor representation of the RPCP within the macular region, its marginal density is taken into account together with the SVP, as part of the SVC.

Herein, we propose the segmentation boundaries that we routinely use to isolate each capillary plexus within the macula<sup>14</sup> (Figure 1):

SVC: between the inner limiting membrane (ILM) and 9  $\mu\text{m}$  above the IPL-INL junction;

DVC: between 9  $\mu\text{m}$  above the IPL-INL junction and 9  $\mu\text{m}$  below the OPL-ONL junction;

ICP: between 9  $\mu\text{m}$  above the IPL-INL junction and 6

$\mu\text{m}$  below the INL-OPL junction; and DCP: between 6  $\mu\text{m}$  below the INL-OPL junction and 9  $\mu\text{m}$  below the OPL-ONL junction.

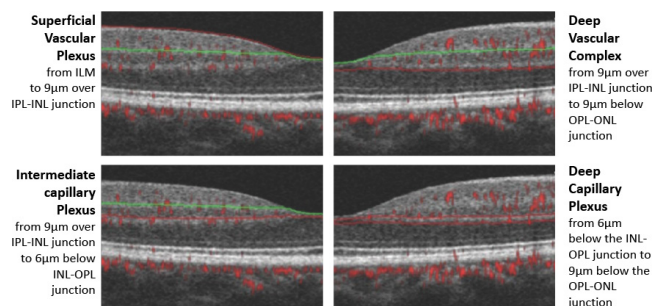


**Figure 1:** Segmentation of OCTA used to obtain the en face images of the retinal capillary plexuses.

## MORPHOLOGY OF EACH RETINAL CAPILLARY PLEXUS

In the RPCP, the radial capillaries are immersed in the ONFL and are composed of long capillary segments oriented radially along the ganglion cell axons (Figure 2). Smaller interconnecting capillaries are oriented orthogonally to the long capillaries<sup>15</sup>. Fouquet et al<sup>16</sup> have found that these capillary segments are connected at one side to the superficial capillary plexus (SCP) and at the other side to the deeper capillaries. In the macula, the RPCP is negligible and the capillary structure is composed of 3 levels (Figure 3).

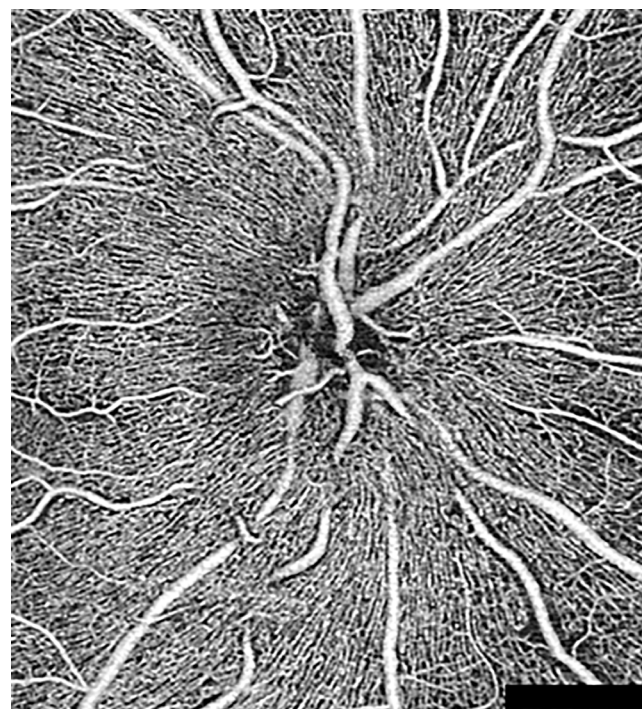


**Figure 2:** Radial peripapillary capillaries.

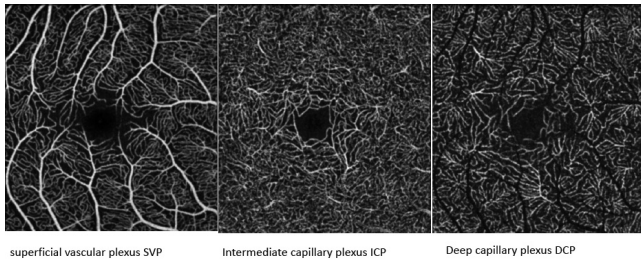


**Figure 3:** Three capillary plexuses in the macula (with averaging).

The SVP is composed of precapillary arterioles, capillaries and post-capillary venules (Figure 4). The arterioles are surrounded by wider capillary-free areas that allow differentiating them from the venules. There are a few anastomotic capillaries directly connecting the arterioles to the venules. However, most superficial capillaries branch out in the thickness of the GCL and give rise to capillaries that plunge backwards in the ICP or directly in the DCP. Overall, the SVP forms a 3D capillary meshwork<sup>8</sup>, fed by retinal arterioles and distributing

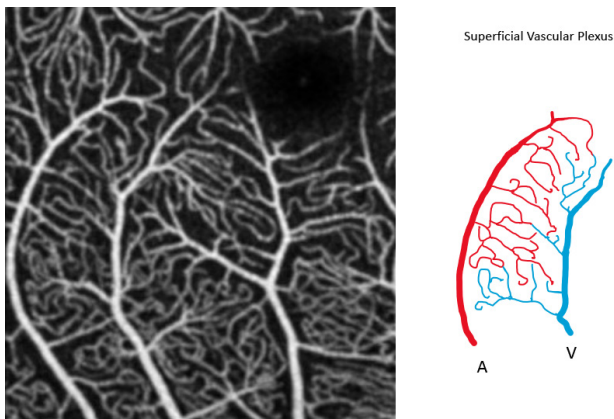


**Figure 4:** Details of the SCP and schematic illustration. Only a few capillaries connect directly the arteriole to the venule.

blood to the underlying capillary plexuses<sup>16,17</sup>. An anastomotic capillary arcade at the end of the arterioles and venules of the SVP delimits a roundish avascular zone (FAZ) about 400-500  $\mu\text{m}$  wide, in the middle of the foveal slope. Capillaries coming from deeper plexuses also contribute to this arcade. Many OCTA parameters have been studied to evaluate the FAZ, including its area, perimeter and circularity (18-20). The ICP also forms a 3D meshwork of capillaries located at the boundary between the IPL and the INL. Some anastomoses are visible while other capillaries come from and are oriented towards the SVP and the DCP. The DCP shows a unique uniplanar pattern. Capillaries drained by vertically-oriented capillaries<sup>17,21</sup> are organized in polygonal units in which the capillaries converge, in a vortex pattern, into a post-capillary venule draining

directly into a superficial retinal venule<sup>16, 17, 21</sup>. On histology, this layer is located at the boundary between the INL and the OPL<sup>8,22</sup>.

## QUANTITATIVE ANALYSES

To provide data on the capillary status, several image processing techniques have been developed to quantify the flow measured within the scan area, on both C- and B-scans. Binarization and skeletonization are now routinely used by the OCTA devices to provide data on the flow detected within a scan and to detect a capillary loss. Binarization, that is the transformation in no-flow or flow of a signal less or greater than a certain threshold, is used in the calculation of the vessel density (VD; % of flow signal within a given scan area).

Skeletonization, that is the transformation of flow signal in a trace of virtual width, is used in the calculation of the vessel length within a given scan area.

Both techniques have their advantages and limitations. Binarization includes the width of arterioles and venules in the density calculation so that the term of vascular density is more adapted than capillary density. This does not apply to the deeper plexuses. In the SVC, a decrease in VD may be underestimated because the surface of larger vessels remains unchanged. Skeletonization does not take into account the changes in capillary diameter while they may be dilated as in diabetic retinopathy. Or, on the contrary, the loss of capillaries has the same value than the obstruction of an arteriole of the same length<sup>23</sup>.

Image quality and artifacts may significantly affect the qualitative and quantitative assessments of OCTA scans<sup>11</sup>. For instance, there is a significant positive correlation between the image quality (measured as the signal strength index) and the VD<sup>14</sup>. VD values provided by OCTA devices may present some differences, related to the acquisition technique (e.g., processing algorithms, thresholds) and to the location of the segmentation boundaries.

Finally, all the algorithms are limited by the difficulty to measure the actual density of a 3D meshwork that is projected onto a single plane. This is the case for the SVP and the ICP. Only the DCP is uniplanar<sup>24</sup>.

VD values within the macular region can be obtained from smaller (e.g., 3x3 mm or 10°x10°) or larger scans (e.g., 6x6 mm, 8x8 mm, 9x9 mm). Smaller scans generally have a higher resolution due to a higher number of B-scans per mm and we therefore recommend to use them for quantitative analyzes. OCTA devices normally show the VD values of the whole scan and of standardized sectors (parafoveal, i.e., an annulus centered on the fovea with an inner and outer diameter of 1 and 3 mm, respectively; perifoveal, i.e., an annulus of 6 mm in diameter that encircles the parafovea).

Using the segmentation boundaries proposed in this chapter, the VD is higher in the DVC than in the SVC. The VD in the DCP represents about two thirds of that in the ICP, that is slightly less than that in the SVC. In a series of 148 healthy eyes, we have obtained the following



	VD (%): Mean $\pm$ SD		VD (%) range	
	Whole area	Parafoveal area	Whole area	Parafoveal area
<b>SVC</b>	47.7 $\pm$ 2.8	50.5 $\pm$ 2.8	39.0-54.7	41.4-57.2
<b>ICP</b>	45.4 $\pm$ 4.2	46.9 $\pm$ 4.2	30.8-53.2	32.4-54.4
<b>DCP</b>	31.6 $\pm$ 4.4	32.7 $\pm$ 4.3	19.1-42.4	21.1-43.5
<b>DVC</b>	52.7 $\pm$ 3.3	54.2 $\pm$ 3.2	43.5-59.5	46.1-61.1

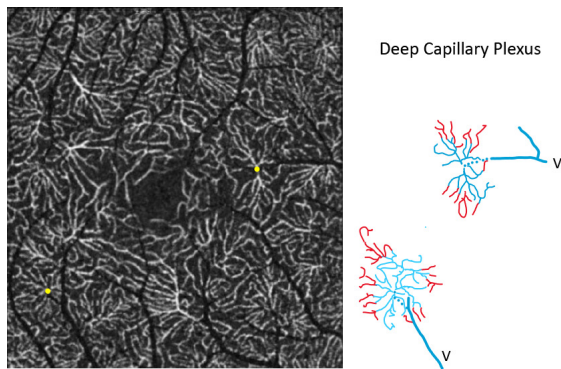


**Figure 5:** Details of the DCP and schematic illustration. The yellow dots point out the centre of the capillary vortices connected to the superficial venule.

VD values using a binarization technique<sup>14</sup> (Figure 5):

Of note, the parafoveal annulus showed higher VD values compared to the whole 3x3-mm scan due to the presence of the FAZ in the latter.

The VD in the SVP in the macular region was greater in the superior and inferior quadrants, followed by the nasal and temporal quadrants, partly due to the presence of the ONFL and RPCP. The VD did not differ between the four quadrants in the ICP, DCP and DVC. The VD in the SVC positively correlated with the inner retinal thickness (i.e., between the ILM and the IPL-INL junction). No correlations were observed between the VD in deeper plexuses and their corresponding retinal thickness. The VD significantly negatively correlated with age in all plexuses, being reduced by 0.064% and 0.076% per year in the SVP and DCP, respectively. No gender-related changes in mean VD values were observed.

Image quality parameters significantly positively correlated with VD values and should be taken in account when performing a quantitative analysis of OCTA data. Each device has its own quality criteria so that specific considerations are difficult to take into account. We suggest to carefully consider them as well as manually check if visible errors are present (e.g., segmentation errors, motion artifacts) before performing any analysis. It should be kept in mind that, due to the OCTA lateral resolution limited to 15  $\mu$ m, the capillary size is overestimated compared to histology, where capillaries appear thinner and more spaced.

The FAZ is generally examined with a thicker slab encompassing both the SVC and the DVC, due to the presence of anastomotic capillaries coming from all plexuses.

The measurement of FAZ parameters is less subject to significant inter- and intra-device-related variability. On the other hand, FAZ metrics significantly differ even between healthy eyes, suggesting that a combination of them may be required to capture local and overall aspects of the FAZ.

In our series of 148 healthy eyes, the FAZ metric values were as follows:

The mean FAZ area was  $0.25 \pm 0.11$  mm<sup>2</sup>. The mean FAZ perimeter was  $1.97 \pm 0.43$  mm. The mean FAZ acircularity was  $1.14 \pm 0.05$ .

The FAZ area significantly negatively correlated with age, being reduced by 0.003 mm<sup>2</sup> per year.

The mean FAZ area was greater in women.

Image quality parameters did not correlate with FAZ metrics.

FAZ parameters have been extensively studied after the advent of OCTA and, even if they have been less investigated than VD values, they are less subject to post-processing analysis. Of note, due to the location of capillaries defining the FAZ at the junction between the SCP and the DVC<sup>25</sup>, we stress the importance of using a thick slab.

Finally, some authors have studied the capillary rarefaction around the FAZ, suggesting its potential use as a biomarker to define early diabetic retinopathy<sup>26</sup>.

## FUNCTIONAL ORGANIZATION OF THE RETINAL CAPILLARY PLEXUSES

OCTA is used in clinical practice since 2014 and the first articles on the human retinal capillary anatomy have been published in 2015. Spaide has noted that OCTA provided high-quality images of the retinal capillary network by separating the two planes of capillaries, the SVP in the GCL and the DCP in the INL<sup>27</sup>. Savastano et al have reported a different pattern of the two capillary beds and that the deep network presented as an interconnected mesh of dense vessels. They have also suggested the presence of vertical anastomoses between the DCP and the SVP as small, slanted, interconnected anastomoses between the superficial and deeper vessels but without explicitly mentioning the venous drainage<sup>28</sup>.

The same year, Bonnín et al<sup>17</sup> have shown that, despite the limitations of the early version of OCTA software, it was possible to observe that the SVP and the DCP had two different topographic organizations. In the DCP, the pattern of the capillary units converging into capillary vortices highly

suggested that they drained into the superficial venules. They have confirmed the hypothesis already put forward by Paques et al in mice. This schematic interpretation of the capillary architecture of the inner retina has been further refined in an editorial by Garrity et al<sup>29</sup>.

Fouquet et al, based on a histological analysis of pig retinas<sup>16</sup>, have proposed an outline of the DCP very similar to that observed on OCTA in human eyes, and have proposed a model of capillary organization, mainly serial, in which the DCP drains directly into the superficial venules. However, the representation of the ICP in their outline is sparse, whereas its density is greater than that of the DCP (Figure 6).

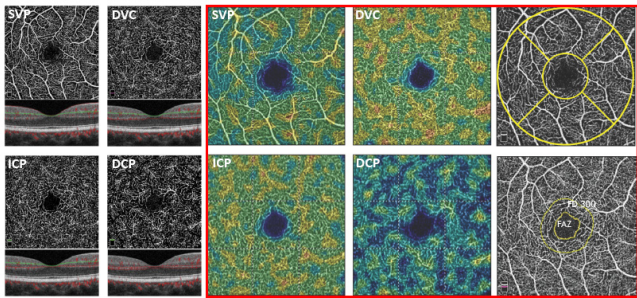


**Figure 6:** Typical normal capillary density in the various plexuses in a healthy eye.

Finally, the role of the DCP in the venous drainage of the retinal blood flow has been indirectly confirmed by the observations that veno-venous anastomoses primarily developed in the DCP in branch retinal vein occlusion<sup>30</sup>. Other conceptions of the retinal capillary architecture have been proposed. Campbell et al have initially assumed that the 3 capillary plexuses worked in parallel from the arterioles to the venules<sup>13</sup> in a “hammock” configuration. Nesper and Fawzi<sup>21</sup> have proposed an alternative hybrid model based on the “hammock” model that integrates elements from their observations and from other studies. For instance, they acknowledge the existence of vortices in the DCP, draining into central conduits that directly connect to the venules in the SVP but they also take into account capillary anastomoses (direct connections) between each of the three plexuses in their model. Whatever the discordances between these models, two constants appear:

1. The ICP and the DCP form a functional unit around the INL, but only the DCP participates in the oxygenation of the ONL.
2. The DCP directly receives blood from vertical capillaries coming from the SVP and drains into venules directly connected to the superficial venules. The latter also collect blood from the ICP.

There is thus no complete consensus on the functional organization of the retinal capillary plexuses, the proposed models being a simplification of the complex *in vivo* capillary meshwork. However, a reliable model is needed to better understand pathological conditions such as posterior acute middle maculopathy or diabetic retinopathy.

## RETINAL CAPILLARIES FROM THE FOVEA TO THE PERIPHERY

The increased speed of B-scan acquisition (up to 200,000 A-scans per second) available since the introduction of Swept-Source OCTA devices has allowed increasing the field of view of OCT/OCTA. Wide-field scans of 9x9, 12x12, 15x9 mm and a combination of them are now available. However, these wide-field images result from a compromise between the acquisition speed and the lateral resolution so that the widest images do not provide a resolution accurate enough to analyze precisely the ICP and the DCP<sup>31,32</sup>, while they are overall useful to detect full-thickness capillary non-perfusion in the mid-periphery.

In order to assess the density of retinal capillaries outside the macula, several publications have used smaller scans, acquired from the fovea towards the periphery with both *en face* and transverse analyzes<sup>13,33</sup>.

We have used a series of overlaid 3x3-mm C-scans from the fovea to 11 mm in temporal and nasal horizontally and 10 mm up and down vertically (34) (Figure 7). We have shown a progressive decrease in VD towards the periphery, consistent with a retinal thinning. The retinal thinning, outside the macular region, involved all the retinal layers but was more pronounced in the inner retina.

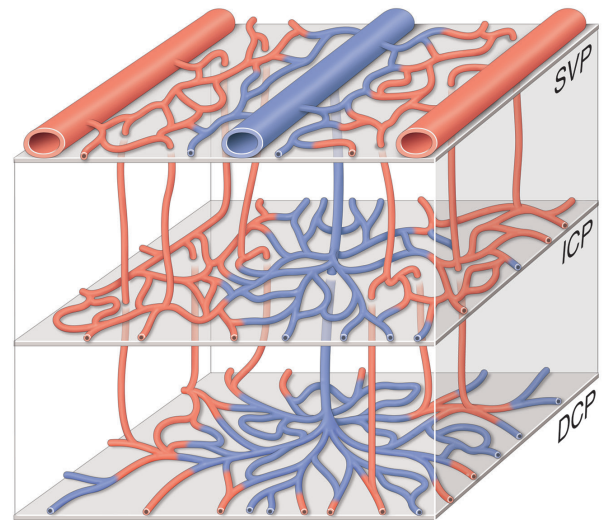


**Figure 7:** Three-dimensional schematic representation of the three capillary plexuses in the macula. Modified from S.Fouquet and M.Paques, 2017<sup>16</sup> and S. Bonnini et al, 2015<sup>17</sup>. SVP: Superficial Vascular Plexus. ICP: Intermediate Capillary Plexus. DCP: Deep Capillary Plexus.

As the retina thinned, both the interplexus distance (i.e., the distance on B-scans between each plexus) and the VD decreased, together with a lower oxygen consumption by ganglion and bipolar cells that became sparser. For instance, in the temporal sector, the VD in the SVP progressively decreased, being halved at about 8 mm from the foveal center, according to a significant

decrease in GC density (by up to 10-fold at 10 mm temporally). In the superior and inferior sectors, the VD in the SVP was almost stable towards the vascular arcades, at about 4 mm from the foveal center. Then, a significant reduction was observed, with VD values that became similar to that of the temporal sector at about 8 mm from the foveal center<sup>34</sup> (Figure 8).

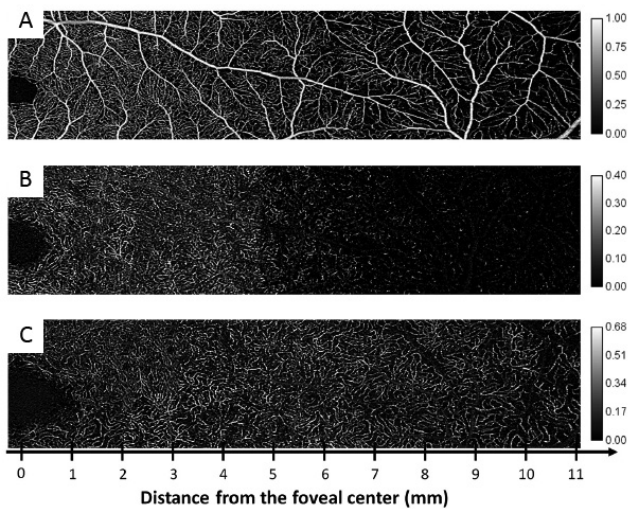


**Figure 8:** Capillary plexuses from the posterior pole to the periphery. The intermediate capillary plexus vanishes between 6 and 8 mm from the fovea in temporal. From Lavia et al 2020<sup>34</sup>.

The VD in the ICP strongly decreased at about 6 mm in the superior, inferior and temporal sectors and 8 mm in the nasal sector, becoming almost undetectable 2 mm more peripherally, so that beyond this limit only two plexuses, the SVP and the DCP, were detected.

The VD in the DCP slightly decreased, being halved at about 10 mm from the fovea in all sectors.

The consequences of the progressive rarefaction of the ICP in the mid-periphery in various retinal vascular diseases are unknown. However, it should be noted that, in diabetic retinopathy, the capillary dropout starts preferentially in this transitional zone, a preferred location that has never been explained until now, but where the ICP vanishes<sup>5,35</sup>. It is noteworthy that beyond the limit of the ICP, the interplexus distance, that was initially of about 24–36  $\mu\text{m}$  between each of the 3 plexuses, increased to 55  $\mu\text{m}$  between the SVP and the DCP while the density in the SVP continued to decrease, and this could have resulted in some vulnerability in the neurovascular coupling in this area.

## SUMMARY

The retinal capillary meshwork is organized in 3 plexuses in the posterior pole: the SVP in the GCL, and the ICP and the DCP in the plexiform layers framing the INL, to which the RPCP is added in the thick ONFL around the optic disc and along the temporal arcades. The blood flow in this complex is mainly serial in the sense that there are

relatively few direct capillary connections between the arterioles and the venules in the SVP, while the ICP and the DCP are fed by plunging capillaries coming from the SVP and the venous drainage occurs through the DCP organized in vortices collecting blood in the venules directly connected to the superficial venules. The ICP and the DCP form a circulation unit called the DVC.

## REFERENCES

1. His W. Abbildungen über das Gefäßsystem der Menschlichen Netzhaut und derjenigen des Kaninchens. Arch Anat Entwicklungslehre 1880;5:224.
2. Wise NG, Dollery CT, Henkind P. The Retinal Circulation. New York: Harper and Row; 1971. 566 p.
3. Toussaint D, Kuwabara T, Cogan DG. Retinal vascular patterns. II. Human retinal vessels studied in three dimensions. Arch Ophthalmol. 1961;65:575 - 81.
4. Henkind P. Microcirculation of the peripapillary retina. Trans Am Acad Ophthalmol Otolaryngol. 1969;73(5):890-7.
5. Shimizu K, Ujje K. Structure of Ocular vessels Tokyo-New-York: Igaku-Shoin 1978. 144p.
6. Snodderly DM, Weinhaus RS, Choi JC. Neural-vascular relationships in central retina of macaque monkeys (*Macaca fascicularis*). J Neurosci. 1992;12(4):1169-93.
7. Paques M, Tadayoni R, Sercombe R, Laurent P, Genevois O, Gaudric A, et al. Structural and hemodynamic analysis of the mouse retinal microcirculation. Invest Ophthalmol Vis Sci. 2003;44(11):4960-7.
8. Chan G, Balaratnasingam C, Yu PK, Morgan WH, McAllister IL, Cringle SJ, et al. Quantitative morphometry of perifoveal capillary networks in the human retina. Invest Ophthalmol Vis Sci. 2012;53(9):5502-14.
9. Tan PE, Yu PK, Balaratnasingam C, Cringle SJ, Morgan WH, McAllister IL, et al. Quantitative confocal imaging of the retinal microvasculature in the human retina. Invest Ophthalmol Vis Sci. 2012;53(9):5728-36.
10. Yu J, Gu R, Zong Y, Xu H, Wang X, Sun X, et al. Relationship Between Retinal Perfusion and Retinal Thickness in Healthy Subjects: An Optical Coherence Tomography Angiography Study. Invest Ophthalmol Vis Sci. 2016;57(9):OCT204-10.
11. Spaide RF, Fujimoto JG, Waheed NK. Image Artifacts in Optical Coherence Tomography Angiography. Retina. 2015;35(11):2163-80.
12. Hwang TS, Zhang M, Bhavsar K, Zhang X, Campbell JP, Lin P, et al. Visualization of 3 Distinct Retinal Plexuses by Projection-Resolved Optical Coherence Tomography Angiography in Diabetic Retinopathy. JAMA Ophthalmol. 2016;134(12):1411-9.
13. Campbell JP, Zhang M, Hwang TS, Bailey ST, Wilson DJ, Jia Y, et al. Detailed Vascular Anatomy of the Human Retina by Projection-Resolved Optical Coherence Tomography Angiography. Sci Rep. 2017;7:42201.
14. Lavia C, Bonnin S, Maule M, Erginay A, Tadayoni R, Gaudric A. Vessel Density of Superficial, Intermediate, and Deep Capillary Plexuses Using Optical Coherence Tomography Angiography. Retina. 2019;39(2):247-58.
15. Yu D-Y, Cringle SJ, Yu PK, Balaratnasingam C, Mehnert A, Sarunic MV, et al. Retinal capillary perfusion: Spatial and

- temporal heterogeneity. *Prog Retin Eye Res.* 2019;70:23 - 54.
16. Fouquet S, Vacca O, Sennlaub F, Paques M. The 3D Retinal Capillary Circulation in Pigs Reveals a Predominant Serial Organization. *Invest Ophthalmol Vis Sci.* 2017;58(13):5754-63.
  17. Bonnin S, Mane V, Couturier A, Julien M, Paques M, Tadayoni R, et al. New Insight into the Macular Deep Vascular Plexus Imaged by Optical Coherence Tomography Angiography. *Retina.* 2015;35(11):2347-52.
  18. Krawitz BD, Mo S, Geyman LS, Agemy SA, Scripsema NK, Garcia PM, et al. Acircularity index and axis ratio of the foveal avascular zone in diabetic eyes and healthy controls measured by optical coherence tomography angiography. *Vision Res.* 2017;139:177-86.
  19. Carpineto P, Mastropasqua R, Marchini G, Toto L, Di Nicola M, Di Antonio L. Reproducibility and repeatability of foveal avascular zone measurements in healthy subjects by optical coherence tomography angiography. *Br J Ophthalmol.* 2016;100(5):671-6.
  20. Corvi F, Pellegrini M, Erba S, Cozzi M, Staurengi G, Giani A. Reproducibility of vessel density, fractal dimension and foveal avascular zone using 7 different optical coherence tomography angiography devices. *Am J Ophthalmol.* 2017.
  21. Nesper PL, Fawzi AA. Human Parafoveal Capillary Vascular Anatomy and Connectivity Revealed by Optical Coherence Tomography Angiography. *Invest Ophth Vis Sci.* 2018;59(10):3858-67.
  22. Yu PK, Mammo Z, Balaratnasingam C, Yu DY. Quantitative Study of the Macular Microvasculature in Human Donor Eyes. *Invest Ophthalmol Vis Sci.* 2018;59(1):108-16.
  23. Pedinielli A, Bonnin S, Sanharawi ME, Mane V, Erginay A, Couturier A, et al. Three Different Optical Coherence Tomography Angiography Measurement Methods for Assessing Capillary Density Changes in Diabetic Retinopathy. *Ophthalmic Surg Lasers Imaging Retina.* 2017;48(5):378-84.
  24. Yu PK, Balaratnasingam C, Cringle SJ, McAllister IL, Provis J, Yu D-Y. Microstructure and network organization of the microvasculature in the human macula. *Invest Ophth Vis Sci.* 2010;51(12):6735 - 43.
  25. Anvari P, Najafi A, Mirshahi R, Sardarina M, Ashrafkhorasani M, Kazemi P, et al. Superficial and Deep Foveal Avascular Zone Area Measurement in Healthy Subjects Using Two Different Spectral Domain Optical Coherence Tomography Angiography Devices. *J Ophthalmic Vis Res.* 2020;15(4):517-23.
  26. Inanc M, Tekin K, Kiziltoprak H, Ozalkak S, Doguizi S, Aycan Z. Changes in Retinal Microcirculation Precede the Clinical Onset of Diabetic Retinopathy in Children With Type 1 Diabetes Mellitus. *Am J Ophthalmol.* 2019;207:37-44.
  27. Spaide RF, Klancnik JM, Jr., Cooney MJ, Yannuzzi LA, Balaratnasingam C, Dansingani KK, et al. Volume-Rendering Optical Coherence Tomography Angiography of Macular Telangiectasia Type 2. *Ophthalmology.* 2015;122(11):2261-9.
  28. Savastano MC, Lumbroso B, Rispoli M. In Vivo Characterization of Retinal Vascularization Morphology Using Optical Coherence Tomography Angiography. *Retina.* 2015;35(11):2196-203.
  29. Garrity ST, Paques M, Gaudric A, Freund KB, Sarraf D. Considerations in the Understanding of Venous Outflow in the Retinal Capillary Plexus. *Retina.* 2017;37(10):1809-12.
  30. Freund KB, Sarraf D, Leong BCS, Garrity ST, Vupparaboina KK, Dansingani KK. Association of Optical Coherence Tomography Angiography of Collaterals in Retinal Vein Occlusion With Major Venous Outflow Through the Deep Vascular Complex. *JAMA Ophthalmology.* 2018;136(11):1262 - 9.
  31. Pellegrini M, Cozzi M, Staurengi G, Corvi F. Comparison of wide field optical coherence tomography angiography with extended field imaging and fluorescein angiography in retinal vascular disorders. *PLoS One.* 2019;14(4):e0214892.
  32. De Pretto LR, Moulton EM, Alibhai AY, Carrasco-Zevallos OM, Chen S, Lee B, et al. Controlling for Artifacts in Widefield Optical Coherence Tomography Angiography Measurements of Non-Perfusion Area. *Sci Rep.* 2019;9(1):9096.
  33. Hirano T, Chanwimol K, Weichsel J, Tepelus T, Sadda S. Distinct Retinal Capillary Plexuses in Normal Eyes as Observed in Optical Coherence Tomography Angiography Axial Profile Analysis. *Sci Rep* 2018;8(1), 9380 (2018).
  34. Lavia C, Mece P, Nassisi M, Bonnin S, Marie-Louise J, Couturier A, et al. Retinal Capillary Plexus Pattern and Density from Fovea to Periphery Measured in Healthy Eyes with Swept-Source Optical Coherence Tomography Angiography. *Sci Rep.* 2020;10(1):1474.
  35. Niki T, Muraoka K, Shimizu K. Distribution of Capillary Nonperfusion in Early-stage Diabetic Retinopathy. *Ophthalmology.* 1984;91(12):1431-9.



## 4.2.

# VASCULAR AUTOREGULATORY FUNCTION OF THE RETINA

David Cordeiro Sousa<sup>\*1,2</sup>, Inês Leal<sup>1,2</sup>, Susana Moreira<sup>3</sup>, Sónia do Vale<sup>4,5</sup>, Ana S Silva-Herdade<sup>6</sup>, Patrício Aguiar<sup>7,8</sup>, Patrícia Dionísio<sup>3</sup>, Luís Abegão Pinto<sup>1,2</sup>, Miguel Castanho<sup>6</sup>, Carlos Marques-Neves<sup>1,2</sup>

1 - Ophthalmology Department, Hospital de Santa Maria, Centro Hospitalar Universitário Lisboa Norte, Av Prof. Egas Moniz, 1649-035, Lisboa, PT

2 - Vision Sciences Study Center, CECV, Faculdade de Medicina, Universidade de Lisboa, 1649-028, Lisboa, PT

3 - Respiratory Medicine Department, Hospital de Santa Maria, Centro Hospitalar Universitário Lisboa Norte, 1649-035, Lisboa, PT

4 - Endocrinology Department, Hospital de Santa Maria, Centro Hospitalar Universitário Lisboa Norte, 1649-035, Lisboa, PT

5 - Endocrinology Department, Faculdade de Medicina, Universidade de Lisboa, 1649-028, Lisboa, PT

6 - Instituto de Bioquímica, Instituto de Medicina Molecular, Faculdade de Medicina, Universidade de Lisboa, 1649-028, Lisboa, PT

7 - Medicine I Department, Centro Hospitalar Universitário Lisboa Norte, Av Prof. Egas Moniz, 1649-035, Lisboa, PT

8 - Clínica Universitária de Medicina I, Faculty of Medicine, University of Lisbon, Lisboa, PT

## 1. INTRODUCTION

### • Anatomy and Physiology

The retina is the highest oxygen consumer by weight in the human body. Therefore, a dedicated and efficient vascular network is needed to meet its demand.<sup>1</sup> In the macula, the retinal vascular network is elegantly organized in three levels: i) superficial capillary plexus (SCP), ii) intermediate capillary plexus (ICP), and iii) deep capillary plexus (Figure 1). The ICP and DCP are usually collectively named as the deep vascular complex (DVC).<sup>2</sup> Although their structure is well-defined, the blood flow dynamics in the macula remains to be completely understood. Previous studies found that retinal venules are found deeper than arterioles, and that direct arterial supply is only found in the SCP and ICP, with the DCP receiving supply only from the overlying plexus. Recent imaging studies suggested the existence of both parallel (i.e. within the same plexus) and in series (i.e. from the superficial to the deep plexuses) circulations, with predominance of the latter (Figure 1).<sup>3,4</sup>

### • Retinal Vascular Autoregulation

Autoregulation is defined as the ability to maintain an appropriate blood flow over a range of scenarios to ensure adequate supply according to the metabolic demand. Retinal vascular autoregulation corresponds to a change in vascular resistance in order to maintain an adequate blood flow in a wide range of conditions.<sup>6,7</sup> Given that the retinal vessels are not innervated, these autoregulatory mechanisms are achieved mainly through local factors. These include both a metabolic and

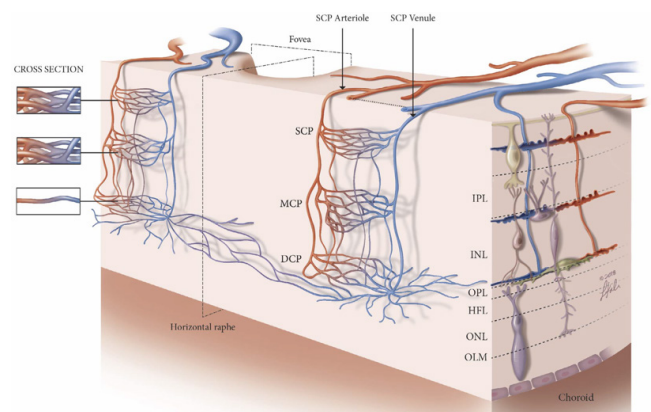


**Figure 1.** Schematic depiction of the retinal circulation and the in-series and parallel macular blood flow.

GCL, ganglion cell layer; HFL, Henle fiber layer; INL, inner nuclear layer; IPL, inner plexiform layer; OLM, outer limiting membrane; ONL, outer nuclear layer; SCP, superficial capillary plexus; MCP, intermediate (middle) capillary plexus; DCP, deep capillary plexus. Adapted from (5) under the terms of a Creative Commons Attribution 4.0 International License

myogenic component. The metabolic factors in play are released by glial, neural or endothelial cells, and can be both tone relaxing (e.g. nitric oxide and prostacyclin) or tone contracting (e.g. endothelin-1, angiotensin II). The myogenic response corresponds to an endothelial response to sensed mechanical forces.<sup>8</sup>

The retinal and cerebral blood flow are not only regulated in response to changes in perfusion pressure, but also dependent on local neural activity – a concept termed as *neurovascular coupling*. In this process, neural feedforward mechanisms contribute for an adequate

supply of nutrients and oxygen to match the demands of active neurons.<sup>9</sup> Interestingly, this response appears to be relatively independent of changes in the perfusion pressure or vascular resistance.<sup>10</sup>

### • Retinal Vasculature Imaging

For structural analysis, a revolution in retinal imaging was the development of the optical coherence tomography (OCT). An extension of OCT, optical coherence tomography angiography (OCTA) provides non-invasive high-resolution depth-resolved images of the retinal microvasculature.<sup>11</sup> This technology depicts with unprecedented detail the retinal capillaries by measuring the amplitude and delay of reflected or backscattered light from moving erythrocytes. It does so by performing multiple B-scans at the same location and detecting motion contrast produced by moving blood cells in the retinal vessels. Since no motion in the retina other than blood flow is expected, stationary objects won't produce much of a change from one image to the next, while moving objects will. By looking at change over time, the final image defines the retinal microvasculature, with the vessels depicted as white pixels on a black background.<sup>11</sup> The dynamic study of retinal vessels behaviour is important to better understand the retinal autoregulatory function, in both health and disease. A number of non-invasive methods have been used for ocular vessels' assessment, including laser Doppler flowmetry, colour Doppler imaging, and laser speckle flowgraphy. However, these techniques are not widely used in clinic, being mostly limited to research purposes.<sup>12</sup> Table 1 summarizes the characteristics, advantages and limitations of various methods.

## 2. A PROTOCOL TO STUDY RETINAL VASCULAR REACTIVITY USING OPTICAL COHERENCE TOMOGRAPHY ANGIOGRAPHY

In 2019, our group published a protocol for the use of OCTA to study retinal vascular responses of both vasodilation and vasoconstriction in a healthy population.<sup>14</sup> For this purpose, as detailed in the manuscript, we used two standardized stress tests, in brief:

- i) *Hypoxia Challenge Test (HCT)*. The HCT, whose protocol is standardized by the British Thoracic Society<sup>15</sup>, consists in a mild hypoxic stimulus performed to people with respiratory disease in order to evaluate their susceptibility to hypoxic environments, such as a long-haul flight. The effects of lower levels of partial pressure of arterial oxygen (PaO<sub>2</sub>) on retinal vessels are similar to the brain vasculature, with hypoxia triggering *vasodilation*.<sup>16</sup>
- ii) *Handgrip Test*. The handgrip manoeuvre is an isometric exercise that induces a sympathetomimetic response with increases in heart rate and arterial pressure. It induces an retinal autoregulatory response of *vasoconstriction* that keeps the blood flow unchanged until the ocular perfusion pressure increases above 35-40% compared to baseline.<sup>17</sup>

The OCTA was performed at baseline conditions and during the stress test. During the hypoxic stimulus, the mean parafoveal vessel density increased significantly in both the superficial and deep plexuses. The vasodilatory response and retinal blood flow increase in response to decreased arterial oxygen values are a physiologic response, and OCTA was able to reliably confirm it.

**Table 1.** Techniques for in vivo study of ocular hemodynamics.

Technique	Measurements	Advantages	Limitations
<i>Laser Doppler Flowmetry</i>	Velocity, Volume and Flow in arbitrary units	Multiple hemodynamic parameters	No absolute measurements and limited interindividual comparisons
<i>Colour Doppler Imaging</i>	Velocity	Vessel selective, no need for clear media	Velocity measurements only, operator-dependent
<i>Laser speckle flowgraphy</i>	Velocity and Flow in arbitrary units	Time evolution of velocity at the same site of the same eye	No absolute measurements and limited interindividual comparisons
<i>OCT Angiography</i>	Flow in arbitrary units	Fast, high-quality images	No absolute measurements, motion/projection artifacts

OCT: optical coherence tomography. Adapted from Prada et al<sup>13</sup>

Although this protocol uses a single mildly hypoxic stimulus, it has been estimated a lower PaO<sub>2</sub> threshold of 32-37 mmHg, until when the retinal arteriolar and venular dilation is able to compensate so that oxygen delivery is maintained constant.<sup>16</sup>

For the handgrip test, a vasoconstrictive autoregulatory response was demonstrated, with the corresponding decrease in vessel density in both the superficial and deep retinal plexuses. In order to maintain the retinal blood flow constant, retinal vasoconstriction constitutes a protective mechanism of autoregulation to ensure the blood flow remains largely unchanged until the mean ocular perfusion pressure increases by an average of 34-60%. The response to increases in blood pressure is triggered not only by local metabolites, but also as a myogenic response to the increase in the intraluminal vascular pressure – *Bayliss effect*.<sup>17</sup>

Recently, a few other groups have been publishing studies using OCTA with the purpose of evaluating retinal vascular responses. For instance, Nesper and Fawzi used dark adaptation, transition from dark to light, and flicker stimulation as stimuli to assess retinal microvascular reactivity.<sup>6</sup> They found the expected increase in vessel density in the superficial plexus during ambient light and flicker stimulation. But interestingly, in the transition from dark to light the vessel density of the deeper plexus was decreased. The authors suggest that the deep plexus is maximally dilated during dark adaptation, constricting after the transition to light to allow for the blood to be redirected to the more superficial layers. The ability to depth-resolve the maximal dilation of the deep plexus may have important implications in pathologic conditions, in which deep capillary loss may be associated with photoreceptor disruption.<sup>18</sup> These results confirm the distinct neurovascular control mechanisms for each plexus and the uniqueness of OCTA in the ability to study them independently.<sup>3</sup>

### 3. RETINAL VASCULAR REACTIVITY IN TYPE 1 DIABETES PATIENTS WITHOUT RETINOPATHY

The endothelial cells and pericytes, which are affected early in the pathogenesis of diabetic retinopathy (DR), are main regulators of retinal vascular contractile status and responsible for an appropriate vascular autoregulation.<sup>8</sup> In cases of shortage of oxygen or nutrients, the inability to adapt the supply to match the demand may lead to tissue hypoxia and permanent damage.<sup>7</sup> Similarly, in response to situations of hyperperfusion, the failure of autoregulatory mechanisms may be responsible for the formation of reactive oxygen species and cell death.

We applied the above-described OCTA protocol to dynamically assess retinal vascular responses in healthy subjects and patients with type 1 diabetes and no clinical evidence of DR.<sup>19</sup> Two tests - hypoxia and isometric exercise - in order to evaluate eventual changes in the vasodilatory or vasoconstrictive retinal autoregulatory responses (Figures 2-3).

Contrary to the healthy subjects, in the diabetic group

the physiological autoregulatory response to hypoxia (i.e., vasodilation) was not observed neither in the superficial, nor in the deep retinal plexuses—Table 2. During isometric exercise, the expected vasoconstrictive retinal response was observed in both plexuses in the control group but only detected in the deep plexus of the patients with diabetes—Table 3.

These results corroborate previous findings of pre-clinical changes in patients with diabetes, not only on the retinal vascular network, but also of retinal function such as with decreased dark adaptation, reduced light sensitivity, hue discrimination, contrast sensitivity, microperimetry defects, and electroretinogram changes.<sup>20,21</sup> The reported functional abnormalities in patients with early or no DR suggest that not only the retinal vascular component is affected, but rather the whole system of neural, glial, and vascular elements that form the neurovascular unit.

Strikingly, in the diabetic cohort, the autoregulatory retinal vasoconstriction in response to the handgrip was preserved in the DCP, although in a lesser magnitude. It is known that it is in the outer retinal layers that the oxygen consumption is higher, that the DCP might have to supply the photoreceptors in high-activity conditions (such as dark environments), and that the retinal capillary plexuses autoregulate independently.<sup>6,7</sup> We hypothesize that the capacity for retinal autoregulation might be preserved in the DCP until later stages, in order to maintain an adequate supply of oxygen and nutrients to the energy-demanding outer retinal layers.

These data highlight the ability of OCTA to document the impaired autoregulatory retinal vascular responses in patients with diabetes before any clinical feature of DR were evident. The identified regional abnormalities in vascular autoregulation suggest there is an important role for retinal imaging to sensitively identify these early changes.

### 4. OCTA - ADVANTAGES & LIMITATIONS

All imaging methods have advantages and limitations, and OCTA is no exception.

As advantages, OCTA does not require any dye and is able to depth-resolve the retinal microvascular plexuses with impressive resolution. It provides quantitative data to be used as potential biomarkers in health and disease. It is a fast and safe exam and can be repeated in short periods of time for the same subject to assess microvascular responses to functional stimulation.<sup>11</sup>

However, OCTA has important limitations. Firstly, the quantification of OCTA metrics may be biased by interindividual factors, such as age and systemic vascular risk. The inexistence of normative databases for vessel density, foveal avascular zone and other OCTA parameters limits the possibility of classifying a single measurement as normal or abnormal. Therefore, one of the advantages of this innovative concept of using OCTA for dynamic retinal vascular analysis is the ability to study an individual functional responses and not a



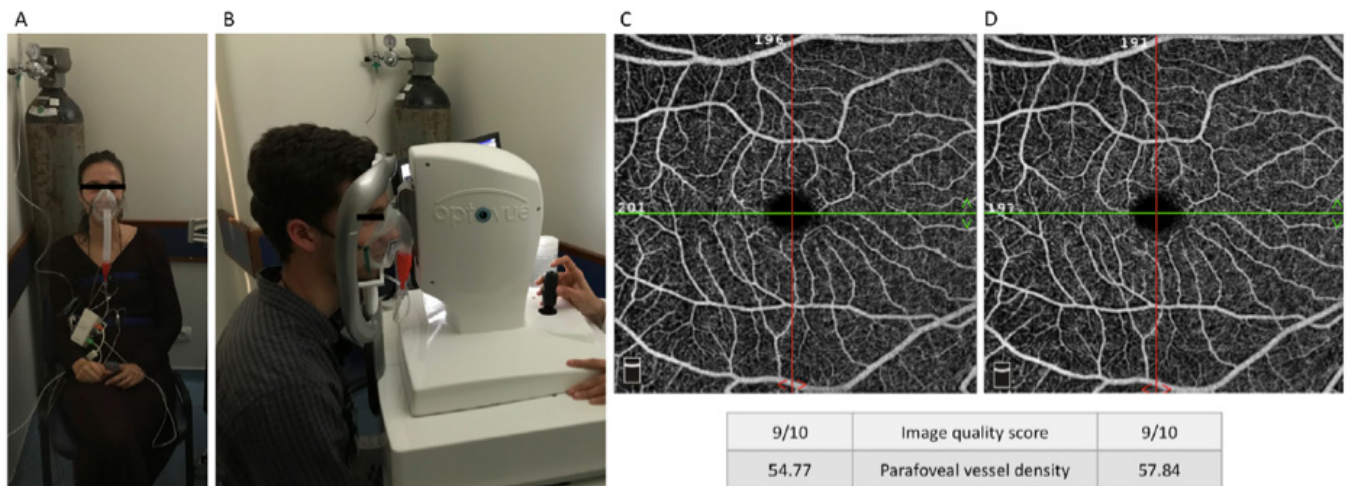


**Figure 2.** Exemplar of the setup during the hypoxia challenge test and OCT-angiography examination (A, B) and macular en-face 6x6 mm angiograms obtained in baseline conditions (C) and during hypoxia (D). Image quality score and vessel density are provided by the built-in angioanalytics® software.

**Table 2.** Retinal Vascular response to the Hypoxia Challenge Test

Parafoveal Vessel Density, Median (IQR)	Control	P Value	Type 1 Diabetes	P Value
Superficial plexus				
Baseline	55.1 (53.1–56.4)	—	53.1 (48.9–55.1)	—
Hypoxia	56.5 (54.0–57.6)	<0.001	52.0 (50.0 - 54.2)	0.81
Deep plexus				
Baseline	60.4 (59.3 - 61.8)	—	57.2 (53.3 - 60.0)	—
Hypoxia	62.0 (59.9 - 62.8)	< 0.001	56.2 (54.4 - 57.9)	0.31

P values (versus baseline) obtained with ANOVA repeated measures. IQR, interquartile range.

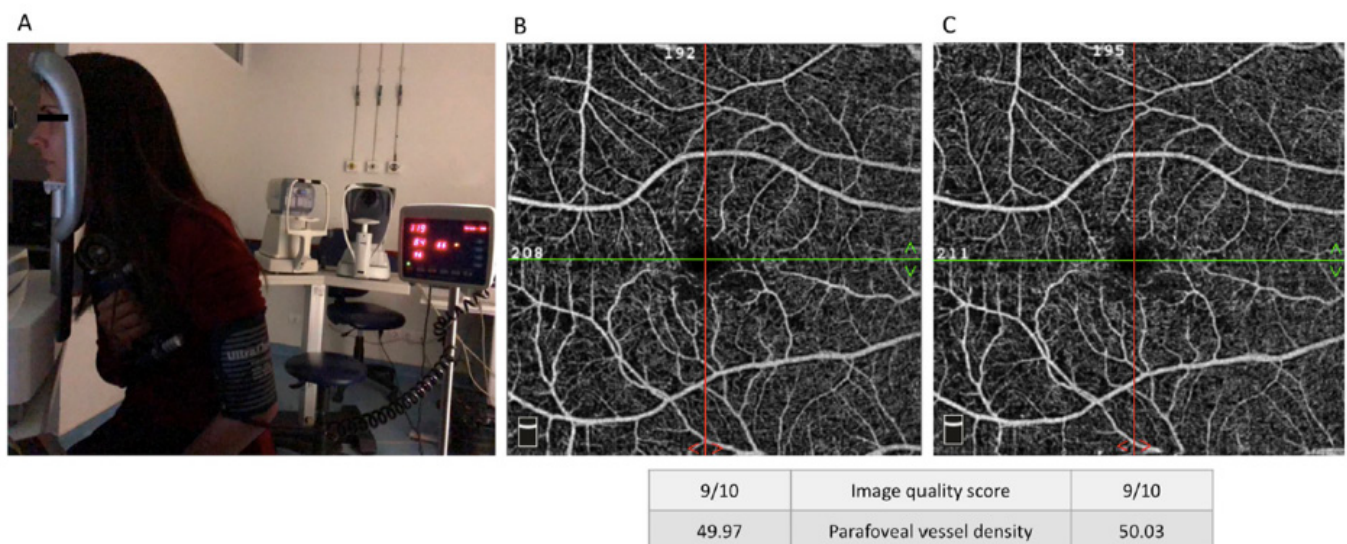


**Figure 3.** Exemplar of the setup during the handgrip test and OCT-angiography examination (A, B) and macular en-face 6x6 mm angiograms obtained in baseline conditions (C) and during the Handgrip manoeuvre (D). The angiograms belong to a volunteer with type 1 diabetes – the physiological decrease in vessel density with isometric exercise was not observed. Image quality score and vessel density are provided by the built-in angioanalytics® software.

**Table 3.** Retinal Vascular response to the Handgrip Test

Parafoveal Vessel Density, Median (IQR)	Control	P Value	Type 1 Diabetes	P Value
Superficial plexus				
Baseline	55.8 (53.5–56.9)	—	53.5 (51.1–55.4)	—
Handgrip	54.1 (52.2–54.5)	<0.0001	52.8 (48.7–54.8)	0.06
Deep plexus				
Baseline	60.4 (58.7–61.2)	—	58.5 (54.1–60.3)	—
Handgrip	57.1 (53.7–58.6)	<0.0001	55.9 (52.5–60.3)	<0.01

P values (versus baseline) obtained with ANOVA repeated measures. IQR, interquartile range.

single structural exam. The *functional* response is likely more accurate to identify of what is normal or abnormal than a cross-sectional quantitative metric.<sup>11</sup> Secondly, there are limitations inherent to the technology, such as the influence of confounding factors in the metrics. For instance, the axial length affects the magnification of the OCTA images as well as the vessel density and FAZ measurements.<sup>22</sup> Thirdly, OCTA technology is not optimized for functional analyses and blood flow metrics. Current methods and technology measure *perfused vessel densities* and not absolute blood flow. And lastly, the OCTA scans may have associated artifacts (e.g. motion, projection) and an understanding of the technology and careful interpretation of the outputs is crucial.<sup>11</sup>

## 5. FUTURE PERSPECTIVES

The use of OCTA technology to assess retinal vascular reactivity is a stepping-stone for several future studies and is tremendously exciting as the applications of OCTA extend well beyond diabetes and ophthalmology.<sup>23</sup> Also, other technologies are emerging to assess blood flow using OCT. One of the most promising is Doppler-OCT, which allows to measure total blood flow. However, accurate quantification remains challenging, with current systems being limited in the maximum velocities measurable, small vessels assessment, and the geometry of the vessel (i.e. the Doppler angle). As a very recent imaging technology, most of OCTA studies are cross-sectional. In DR in particular, future longitudinal studies will allow for a better characterization of the relationship between structural and functional changes and the severity of the disease. And lastly, the incorporation of artificial intelligence in OCTA imaging is promising in the diagnosis and follow-up of multiple conditions.<sup>24</sup> We hope that the ever-increasing interest in OCTA metrics could also serve as encouragement for the development of methods to overcome some of its limitations and for dynamically assessing vascular responses.

## REFERENCES

1. Wong-Riley M. Energy metabolism of the visual system. *Eye Brain*. 2010;2:99-116.
2. Campbell JP, Zhang M, Hwang TS, et al. Detailed Vascular Anatomy of the Human Retina by Projection-Resolved Optical Coherence Tomography Angiography. *Sci Rep*. 2017;7:1–11.
3. An D, Yu P, Freund KB, et al. Three-Dimensional characterization of the normal human parafoveal microvasculature using structural criteria and high-resolution confocal microscopy. *Invest Ophthalmol Vis Sci*. 2020;61(10):3.
4. Cabral D, Pereira T, Ledesma-Gil G, et al. Volume rendering of dense B-scan optical coherence tomography angiography to evaluate the connectivity of macular blood flow. *Investig Ophthalmol Vis Sci*. 2020;61(6):1–3.
5. Nesper PL, Fawzi AA. Human parafoveal capillary vascular anatomy and connectivity revealed by optical coherence tomography angiography. *Investig Ophthalmol Vis Sci*. 2018;59(10):3858–67.
6. Nesper PL, Lee HE, Fayed AE, et al. Hemodynamic response of the three macular capillary plexuses in dark adaptation and flicker stimulation using optical coherence tomography angiography. *Investig Ophthalmol Vis Sci*. 2019;60(2):694–703.
7. Linsenmeier RA, Zhang HF. Retinal oxygen: from animals to humans. *Prog Retin Eye Res*. 2017;58:115–51.
8. Pournaras CJ, Rungger-Brändle E, Riva CE, et al. Regulation of retinal blood flow in health and disease. Vol. 27, *Prog Retin Eye Res*. 2008;27(3):284-330. 2008. p. 284–330.
9. Gerhard G, Chua J, Tan B, et al. Retinal Neurovascular Coupling in Diabetes. *J Clin Med*. 2020;1;9(9):2829..
10. Riva CE, Falsini B, Logean E. Flicker-evoked responses of human optic nerve head blood flow: Luminance versus chromatic modulation. *Investig Ophthalmol Vis Sci*. 2001;42(3):756–62.
11. Spaide RF, Fujimoto JG, Waheed NK, et al. Optical coherence tomography angiography. *Prog Retin Eye Res*. 2018;64:1–55.
12. Wei X, Balne PK, Meissner KE, et al. Assessment of flow dynamics in retinal and choroidal microcirculation. *Surv Ophthalmol*. 2018;63(5):646-664.
13. Prada D, Harris A, Guidoboni G, et al. Autoregulation and neurovascular coupling in the optic nerve head. *Surv Ophthalmol*. 2016;61(2):164–86.

14. Sousa DC, Leal I, Moreira S, et al. A protocol to evaluate retinal vascular response using optical coherence tomography angiography. *Front Neurosci.* 2019;13:566.
15. Ahmedzai S, Balfour-Lynn IM, et al. Managing passengers with respiratory disease planning air travel: British Thoracic Society recommendations. *Thorax.* 2002 Sep 1;57(4):289–304.
16. Cheng RW, Yusof F, Tsui E, et al. Relationship between retinal blood flow and arterial oxygen. *J Physiol.* 2016;594(3):625–40.
17. Blum M, Bachmann K, Wintzer D, et al. Noninvasive measurement of the Bayliss effect in retinal autoregulation. *Graefes Arch Clin Exp Ophthalmol.* 1999;237(4):296–300.
18. Nesper PL, Scarinci F, Fawzi AA. Adaptive Optics Reveals Photoreceptor Abnormalities in Diabetic Macular Ischemia. *PLoS One.* 2017;12(1):e0169926.
19. Sousa DC, Leal I, Moreira S, et al. Retinal Vascular Reactivity in Type 1 Diabetes Patients Without Retinopathy Using Optical Coherence Tomography Angiography. *Invest Ophthalmol Vis Sci.* 2020 Jun;61(6):49.
20. Sacconi R, Casaluci M, Borrelli E, et al. Multimodal Imaging Assessment of Vascular and Neurodegenerative Retinal Alterations in Type 1 Diabetic Patients without Fundoscopic Signs of Diabetic Retinopathy. *J Clin Med.* 2019;8(9):1409.
21. McAnany JJ, Park JC. Reduced Contrast Sensitivity is Associated With Elevated Equivalent Intrinsic Noise in Type 2 Diabetics Who Have Mild or No Retinopathy. *Invest Ophthalmol Vis Sci.* 2018 May;59(6):2652–8.
22. Llanas S, Linderman RE, Chen FK, Carroll J. Assessing the Use of Incorrectly Scaled Optical Coherence Tomography Angiography Images in Peer-Reviewed Studies: A Systematic Review. *JAMA Ophthalmol.* 2019
23. Pellegrini M, Vagge A, Ferro Desideri LF, et al. Optical Coherence Tomography Angiography in Neurodegenerative Disorders. *J Clin Med.* 2020;9(6).
24. Gunasekeran D V, Ting DSW, Tan GSW, Wong TY. Artificial intelligence for diabetic retinopathy screening, prediction and management. *Curr Opin Ophthalmol.* 2020;31(5):357–65.

# 5. THE CHOROID



## 5.1.

# MIDDLE AND OUTER CHOROID

Lilianne Duarte, Jeniffer Jesus, Maria João Matias  
Centro Hospitalar de Entre o Douro e o Vouga

The choroid is a part of the uveal tract of the eye. It is an extensive vascular network involved by connective tissue that goes from the *ora serrata* up to the optic nerve and lies between the sclera and the retina.

It is supplied by ciliary arteries derived from the first branch of the internal carotid artery that pierce the sclera more anteriorly by the long posterior ciliary arteries and peripapillary by the short posterior ciliary arteries, until the choriocapillaris. The venous drainage is made by the vortex vein system that ultimately drain to the superior and inferior ophthalmic veins.

The enervation has parasympathetic and sympathetic nerves, but only the latter has an autoregulatory influence in the choroidal blood flow.

The choroid has a very specific anatomic architecture. Histologically, it is divided in four layers: the Bruch's membrane, the choriocapillaris, the stroma and the suprachoroid (Figure 1).

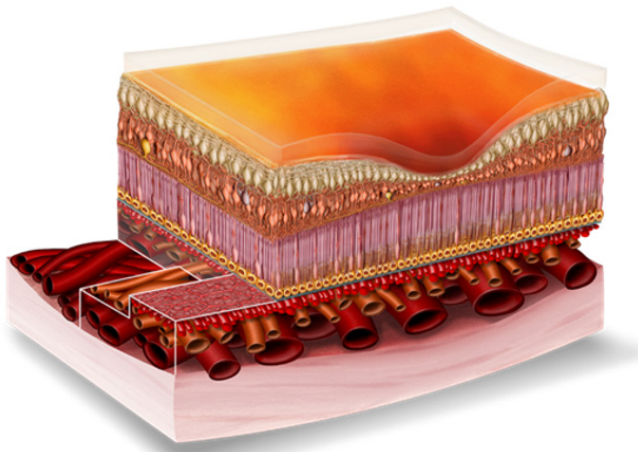


**Figure 1.** Choriocapillaris, Sattler and Haller's layers. Source: Lilianne Duarte et al: *Choroidal thickness and morphology analysis by optical coherence tomography as a method to approach diabetic ocular disease prognosis and progression.* <http://hdl.handle.net/10550/69543>. Design copyright Jirehdesign.com licensed to Lilianne Duarte.

The Bruch's membrane separates the retinal pigmented epithelium (RPE) from the choriocapillaris.

The choriocapillaris will be detailed on the next chapter.

The stroma is composed of larger vessels than those found on the choriocapillaris. The vessel diameter increases from the choriocapillaris to the posterior or scleral side. Involving the vessels there is connective tissue, melanocytes, nerve fibers, fibroblasts and non-vascular smooth muscle, macrophages, lymphocytes, plasma and mast cells. The stroma is divided in the medium diameter vessel layer or Sattler's layer, and the large vessel layer or the Haller's layer. The vessels of the stroma are not fenestrated or organized in lobules, they are rather intertwined and, especially in the Haller's layer, the arteries are similar to those elsewhere with contractile ability due to the presence of internal elastic lamina and smooth muscle. They do not leak. The vessel system is supported by the involving tissue and cells, and it was suggested that the non-vascular smooth muscle and fibroblasts plays a role in the choroidal thickness changes occurring in physiologic states as on retinal defocus.

The suprachoroid, an avascular layer, separates the Haller's layer from the lamina fusca.

It is important to know the anatomy of the choroid to better interpret OCT images. The physiological role of the choroid is highly related to its blood flow. It is responsible for the major supply of oxygen and nutrients to the outer retina with particular influence on the metabolic processes of the photoreceptors and light absorption due to its rich melanocytes content; it has a retinal thermoregulation role; it is important in the immunologic response of the eye since it works as a provider of mast and inflammatory cells to the eye and a barrier for certain kind of molecules; and it is responsible for about 35% of the humor aqueous drainage with a role in the ocular pressure control.

Choroidal and retinal disorders are intimately related due to the high dependence of the normal outer retina function to choroidal blood flow supply.

Since it is a highly vascular structure with elevated blood flow speed, it is also susceptible to systemic changes. Systemic diseases affecting vascular system or spread by blood can affect both the choroid and the retina. A malfunction of the choroid will have a strong effect on the outer retina and photoreceptor metabolism. Until now it is not clear if the choroid might have an autoregulation mechanism, but the choroid may react in response to retinal pathology, as a response to an

increased or decreased need for nutrition or metabolic input of retinal cells, or to the excessive retinal metabolic products to be expelled to blood circulation.<sup>1,2</sup>

Advances in OCT technology have facilitated choroidal imaging with longer wavelengths, namely the standard OCT with Enhanced Depth Imaging (EDI) or with Swept-source, which had improved in-depth imaging allowing good penetration at the RPE and visualization of the choroidal/scleral interface. However, definite separation of choroidal layers is not ever possible, as it can be affected by age or pathologic changes.<sup>3</sup> OCT Angiography (OCT-A) has brought new perspectives in choroidal analysis. Combining analysis obtained with Standard OCT such as Choroidal thickness, Choroidal layers segmentation, Choroidal volume, Choroidal vascularity, *En-face* or coronal layer views, OCT-A allows detailed visualization of the microvasculature and somehow flow features.

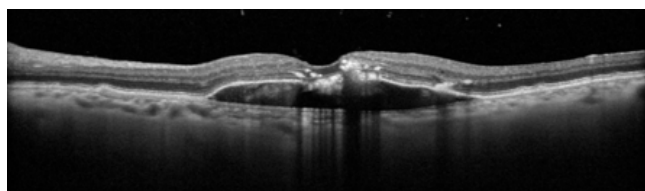


**Figure 2.** EDI-OCT showing areas of affected choroidal visualization due to anterior signal block.

Despite technological development, choroidal visualization may be affected by poor in-depth imaging, signal attenuation by the RPE block, projection artifacts (Figure 2), even with software correction improvements. To segment choroidal layers in the OCT/OCT-A images, it is commonly accepted to consider the choriocapillaris from the Bruch's 10-20  $\mu\text{m}$  thickness slab below, the Sattler's layer with a 30-40  $\mu\text{m}$  thickness, and below the Haller's layer.<sup>5,6</sup> As manual segmentation is time-consuming and subjective, several algorithms were developed for automatically determined Haller's and Sattler's segmentation, helping to interpret the images when data signal is weak.<sup>7,8</sup> But with high variability of choroidal and layers thickness either within normal or from pathologic changes, limits the standardization of layer's depth.

### THE SATTLE'S LAYER ON OCT-ANGIOGRAPHY

On OCT-A B-scans, Sattler layer can be identified as the layer below ( $\pm 20 \mu\text{m}$ ) the mosque layer immediately below the Bruch's membrane (choriocapillaris), with a 30  $\mu\text{m}$  thickness (Figure 3), with alternate hyper and hypo-reflective structures, larger than the layer above. When visualizing the *En-face* or C-scans a greyish sinuous structure with thin hypo-reflective spaces.

### THE HALLER'S LAYER ON OCT-ANGIOGRAPHY

On B-scans the large vessels of this layer are visualized

as large round or oval hyporeflective spaces surrounded by thinnest greyish lines or mesh (Figure 4). On *En-face* images larger hyporeflective and sinuous structures become predominant than the greyish mesh.

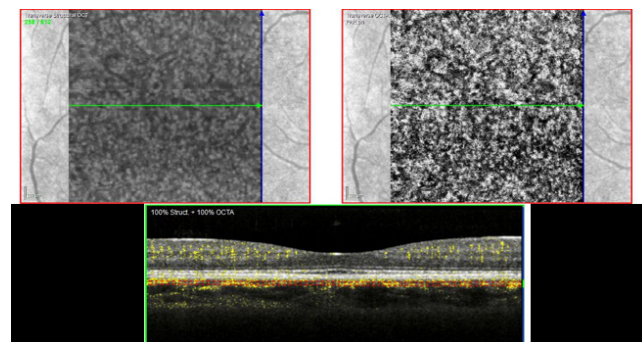


**Figure 3.** *En face* OCT-A image and horizontal B-scan of their layer segmentation of a healthy individual. The OCT angiogram of the Sattler's layer was segmented within a thin 30  $\mu\text{m}$  slab below the Bruch membrane (red dotted-line).

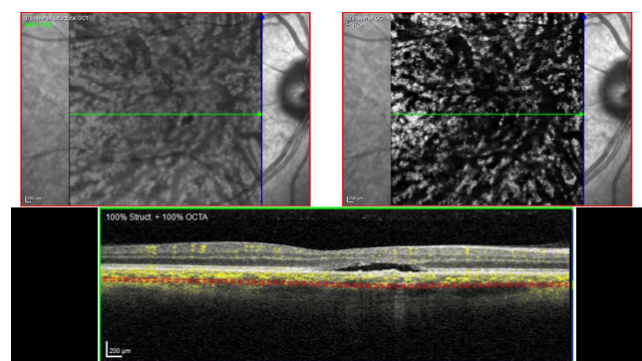


**Figure 4.** *En face* OCT-A image and horizontal B-scan of their layer segmentation of a healthy individual. The OCT angiogram of the Haller's layer was segmented below the Sattler's Layer (red dotted-line).

## VASCULAR QUANTITATIVE ANALYSIS

OCT-A images allowed the analysis of Choroidal Vascularity (choroidal vascular index (CVI) and choroidal vascular density (CVD).

CVI is measured using binarized OCT B-scans (Figure 5) where anterior and posterior boundaries of the choroid are marked to get the total choroidal area (TCA). Black spaces are identified as the luminal choroidal area (LCA), and CVI is calculated as the proportion of LCA from the TCA.<sup>9,10</sup>

CVD is measured using binarized *en-face* OCT-A images. Black areas are considered as vessels and white areas as stroma (Figure 6). The CVD is calculated as the proportion of black pixels from the total pixels in a image.<sup>11,12</sup> Limitations are related to dependence of OCT-A flow speed, so greater variations on flow can affect vascular imaging. The position of the slab analysis can vary, from studies, but also depending on individual

variability layers thickness, making difficult to establish a fixed threshold depth slab.

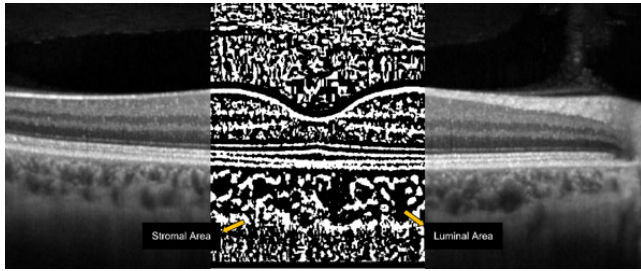


**Figure 5.** EDI-OCT image and converted binary image of fovea using ImageJ Software. Binarization was made with Niblack auto local threshold method. The white pixels were accepted as the stromal area, and the dark pixels were accepted as the luminal area.

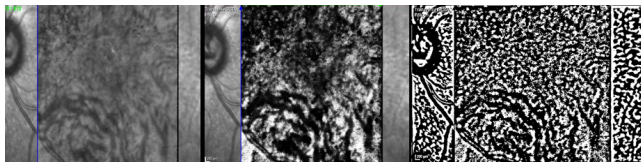


**Figure 6.** OCT-A image of a choroidal slab and converted binary image using ImageJ Software. Binarization was made with Niblack auto local threshold method. The white pixels were accepted as the stromal area, and the dark pixels were accepted as the luminal area.

## FLOW ANALYSIS

Actual commercially available OCT/OCT-A devices only allow a color-coded flow information as flow or no flow, without quantification software analysis.<sup>13</sup> Middle and outer choroid appears in an inverted code of that from choriocapillaris and retinal vessels, where vessels appear as no colored.

Investigative methods to quantify and map flow as the Variable Interscan Time Analysis (VISTA)<sup>13</sup> were described but still have some limitations of inability of dynamic information such as leakage obtained with the standard dye angiographies.

Some publications regarding choroidal flow results are in fact CVI or CVD analysis, since real flow data refers to a dynamic process requiring temporal resolution that OCT-A is still unable to evaluate.

Pathological features will be approached in specific chapters ahead.

## REFERENCES

1. Nickla DL, Wallman J. The multifunctional choroid. *Prog Retin Eye Res.* 2010;29(2):144-168.
2. Gonçalves Duarte L, Dolores Pinazo-Duran M, Salgado-Borges J, Gallego-Pinazo R. Choroidal thickness and morphology analysed by optical coherence tomography as a method to approach diabetic ocular disease prognosis and progression doctoral thesis.; 2018. <https://roderic.uv.es/handle/10550/69543>. Accessed may 24, 2021.
3. McLeod DS, Luttj G. High-Resolution Histologic Analysis Of The Human Choroidal Vasculature. *Investig Ophthalmol Vis Sci.* 1994;35(11):3799-3811. File:///C:/Users/Lilianne/Downloads/3799.Pdf. Accessed July 3, 2017.
4. Duarte L, Ruão M, Gallego R. Focal Choroidal Changes On Diabetic Macular Edema. *Acta Ophthalmol.* 2015;93(S255):N/A-N/A.
5. Coscas G, Lupidi M, Coscas Paris F, Authors Gabriel Coscas P, Coscas F. Atlas Oct-angiography in amd 1 atlas: oct-angiography in amd comparison with multimodal imaging optical coherence tomography angiography in age-related macular degeneration atlas of oct-angiography in exudative amd.
6. Greig EC, Duker JS, Waheed NK. A practical guide to optical coherence tomography angiography interpretation. *Int J Retin Vitreol.* 2020;6(1):1-17.
7. Esmacelpour M, Kajić V, Zabihian B, et al. Choroidal Haller's and Sattler's layer thickness measurement using 3-dimensional 1060-nm optical coherence tomography. *PLoS One.* 2014;9(6):e99690.
8. Kajić V, Esmacelpour M, Glittenberg C, et al. Automated three-dimensional choroidal vessel segmentation of 3D 1060 nm OCT retinal data. *Biomed Opt Express.* 2013;4(1):134.
9. Agrawal R, Salman M, Tan KA, et al. Choroidal vascularity index (CVI) - A novel optical coherence tomography parameter for monitoring patients with panuveitis? *PLoS One.* 2016; 11;11(1):e0146344.
10. Iovino C, Pellegrini M, Bernabei F, et al. Choroidal Vascularity Index: An In-Depth Analysis of This Novel Optical Coherence Tomography Parameter. *J Clin Med.* 2020;9(2):595.
11. Wang E, Zhao X, Yang J, Chen Y. Visualization of deep choroidal vasculatures and measurement of choroidal vascular density: a swept-source optical coherence tomography angiography approach. *BMC Ophthalmol.* 2020;20(1):1-9.
12. Wang JC, Láíns I, Silverman RF, et al. Visualization of choriocapillaris and choroidal vasculature in healthy eyes with en face swept-source optical coherence tomography versus angiography. *Transl Vis Sci Technol.* 2018;7(6).
13. Arya M, Rashad R, Sorour O, Moulton EM, Fujimoto JG, Waheed NK. Optical coherence tomography angiography (OCTA) flow speed mapping technology for retinal diseases. *Expert Rev Med Devices.* 2018;15(12):875-882.





## 5.2.

# THE CHORIOCAPILLARIS

António Campos

Department of Ophthalmology, Centro Hospitalar Leiria E. P. E., Leiria, Portugal

ciTechCare, Center for Innovative Care and Health Technology, Polytechnic Institute of Leiria, Leiria, Portugal

## INTRODUCTION

The medium-sized arteries of the Sattler's layer give rise at a right angle after a short trajectory to the patch-like structure of the choriocapillaris (CC) (Figure 1)<sup>1,2</sup>. The CC is a single-layered network of fine flattened fenestrated channels about 10-20  $\mu\text{m}$  thick at the fovea, thinning to about 8  $\mu\text{m}$  at the periphery, originating from end-arteries, arranged in a lobular hexagonal pattern<sup>3,4</sup>. The lobules of the CC are smaller and more densely packed in the submacular region (200-350  $\mu\text{m}$  in diameter), making the capillaries of the CC more numerous at this area<sup>5</sup>. The CC lobules illustrate a characteristic patchy lobular filling pattern with fluorescein angiography (FA). Each piece of the jig-saw pattern has a well-defined margin which forms the watershed zones. A watershed zone is the border between the territories of distribution of any two end-arteries and is most vulnerable to ischemia<sup>6</sup>.

At the level of the outer CC, columns of collagen fibers run between the capillaries and attach to the outer fibrous layer of the Bruch's membrane (BM), probably supporting the capillaries network. The BM is a five layered structure 2-4  $\mu\text{m}$  thick, comprehending the basement membrane of the CC, an outer collagenous zone, an elastic layer, an inner collagenous zone, and the basement membrane of the retinal pigment epithelium (RPE)<sup>7</sup>. It is structurally analogous to the renal glomerulus, with a vascular intima, a subendothelial extracellular matrix and an elastic layer equivalent to the internal elastic layer of blood vessels. Thus, it possesses a basal membrane in its abluminal surface (RPE's basal membrane, a parallel to Bowman's capsule visceral layer) and a fenestrated vascular endothelium with its own luminal basal lamina. As in the glomerulus, transport and filtration are its most important functions. However, BM stands as a barrier to preclude the CC progression into the retina, either by being a mechanical barrier or by its elastic layer's intrinsic anti-angiogenic properties. With ageing, BM increases in thickness and its elastic layer loses elasticity and continuity<sup>8</sup>. The RPE is so intimately related with the CC under homeostasis and disease that photoreceptors, RPE, BM and CC, may be considered as the tapetoretinal unit<sup>9,10</sup>.

The CC nourishes the outer retina and the macula and regulates temperature by conveying heat. The nutrients bypass the RPE/BM, through specific adaptations in the

choroid: a blood flow ten-fold higher than in the brain, a high oxygen tension (arterial/venous difference of about 3% compared with 38% in the retinal circulation) and the CC pores disposed mainly on the BM side of the flattened CC network<sup>5</sup>.

On optical coherence tomography (OCT) the CC is located underneath the complex RPE/BM, and has a rough estimated thickness of 10  $\mu\text{m}$ . It may be absent in case of atrophy or it may be thickened due to multifocal choroiditis. FA does not give much information on the CC due to the block of visible light by the RPE and the rapid diffusion in the interstitial space during the early arterial phase. Indocyanin green angiography (ICGA) bypasses the RPE, however it cannot separate properly the different layers of the choroid. Nevertheless, ICGA is most important in identifying the polyps or the aneurysmatic dilations of the CC in polypoidal choroidal vasculopathy (PCV) and contributes to differentiating the wet age-related macular degeneration (AMD) subtypes<sup>11</sup>. Optical coherence tomography angiography (OCTA) is the imaging tool capable of separating the different choroidal layers based on angiographic properties.

## OPTICAL COHERENCE TOMOGRAPHY ANGIOGRAPHY

Combining structural information of OCT scan with blood flow visualization, OCTA allows to visualize the retinal capillary plexuses and the inner choroidal layers. Intrinsic movement of cells within the blood vessels accessed by multiple OCT scans at the same location allows to build up a lumen-based vascular profile of the biological tissue in a dual image of dark and white pixels, where white pixels represent areas of blood flow above the decorrelation threshold. OCTA is most commonly used in the en face representation due to the analogy with the dye-based angiography. However, the structural OCT and the B-scan with flow overlay are invaluable auxiliary tools to qualitative and quantitative analyses<sup>12</sup>. The depth resolved capability and high spatial resolution ( $\sim 15\text{-}20$   $\mu\text{m}$  laterally,  $\sim 6$   $\mu\text{m}$  axially) of OCTA is suitable for quantification and in vivo imaging of the retinal vessels, as the inter-capillary distances are generally larger ( $71.30 \pm 5.17$   $\mu\text{m}$ ) than the system's lateral resolution ( $\sim 15\text{-}20$   $\mu\text{m}$ ). Conversely, the CC denser capillary network (5-20  $\mu\text{m}$  of inter-capillary distance in the

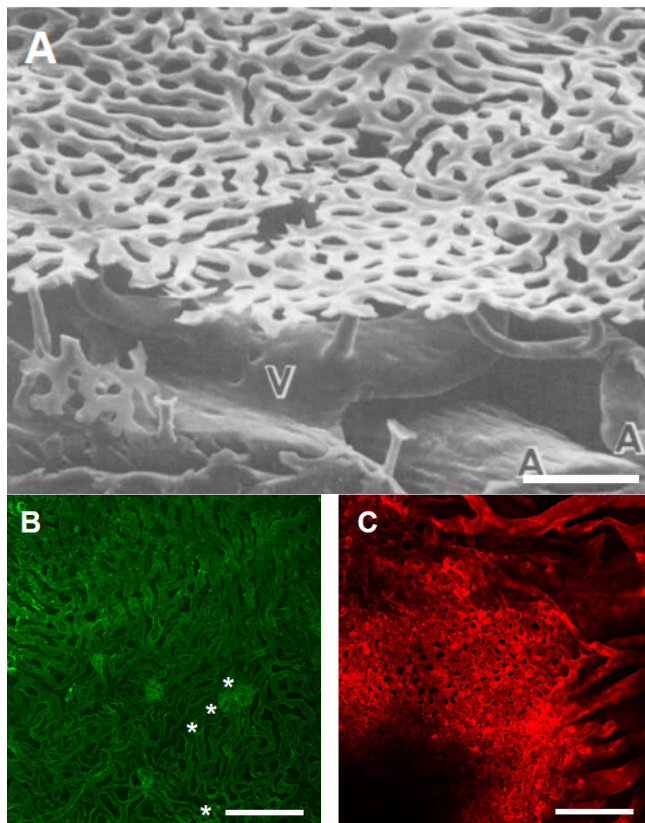


**Figure 1.** The choriocapillaris (CC) and choroidal feeding vessels. A. Scanning electron micrograph of the human CC network from vascular casts. The CC is a network of low resistance flattened capillaries whose larger horizontal lumen is up to 50  $\mu\text{m}$ , allowing a high speed blood flow. As the terminal arteries join the CC lobules in their center, the blood flow in the periphery of the lobules is slower than in the center<sup>6</sup>. Choroidal arteries (A) and veins (V) beneath the CC network (adapted from Risco and Nopanitaya), Scale bar = 100  $\mu\text{m}$  (1). Permission granted by The Association for Research in Vision and Ophthalmology, ARVO. B. Rat CC immunolabeled with anti-endothelial cell antibody (RECA-1) viewed from retinal aspect by confocal microscopy (2). The structure of rat CC resembles man's and monkey's. Venular dilated sinuses at the same plane of the CC are visible (white asterisks), but a clear lobular arrangement of the choriocapillaris is absent. Scale bar: 150  $\mu\text{m}$ . C. Rat choroid (2). Choroid single confocal plane visualized from the RPE side, showing choroidal medium-sized arteries perfused by 1,1'-diocadecyl-3,3,3',3'-tetramethylindocarbocyanine perchlorate (DiI) running parallel to the CC plane. They originate the CC through short pre-terminal arteries (actually, arterioles) emerging at right angles that are not visualized as they are perpendicular to the plane of acquisition. Note that the image enrolls different in-depth planes due to the wavy disposition of the choroid-scleral whole-mount. Laser scanning microscope LSM 710 (Zeiss). Scale bar = 350  $\mu\text{m}$ .

posterior pole) surpasses the system's lateral resolution, which is not able to tell them apart. Therefore, OCTA is able to examine nonperfusion but not detailed vascular patterns, since the CC is as thin as 10-20  $\mu\text{m}$  (Figure 2)<sup>13</sup>. Furthermore, the dynamic aspect of the CC circulation and various artifacts associated with OCTA imaging limit the value and the correct interpretation of collected

data. A capillary segment may be closed and/or may not show flow just for a while. These dynamic changes have implications for the repeatability of CC measurements as the percentage of CC with flow may vary over time. The three artifacts that most dramatically and significantly impact CC assessment include: (i) segmentation errors,

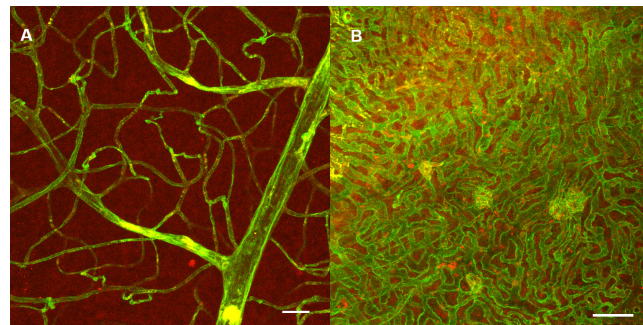


**Figure 2.** Rat retina and choriocapillaris (CC) vascular profiles immunolabeled with anti-endothelial cell antibody (RECA-1, green) and phagocytic cells immunolabeled with Cx3Cr1 antibody (red) (2). A. Retina superficial plexus immunolabeled with RECA-1 (green). B. CC immunolabeled with RECA-1 viewed from retinal aspect by confocal microscopy. Pre-venular dilated sinuses at the same plane of the CC are visible (white asterisks), but a clear lobular arrangement of the CC is absent. Please note that while the retinal capillaries lumen size is 3.5 to 6  $\mu\text{m}$ , the CC lumen size may be up to 50  $\mu\text{m}$ , many times that of the lumen size of normal capillaries. Scale bar: 50  $\mu\text{m}$ . I am extremely grateful to João C. Martins, PhD (<https://orcid.org/0000-0001-7764-286X>), for reviewing the original figures and checking for the exact scale.

(ii) projection artifacts, and (iii) shadowing artifacts<sup>12</sup>. The CC presents a significant segmentation challenge as it is variable and extremely thin (10  $\mu\text{m}$  under the fovea), thus even small or subtle segmentation errors can cause regions of CC to be displaced outside the boundaries of the en face slab. En face OCTA images of the CC are generated by segmenting the BM, and then positioning a second boundary several microns below, to yield a thin slab 10–30  $\mu\text{m}$  thick. In these en face images of a grainy appearance, small dark regions alternate with granular bright areas, the latter thought to represent CC flow, and the former more likely to be secondary to CC vascular dropout or flow reduction. Nevertheless, due to several histologic and device's tradeoffs, there is no consensus on the best position and thickness of the CC slab<sup>12</sup>. Many research groups and instrument manufacturers utilize an en face slab from a position deeper than the physical location of the CC (thereby imaging the projection artifact from the CC). The resultant image is probably not only the CC. However, this "CClike" structure or "inner choroidal slab" has provided new insights into normal aging and various macular diseases<sup>12,14</sup>. The dark areas have recently been renamed signal voids, because they represent a flow signal strength below the decorrelation threshold that will be undetectable in the en face image. For there to be a dark area there has to be

a relative decrease in local flow signal, neither necessarily irreversible nor meaning always absent flow. Indeed, the dark areas do not match the anatomic structure of the CC. As such, signal voids do not necessarily correspond to a true absence of the capillary bed. In fact, flow abnormalities implied by the signal voids are commonly smaller than the size of a CC lobule<sup>15</sup>. Experimental work revealed arterial-arterial pre-terminal anastomoses and CC remodeling under pericyte mediation, which may contribute to the transient nature of some of these flow alterations<sup>16,17</sup>.

Different strategies have been used to quantify CC perfusion density and signal voids. Those include projection artifact removal methods, brightness/contrast adjustment, avoidance of tilting the acquisition slab, signal strength, threshold strategies and multiple en face image averaging.

Image binarization allows to quantify the vessel density, the total amount of the vascular dropout, as well as to count and measure the size of the signal voids (Figure 3)<sup>12,18,19</sup>. Averaging sequential en face OCTA images enhances the image quality, transforming the poorly defined granular appearance into a morphologic pattern resembling the meshwork pattern of histology. Averaged images show a reduction in the signal void area, confirming that the flow pattern changes between different frames<sup>19,20</sup>. Likewise, in diseases without permanent damage, such as diabetes without retinopathy, alterations in the fractal image of the CC with increase in signal voids may be due to reduced flow, CC remodeling, interstitial edema, increased inflammatory cells on the CC's choroidal side or true CC's segment malfunction<sup>14,21</sup>. Recently, frame-averaged

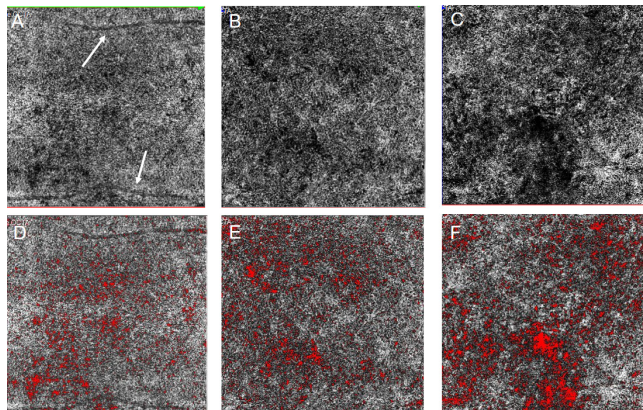


**Figure 3.** OCTA regular single frames and binarization by the Otsu method (18). A. Choriocapillaris (CC) in a control subject aged 29. Projection artifacts are clearly visible even after activating the artifact removal tool (white arrows). B. CC in a control subject aged 58. C. CC in an eye of a patient with paracentral acute middle maculopathy associated with inferior branch retinal vein occlusion, after being treated with an anti-VEGF drug, without edema. D, E and F. Corresponding binarized images of the frame above, respectively. Lacunarity seems to be increased in the older control subject and is clearly increased in the central and inferior macular area of the eye of the patient depicted in C. I am extremely grateful to João C. Martins, PhD (<https://orcid.org/0000-0001-7764-286X>), for the binarization of images D, E and F for me.

images of the CC, binarized and skeletonized, revealed that pachychoroid without disease eyes had normal fractal dimension, mean CC vessel segment length and diameter, indicating that the finding of a pachychoroid is not *per se* pathologic<sup>19</sup>. There is agreement that the high vascular density of the CC underneath the fovea decreases with age, being independent of gender or choroidal thickness, and that has been related to the continuous CC's high blood flow speed and high metabolic demands of the outer retina at this location<sup>12</sup>. Altogether, these findings bring the focus back on the tapetoretinal unit, in lieu of the choroidal thickness, as a prominent locus and marker of outcome of many retinal diseases.

## CHORIOCAPILLARIS AND DISEASE

Currently, it is considered that CC changes may be related with the pathogenesis of several retinal diseases. CC atrophy is associated with high myopic retinal degeneration and atrophic AMD. RPE-BM dysfunction relates to proliferative AMD<sup>22</sup>. Correlation between CC loss and drusen density was reported in early AMD<sup>23</sup>. CC hyperpermeability, aneurisms, type 1 neovascularization, attenuation and smaller fractal dimension were described in the pachychoroid disease<sup>24</sup>.

In diabetes, the choroid behaves as a pro-inflammatory environment<sup>21</sup>. On OCTA, vascular abnormalities in the CC, more and larger sized CC signal voids in diabetic eyes without retinopathy and an association between impaired flow in the CC and photoreceptor damage were reported<sup>25</sup>. The decrease in the CC vascular density correlates with the deep retinal capillary plexus decreased vascular density found with increased grading in diabetic retinopathy<sup>26</sup>.

CC segmental non-perfusion in ICGA has been demonstrated in multiple evanescent white dot syndrome (MEWDS), acute posterior multifocal placoid pigment epitheliopathy (APMPPE) and other white dot syndromes. While once these entities were considered to be related one another by a matter of grade of severity, MEWDS is currently considered to be a choriocapillaritis or photoreceptoritis, while APMPPE may actually be a terminal occlusive arteriolitis, due to the clear defined border of the lesions measuring about 0.8 mm of diameter, resembling the choroidal lobules described by Hayreh and Torczynski (Figure 4)<sup>6,27,28</sup>. Unlike APMPPE, the paradoxical presence of flux in MEWDS concurring with hypofluorescent lesions may actually be attributed to a reduction but not stoppage in the CC fast blood flow speed, detected by OCTA along with a wash out of the indocyanine dye or, on the other hand, CC flux in MEWDS may be almost normal and the hypofluorescent lesions may actually result from a masking effect of the focal inflammation on ICGA<sup>28</sup>. Likewise, polyps in PCV may appear as hypo or hyper reflective aneurysmatic structures, depending on different flow speeds within<sup>29</sup>.

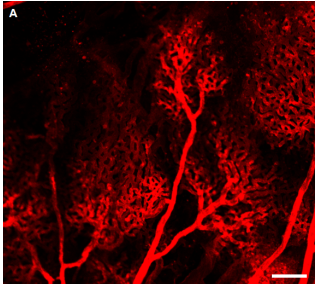


**Figure 4.** Arteries, end-terminal arterioles and choriocapillaris (CC) lobules viewed from the choroidal side (2). Terminal choroidal arterioles visualized by Dil (red) in a 16-week Wistar rat. Arteries dividing in pre-terminal arterioles that originate the multiple lobular network of the CC. Laser scanning microscope LSM 710 (Zeiss), 10x Full size: x: 850.19  $\mu\text{m}$ , y: 850.19  $\mu\text{m}$ . Scale bar: 100  $\mu\text{m}$ .

## REFERENCES

- Risco JM, Nopanitaya W. Ocular microcirculation. Scanning electron microscopic study. *Invest Ophthalmol Vis Sci.* 1980;19(1):5-12.
- Campos A. Study on the Contribution of the Choroid to the Pathophysiology of Diabetic Retinopathy [Thesis Doctorat]. Coimbra: Coimbra University 2020. Accessed at: [https://www.researchgate.net/publication/346061663\\_Study\\_on\\_the\\_Contribution\\_of\\_the\\_Choroid\\_to\\_the\\_Pathophysiology\\_of\\_Diabetic\\_Retinopathy](https://www.researchgate.net/publication/346061663_Study_on_the_Contribution_of_the_Choroid_to_the_Pathophysiology_of_Diabetic_Retinopathy).
- Olver JM. Functional anatomy of the choroidal circulation: methyl methacrylate casting of human choroid. *Eye.* 1990;4 ( Pt 2):262-72.
- Forrester J. V., Dick A. D., Paul G. McMenamin P. G., Roberts F., Pearlman E. Anatomy of the eye and orbit. In: Saunders WB, editor. *The Eye.* 4th ed. Edinburgh; New York: Saunders/Elsevier 2016. p. 1-102.
- Federman JL. The fenestrations of the choriocapillaris in the presence of choroidal melanoma. *Trans Am Ophthalmol Soc.* 1982;80:498-516.
- Hayreh SS. The choriocapillaris. *Graefes Arch Clin Exp Ophthalmol.* 1974;12(3):165-79.
- Campos A, Campos EJ, Martins J, Ambrosio AF, Silva R. Viewing the choroid: where we stand, challenges and contradictions in diabetic retinopathy and diabetic macular oedema. *Acta Ophthalmol.* 2017;95(5):446-59.
- Curcio CA, Johnson M. Structure, Function, and Pathology of Bruch's Membrane In: Ryan SJ, editor. *Retina.* 5th ed. Philadelphia, PA: Elsevier; 2013. p. 465-81.
- Baba T, Grebe R, Hasegawa T, Bhutto I, Merges C, McLeod DS, et al. Maturation of the fetal human choriocapillaris. *Invest Ophthalmol Vis Sci.* 2009;50(7):3503-11.
- Fields MA, Del Priore LV, Adelman RA, Rizzolo LJ. Interactions of the choroid, Bruch's membrane, retinal pigment epithelium, and neurosensory retina collaborate to form the outer blood-retinal-barrier. *Prog Retin Eye Res.* 2020;76:100803.
- Silva RM, Figueira J, Cachulo ML, Duarte L, Faria de Abreu JR, Cunha-Vaz JG. Polypoidal choroidal vasculopathy and photodynamic therapy with verteporfin. *Graefes Arch Clin Exp Ophthalmol.* 2005;243(10):973-9.
- Corvi F, Su L, Sadda SR. Evaluation of the inner choroid using OCT angiography. *Eye.* 2021;35(1):110-20.
- Chu Z, Gregori G, Rosenfeld PJ, Wang RK. Quantification of Choriocapillaris with Optical Coherence Tomography Angiography: A Comparison Study. *Am J Ophthalmol.* 2019;208:111-23.
- Byon I, Alagorie AR, Ji Y, Su L, Sadda SR. Optimizing the Repeatability of Choriocapillaris Flow Deficit Measurement From Optical Coherence Tomography Angiography. *Am J Ophthalmol.* 2020;219:21-32.
- Spaide RF, Fujimoto JG, Waheed NK, Sadda SR, Staurengi G. Optical coherence tomography angiography. *Prog Retin Eye Res.* 2018;64:1-55.
- Castro Correia J. *Vascularização da coróideia. Anatomofisiologia da coróideia.* [Thesis Doctorat]. Porto: Porto University; 1958.
- Campos A, Martins J, Campos EJ, Silva R, Ambrosio AF. Choroidal and retinal structural, cellular and vascular changes in a rat model of Type 2 diabetes. *Biomed Pharmacother.* 2020;132:110811.
- Otsu N. A Threshold Selection Method from Gray-Level Histograms. *IEEE Trans Syst Man Cybern* 1979;9:62-66.
- Spaide RF, Ledesma-Gil G. Choriocapillaris Vascular Parameters in Normal Eyes and Those with Pachychoroid with and without Disease. *Retina.* 2021;41(4):679-85.
- Borrelli E, Sarraf D, Freund KB, Sadda SR. OCT angiography and evaluation of the choroid and choroidal vascular disorders. *Prog Retin Eye Res.* 2018;67:30-55.
- Campos A, Campos EJ, Martins J, Rodrigues FSC, Silva R, Ambrosio AF. Inflammatory cells proliferate in the choroid and retina without choroidal thickness change in early Type 1 diabetes. *Exp Eye Res.* 2020;199:108195.
- Ruiz-Medrano J, Montero JA, Flores-Moreno I, Arias L, Garcia-Layana A, Ruiz-Moreno JM. Myopic maculopathy: Current status and proposal for a new classification and grading system (ATN). *Prog Retin Eye Res.* 2019;69:80-115.
- Arya M, Sabrosa AS, Duker JS, Waheed NK. Choriocapillaris changes in dry age-related macular degeneration and geographic atrophy: a review. *Eye Vis.* 2018;5:22.
- Cheung CMG, Lee WK, Koizumi H, Dansingani K, Lai TYY, Freund KB. Pachychoroid disease. *Eye.* 2019;33(1):14-33.
- Chua J, Sim R, Tan B, Wong D, Yao X, Liu X, et al. Optical Coherence Tomography Angiography in Diabetes and Diabetic Retinopathy. *J Clin Med.* 2020;9(6).
- Ra H, Kang NY, Song J, Lee J, Kim I, Baek J. Discordance in Retinal and Choroidal Vascular Densities in Patients with Type 2 Diabetes Mellitus on Optical Coherence Tomography Angiography. *J Ophthalmol.* 2021;2021:8871602.
- Torczyński E, Tso MO. The architecture of the choriocapillaris at the posterior pole. *Am J Ophthalmol.* 1976;81(4):428-40.
- Lages V, Mantovani A, Papadia M, Herbort CP. MEWDS is a true primary choriocapillaritis and basic mechanisms do not seem to differ from other choriocapillaritis entities. *J Curr Ophthalmol.* 2018;30(4):281-6.
- Serra R, Coscas F, Pinna A, Cabral D, Coscas G, Souied EH. Fractal analysis of polypoidal choroidal neovascularisation in age-related macular degeneration. *Br J Ophthalmol.* 2021;105(10):1421-1426.

# 6. OPTIC NERVE HEAD

João Barbosa-Breda

Cardiovascular R&D Center, Faculty of Medicine of the University of Porto, Porto, Portugal

Department of Ophthalmology, Centro Hospitalar e Universitário São João, Porto, Portugal

KULeuven, Research Group Ophthalmology, Department of Neurosciences, Leuven, Belgium

The optic nerve head (ONH) is currently a difficult location to be evaluated through OCT-A. First of all, it is anatomically challenging due to the abrupt changes in the direction of layers and even cessation of some of them, such as the external retinal layers. Furthermore, there are plenty of shadow effects from large retinal vessels that traverse the whole depth of the ONH. Finally, this region is angiographically complex since it is supplied by several arterial systems, all ultimately deriving from the ophthalmic artery<sup>1</sup>.

The innermost region, corresponding to the nerve fiber layer, is supplied by branches of the central retinal artery, creating the radial peripapillary capillary network (Figure 1 left). In some cases, the posterior ciliary arteries can also provide arterial supply to the temporal sector of the superficial layer through the cilioretinal artery.

At deeper levels, the short posterior ciliary arteries create a vascular complex surrounding the ONH, called the circle of Zinn-Haller, which is the main supply to the prelaminar, laminar and retrolaminar regions of the ONH<sup>2</sup>. Moreover, the peripapillary choroid also provides centripetal branches. Noteworthy, the blood supply at these deeper levels has a sectoral distribution with watershed zones, which explains the cases of segmental visual loss in some ischemic disorders<sup>1</sup>.

The autoregulatory capacity of these vascular networks has never been fully established. It is known that retinal vessels have a considerably higher ability to autoregulate, while choroidal vessels are considered to have none or a slight ability to do so<sup>3</sup>. Nonetheless, the intricate network surrounding the ONH has proven difficult to study. Ongoing studies including dynamic analyses of OCT-A with concomitant vascular stimuli might help shed more light into this subject<sup>4</sup>.

The most studied layer is currently the superficial layer, comprising the radial peripapillary capillaries that run through the retinal nerve fiber layer. The two main reasons for this are the easy access to automatic quantification from current built-in software tools, but also the fact that it is the least affected layer by artefacts (all other layers have some posterior projection of innermost layers). Nonetheless, many softwares do not automatically remove the large retinal vessels, thus diluting the changes that can be detected at the microvascular capillary level, which are seen as more relevant, at least for ONH-

centered diseases<sup>5</sup>.

Deeper layers have also proven to be fruitful in terms of research and clinical usefulness. Moreover, many authors have turned to these layers as a potential source for further physiopathological understanding of optic nerve diseases, such as glaucoma, which is thought to have progression derived from vascular insults to these deeper vascular layers<sup>6</sup>.

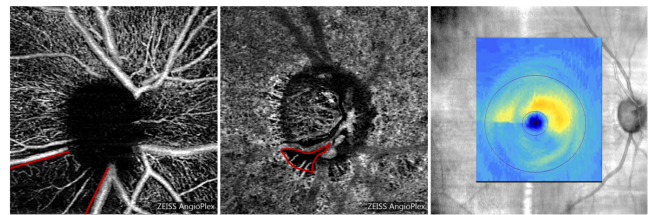


**Figure 1.** OCT angiography en-face image of the superficial layer showing the radial peripapillary capillary network with a sectoral reduction of vessel density (left image, vessel density defect delimited by red lines); OCT angiography en-face image of the choriocapillaris layer with a localized microvascular dropout area (central image, defect delimited with red lines); macular ganglion cell thickness map with a profound loss in the inferior half respecting the horizontal midline, which corresponds to the area of severe vessel density reduction depicted in the OCT angiography images (right image). Images from a glaucoma case.

The choroidal layer peripapillary defects, also called microvascular dropout (MvD) areas, have been shown to have diagnostic and prognostic abilities<sup>7,8</sup>, being linked to glaucoma progression and peripapillary hemorrhages (Figure 2). These are best seen when peripapillary atrophy is present, due to the absence of the highly reflective outer retinal layers.

OCT-A can improve our ability to follow patients with difficult ONH features, such as myopic discs, which prove hard to study through standard OCT parameters<sup>9</sup>. Moreover, data show that larger scans (larger than 3x3 mm) might hold significant information in these elongated eyes (despite the loss of resolution)<sup>9</sup>. Nonetheless, in the case of healthy macular areas, the macula might still be the best location to study glaucomatous eyes. When compared to standard OCT, OCT-A has clearly shown a high diagnostic ability, in many cases comparable between systems<sup>10-12</sup>. Nonetheless, OCT-A seems to have

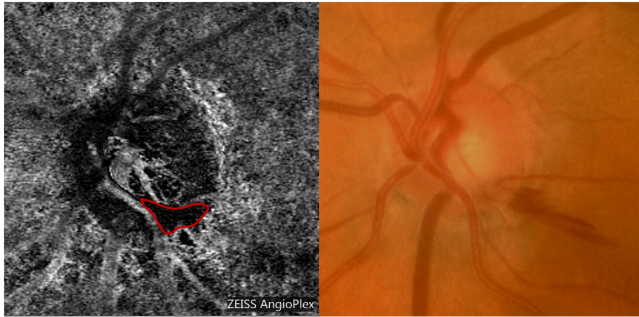


**Figure 2.** OCT angiography en-face image of the choriocapillaris layer with a localized microvascular dropout area (left image, defect delimited with red lines); ONH-centered retinography with a peripapillary hemorrhage at the same location as the microvascular dropout (right image). Images from a glaucoma case.

the ability to detect progression until more advanced disease stages, after standard OCT has reached its so called “floor effect”<sup>13,14</sup>.

Glaucoma is definitely the most studied disease in the ONH region with OCT-A. Nonetheless, other optic neuropathies and even retinopathies benefit from the study of the ONH diverse vasculature.

OCT-A studies in arteritic and non-arteritic anterior ischemic optic neuropathies have shown the ability of this technique to show a reduction of peripapillary and ONH vasculature, in most cases circumferential with a more pronounced defect at a specific focal area, mainly at the superficial layers but also at the level of the choriocapillaris<sup>15-19</sup>. Some studies found a correlation between OCT-A metrics and visual field (defect location and overall severity) and visual acuity<sup>15,16,18</sup>. Regarding diabetic retinopathy (DR), in a study with 94 patients, the peripapillary superficial vessel density reduction correlated with DR severity, while the whole image ONH vessel density correlated with visual acuity<sup>20</sup>. Finally, systemic cardiovascular diseases, such as arterial hypertension and diabetes mellitus also lead to ONH vessel density reduction identified through OCT-A, even when no ocular disease is yet identified<sup>21</sup>.

The key to enhance our diagnostic and prognostic yield seems to be by combining information from multiple regions but also multiple layers. The use of artificial intelligence algorithms to this end was able to improve the AUC values for glaucoma diagnosis and severity grading<sup>22</sup>.

Current automatic quantification software systems still require improvement. Apart from dealing with artefacts, such as the posterior projection removal, which are inherent to any OCT-A region being analyzed, the ONH requires special attention. Potential improvements could be taking into account the optic disc size (and the corresponding ONH optically hollow area) when performing peripapillary annular analyses, the ability to customize the angle of sectors in the peripapillary annulus (since the Early Treatment Diabetic Retinopathy Study grid is many times not ideal), automatic large

retinal vessel removal (some softwares are already able to perform this task) and automatic quantification and follow-up of focal defects, mainly at deeper levels, such as the MvD in the choroidal layers. Moreover, systemic cardiovascular diseases should also be taken into account since they have a clear impact in almost all OCT-A metrics, in most cases reducing the vessel density<sup>21</sup>. Overall, OCT-A in the ONH region still has a long way to go before it can reach its full potential in clinical practice. A similar path is still ongoing regarding standard OCT (which is still not able to automatically generate several ONH metrics) which will definitely help improve OCT-A.

## REFERENCES

1. Hayreh SS. Ischemic optic neuropathy. *Prog Retin Eye Res.* 2009;28(1):34-62.
2. Mackenzie PJ, Cioffi GA. Vascular anatomy of the optic nerve head. *Can J Ophthalmol.* 2008;43(3):308-312.
3. Polska E, Simader C, Weigert G, et al. Regulation of choroidal blood flow during combined changes in intraocular pressure and arterial blood pressure. *Invest Ophthalmol Vis Sci.* 2007;48(8):3768-3774.
4. Barbosa Breda J, Van Eijgen J, Stalmans I. Advanced vascular examinations of the retina and optic nerve head in glaucoma. *Progr Brain Res.* 2020;257:77-83.
5. Jia Y, Morrison JC, Tokayer J, et al. Quantitative OCT angiography of optic nerve head blood flow. *Biomed Opt Express.* 2012;3(12):3127-3137.
6. Zeitz O, Galambos P, Wagenfeld L, et al. Glaucoma progression is associated with decreased blood flow velocities in the short posterior ciliary artery. *Br J Ophthalmol.* 2006;90(10):1245-1248.
7. Park HL, Kim JW, Park CK. Choroidal Microvasculature Dropout Is Associated with Progressive Retinal Nerve Fiber Layer Thinning in Glaucoma with Disc Hemorrhage. *Ophthalmology.* 2018;125(7):1003-1013.
8. Kwon JM, Weinreb RN, Zangwill LM, Suh MH. Parapapillary Deep-Layer Microvasculature Dropout and Visual Field Progression in Glaucoma. *Am J Ophthalmol.* 2019;200:65-75.
9. Lee K, Maeng KJ, Kim JY, et al. Diagnostic ability of vessel density measured by spectral-domain optical coherence tomography angiography for glaucoma in patients with high myopia. *Sci Rep.* 2020;10(1):3027.
10. Varma R, Xu BY, Richter GM, Reznik A. ed. *Advances in Ocular Imaging in Glaucoma.* 2020. New York, NY: Springer; 2020.
11. Miguel AIM, Silva AB, Azevedo LF. Diagnostic performance of optical coherence tomography angiography in glaucoma: a systematic review and meta-analysis. *The Br J Ophthalmol.* 2019;103(11):1677-1684.
12. Van Melkebeke L, Barbosa-Breda J, Huygens M, Stalmans I. Optical Coherence Tomography Angiography in Glaucoma: A Review. *Ophthalmic Res.* 2018:1-13.
13. Barbosa-Breda J, Andrade de Jesus D, Van Keer K, et al. AngioOCT peripapillary microvascular density outperforms standard OCT parameters as a discriminant between different glaucoma severity levels – The Leuven Eye Study. *Invest Ophthalmol Vis Sci.* 2018;59(9):4478-4478.

14. Rao HL, Pradhan ZS, Weinreb RN, et al. Relationship of Optic Nerve Structure and Function to Peripapillary Vessel Density Measurements of Optical Coherence Tomography Angiography in Glaucoma. *J Glaucoma*. 2017;26(6):548-554.
15. Augstburger E, Zeboulon P, Keilani C, Baudouin C, Labbe A. Retinal and Choroidal Microvasculature in Nonarteritic Anterior Ischemic Optic Neuropathy: An Optical Coherence Tomography Angiography Study. *Invest Ophthalmol Vis Sci*. 2018;59(2):870-877.
16. Hata M, Oishi A, Muraoka Y, et al. Structural and Functional Analyses in Nonarteritic Anterior Ischemic Optic Neuropathy: Optical Coherence Tomography Angiography Study. *J Neuroophthalmol*. 2017;37(2):140-148.
17. Wright Mayes E, Cole ED, Dang S, et al. Optical Coherence Tomography Angiography in Nonarteritic Anterior Ischemic Optic Neuropathy. *J Neuroophthalmol*. 2017;37(4):358-364.
18. Gandhi U, Chhablani J, Badakere A, et al. Optical coherence tomography angiography in acute unilateral nonarteritic anterior ischemic optic neuropathy: A comparison with the fellow eye and with eyes with papilledema. *Indian J Ophthalmol*. 2018;66(8):1144-1148.
19. Rougier MB, Delyfer MN, Korobelnik JF. OCT angiography of acute non-arteritic anterior ischemic optic neuropathy. *J Fr Ophthalmol*. 2017;40(2):102-109.
20. Ghassemi F, Berijani S, Roohipoor R, et al. Vascular density of optic nerve head in diabetic retinopathy using optical coherence tomography angiography. *Int J Retina Vitreous*. 2020;6(1):62.
21. Monteiro-Henriques I, Rocha-Sousa A, Barbosa-Breda J. Optical coherence tomography angiography changes in cardiovascular systemic diseases and risk factors: A Review. (ahead of print).
22. Andrade De Jesus D, Sanchez Brea L, Barbosa Breda J, et al. OCTA Multilayer and Multisector Peripapillary Microvascular Modeling for Diagnosing and Staging of Glaucoma. *Transl Vis Sci Technol*. 2020;9(2):58.





7.

# OCCLUSIVE DISEASES AND THE ISCHEMIC CASCADE



## 7.1.

# PARACENTRAL ACUTE MIDDLE MACULOPATHY

Filipe Mira<sup>1</sup>, Sara Vaz-Pereira<sup>2,3</sup>

1- Department of Ophthalmology, Centro Hospitalar Médio Tejo, EPE, Portugal

2- Department of Ophthalmology, Centro Hospitalar Universitário de Lisboa Norte, EPE - Hospital de Santa Maria, Lisbon, Portugal

3- Department of Ophthalmology, Faculdade de Medicina, Universidade de Lisboa, Lisbon, Portugal

Paracentral acute middle maculopathy (PAMM) was originally described by Sarraf et al in 2013<sup>1</sup> as a variant of acute macular neuroretinopathy, however it is now considered a different entity<sup>2,4</sup>.

PAMM is a nonspecific tomographic sign of retinal ischemia involving the intermediate and deep capillary plexuses<sup>2,5</sup>. Using spectral domain-optical coherence tomography (SD-OCT) lesions are characteristically hyperreflective and band-like and located in the inner nuclear layer (INL) in the acute phase (Figures 1 and 2) with subsequent INL thinning and outer plexiform layer elevation with sparing of the outer retina layers in the convalescent phase (Figure 1)<sup>1,2,5,6</sup>.

PAMM may be idiopathic or secondary to retinal or systemic diseases, such as diabetic retinopathy, retinal artery occlusion, central vein occlusion, sickle cell retinopathy,

Purtscher's retinopathy and flu-like disease<sup>1,4,5,7-15</sup>. It may also be related to vasculopathic risk factors including hypotension, dyslipidemia, oral contraceptives, migraine disorder, anemia, and caffeine intake<sup>1,2,4,16</sup>.

Regarding its presentation, patients typically present with sudden onset of unilateral or bilateral paracentral scotomas. Mean age at presentation is 41-53 years, with no gender preference<sup>2,4,17</sup>. On clinical examination, funduscopy may be otherwise unremarkable or, less frequently, deeper and smoother gray lesions may be observed<sup>1,2,4,5</sup>.

A multimodal retinal imaging approach has allowed for a more detailed analysis and quantification of PAMM lesions and provided new insights into its pathogenesis with integrated information from SD-OCT, near-infrared imaging (NIR), fundus autofluorescence (FAF) and OCT-angiography (OCTA) (Figure 1)<sup>1,4,5,17-22</sup>.

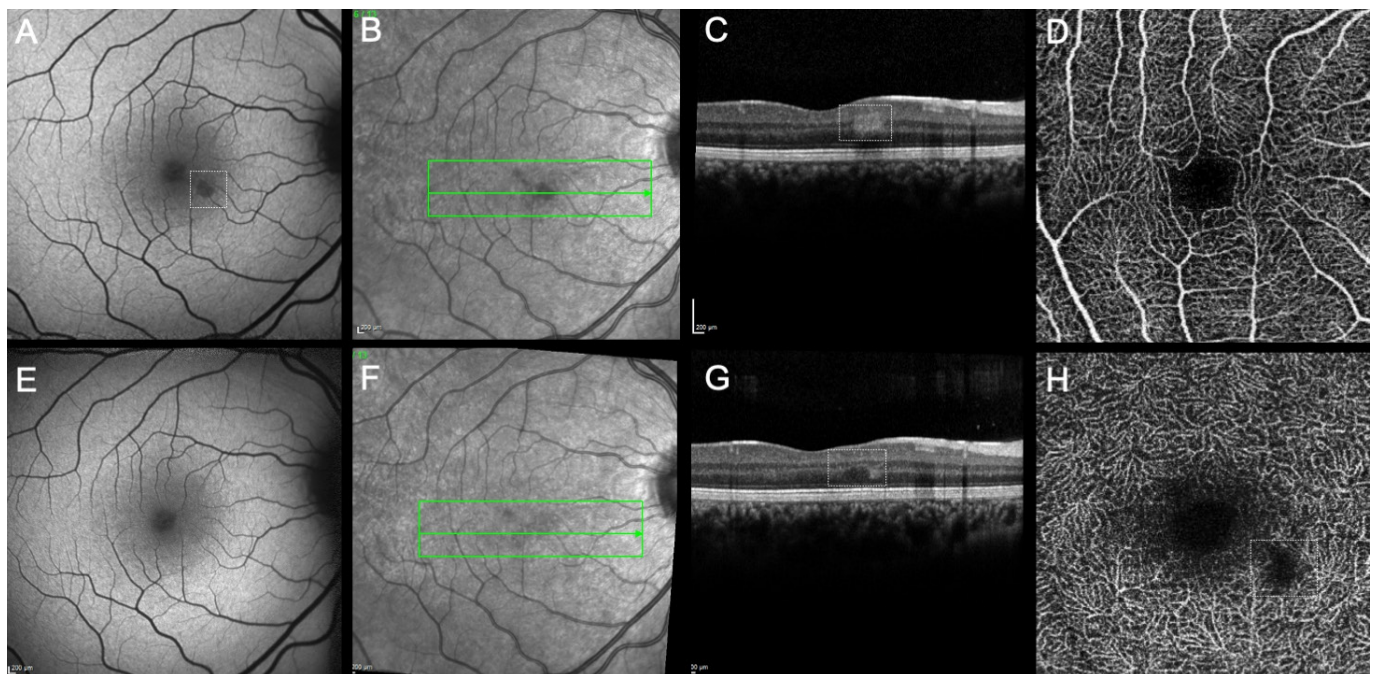


**Figure 1.** Multimodal imaging of idiopathic focal PAMM. Baseline fundus autofluorescence (A) and near-infrared reflectance (B) imaging revealed a paracentral dark wedge-shaped lesion (annotated). Matching SD-OCT (C) showed a hyperreflective lesion at the level of the inner nuclear layer in accordance with PAMM (depicted). OCTA of the superficial capillary plexus (D) was unremarkable. At 3 months-follow up, no changes were noted either in fundus autofluorescence (E) or near-infrared reflectance (F) images. Same visit SD-OCT (G) showed a convalescent phase PAMM lesion with inner nuclear layer thinning and outer plexiform layer elevation (annotated). OCTA of the deep capillary plexus (H) presented a persisting focal area of loss of flow (annotated), matching the location of the PAMM lesion. (Adapted with permission from Vaz-Pereira S. *Revista Sociedade Portuguesa De Oftalmologia*. 2015;39(2):115-8).

The typical SD-OCT features of PAMM were already described above. In NIR, PAMM presents as well demarcated dark wedge-shaped lesions and in FAF as matching hypoautofluorescent lesions, which fade from the acute to the convalescent phase (Figure 1)<sup>1, 4, 5, 15, 23</sup>. Conventional fundus fluorescein angiography (FFA) has limited value in PAMM, albeit it may reveal several findings such as delayed filling, areas of hypofluorescence and intracapillary spacing, particularly when PAMM is associated with retinal vascular disease that involves the superficial capillary plexus (SCP)<sup>4, 5, 8, 12, 23</sup>. Nonetheless, it has limited depth resolution in distinguishing the intermediate capillary plexus (ICP) from the deep capillary plexus (DCP)<sup>5, 11, 24</sup>. It should be remembered that in the central macula the retinal plexus network exists within a superficial, intermediate and deep triplanar system<sup>25, 26</sup>. The deeper system is composed of an ICP and a DCP and the ICP has shown to be more dependent on the hypoxia-inducible factor 1(HIF1)<sup>27</sup>. As noted, PAMM lesions result from ischemia in the deep retinal plexus and thus may be unapparent in conventional FFA<sup>5, 21</sup>.

OCTA is a recent imaging modality that provides enhanced anatomic detail with an improved retinal vascular flow visualization<sup>24, 28</sup>. This permits an enhanced visualization of the deep retinal plexus and its ischemic changes in a noninvasive way<sup>28</sup>. With this technology we have the ability to identify the SCP traditionally seen on FFA but also the flow of the DCP, unseen in FFA<sup>24, 28, 29</sup>. Indeed, with OCTA, PAMM is confirmed as a vascular disorder resulting from ischemia of the ICP and DCP, which are responsible for the blood supply to the middle retinal layers (Figure 1)<sup>1, 2, 13, 20, 22, 30-32</sup>. Yu et al<sup>18</sup> concluded that the parafoveal macula, particularly the middle retinal layers, were a watershed-like zone, that may be most vulnerable to ischemia. This understanding of the retinal anatomy aligns itself with an ischemic etiology for PAMM<sup>2</sup>.

Acute lesions of PAMM may be focal (Figure 1), multifocal (Figure 2) or diffuse<sup>32</sup>. OCTA may demonstrate patent perfusion of the DCP in focal or multifocal forms (Figure 2), whereas in diffuse PAMM (from large vessel obstruction), it may reveal decreased perfusion within the DCP<sup>32</sup>. In chronic lesions/convalescent phase, OCTA shows loss of flow within the DCP with decreased vascular density and sometimes patchy voids<sup>32</sup>.

Information from OCTA, using both the en face image and the structural image with flow signal, can be used to assess the degree of ischemia: capillary density, foveal avascular zone, degree of capillary remodeling and pruning at the DCP<sup>12, 33-37</sup>. Indeed, three patterns of PAMM have been described based on the presumed pathophysiology and using the OCTA en face and structural image: arteriolar, globular and fern-like patterns (Figure 2)<sup>4, 12, 20, 23, 32</sup>. Obviously, for this assessment and to have accurate images, it is important to have a correct segmentation of the retinal plexuses. While standardized segmentation may be enough for acute lesions, manual segmentation is sometimes necessary for chronic lesions with severe INL thinning. Vessel density, analysis and

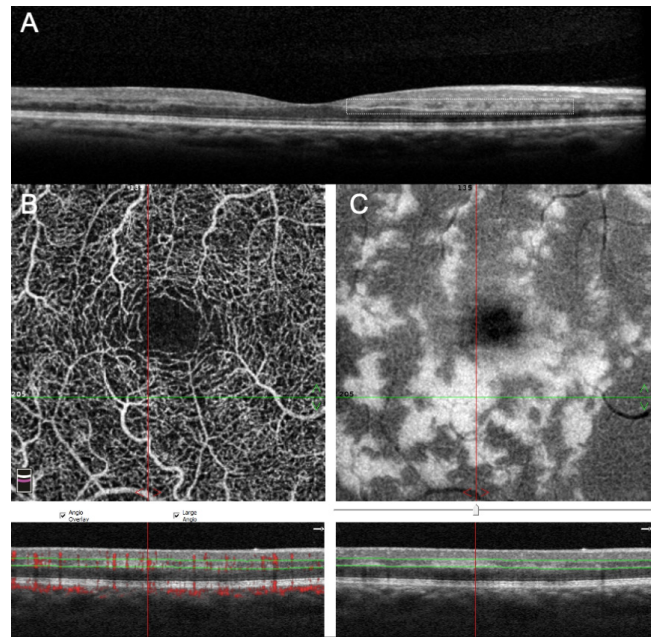


**Figure 2.** OCT imaging of PAMM secondary to vascular disease. Acute phase SD-OCT (A) showed multifocal band-like hyperreflective lesions at the level of inner nuclear layer (annotated) characteristic of PAMM. OCTA demonstrated patent perfusion of the deep capillary plexus (B) and the en face image revealed a typical fern-like pattern (C).

quantification of the SCP and DCP may be performed using special software that binarize and skeletonize scans<sup>38</sup>, albeit less feasible in routine clinical practice.

In summary, OCTA is currently an important tool to evaluate the retina, including PAMM lesions. The development of SD-OCT and OCTA technology provided us with a better understanding of PAMM and recognized that PAMM is far more common than initially anticipated. However, there are still some challenges, such as projection artifacts from the SCP to the DCP along with OCT signal attenuation underneath the INL hyperreflective lesions<sup>21, 32</sup>. We hope that the continuous development of multimodal imaging will give Ophthalmologists a greater acknowledgment of the pathophysiology and perhaps a better management of this entity.

## REFERENCES

1. Sarraf D, Rahimy E, Fawzi AA, Sohn E, Barbazetto I, Zacks DN, et al. Paracentral acute middle maculopathy: a new variant of acute macular neuroretinopathy associated with retinal capillary ischemia. *JAMA Ophthalmol.* 2013;131(10):1275-87.
2. Rahimy E, Kuehlewein L, Sadda SR, Sarraf D. Paracentral Acute Middle Maculopathy: What We Knew Then and What We Know Now. *Retina.* 2015;35(10):1921-30.
3. Dansingani KK, Freund KB. Paracentral Acute Middle Maculopathy and Acute Macular Neuroretinopathy: Related and Distinct Entities. *Am J Ophthalmol.* 2015;160(1):1-3.e2.
4. Moura-Coelho N, Gaspar T, Ferreira JT, Dutra-Medeiros M, Cunha JP. Paracentral acute middle maculopathy-review of the literature. *Graefes Arch Clin Exp Ophthalmol.*

- 2020;258(12):2583-96.
5. Vaz-Pereira S. Paracentral Acute Middle Maculopathy: a novel clinical finding. *Revista Sociedade Portuguesa De Oftalmologia*. 2015;39(2):115-8.
  6. Maltsev DS, Kulikov AN, Burnasheva MA, Freund KB. Vascular Microanatomy of Small Resolved Paracentral Acute Middle Maculopathy Lesions. *Ophthalmol Retina*. 2020;S2468-6530(20)30485-1.
  7. Querques G, La Spina C, Miserocchi E, Gagliardi M, Corvi F, Bandello F. Angiographic evidence of retinal artery transient occlusion in paracentral acute middle maculopathy. *Retina*. 2014;34(10):2158-60.
  8. Rahimy E, Sarraf D, Dollin ML, Pitcher JD, Ho AC. Paracentral acute middle maculopathy in nonischemic central retinal vein occlusion. *Am J Ophthalmol*. 2014;158(2):372-80.e1.
  9. Ilginis T, Keane PA, Tufail A. Paracentral acute middle maculopathy in sickle cell disease. *JAMA Ophthalmol*. 2015;133(5):614-6.
  10. Yu S, Pang CE, Gong Y, Freund KB, Yannuzzi LA, Rahimy E, et al. The spectrum of superficial and deep capillary ischemia in retinal artery occlusion. *Am J Ophthalmol*. 2015;159(1):53-63.e1-2.
  11. Casalino G, Williams M, McAvoy C, Bandello F, Chakravarthy U. Optical coherence tomography angiography in paracentral acute middle maculopathy secondary to central retinal vein occlusion. *Eye (Lond)*. 2016;30(6):888-93.
  12. Phasukkijwatana N, Rahimi M, Iafe N, Sarraf D. Central Retinal Vein Occlusion and Paracentral Acute Middle Maculopathy Diagnosed With En Face Optical Coherence Tomography. *Ophthalmic Surg Lasers Imaging Retina*. 2016;47(9):862-4.
  13. Chen X, Rahimy E, Sergott RC, Nunes RP, Souza EC, Choudhry N, et al. Spectrum of Retinal Vascular Diseases Associated With Paracentral Acute Middle Maculopathy. *Am J Ophthalmol*. 2015;160(1):26-34.e1.
  14. Ong SS, Ahmed I, Scott AW. Association of Acute Macular Neuroretinopathy or Paracentral Acute Middle Maculopathy with Sickle Cell Disease. *Ophthalmol Retina*. 2021;S2468-6530(21)00013-0.
  15. Rivera-De La Parra D, Fromow-Guerra J. Paracentral Acute Middle Maculopathy in Purtscher Retinopathy. *Retin Cases Brief Rep*. 2020;14(3):275-7.
  16. Coulon SJ, Dedania VS. Paracentral Acute Middle Maculopathy Associated with Hypercoagulability in Pregnancy. *Retin Cases Brief Rep*. 2020.
  17. Shah A, Rishi P, Chendilnathan C, Kumari S. OCT angiography features of paracentral acute middle maculopathy. *Indian J Ophthalmol*. 2019;67(3):417-9.
  18. Yu S, Wang F, Pang CE, Yannuzzi LA, Freund KB. Multimodal imaging findings in retinal deep capillary ischemia. *Retina*. 2014;34(4):636-46.
  19. Riazi-Esfahani H, Khalili Pour E, Fadakar K, Ebrahimiadib N, Ghassemi F, Nourinia R, et al. Multimodal imaging for paracentral acute maculopathy; the diagnostic role of en face OCT. *Int J Retina Vitreous*. 2021;7(1):13.
  20. Sridhar J, Shahlae A, Rahimy E, Hong BK, Khan MA, Maguire JI, et al. Optical Coherence Tomography Angiography and En Face Optical Coherence Tomography Features of Paracentral Acute Middle Maculopathy. *Am J Ophthalmol*. 2015;160(6):1259-68.e2.
  21. Chu S, Nesper PL, Soetikno BT, Bakri SJ, Fawzi AA. Projection-Resolved OCT Angiography of Microvascular Changes in Paracentral Acute Middle Maculopathy and Acute Macular Neuroretinopathy. *Invest Ophthalmol Vis Sci*. 2018;59(7):2913-22.
  22. Schwartz R, Hykin P, Sivaprasad S. Localization of Paracentral Acute Middle Maculopathy Using Optical Coherence Tomography Angiography. *Ophthalmic Surg Lasers Imaging Retina*. 2018;49(8):619-24.
  23. Chen Y, Hu Y. The optical imaging of idiopathic paracentral acute middle maculopathy in a Chinese young man and review of the literature. *Photodiagnosis Photodyn Ther*. 2017;19:383-7.
  24. Spaide RF, Klancnik JM, Jr, Cooney MJ. Retinal vascular layers imaged by fluorescein angiography and optical coherence tomography angiography. *JAMA Ophthalmol*. 2015;133(1):45-50.
  25. Snodderly DM, Weinhaus RS, Choi JC. Neural-vascular relationships in central retina of macaque monkeys (*Macaca fascicularis*). *The Journal of neuroscience : the official journal of the Society for Neuroscience*. 1992;12(4):1169-93.
  26. Tan PE, Yu PK, Balaratnasingam C, Cringle SJ, Morgan WH, McAllister IL, et al. Quantitative confocal imaging of the retinal microvasculature in the human retina. *Invest Ophthalmol Vis Sci*. 2012;53(9):5728-36.
  27. Caprara C, Thiersch M, Lange C, Joly S, Samardzija M, Grimm C. HIF1A is essential for the development of the intermediate plexus of the retinal vasculature. *Invest Ophthalmol Vis Sci*. 2011;52(5):2109-17.
  28. Puliafito CA. OCT angiography: the next era of OCT technology emerges. *Ophthalmic Surg Lasers Imaging Retina*. 2014;45(5):360.
  29. Savastano MC, Lumbroso B, Rispoli M. In Vivo Characterization of Retinal Vascularization Morphology Using Optical Coherence Tomography Angiography. *Retina*. 2015;35(11):2196-203.
  30. Rahimy E, Sarraf D. Paracentral acute middle maculopathy spectral-domain optical coherence tomography feature of deep capillary ischemia. *Curr Opin Ophthalmol*. 2014;25(3):207-12.
  31. Nemiroff J, Kuehlewein L, Rahimy E, Tsui I, Doshi R, Gaudric A, et al. Assessing Deep Retinal Capillary Ischemia in Paracentral Acute Middle Maculopathy by Optical Coherence Tomography Angiography. *Am J Ophthalmol*. 2016;162:121-32.e1.
  32. Nemiroff J, Phasukkijwatana N, Sarraf D. Optical Coherence Tomography Angiography of Deep Capillary Ischemia. *Dev Ophthalmol*. 2016;56:139-45.
  33. Hufendiek K, Gamulescu MA, Hufendiek K, Helbig H, Marker D. Classification and characterization of acute macular neuroretinopathy with spectral domain optical coherence tomography. *Int Ophthalmol*. 2018;38(6):2403-16.
  34. Garrity ST, Tseng VL, Sarraf D. Paracentral Acute Middle Maculopathy in a Perivenular Fern-Like Distribution with En Face Optical Coherence Tomography. *Retin Cases Brief Rep*. 2018;12 Suppl 1:S25-S8.
  35. Haskes C, Santapaola S, Zinn J. An Atypical Case of Paracentral Acute Middle Maculopathy. *Optom Vis Sci*. 2017;94(8):845-50.
  36. Mendis KR, Balaratnasingam C, Yu P, Barry CJ, McAllister IL, Cringle SJ, et al. Correlation of histologic and clinical images to determine the diagnostic value of fluorescein angiography for studying retinal capillary detail. *Invest Ophthalmol Vis Sci*. 2010;51(11):5864-9.

37. Kulikov AN, Maltsev DS, Leongardt TA. Retinal Microvasculature Alteration in Paracentral Acute Middle Maculopathy and Acute Macular Neuroretinopathy: A Quantitative Optical Coherence Tomography Angiography Study. *Retin Cases Brief Rep.* 2020;14(4):343-51.
38. Iafe NA, Onclinx T, Tsui I, Sarraf D. Paracentral Acute Middle Maculopathy and Deep Retinal Capillary Plexus Infarction Secondary to Reperfused Central Retinal Artery Occlusion. *Retin Cases Brief Rep.* 2017;11 Suppl 1:S90-S3.

## 7.2.

# ACUTE MACULAR OUTER RETINOPATHY

Rita Anjos<sup>1</sup>, Diogo Maleita<sup>1</sup>, Giuseppe Casalino<sup>2</sup>

1 - Centro Hospitalar Universitário Lisboa Central

2- Oftalmico Hospital, ASST Fatebenefratelli Sacco, Milan, Italy

Acute Macular Neuroretinopathy, is an uncommon retinal condition characterized by a sudden onset of one or more paracentral scotomas<sup>1</sup>. Bos and Deutman first described this entity in 1975, reporting four young women presenting with slightly decreased visual acuity and dark-reddish, wedge-shaped intraretinal lesions pointing to the fovea<sup>1</sup>. Although initially thought as a disease of the inner retina, recent multimodal studies found the outer retina as the location for the architectural changes of this disease with no typical involvement of the optic nerve<sup>1,2</sup>. Therefore, some authors have proposed to adopt the term Acute Macular Outer Retinopathy (AMOR)<sup>2</sup>.

AMOR is a rare disease with just over 100 cases reported since its initial description<sup>3</sup>. A vascular-occlusive aetiology seems to be the most likely culprit of AMOR, but the origin and location of the vascular insult is still unclear<sup>4</sup>. Women are more commonly affected (F:M ratio 6.25:1), and most patients are in the 3<sup>rd</sup> to 4<sup>th</sup> decade of life<sup>1</sup>. The most significant environmental factors identified are infection, fever and oral contraceptives<sup>3</sup>. Other triggers including epinephrine, caffeine, trauma and system shock have also been reported<sup>3,5</sup>. This disease is characterized by a sudden onset of paracentral scotomas and mild visual impairment, with most patients presenting with 20/40 or better visual acuity. Visual improvement, if any, develops slowly over months, but most patients remain with persistent symptoms<sup>1,3</sup>. AMOR may be a challenging diagnosis since on fundus examination the lesions may be barely visible and easily overlooked, thus requiring multimodal retinal imaging, especially high resolution optical coherence tomography (OCT).

Several diagnostic tests have been used in the diagnosis of AMOR. Amsler grid or perimetry testing reveal at least one paracentral scotoma in the majority of patients<sup>3</sup>. The most striking features of this condition are the perifoveal hyporeflective wedge-shaped areas with well demarcated margins in the near infrared reflectance imaging that correlate with the described scotomata and with the lesions shape visible on biomicroscopy<sup>3</sup>. Petaloid, oval and tear-drop lesions shape have also been reported<sup>3,5</sup>. Fundus autofluorescence changes are less prominent and frequently non-existent, although corresponding areas of hypo or hyperautofluorescence have been described<sup>3</sup>. OCT is sensitive for the detection of structural abnormalities in AMOR. Earliest abnormalities occur

at the outer plexiform layer, even before the appearance of lesions on near-infrared reflectance imaging<sup>6</sup>. In the course of disease, almost all AMOR eyes have OCT changes such as outer retinal hyper-reflectivity, ellipsoid zone disruption, outer nuclear layer thinning and/or hyperreflectivity as well as generalized retinal thinning. Although not all patients develop persistent changes over time, thinning of the outer nuclear layer associated with permanent scotomata frequently occur<sup>3,6</sup>. Fluorescein angiography is usually silent in this disease, although some abnormalities such as subtle hypofluorescence of the lesion or, less frequently, dilatation of the perimacular capillaries or punctate hyperfluorescence with late staining have been reported. Indocyanine green angiography is typically normal in AMOR, with a few reports of early hypofluorescence<sup>6</sup>.

OCT angiography (OCTA) came as a promising opportunity for the diagnosis and physiopathology clarification of this disease. Although AMOR is rare, several OCTA studies have been recently published with interesting findings. Perfusion of the deep capillary plexus (DCP) in this disease is not consensual between authors. Although some papers have reported a reduction in the perfusion of the DCP in the corresponding lesion area<sup>4,7,8</sup>, others failed to find any abnormality in this vascular network<sup>9,10</sup>. Choriocapillaris (CC) flow abnormalities in the same location of AMOR lesions have been also described and seem to be present even after artifact removal<sup>4,8-10</sup>. One study also found a general flow void in these patients although preservation of the global vascular perfusion of the retinal plexus was observed<sup>4</sup>.

These novel findings from OCTA and OCT imaging led to several hypothesis for the location of the primary vascular insult: either on the CC with secondary focal involvement of the DCP at the level of impaired photoreceptors axon terminals; or at the DCP with a decrease of photoreceptor function and subsequent less oxygen demand leading to a secondary CC dysfunction<sup>4</sup>. The choroid is the main oxygen supplier of the photoreceptors that seems to be the ultimate target of this disease<sup>4</sup>. The morphology and location of the lesions in AMOR are also identical to the histological descriptions of the CC lobules anatomy<sup>4</sup> and the multilobular pattern frequently seen could be the result of an insult to collecting veins<sup>9</sup>. Some authors have even considered a possible shared pathophysiologic



mechanism between AMOR and APMPPE, with both representing a spectrum of disorders depending on the level of choroidal involvement<sup>9</sup>. It is possible that a reduction in the perfusion of the DCP that supply oxygen to several cells involved in the photoreceptor homeostasis could also be responsible for the AMOR lesions<sup>4</sup>. This vascular network may be detrimental for the photoreceptors axons terminals located in the outer plexiform layer and could explain the infrequent location

on these lesions in the fovea where this layer is absent<sup>9</sup>. An alternative hypothesis is that a vascular primary insult could initially occur in either vascular bed with secondary injury of the other through an inflammatory mechanism<sup>8</sup>. In conclusion, multimodal retinal imaging is essential for the diagnosis of AMOR which is quite a rare and challenging condition to diagnose. Latest developments of retinal imaging such as OCTA have made it possible to highlight insights on the pathogenesis of this condition.

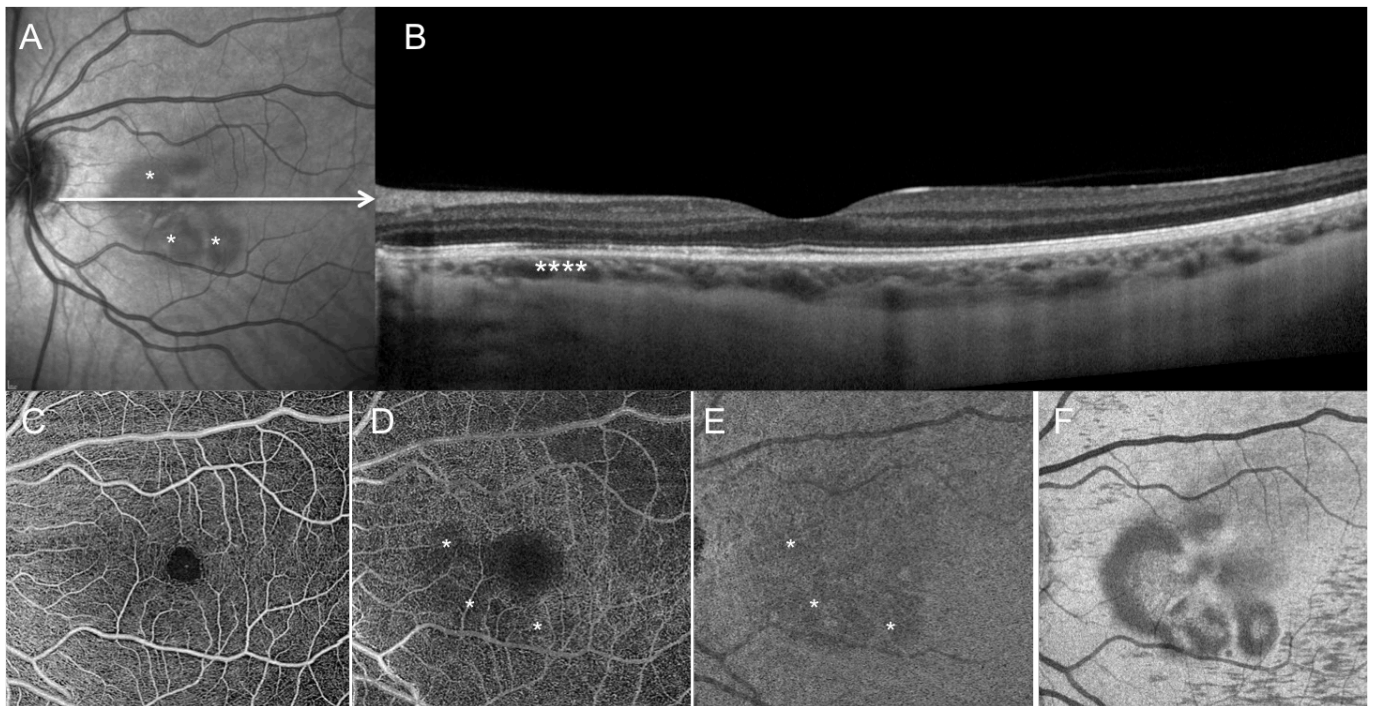


**Figure 1.** Multimodal imaging features of acute macular outer retinopathy in the left eye.

Near-infrared reflectance (NIR) imaging (A) shows wedge-shaped perifoveal hyporeflective lesions. (B) Simultaneous acquisition of optical coherence tomography (OCT) shows attenuation of the ellipsoid zone (asterisks) and overlying thinning of the outer nuclear layer. OCT angiography shows normal vascular flow at the level of the superficial capillary plexus (C) and vascular flow void (asterisks) in the deep capillary plexus (D) and choriocapillaris (E). Enface OCT slab at the level of the ellipsoid zone (F) shows hyporeflective lesions that colocalise with the hyporeflectivity seen on NIR imaging.

## REFERENCES

1. Bos PJM, Deutman AF. Acute macular neuroretinopathy. *Am J Ophthalmol.* 1975;80(4):573–84.
2. Yeh S, Hwang TS, Weleber RG, Watzke RC FP. Acute Macular Outer Retinopathy (AMOR): A Reappraisal of Acute Macular Neuroretinopathy Using Multimodality Diagnostic Testing. *Arch Ophthalmol.* 2011;129(3):360–371.
3. Bhavsar K V, Lin S, Rahimy E, Joseph A, Freund KB, Sarraf D, et al. Acute macular neuroretinopathy: A comprehensive review of the literature. *Surv Ophthalmol.* 2016;61(5):538–65.
4. Casalino G, Arrigo A, Romano F, Munk MR, Bandello F, Parodi MB. Acute macular neuroretinopathy: Pathogenetic insights from optical coherence tomography angiography. *Br J Ophthalmol.* 2019;103(3):410–4.
5. Rahimy E, Kuehlewein L, Sadda SR SD. Paracentral Acute Middle Maculopathy: What We Knew Then and What We Know Now. *Retina.* 2015;35(10):1921–30.
6. Fawzi AA, Pappuru RR, Sarraf D, Le PP, McCannel CA, Sobrin L, et al. Acute macular neuroretinopathy: Long-term insights revealed by multimodal imaging. *Retina.* 2012;32(8):1500–13.
7. Nemiroff J, Sarraf D, Davila JP, Rodger D. Optical coherence tomography angiography of acute macular neuroretinopathy reveals deep capillary ischemia. *Retin Cases Brief Rep.* 2018;12:S12–5.
8. Hwang CK, Sen HN. Concurrent vascular flow defects at the deep capillary plexus and choriocapillaris layers in acute macular neuroretinopathy on multimodal imaging: A case series. *Am J Ophthalmol Case Reports.* 2020;20.
9. Lee SY, Cheng JL, Gehrs KM, Folk JC, Sohn EH, Russell SR, et al. Choroidal features of acute macular neuroretinopathy via optical coherence tomography angiography and correlation with serial multimodal imaging. *JAMA Ophthalmol.* 2017;135(11):1177–83.
10. Thanos A, Faia LJ, Yonekawa Y, Randhawa S. Optical coherence tomographic angiography in acute macular neuroretinopathy. *JAMA Ophthalmol.* 2016;134(11):1310–4.



## 7.3.

# CENTRAL RETINAL VEIN OCCLUSION

Lígia Ribeiro, Filipe Sousa Neves  
Centro Hospitalar Vila Nova de Gaia/Espinho

## INTRODUCTION

Central Retinal Vein occlusion (CRVO) is a common retinal vascular disorder that may lead to significant visual morbidity. Visual outcome depends on the severity of retinal ischemia and macular edema (ME). Therefore, evaluation of the retinal vasculature is important for determining the therapeutic strategy and prognosis<sup>1-3</sup>. Fluorescein angiography (FA) is the gold standard for evaluation of retinal capillary non-perfusion and neovascularization, while spectrum-domain optical coherence tomography (OCT) enables assessment of the structural changes of the retina, including the presence and amount of ME<sup>4</sup>. Conventional FA provides two-dimensional images with dynamic visualization of blood flow in both central and peripheral retina and information concerning the health of vessels can be assessed by looking for patterns of leakage, pooling and staining. However, FA is time-consuming and involves the use of intravenous contrast agent, which is associated with common minor adverse effects and a small risk of serious complications<sup>5</sup>. Precise evaluation of the vasculature at different capillary levels is not feasible with FA and it may not always yield clear images of the foveal avascular zone (FAZ) which has prognostic value in CRVO, due to the presence of hemorrhage or edema<sup>6</sup>.

Evidence suggests that the superficial and deep retinal capillary plexus may be disproportionately affected in retinal vascular diseases. Optical coherence tomography angiography (OCTA) can evaluate the microvascular structures of the retina and the choriocapillaris, layer by layer, and provide additional information in patients with CRVO<sup>4,7</sup>.

## ADVANTAGES AND LIMITATIONS OF OCTA

OCTA's advantages include its rapid, easy and comfortable image acquisition, and dye independency. The absence of leakage and tissue staining, and the better penetration of the longer wavelengths used in OCTA through intraretinal hemorrhage, allows better visualization of the microvascular abnormalities, including delineation of the FAZ<sup>5</sup>. The ability of OCTA to outline microvascular changes and ischemia in both the superficial capillary plexus (SCP) and the deep capillary plexus (DCP) is a

major advantage because many of the vascular changes in CRVO occur in the DCP, which cannot be visualized by FA. OCT angiograms come cross-registered with OCT B-scans enabling accurate correlation between the vascular to the structural scans<sup>6,8</sup>.

Limitations of OCTA in CRVO include restricted field of view, motion artifacts in patients with poor fixation or poor vision and the absence of dynamic flow and vascular leakage information. The main concern about OCTA image interpretation is the presence of artifacts, mainly segmentation, projection, and masking artifacts. Significant retinal thinning or macular edema causes distortion of the retinal architecture, making delineation of the retinal layers for automated segmentation of the SCP and DCP challenging and less accurate. Assessment of vascular nonperfusion in CRVO may be limited by signal attenuation in the presence of macular edema, shadowing artifacts caused by retinal hemorrhages and projection artifacts of the superficial vessels over the deeper retinal layers<sup>9,10</sup>.

Software platforms lack normalized data to determine whether microvascular changes are abnormal, and the reliability of FAZ measurements using OCTA in vascular retinal disease is unclear<sup>11</sup>.

## OCTA QUALITATIVE FINDINGS IN EYES WITH CRVO

OCTA may be used to identify microvascular changes of acute and chronic CRVO in both the superficial and deep capillary networks of the retina. Findings include vascular tortuosity, capillary engorgement and telangiectasias, disruption of the perifoveal arcade, impaired capillary perfusion, macular edema and formation of collateral vessels<sup>6-9</sup>.

OCTA showed to be more effective than FA in CRVO in displaying and analyzing the macular capillary network and the perifoveal capillary arcade (Figure 1) and also to detect the presence of macular edema<sup>7,12</sup>. Coscas et al. found that the degree of disruption of the perifoveal capillary network is correlated with the presence of peripheral ischemia in FA and the degree of non-perfusion in the DCP. On FA, peripheral ischemia in cases with an intact perifoveal capillary network was not found and they suggested that OCTA may be a screening tool to decide whether to perform FA<sup>7</sup>.

Non-perfusion areas (NPA) correspond to hypointense dark areas of undetectable flow on OCTA<sup>7,9</sup>. Patients with retinal vein occlusion (RVO) may show decreased vascular perfusion in both the SCP and the DCP of the fellow eye, compared to controls, suggesting that structural alterations may indicate a predisposition to ocular vascular complications<sup>13-15</sup>.

Cystoid macular edema appears as round dark areas with smooth borders (Figure 2). The presence of cystoid

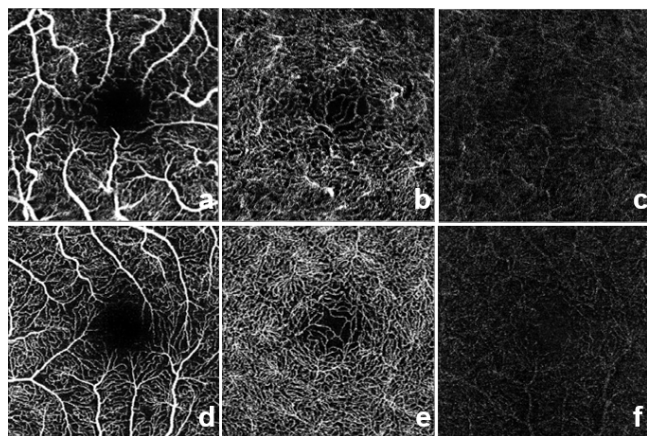


**Figure 1.** OCT angiogram of a 61 year-old female with central retinal vein occlusion with resolved macular edema in the right eye. (a-c) showing structural vascular changes compared to the fellow eye (d-e). a,d. Superficial Vascular complex b,e. Deep Vascular complex c,f. Avascular complex.

edema may lead to the displacement of vessels, inaccurate segmentation and signal attenuation. This may hamper detection of capillaries and result in overestimation of the degree of non-perfusion<sup>8</sup>.

Several studies showed consistent findings of more marked vascular changes in the DCP versus the SCP that may reflect greater susceptibility to damage in the DCP<sup>7,9,16,17</sup>.

OCTA shows optic disc venous collaterals (OVC) as small, loopy vessels at the level of the superficial peripapillary plexus (Figure 3) whereas neovascular vessels (NVD) are visible as a mesh of fine vessels above the retina at the level of the vitreous. OCTA delineates OVCs better than fundus photographs or FA. Furthermore, new vessels are more clearly visible, due to the absence of leakage in OCTA<sup>18</sup>.

### OCTA QUANTITATIVE FINDINGS IN EYES WITH CRVO

Quantitative measurements of the FAZ and NPA areas, vascular density, perfusion in the SCP, DCP and choriocapillaris, their correlation with macular function, and their changes after treatment, are areas of active research in RVO<sup>7,12,14-17,19-21</sup>.

Despite the variability of the FAZ size in normal individuals, it is enlarged in the DCP of RVO eyes, comparing to normal controls and fellow eyes, and to the FAZ of the SCP<sup>12,22</sup>. De Salles et al. showed a significant correlation between an enlarged FAZ and poorer visual outcome in patients who have CRVO without macular

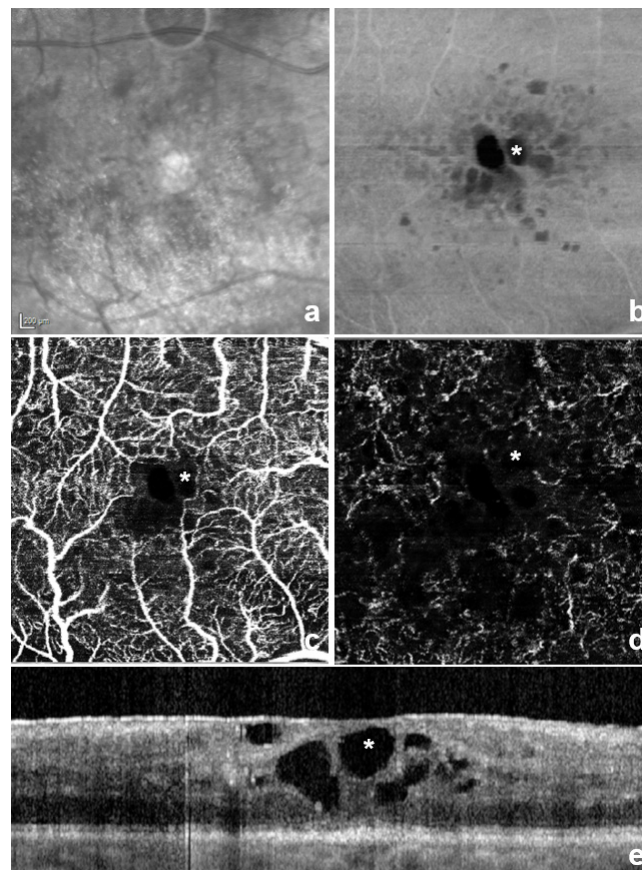


**Figure 2.** Macular edema in a 77 year-old male with acute central retinal vein occlusion. a. Infra-red image b. En face OCT c. OCT angiogram of the Superficial Vascular Complex d. OCT angiogram of the Deep Vascular Complex e. OCT B-scan (white asterisk correspond to intraretinal cysts).

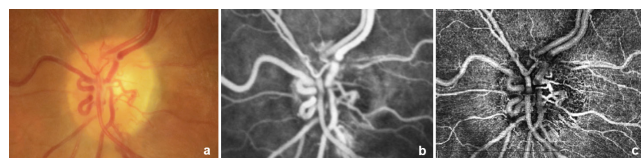


**Figure 3.** Optociliary shunt vessels in a 63 year-old female with central retinal vein occlusion. a. Color fundus photograph of the optic nerve b. Mid-late-phase fluorescein angiography c. OCT angiogram of the optic nerve.

edema<sup>22</sup>. Suzuki et al proposed that the FAZ size may be related to the intraocular VEGF levels, as they found larger FAZs in both plexuses in eyes receiving fewer intraocular injections<sup>12</sup>. The macular NPA measured by OCTA was found to correlate strongly with the visual acuity and macular sensitivity in patients with CRVO who have had previous ME<sup>23</sup>. These results support the notion that, in addition to foveal photoreceptor integrity, macular perfusion contributes to visual outcomes in eyes with RVO and reflects macular sensitivity more closely than visual acuity.

Several studies reported a positive correlation between

microvascular changes in the macula in OCTA and peripheral ischemia<sup>7,14,16,19</sup>. In a retrospective study that automatically quantified macular vascular density on OCTA, Seknazy et al. found that when the DCP vascular density decreased to less than 46% in eyes with CRVO, peripheral retinal non-perfusion becomes probable. Therefore, the use of this limit was suggested as an indication for performing FA in CRVO patients<sup>19</sup>. Khodabandeh et al. proposed a reducing formula using OCTA parameters to recognize the ischemic type of CRVO<sup>14</sup>.

Using conventional OCTA parameters and fractal-based potential biomarkers, Cabral et al. identified vascular patterns in the central macula associated with peripheral nonperfusion on FA<sup>24</sup>. Significant ischemia was defined as nonperfusion areas superior or equal to the equivalent of one retinal quadrant on FA. These findings suggest that perifoveal and foveal changes seen on OCTA are surrogates of ischemic changes in the peripheral retina on FA.

The utility of OCTA quantitative parameters in monitoring treatment response is a promising application of OCTA in the CRVO management. Sellam et al. investigated 28 eyes with RVO treated with anti-VEGF agents<sup>20</sup>. Post-treatment OCTA showed significant decreases in the perifoveal capillary arcade, disruption, macular cysts, and vascular dilation in the SCP and DCP. NPA size has been shown to decrease, while the blood flow area increases following anti-VEGF treatment, mostly in DCP<sup>12</sup>.

## CONCLUSION

OCTA visualizes the CRVO-related vessel changes spatially separated into different retinal layers, which has been unachievable so far by conventional FA, and will help us understand findings in the complex microvasculature of the macula after vein occlusions. It may have a prognostic value in the visual outcome and in distinguishing presumable ischemic from non-ischemic CRVO. OCTA has great potential for measuring and monitoring macular ischemia during and after treatment. Further improvement of OCTA is still required for there to be as prominent in the daily routine practice as FA is. However, currently, OCTA may provide most of the multidimensional information needed to manage patients with vein occlusions, obviating the need for invasive techniques in some cases. Future larger, prospective studies will help to define the role of OCTA in the workup and management of CRVO.

## REFERENCES

- Hayreh SS, Podhajsky PA, Zimmerman MB. Natural history of visual outcome in central retinal vein occlusion. *Ophthalmology*. 2011;118(1):119-133.e2.
- McIntosh RL, Rogers SL, Lim L, Cheung N, Wang JJ, Mitchell P, et al. Natural History of Central Retinal Vein Occlusion: An Evidence-Based Systematic Review. *Ophthalmology*. 2010;117(6):1094-1101.e5. 2010;117(6):1113-1123.e15.
- Hayreh SS, Zimmerman MB. Fundus changes in central retinal vein occlusion. *Retina*. 2015;35(1):29-42.
- Hirano Y, Suzuki N, Tomiyasu T, Kurobe R, Yasuda Y, Esaki Y, et al. Multimodal Imaging of Microvascular Abnormalities in Retinal Vein Occlusion. *J Clin Med*. 2021;10(3):405.
- Spaide RF, Klancnik JM, Cooney MJ. Retinal vascular layers imaged by fluorescein angiography and optical coherence tomography angiography. *JAMA Ophthalmol*. 2015;133(1):45-50.
- Tsai G, Banaee T, Conti FF, Singh RP. Optical coherence tomography angiography in eyes with retinal vein occlusion. *J Ophthalmic Vis Res*. 2018;13(3):315-32.
- Coscas F, Glacet-Bernard A, Miere A, Caillaux V, Uzzan J, Lupidi M, et al. Optical Coherence Tomography Angiography in Retinal Vein Occlusion: Evaluation of Superficial and Deep Capillary Plexa. *Am J Ophthalmol*. 2016;161:160-171.e2.
- Novais EA, Waheed NK. Optical Coherence Tomography Angiography of Retinal Vein Occlusion. *Dev Ophthalmol*. 2016;56:132-8.
- Kashani A, Lee S, Moshfeghi A, Durbin M, Puliafito C. Optical Coherence Tomography Angiography of Retinal Venous Occlusion. *Retina*. 2015;35(11):2323-31.
- Nobre Cardoso J, Keane PA, Sim DA, Bradley P, Agrawal R, Addison PK, et al. Systematic Evaluation of Optical Coherence Tomography Angiography in Retinal Vein Occlusion. *Am J Ophthalmol*. 2016;163:93-107.e6.
- De Oliveira BMR, Nakayama LF, De Godoy BR, De Azevedo AGB, Hirai FE, Mitne S. Reliability of foveal avascular zone measurements in eyes with retinal vein occlusion using optical coherence tomography angiography. *Int J Retin Vitre*. 2020;6(1):1-6.
- Suzuki N, Hirano Y, Tomiyasu T, Esaki Y, Uemura A, Yasukawa T, et al. Retinal hemodynamics seen on optical coherence tomography angiography before and after treatment of retinal vein occlusion. *Invest Ophthalmol Vis Sci*. 2016;57(13):5681-7.
- Wang Q, Chan SY, Yan Y, Yang J, Zhou W, Jonas JB, et al. Optical coherence tomography angiography in retinal vein occlusions. *Graefes Arch Clin Exp Ophthalmol*. 2018;256(9):1615-22.
- Khodabandeh A, Shahraki K, Roohipoor R, Riazi-Esfahani H, Yaseri M, Faghihi H, et al. Quantitative measurement of vascular density and flow using optical coherence tomography angiography (OCTA) in patients with central retinal vein occlusion: Can OCTA help in distinguishing ischemic from non-ischemic type? *Int J Retin Vitre*. 2018;4(1):1-11.
- Adhi M, Bonini Filho MA, Louzada RN, Kuehlewein L, De Carlo TE, Bauman CR, et al. Retinal capillary network and foveal avascular zone in eyes with vein occlusion and fellow eyes analyzed with optical coherence tomography angiography. *Invest Ophthalmol Vis Sci*. 2016;57(9):486-94.
- Mastropasqua R, Toto L, Di Antonio L, Borrelli E, Senatore A, Di Nicola M, et al. Optical coherence tomography angiography microvascular findings in macular edema due to central and branch retinal vein occlusions. *Sci Rep*. 2017;7(December 2016):40763.
- Kang JW, Yoo R, Jo YH, Kim HC. Correlation of microvascular structures on optical coherence tomography angiography with visual acuity in retinal vein occlusion. *Retina*. 2017;37(9):1700-9.
- Singh A, Agarwal A, Mahajan S, Karkhur S, Singh R, Bansal

- R, et al. Morphological differences between optic disc collaterals and neovascularization on optical coherence tomography angiography. *Graefes Arch Clin Exp Ophthalmol*. 2017;255(4):753–9.
19. Seknazi D, Coscas F, Sellam A, Rouimi F, Coscas G, Souied EH, et al. Optical Coherence Tomography Angiography in Retinal Vein Occlusion. *Retina*. 2018;38(8):1562–70.
  20. Sellam A, Glacet-Bernard A, Coscas F, Miere A, Coscas G, Souied EH. Qualitative and quantitative follow-up using optical coherence tomography angiography of retinal vein occlusion treated with anti-vegf. *Retina*. 2017;37(6):1176–84.
  21. Kaidonis G, Leng T. Optical Coherence Tomography Angiography in Retinal Vein Occlusion: Quantifying Macular Ischemia. *Curr Ophthalmol Rep*. 2018;6(1):1–6.
  22. De Salles MC, Kvanta A, Amrén U, Epstein D. Optical coherence tomography angiography in central retinal vein occlusion: Correlation between the foveal avascular zone and visual acuity. *Invest Ophthalmol Vis Sci*. 2016;57(9):OCT242–6.
  23. Ghashut R, Muraoka Y, Ooto S, Iida Y, Miwa Y, Suzuma K, et al. Evaluation of Macular Ischemia in Eyes With Central Retinal Vein Occlusion. *Retina*. 2018;38(8):1571–80.
  24. Cabral D, Coscas F, Glacet-Bernard A, Pereira T, Geraldès C, Cachado F, et al. Biomarkers of peripheral nonperfusion in retinal venous occlusions using optical coherence tomography angiography. *Transl Vis Sci Technol*. 2019;8(3).

## 7.4.

# BRANCH RETINAL VEIN OCCLUSION

Teresa Quintão<sup>1</sup>, Sandra Barrão<sup>2</sup>

1 - Santa Casa da Misericórdia de Lisboa, Instituto de Retina de Lisboa

2 - Instituto de Oftalmologia Dr Gama Pinto

Branch Retinal Vein Occlusion (BRVO) is the most common form of presentation of retinal venous occlusion. A review of 2019<sup>1</sup> estimates a mean overall prevalence of 0.64% (23.38 million affected individuals). Several studies have been published in last years reporting OCTA findings in patients with retinal venous occlusion, allowing mainly for evaluation of ischemia.

Moussa<sup>2</sup> et al. described ischemia of the superficial capillary plexus and of the deep capillary plexus as predictors of poor visual outcome.

OCTA contributes to the study of the vascular network, without the need of invasive procedures. However it has limitations comparatively to fluorescein angiography, in particular the limited field of the analysis and the impossibility of confirming leakage from abnormal vessels. Widefield OCTA overcomes the first of this limitations when accessible.<sup>3,4</sup>

Several works have reported<sup>5-9</sup> multiple microvascular changes related with ischemia and vascular abnormalities

found in OCTA - decrease in vascular densities, enlargement of foveal avascular zone, capillary non-perfusion areas, microvascular abnormalities, capillary engorgement and telangiectasias, vascular tortuosity, microaneurysms and collateral vessels.

Iida et al.<sup>10</sup> evaluated arteriovenous crossing patterns with OCTA allowing its classification as arterial overcrossing, venous overcrossing and helical overcrossing being the proportion of patterns observed superior to fluorescein angiography. Same authors concluded macular and peripheral non perfusion area was larger in eyes with venous overcrossing comparatively with those eyes with arterial overcrossing. These authors also reported regarding collateral vessel formation patients with good prognosis showed either abundant collateral formation and venous narrowing near the arteriovenous crossing or minimal collateral formation and non perfusion area around the crossing.

Some cases of BRVO are illustrated in Figures 1-5.

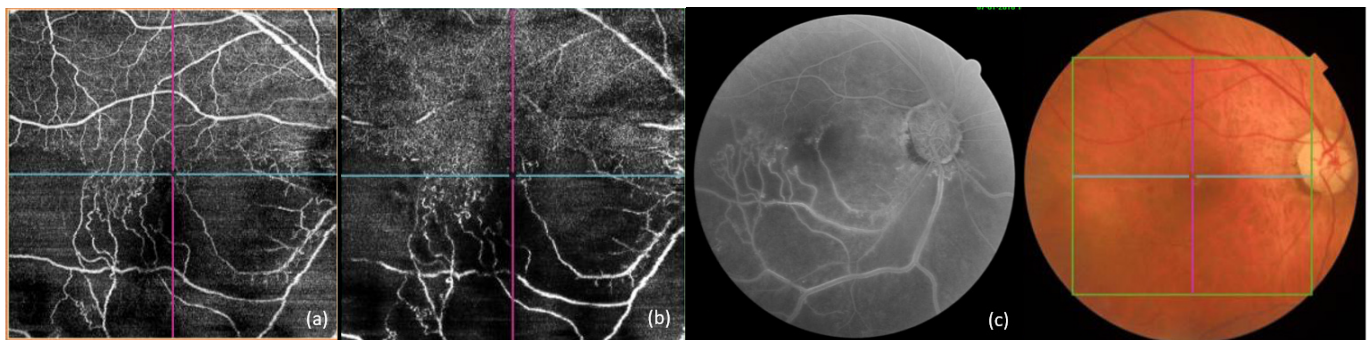


**Figure 1.** Inferior BRVO

(a) OCTA (12x12 mm) at the level of the superficial capillary plexus (SCP) showing vascular tortuosity, dilation and telangiectasia along non-perfusion areas in the inferior region. (b) OCTA at the level of the deep capillary plexus (DCP). (c) Fluorescein angiography (FA). (d) Fundus coloured retinography.



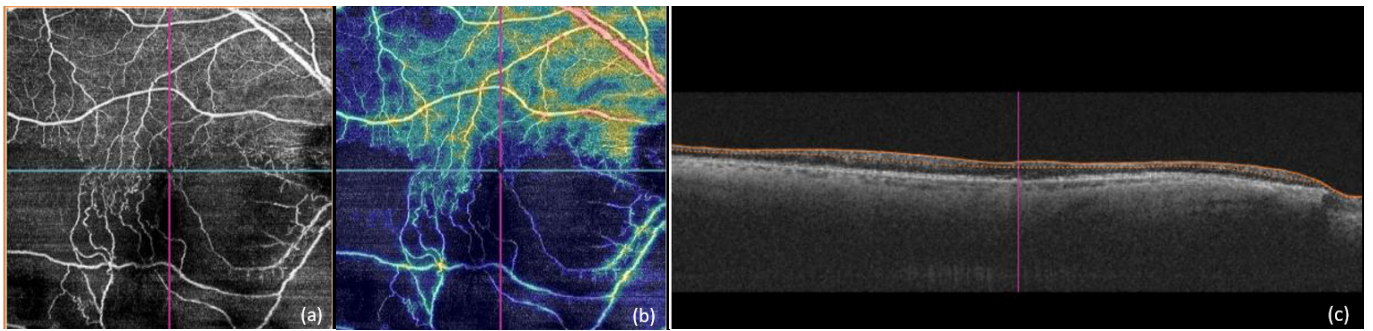


**Figure 2.** Inferior BRVO (same case of Fig. 1)

(a) OCTA (12x12 mm) at the level of the superficial capillary plexus (SCP) showing vascular tortuosity, dilation and telangiectasia along non-perfusion areas in the inferior region. (b) Color-coded vascular density map showing decreased vascular density corresponding to non-perfusion/no flow detected areas. (c) Horizontal cross-sectional B-scan OCT with segmentation lines showing atrophy in the level of OCTA in (a).

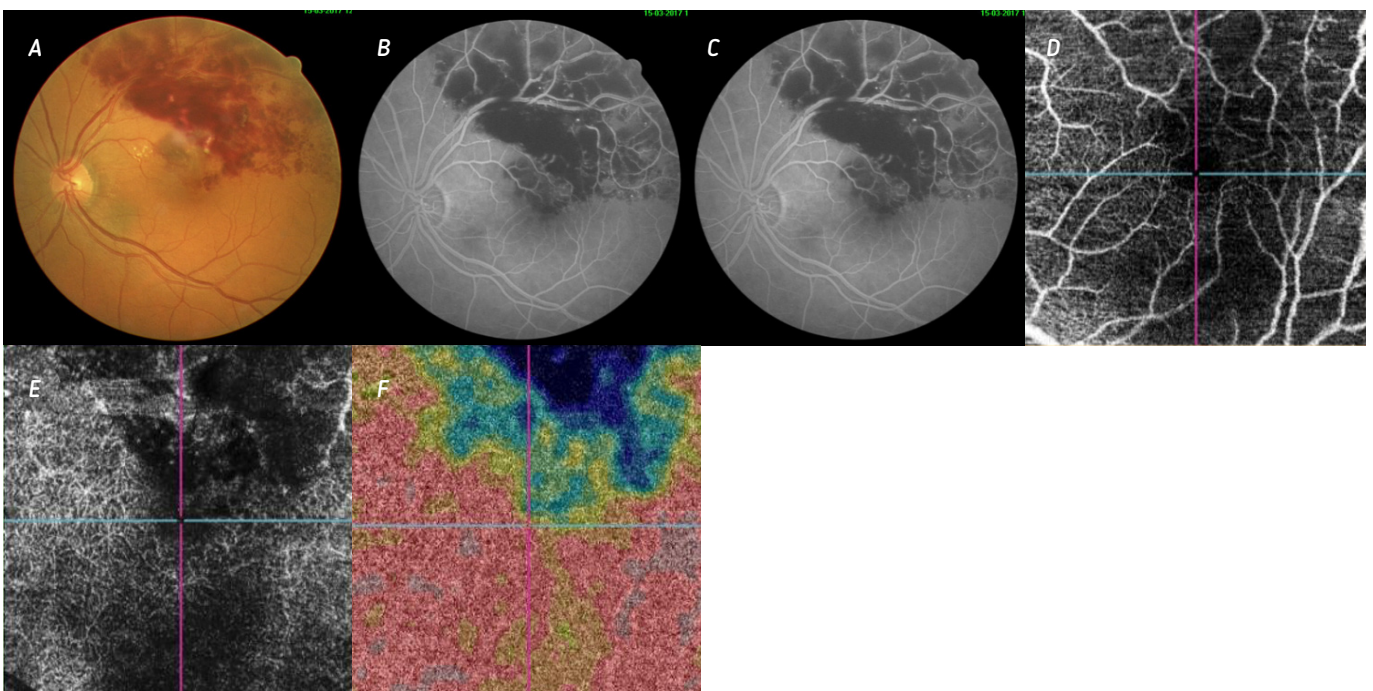


**Figure 3.** Superotemporal BRVO. (a) Fundus coloured retinography showing hemorrhages and exudates. (b) Fluorescein angiography (FA) showing mask effects of hemorrhage. (c) fundus localizing 3D macular acquisition OCTA (4,5x4,5 mm). (d) OCTA at the level of the superficial capillary plexus (SCP) showing vascular tortuosity, dilation and telangiectasia along non-perfusion areas in the superotemporal region. (e) OCTA at the level of the deep capillary plexus (DCP) showing non-perfusion/no flow detected areas, more evident than in SCP. Also note the irregular and enlarged foveal avascular zone. (f) Color-coded vascular density map showing decreased vascular density corresponding to non-perfusion areas.

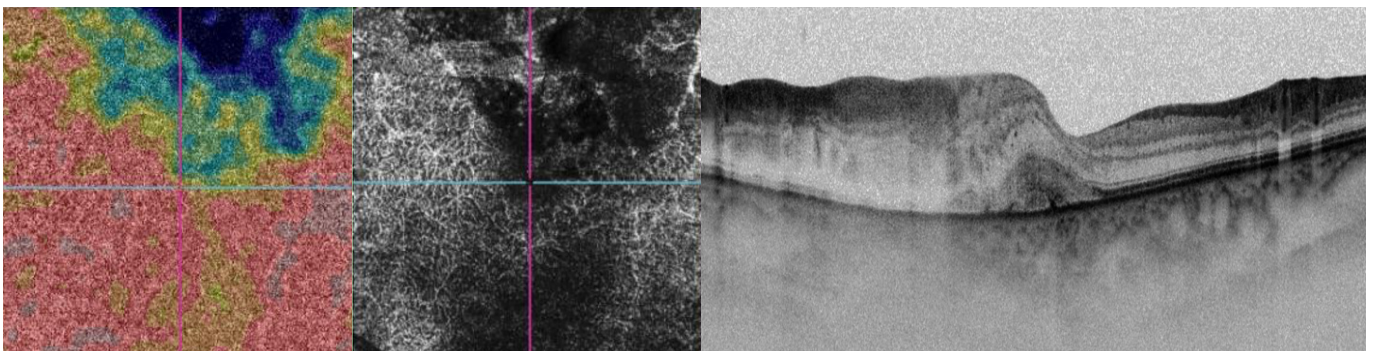


**Figure 4.** Superotemporal BRVO (same case of Fig.3). (a) OCTA at the level of the superficial capillary plexus (SCP). (b) OCTA at the level of the deep capillary plexus (DCP) showing areas of non-perfusion/no flow detected areas. (c) Vertical cross-sectional B-scan OCT. Note the presence of macular edema in the affected area that may cause misinterpretation when cystoid considering automatic layers segmentation.

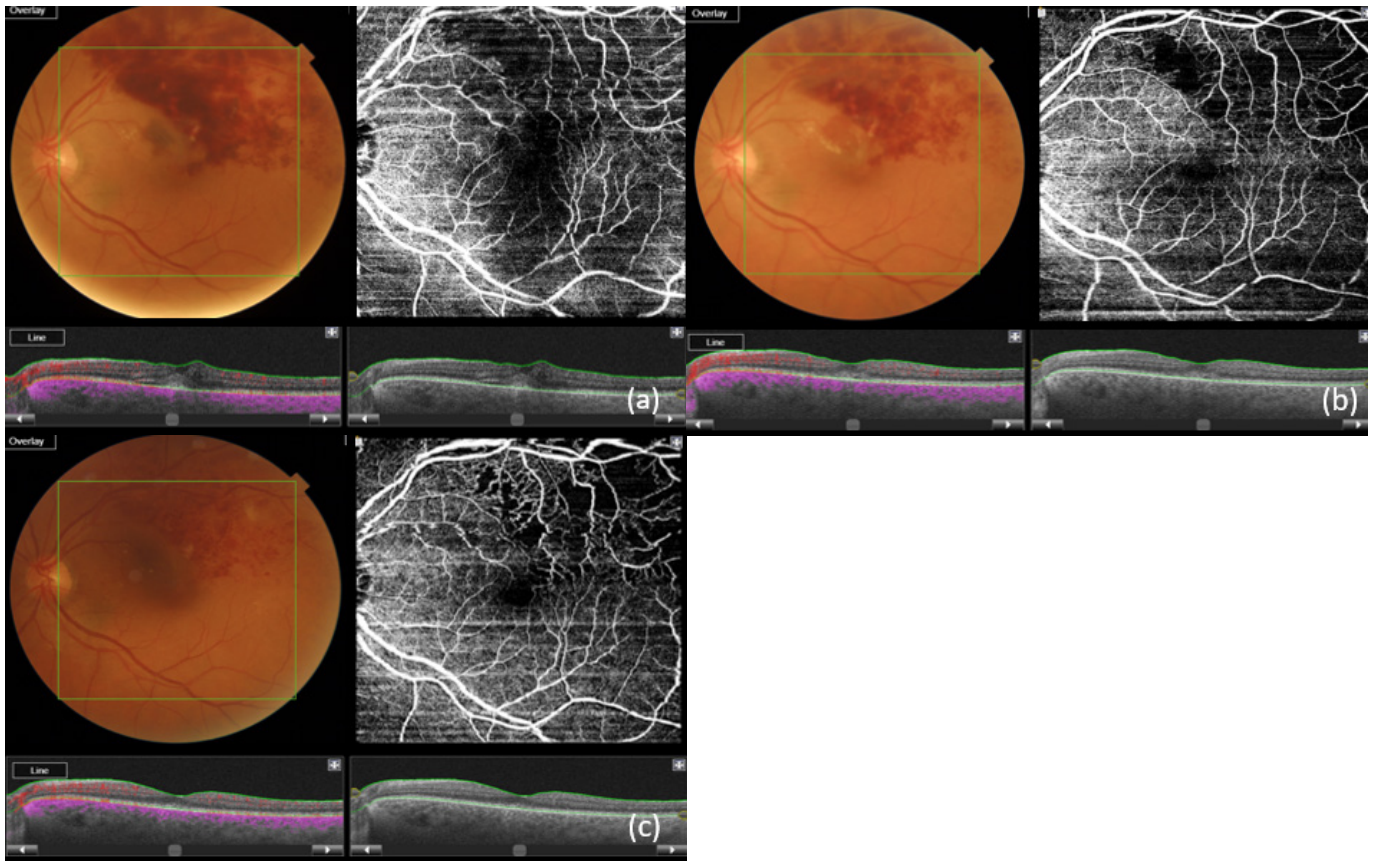


**Figure 5.** BRVO follow up (a) one week. (b) one month. (c) four months.

Fundus coloured retinography, OCTA (12x12 mm) full macula (SCP + DCP), B-scan OCT with perfusion overlay and segmentation lines showing the level of OCTA. It is possible to identify macular edema reabsorption in B-scan, partial reperfusion of ischemic areas.

Although treatment is to be done based in visual acuity and central retinal thickness measured in OCT, OCTA seems to be an interesting way of evaluating vascular features and ischemia evolution.

Stratified analysis of the retina in cases of BRVO allows a detailed study of the retina of these patients contributing to a better understanding of the mechanisms behind vascular occlusion and also provides means of detailed clinical evaluation, improving treatment and follow-up.<sup>11</sup>

## REFERENCES

- 1 - Song P, Xu Y, Zha M, Zhang Y, Rudan I. Global epidemiology of retinal vein occlusion: a systematic review and meta-analysis of prevalence, incidence, and risk factors. *J Glob Health*. 2019;9(1):010427.
- 2 - Moussa M, Leila M, Bessa AS, Lolah M, Abou Shousha M, El Hennawi HM, Hafez TA. Grading of macular perfusion in retinal vein occlusion using en-face swept-source optical coherence tomography angiography: a retrospective observational case series. *BMC Ophthalmol*. 2019;19(1):127.
- 3 - Kadomoto S, Muraoka Y, Uji A, Tamiya R, Oritani Y, Kawai K, Ooto S, Murakami T, Iida-Miwa Y, Tsujikawa A. Nonperfusion Area Quantification in Branch Retinal Vein Occlusion: a Widefield Optical Coherence Tomography Angiography Study. *Retina*. 2021;41(6):1210-1218.
- 4 - Shiraki A, Sakimoto S, Tsuboi K, Wakabayashi T, Hara C, Fukushima Y, Sayanagi K, Nishida K, Sakaguchi H, Nishida K. Evaluation of retinal nonperfusion in branch retinal vein occlusion using wide-field optical coherence tomography angiography. *Acta Ophthalmol*. 2019;97(6):e913-e918.
- 5 - Tsai G, Banaee T, Conti FF, Singh RP. Optical Coherence Tomography Angiography in Eyes with Retinal Vein Occlusion. *J Ophthalmic Vis Res*. 2018;13(3):315-332.
- 6 - Rispoli M, Savastano MC, Lumbroso B. Capillary Network Anomalies in Branch Retinal Vein Occlusion on Optical Coherence Tomography Angiography. *Retina*. 2015 ;35(11):2332-8.
- 7 - Chen L, Yuan M, Sun L, Wang Y, Chen Y. Evaluation of microvascular network with optical coherence tomography angiography (OCTA) in branch retinal vein occlusion (BRVO). *BMC Ophthalmol*. 2020;20(1):154.
- 8 - Kim JT, Chun YS, Lee JK, Moon NJ, Yi DY. Comparison of Vessel Density Reduction in the Deep and Superficial Capillary Plexuses in Branch Retinal Vein Occlusion. *Ophthalmologica*. 2020;243(1):66-74.
- 9 - Suzuki N, Hirano Y, Tomiyasu T, Kurobe R, Yasuda Y, Esaki Y, Yasukawa T, Yoshida M, Ogura Y. Collateral vessels on optical coherence tomography angiography in eyes with branch retinal

- vein occlusion. *Br J Ophthalmol.* 2019;103(10):1373-1379.
- 10 - Iida Y, Muraoka Y, Ooto S, Suzuma K, Murakami T, Iida-Miwa Y, Ghashut R, Tsujikawa A. Morphologic and Functional Retinal Vessel Changes in Branch Retinal Vein Occlusion: An Optical Coherence Tomography Angiography Study. *Am J Ophthalmol.* 2017; 182:168-179.
- 11 - Choi KE, Yun C, Cha J, Kim SW. OCT angiography features associated with macular edema recurrence after intravitreal bevacizumab treatment in branch retinal vein occlusion. *Sci Rep.* 2019;9(1):14153.

# ARTERIAL OCCLUSIONS

Luísa Vieira, Catarina Mota  
Centro Hospitalar Universitário de Lisboa Central

Retinal artery occlusion (RAO) includes transient monocular vision loss (TMVL, amaurosis fugax or retinal transient ischemic attack), branch retinal artery occlusion (BRAO) and central artery retinal occlusion (CRAO). While TMVL does not produce permanent ischemic damage of internal retina, BRAO and CRAO do so. In a consensus statement in 2013<sup>1</sup>, the American Heart Association and American Stroke Association defined central nervous system infarction as “brain, spinal cord, or retinal cell death attributable to ischemia”. TMVL is considered the retinal equivalent of a cerebral transient ischemic attack and BRAO and CRAO are considered the retinal equivalent of cerebral ischemia<sup>2</sup>.

TMVL is the most common form of acute retinal arterial ischemia and its incidence has been estimated to be approximately 14 per 100.000 people per year, while the incidence of CRAO is approximately 1–2 in 100.000<sup>3</sup>. The incidence of acute retinal arterial ischemia increases with age, likely due to an increased prevalence of cardiovascular disease associated with aging.

The most common cause of acute retinal arterial ischemia is an embolic phenomenon from the ipsilateral carotid artery, aortic arch or heart, often associated with carotid atheromatous stenosis, cardiac valve disease or atrial fibrillation<sup>4</sup>. In patients less than 50 years old and/or without associated cardiovascular risk factors coagulation disorders, inflammatory and infectious diseases, and less frequently, trauma induced or ocular conditions must be ruled out. Although less common, any patient over 50 years old who presents with CRAO and has systemic symptoms, such as temporal headache, temporal artery tenderness on palpation or jaw claudication, giant cell arteritis needs to be considered, as the treatment differs. Treatment can be divided into acute treatment, directed at resolving the BRAO/CRAO and improving visual outcome and secondary prevention of subsequent ischemic events and ocular complications. To date, there is no consensus in what concerns the best treatment in the acute phase<sup>4</sup>. There is a lack of randomized clinical trials (RCT), which is related to the low prevalence of the disease and also to the known narrow temporal window of intervention. Although multiple interventions have been attempted to restore ocular perfusion, the majority

failed to improve visual outcome beyond what is expected based upon the natural history of BRAO/CRAO and some of them had deleterious effects<sup>5</sup>. Hyperbaric therapy shows interesting results in some case-control studies<sup>6,7,8</sup>. Intravenous fibrinolysis is being used in the USA, mainly by Neurologists, and was recently recommended by MacGrory *et al*<sup>9</sup>, if the occlusion happened in less than 4.5 hours, with low hemorrhagic risk.

Acute retinal arterial ischemia is not only an important cause of sudden and painless vision loss but also a medical emergency. Patients with acute retinal arterial ischemia are at a high risk of having concomitant or subsequent vascular events, such as stroke and myocardial infarction, valvular disease, auricular fibrillation and even death. Up to 25% need a surgical procedure and up to 90% a medication change<sup>10</sup>. A systemic evaluation with blood analysis, electrocardiogram, echocardiogram, carotid ecodoppler, angio-CT or angio-RM and cranioencephalic-CT or cranioencephalic-TM with DWI is mandatory and should be done, ideally in the first 24 hours<sup>5</sup> or up to 1 week<sup>11</sup>.

Medical Retina evaluation has also the purpose to prevent/treat neovascular complications. Although they tend to occur rarely in CRAO and residually in BRAO, due to recanalization of the vessel in the majority of the cases, ischemic areas need to be assessed. Fluorescein angiography (FA) is the gold-standard method to evaluate the blood flow and peripheral ischemia. Macular ischemia is better evaluated with optical coherence tomography angiography (OCTA). In contrast to FA, OCTA allows a morphological study of superficial and deep capillary networks, without dye injection. However, OCTA can be difficult to acquire and analyze due to poor fixation and motion artifacts.

In the acute phase of RAO, qualitative analysis of the OCTA enface scans shows a decreased vascular flow in both superficial (SCP) and deep capillary plexus (DCP). These OCTA changes correlate to the FA delayed perfusion areas and to the inner retina increased reflectivity on the OCT b-scans<sup>12, 13</sup> – Figure 1 and 2. Quantitatively, Yang *et al*<sup>14</sup> reported a decreased SCP and DCP vessel density and an increased acircularity index of the foveal avascular zone in these eyes comparative to fellow or normal eyes.

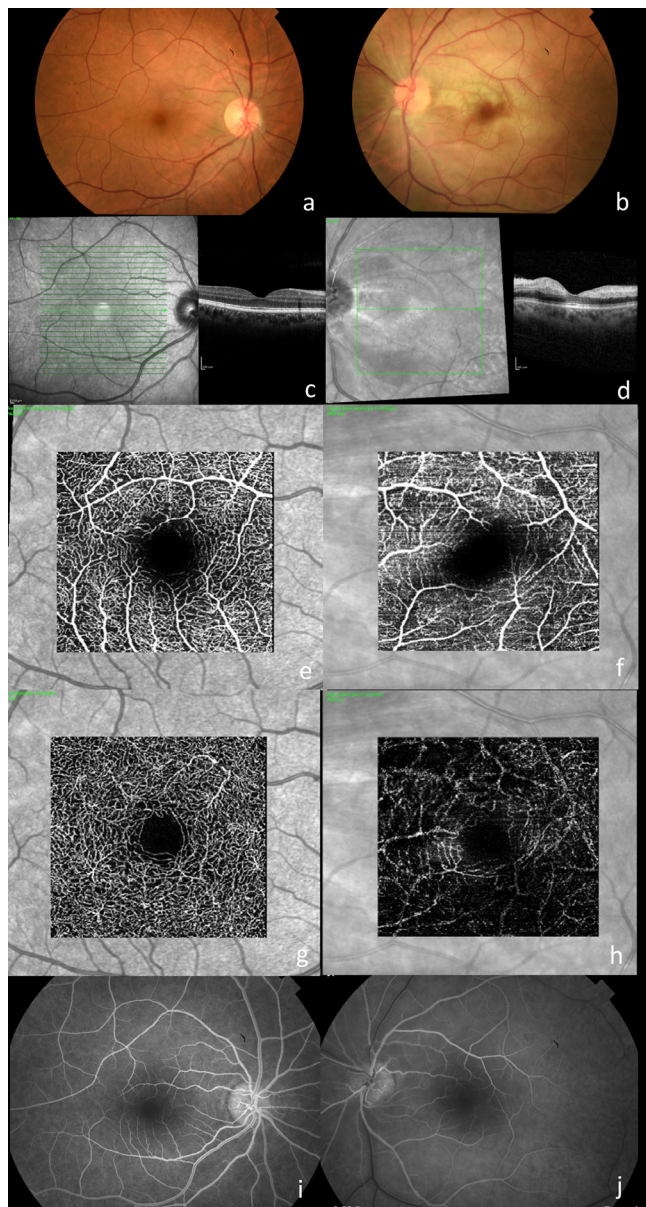


**Figure 1.** Acute phase of a left eye CRAO: a) and b) Retinography showing cherry red spot on the left eye. c) and d) OCT showing inner retina increased reflectivity due to intracellular edema e) and f) SCP OCTA showing decreased vascular flow in the CRAO eye g) and h) DCP OCTA showing decreased vascular flow in the CRAO eye i) and j) Fluorescein Angiography demonstrating a delayed retinal filling.

Care should be taken when evaluating the DCP in the acute phase. The inner retina increased reflectivity can induce a signal attenuation artifact (masking as hypoperfusion), increase superficial layers projection artifacts and also induce segmentation artifacts.

During the recanalization process, the perfusion of the DCP may partially restore in areas where superficial capillary plexus is still compromised<sup>12</sup>.

In the chronic phase, care should also be taken when evaluating both SCP and DCP, as the atrophic inner retina can induce segmentation artifacts and may not allow to differentiate the two individual vascular layers (Figure 3).

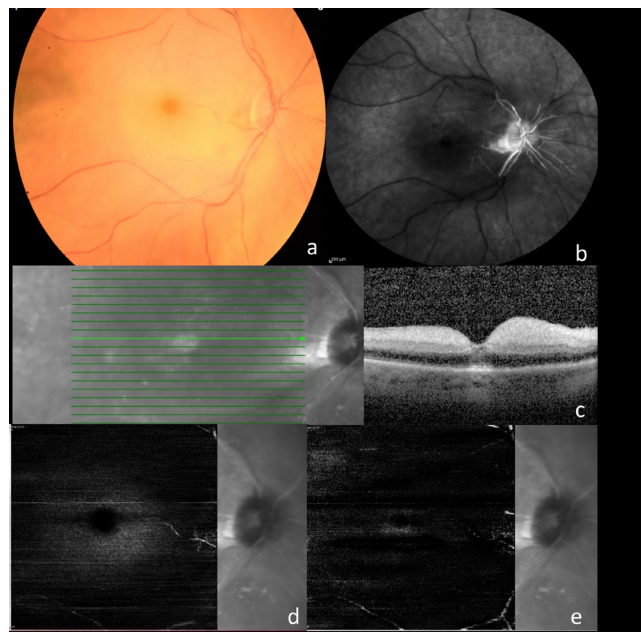


**Figure 2.** Acute phase of a CRAO patient without recanalization: a) Retinography showing cherry red spot b) Fluorescein Angiography demonstrating absence of recanalization with extensive ischemia. c) OCT showing inner retina increased reflectivity due to intracellular edema d) and e) SCP and DCP OCTA showing a severe decrease of vascular flow.

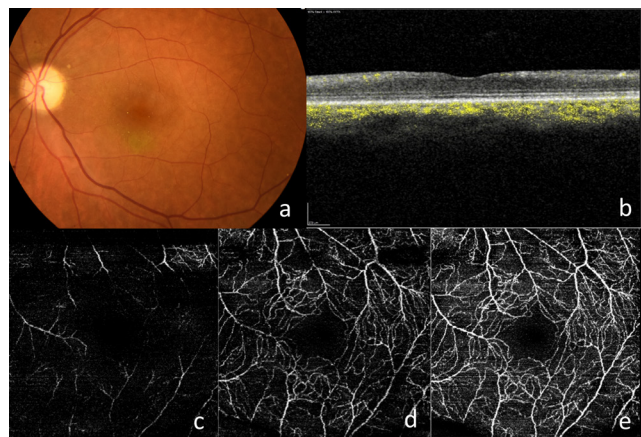


**Figure 3:** Chronic phase of a CRAO patient: a) Retinography demonstrating almost absence of retinal whitening b) OCT showing inner retina atrophic changes c,d,e) OCTA SCP, DCP and SCP + DCP, respectively: Segmentation of the atrophic inner retina may not be reliable and so a combined evaluation of SCP and DCP may be of value.

Although the OCTA alone was already used to diagnose a RAO<sup>15</sup>, its diagnosis is often clinical and can be confirmed by OCT distinctive findings even in the absence of clear fundus signs. OCTA may help but it cannot be performed in all cases and its analysis may be biased due to the attenuation, projection and segmentation artifacts. Some case reports<sup>15, 16, 17</sup> suggest the OCTA to play a role on monitoring patients in order to detect restoration of blood flow, which is known to have better prognosis in

what concern neovascular complications. However, there is a lack of studies documenting its importance.

## REFERENCES

1. Sacco RL, Kasner SE, Broderick JP, et al. An updated definition of stroke for the 21st century: a statement for healthcare professionals from the American Heart Association/American Stroke Association. *Stroke* 2013;44:2064–89.
2. Tanaka K, Uehara T, Kimura K, et al. Comparison of Clinical Characteristics among Subtypes of Visual Symptoms in Patients with Transient Ischemic Attack: Analysis of the PROspective Multicenter registry to Identify Subsequent cardiovascular Events after TIA (PROMISE-TIA) Registry. *J Stroke Cerebrovasc Dis* 2018;27:1711–6.
3. Lawlor M, Perry R, Hunt BJ, et al. Strokes and vision: The management of ischemic arterial disease affecting the retina and occipital lobe. *Surv Ophthalmol* 2015;60:296–309.
4. Dattilo, Michael & Newman, Nancy & Biousse, Valérie. (2018). Acute retinal arterial ischemia. *Ann Eye Sci.* 2018;3:28.
5. Flaxel CJ, Adelman RA, Bailey ST, et al. Retinal and Ophthalmic Artery Occlusions Preferred Practice Pattern® [published correction appears in *Ophthalmology*. 2020 Sep;127(9):1280]. *Ophthalmology*. 2020;127(2):259-287.
6. Menzel-Severing J, Siekmann U, Weinberger A, Roessler G, Walter P, Mazinani B. Early hyperbaric oxygen treatment for nonarteritic central retinal artery obstruction. *Am J Ophthalmol*. 2012;153(3):454-459.e2.
7. Masters TC, Westgard BC, Hendriksen SM, et al. Case series of hyperbaric oxygen therapy for central retinal artery occlusion *Retin Cases Brief Rep*. 2021;15(6):783-788
8. Schmidt I, Walter P, Siekmann U, et al. Development of visual acuity under hyperbaric oxygen treatment (HBO) in non arteritic retinal branch artery occlusion. *Graefes Arch Clin Exp Ophthalmol*. 2020;258(2):303-310.
9. Mac Grory B, Lavin P, Kirshner H, Schrag M. Thrombolytic Therapy for Acute Central Retinal Artery Occlusion. *Stroke*. 2020;51(2):687-695.
10. Lavin P, Patrylo M, Hollar M, Espaillet KB, Kirshner H, Schrag M. Stroke Risk and Risk Factors in Patients With Central Retinal Artery Occlusion. *Am J Ophthalmol*. 2018;196:96-100.
11. Biousse V, Nahab F, Newman NJ. Management of Acute Retinal Ischemia: Follow the Guidelines!. *Ophthalmology*. 2018;125(10):1597-1607.
12. Bonini Filho MA, Adhi M, de Carlo TE et al. Optical coherence tomography angiography in retinal artery occlusion. *Retina*. 2015;35(11):2339-46.
13. Abdellah MM. Multimodal Imaging of Acute Central Retinal Artery Occlusion. *Med Hypothesis Discov Innov Ophthalmol*. Winter 2019;8(4):283-290.
14. Yang S, Lui X, Li H, et al. Optical coherence tomography angiography characteristics of acute retinal arterial occlusion. *BMC Ophthalmol*. 2019;19(1):147.
15. Damento G, Chen MH, Leng T. Spectral-Domain Optical Coherence Tomography Angiography of Central Retinal Artery Occlusion. *Ophthalmic Surg Lasers Imaging Retina*. 2016;47(5):467-70.
16. Philippakis E, Dupas B, Bonnin P, Hage R, Gaudric A, Tadayoni R. Optical Coherence Tomography Angiography Shows Deep Capillary Plexus Hypoperfusion in Incomplete Central Retinal Artery Occlusion. *Retin Cases Brief Rep*. 2015;9(4):333-8.
17. Bhanushali DR, Yadav NK, Dabir S, Chidambara L, Srinivasan P, Shetty R. Spectral Domain Optical Coherence Tomography Angiography Features in a Patient of Central Retinal Artery Occlusion Before and After Paracentesis. *Retina*. 2016;36(5):e36-8.



8.

# DIABETIC RETINOPATHY





## 8.1.

# NON-PROLIFERATIVE DIABETIC RETINOPATHY

Ana Rita Santos<sup>1,2</sup>, João Figueira<sup>1,3,4</sup>

1- AIBILI - Association for Innovation and Biomedical Research on Light and Image, Coimbra, Portugal;

2- Department of Orthoptics, School of Health, Polytechnic of Porto, Porto, Portugal

3- Centro Hospitalar e Universitário de Coimbra, Coimbra, Portugal;

4- Faculty of Medicine of the University of Coimbra, Coimbra, Portugal;

## INTRODUCTION

Optical coherence tomography angiography (OCTA) acquired an important position in the study of Diabetic Retinopathy (DR). As a non-invasive technology that provides depth-resolved images of the retinal microvasculature, it allows the identification of significant features of this disease. OCTA is a repeatable and objective method that not only can provide qualitative information but also important quantitative information about vessel density and perfusion changes in both retinal and choroidal vascular plexus. Therefore, several authors have shown that this technique may be more sensitive to the earliest manifestations of the disease than the currently gold-standard imaging methods like Color Fundus Photography (CFP) or Fluorescein Angiography (FA)<sup>1,2</sup>.

The aim of this chapter is to review the use of OCTA in the detection of retinal key features currently used as diagnostic markers of DR in its non-proliferative stages.

## OCTA BEFORE VISIBLE RETINOPATHY

Before DR becomes clinically visible with the appearance of microaneurysms (MAs) and/or retinal hemorrhages, OCTA has been able to demonstrate microvascular changes such as capillary dropout<sup>3</sup>, dilated capillaries, vessels tortuosity<sup>4</sup>, reduced capillary perfusion or irregularities and enlargement of foveal avascular zone (FAZ)<sup>5</sup> in eyes of patients with diabetes but no retinopathy.

## MICROANEURYSMS

MAs are normally the earliest fundus visible alterations related with DR and CFP but specially FA has been considered the gold standard exams for detection those microvascular dilatations. MAs can be recognised in the OCTA as saccular, fusiform or focal bulge originating from a retinal vessel in DCP or SCP, but this new non-invasive modality showed to be less sensitive, visualising lower number of MAs compared with FA<sup>6</sup>. This could be explain due to the very slow blood flow or even flow

turbulency inside MAs that can't be detected by OCTA machines.

## FAZ PARAMETERS

FAZ parameters are frequently used as a measure of macular ischemia, which has been associated with functional retinal damage and DR progression<sup>1</sup>. The FAZ area/ diameter is known to vary greatly even in the normal population but enlargement and loss of circularity are reported to correlate with increasing severity of DR<sup>7</sup> and even capable of differentiating Proliferative DR (PDR) and mild non proliferative DR (NPDR) stages<sup>8,9</sup>. Despite the described variability<sup>5</sup>, FAZ characteristics are easily evaluated with any OCTA equipment and can be monitored over time to deduce disease progression in individual patients making this a good feature for screening purposes and follow up. The most frequent FAZ changes that can be found since the early stages of DR are small areas of capillary non-perfusion around FAZ contour, presence of microaneurysms, vascular tortuosity and capillary dilations (Figure 1). These changes can be easily seen in the superficial capillary plexus but are frequently much more apparent in the deep capillary plexus<sup>9</sup>.

## VESSEL ARCHITECTURE

Several vessel architecture parameters have being proposed as possible markers of DR stage and progression<sup>4,10,11</sup>.

Lee H et al<sup>4</sup> reported an increase of vessel tortuosity as the stage of NPDR was more severe, but decreased in PDR, which make it potentially useful as an indicator of progression to PDR minimizing the need of Fluorescein Angiography (FA). Fractal dimension (FD), an index of the branching complexity of the capillary network, and vessel diameter index (the average vessel caliber), are also other vessel parameters indicated as possible markers of DR<sup>10</sup>. Decreased branching complexity (FD), and increasing average vascular caliber were associated with worsening DR as they are indirect measures of capillaries

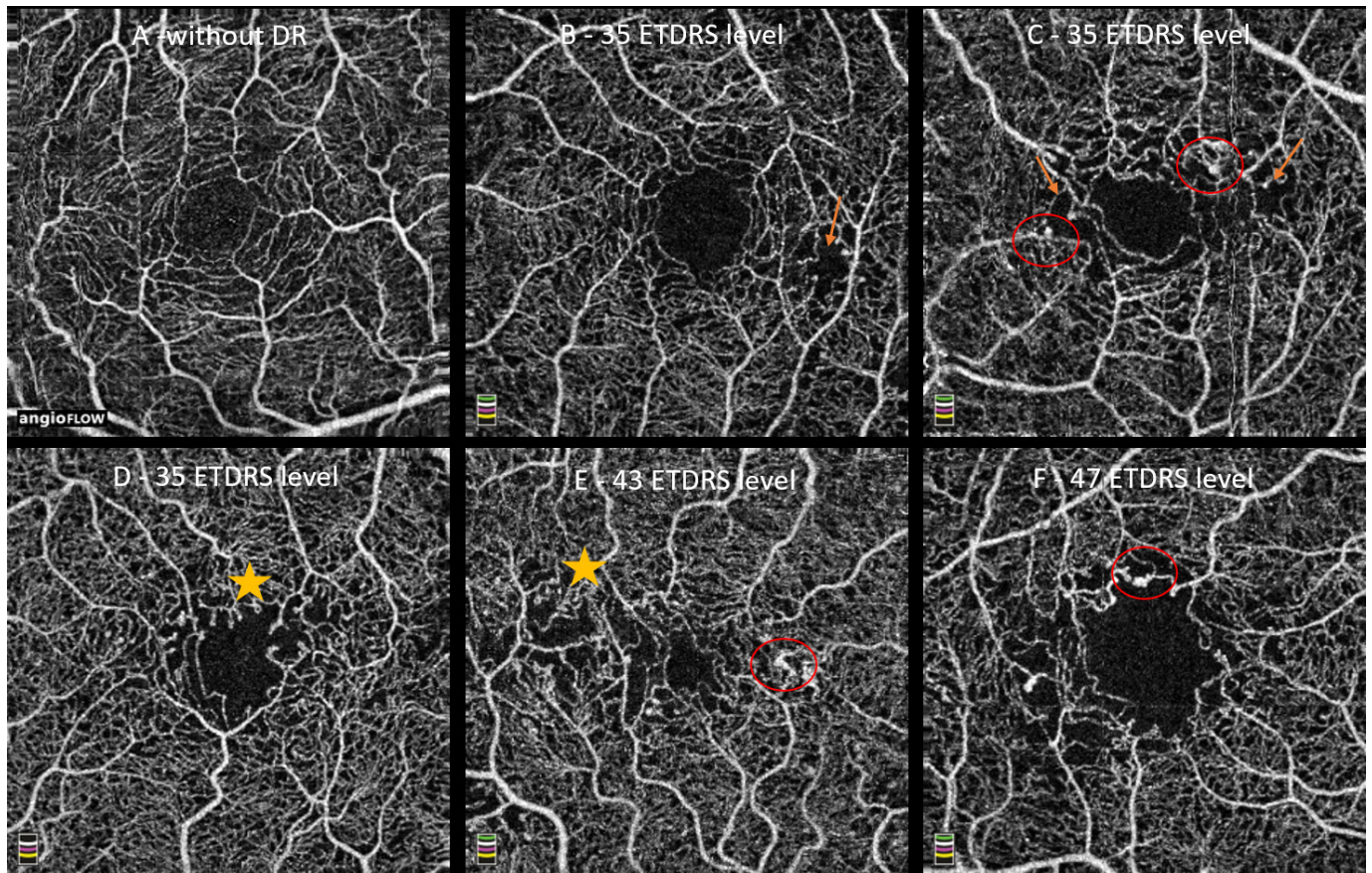


**Figure 1.** Several 3x3 mm acquisitions from diabetic patients with different stages of the disease, showing distinct FAZ changes. Areas with capillary non-perfusion (orange arrows), microaneurysms (red circles), capillary tortuosity and dilations (yellow star). (Adapted from Mario et al (8) and reproduced with author's permission).

loss or vessels dilation, two common occurrences in DR pathophysiology<sup>11</sup>.

### VESSEL DENSITY - CAPILLARY CLOSURE

Vessel density, measured by OCTA provides a quantitative metric of capillary closure or dropout that has shown correlation with severity of DR and its progression, being strongly associated with the clinical features of NPDR<sup>9,12</sup>.

Durbin et al<sup>13</sup>, showed that vessel density measured in the superficial capillary plexus can discriminate healthy from DR eyes. Other authors<sup>12</sup> showed that reduction in retinal vessel density in both the superficial and deep plexuses, mainly at macular area has been correlated to visual acuity and may be a potential indicator for macular ischemia and vision loss during disease progression.

There is still some controversy about which plexus is primarily affected in DR<sup>3</sup> but most studies indicate the deep capillary plexus as more susceptible to ischemic damage and therefore more sensitive to detect DR severity<sup>9,14</sup> and visual function changes<sup>15</sup> (Figure 2).

### PERIPHERY NON-PERFUSION - WIDEFIELD OCTA

The regional distribution of retinal capillary changes may be particularly relevant in staging DR<sup>16,17</sup> optical coherence tomography angiography (OCTA. Studies with widefield FA have also shown that peripheral nonperfusion lesions are associated with higher risks of DR progression<sup>15</sup>.

Swept Source-OCT instruments enables OCTA visualization of retinal vasculature over larger fields of view, like 12x12 mm or 15x9 mm, instead of the common 3x3mm perifoveal acquisitions. Also, it provides advantages in the speed of acquisition, penetration capability and improved sensitivity due to the density of A-scans, compared with conventional OCTA equipment's<sup>18</sup>.

Combining the results of 3x3 mm and 15x9 mm acquisitions, Santos T et al<sup>14</sup>, distinguished patients from two major stages of NPDR: mild retinopathy (ETDRS<sup>20-35</sup>), with capillary closure limited to the perifovea; and moderate to severe NPDR (ETDRS<sup>43-53</sup>) with a significant increase of retinal capillary closure in

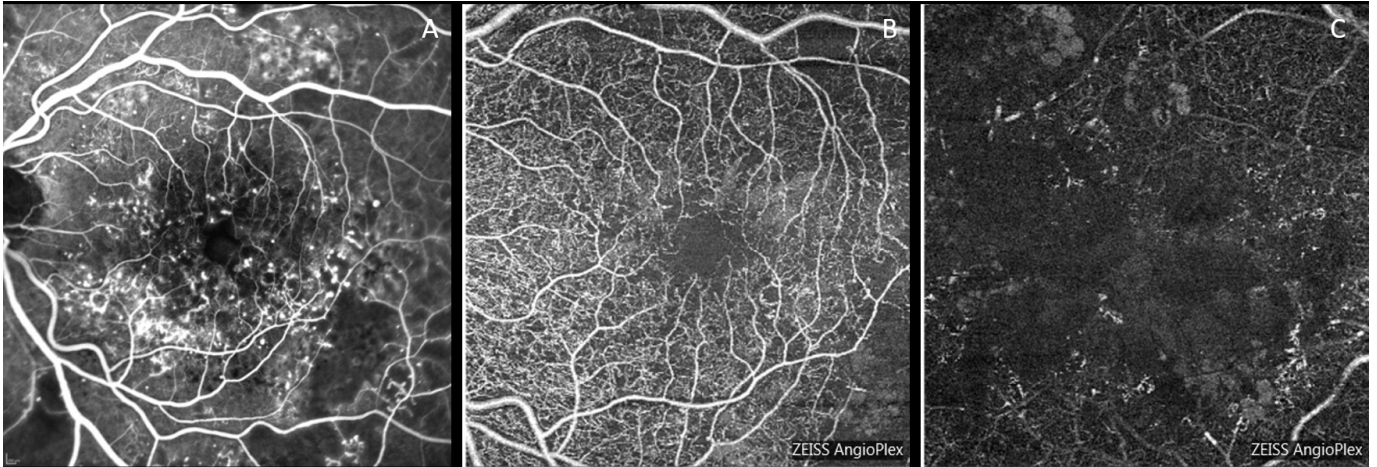


**Figure 2.** (A) FA image showing several NPDR lesions like microaneurysms, capillary dilations, IRMAS and non-perfusion areas. (B) 6x6 mm OCTA acquisition of the same patient on superficial capillary plexus showing microaneurysms and areas of non-perfusion. (C) 6x6 mm OCTA acquisition of the same patient on deep capillary plexus showing larger areas of non-perfusion, capillaries dilation and hyperreflective artifacts compatible with cystoid spaces.

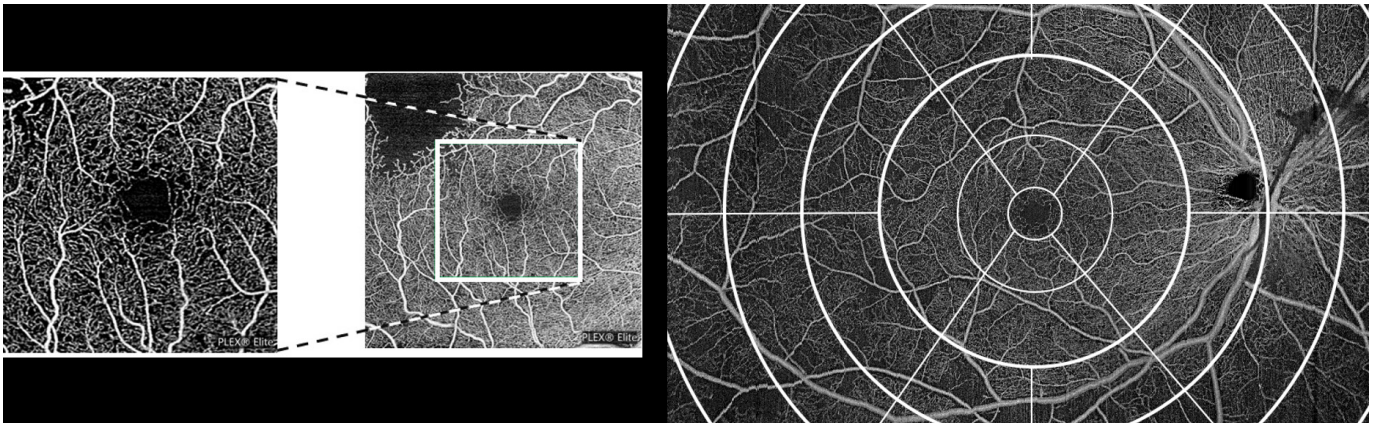


**Figure 3.** (Left side) 3x3 mm acquisition example and the area it occupies in the 6x6 mm acquisitions. (Right side) 15x9 mm acquisition with a representative scheme of perifovea vs mid-periphery retinal locations. (Adapted from Santos T et al (14) and reproduced with author's permission).

more peripheral regions of the retina (Figure 3). Similar findings were also reported by Tan et al<sup>19</sup>. Using 12x12mm acquisitions, showed a stepwise decrease in retinal and capillary perfusion density as well as in capillary dropout density in diabetic patients with no DR, mild NPDR, and moderate to severe NPDR.

Wide-field OCTA has also shown its value in detecting IRMAs and retinal neovascularization (Figure 4) when compared with Wide-field color fundus photography<sup>15</sup>. Analysis of the periphery with wide-field OCTA may allow staging, diagnosis, and monitoring of DR, decreasing the need of subjective evaluation of fundus images or invasive ophthalmic examinations like FA.

### CAN OCT-A BECOME A USEFUL TOOL FOR DR SCREENING?

The prevalence of diabetes will increase substantially in the next years, so it's important to identify patients that

develop ocular manifestations of the disease, especially those with retinopathy progression in particular when threatening vision complications as DME and PDR are present. OCTA can detect vascular retina alterations in very mild stages of DR or even before visible DR lesions, being also correlated with DR severity and can be useful for staging and monitoring patients evolution and treatment response<sup>9,20</sup>.

However, this non-invasive attractive method for DR screening has some disadvantages: it is expensive, only available in some health units, and there is a lack of standardized outcomes obtained in a reproducible way which makes this technique inappropriate to be used in large populations programs at present.

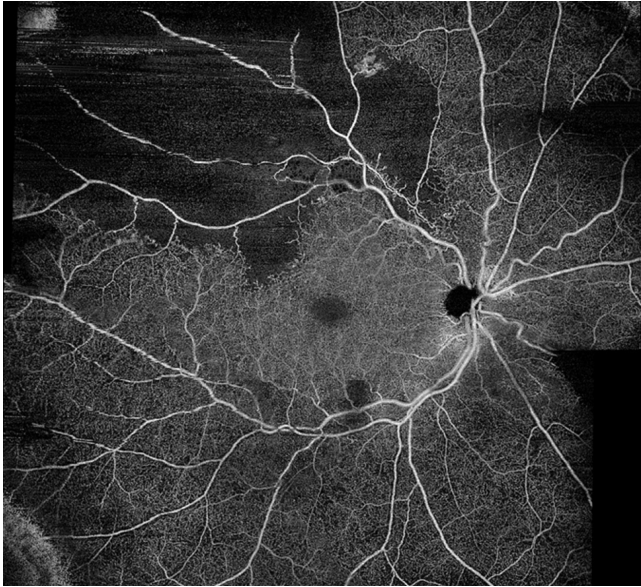


**Figure 4.** 12x12 mm Plex Elite acquisition example showing a large area of non-perfusion in the temporal arcade as well as the presence of retina neovascularization.

## REFERENCES

1. Akil H, Karst S, Heisler M, Etminan M, Navajas E, Maberley D. Application of optical coherence tomography angiography in diabetic retinopathy: a comprehensive review. *Can J Ophthalmol* . 2019;54(5):519–28.
2. Soares M, Neves C, Marques IP, Pires I, Schwartz C, Costa MÂ, et al. Comparison of diabetic retinopathy classification using fluorescein angiography and optical coherence tomography angiography. *Br J Ophthalmol* . 2016;101(1):62–8.
3. Schottenhamml J, Moulton EM, Ploner S, Lee B, Novais EA, Cole E, et al. An automatic, intercapillary area-based algorithm for quantifying diabetes-related capillary dropout using optical coherence tomography angiography. *Retina*. 2016;36:S93–101.
4. Lee H, Lee M, Chung H, Kim HC. Quantification of Retinal Vessel Tortuosity in Diabetic Retinopathy Using Optical Coherence Tomography Angiography. *Retina*. 2017;1–10.
5. Johannesen SK, Viken JN, Vergmann AS, Grauslund J. Optical coherence tomography angiography and microvascular changes in diabetic retinopathy: a systematic review. *Acta Ophthalmol*. 2019;97(1):7–14.
6. Parrulli S, Corvi F, Cozzi M, Monteduro D, Zicarelli F, Staurenghi G. Microaneurysms visualisation using five different optical coherence tomography angiography devices compared to fluorescein angiography. *Br J Ophthalmol* . 2021;105(4):526 LP – 530.
7. Al-Sheikh M, Akil H, Pfau M, Satta SR. Swept-source OCT angiography imaging of the foveal avascular zone and macular capillary network density in diabetic retinopathy. *Investig Ophthalmol Vis Sci*. 2016;57(8):3907–13.
8. Soares M, Neves C, Marques IP, Pires I, Schwartz C, Costa MÂ, et al. Comparison of diabetic retinopathy classification using fluorescein angiography and optical coherence tomography angiography. *Br J Ophthalmol*. 2017;101(1):62–8.
9. Rodrigues TM, Marques JP, Soares M, Simão S, Melo P, Martins A, et al. Macular OCT-angiography parameters to predict the clinical stage of nonproliferative diabetic retinopathy: an exploratory analysis. *Eye*. 2019;33(8):1240–7.
10. Kim AY, Chu Z, Shahidzadeh A, Wang RK, Puliafito CA, Kashani AH. Quantifying microvascular density and morphology in diabetic retinopathy using spectral-domain optical coherence tomography angiography. *Investig Ophthalmol Vis Sci*. 2016;57(9):OCT362–70.
11. Fayed AE, Abdelbaki AM, El Zawahry OM, Fawzi AA. Optical coherence tomography angiography reveals progressive worsening of retinal vascular geometry in diabetic retinopathy and improved geometry after panretinal photocoagulation. *PLoS One* . 2019;14(12):1–13.
12. Samara WA, Shallice A, Adam MK, Khan MA, Chiang A, Maguire JJ, et al. Quantification of Diabetic Macular Ischemia Using Optical Coherence Tomography Angiography and Its Relationship with Visual Acuity. *Ophthalmology* . 2017;124(2):235–44.
13. Durbin MK, An L, Shemonski ND, Soares M, Santos T, Lopes M, et al. Quantification of Retinal Microvascular Density in Optical Coherence Tomographic Angiography Images in Diabetic Retinopathy. *JAMA Ophthalmol* . 2017;94568:1–7.
14. Santos T, Warren LH, Santos AR, Marques IP, Kubach S, Mendes LG, et al. Swept-source OCTA quantification of capillary closure predicts ETDRS severity staging of NPDR. *Br J Ophthalmol*. 2020;1–7.
15. Cui Y, Zhu Y, Wang JC, Lu Y, Zeng R, Katz R, et al. Comparison of widefield swept-source optical coherence tomography angiography with ultra-widefield colour fundus photography and fluorescein angiography for detection of lesions in diabetic retinopathy. *Br J Ophthalmol*. 2021;105(4):577–581.
16. Chua J, Sim R, Tan B, Wong D, Yao X, Liu X, et al. Optical Coherence Tomography Angiography in Diabetes and Diabetic Retinopathy. *J Clin Med*. 2020;9(6):1723.
17. Ashraf M, Sampani K, Rageh A, Silva PS, Aiello LP, Sun JK. Interaction between the Distribution of Diabetic Retinopathy Lesions and the Association of Optical Coherence Tomography Angiography Scans with Diabetic Retinopathy Severity. *JAMA Ophthalmol*. 2020;138(12):1291–1297.
18. Vira J, Marchese A, Singh RB, Agarwal A. Swept-source optical coherence tomography imaging of the retinobulbar and beyond. *Expert Rev Med Devices* . 2020;17(5):413–26.
19. Tan B, Chua J, Lin E, Cheng J, Gan A, Yao X, et al. Quantitative Microvascular Analysis With Wide-Field Optical Coherence Tomography Angiography in Eyes With Diabetic Retinopathy. *JAMA Netw open*. 2020;3(1):e1919469.
20. Sun Z, Tang F, Wong R, Lok J, Szeto SKH, Chan JCK, et al. OCT Angiography Metrics Predict Progression of Diabetic Retinopathy and Development of Diabetic Macular Edema: A Prospective Study. *Ophthalmology*. 2019;126(12):1675–84.

# DIABETIC MACULAR EDEMA

José Henriques<sup>1,2</sup>, Catarina Rodrigues<sup>2</sup>, Susana Henriques<sup>3</sup>

1- Lisbon Retina Institute (IRL)

2- Instituto de Oftalmologia Dr. Gama Pinto, Lisboa (IOGP)

3- Ophthalmology Department of Hospital Professor Doutor Fernando da Fonseca

## INTRODUCTION

Diabetic Retinopathy (DR) is a chronic, subclinical, inflammatory, neuro-microvascular disease, a common complication of diabetes mellitus, which leads to progressive microstructural and functional alterations causing progressive vision loss<sup>1,2</sup>. The initial features are characterized by capillary occlusion and/or microaneurysm, hyperpermeability and retinal neovascularization<sup>2</sup>.

Diabetic Macular Edema (DME) is characterized by the breakdown of the blood-retina barrier at the level of internal retinal capillaries and/or retinal pigment epithelium (RPE) and consequent leakage of water, electrolytes, and lipoproteins from blood vessels. The water and electrolytes are normally reabsorbed by the healthy nearby capillaries and lipoproteins are phagocytized by macrophages. However, if there are local loss of capillaries or excessive capillary workload, water and electrolytes cannot be absorbed and there is an accumulation of fluid within the retina, either diffusely or forming cystic cavities, with loss of clearly defined retinal layers<sup>3</sup>. Simultaneously, the macrophages are not able to phagocyte all the lipoproteins and they accumulate within the retinal layers, increasingly distorting the layers' boundaries as the condition becomes chronic.

Conventionally, fluorescein angiography (FA) is used for qualitative and functional clinical assessment of retinal vasculature, providing two-dimensional (2D) images of ocular circulation. It has the advantage of visualization of leakage from capillaries, the main cause of DME. However, FA has a limited depth perception and limited detailed investigation of the retinal and choroidal vasculatures<sup>4</sup>.

The association of structural OCT and *en face* OCT, allows a more precise identification of the pathological retinal features: cysts, microaneurysms, IRMA and hard exudates<sup>5</sup>. The OCTA, despite its limitations, has the capability of producing high-resolution, 3D angiograms of the retinal (and choroidal) vascular networks<sup>6,7</sup> and the potential to improve our knowledge of the physiology and pathophysiology of the diabetic eye as well as the monitoring of the outcomes of the treatment<sup>4</sup>.

## 1. OCTA as a new imaging modality in DME

### 1. A non-invasive method

OCTA detects the motion of blood using intrinsic signals to capture the location of blood vessels, without exogenous contrast. This is a significant advantage over FA as it is a non-invasive method of retina imaging.

### 2. Possibility of quantitative evaluation

Quantification is important for objective evaluation of retinal abnormalities. Vessel density and flow index are two commonly used metrics which can be obtained by the *en face* angiograms of the OCT.

#### a) Vessel density

Vessel density is defined as a percentage of the area occupied by the blood vessels. Vessel length density and perfusion density of the superficial retinal vasculature can be obtained from OCTA images with high levels of repeatability and reproducibility but can vary with scan pattern and location<sup>4,8</sup>.

#### b) Flow index

Flow index is calculated as the average flow signal in the area of interest. Flow index carries information on both vessel area and blood velocity. However, it cannot be considered a volumetric measurement of blood flow because of the saturation effect of the flow signal value with high flow velocity<sup>4,9</sup>.

## 3. Individualization of retinal plexus/segmentation

The superficial vascular complex (SVC) is located in the ganglion cell layer; the radial peripapillary capillary plexus (RPCP) in retinal nerve fiber layer; the deep vascular complex (DVC) consists of the intermediate capillary plexus (ICP) above inner nuclear layer (INL) and deep capillary plexus (DCP) below INL<sup>4,5</sup>.

OCTA is able to penetrate the retinal layers and image the various different capillary plexuses, thereby providing the unique ability to reconstruct and view the retinal vasculature in a 3-dimensional fashion, as well as to visualize in isolation the individual retinal plexuses<sup>10</sup>. This

achievement overcomes one of the major limitations of FA namely, the light scattering in the retina rendering it unable to capture the alterations in the deep capillary plexus (DCP) of the retina, such as capillary dropout and enlargement of the foveal avascular zone.

### a) Importance of accurate segmentation and the challenge of DME

In DME, anatomical features and boundaries are usually distorted, and segmentation algorithms can fail, requiring manual correction and careful interpretation of OCTA images<sup>11</sup>. The edematous layers are thicker than the segmentation slabs used, and the segmentation slabs are often not in the correct layer. (Fig.1)

### b) Cross-sectional OCT scans with an OCTA flow overlay in DME

Given the complexity of DR features, such as edema, cyst formation, subretinal fluid and neovascularization, it is currently, virtually impossible for a computer algorithm to accurately identify retinal layers in the presence of all these pathologic features. For this reason, viewing cross-sectional OCT scans with an OCTA flow overlay is helpful in DME<sup>10</sup>.(Fig.2, E-H)

## II. CHARACTERISTICS OF DME ON OCTA

### 1. DME appearance

DME is visualized in OCTA by the presence of cystic round spaces without perfusion. This may be confused with ischemic capillary areas. However, simultaneous *en face* imaging with the B-scan helps to differentiate one image from another. In addition, on *en face* imaging, the cystoid spaces present typical characteristics such as rounded/elongated shapes and are totally black due to the absence of signal reflection, while the ischemic areas present a grayish appearance and more irregular contours<sup>12</sup>. (Fig. 1)

### 2. Microaneurysms, the DR hallmark

Microaneurysms, that are seen as focal dilations of the retinal capillaries on FA, are the hallmark of the disease and can be visualized on OCTA as small focal dilations of the vessels<sup>7,13</sup>. However, studies show that only around 62% of the microaneurysms seen on FA are visualized on OCTA<sup>7,14</sup>. This seems to be related to the inability of OCTA to detect slow flow. In addition, some of the volume of a microaneurysm may be occupied by thrombus, which has no flow<sup>10</sup>. DME may be associated with a profusion of microaneurysms in both plexuses but especially in the deep retinal plexus<sup>15</sup>. The presence of microaneurysms near non-perfusion areas and/or cystoid spaces, is a common finding<sup>15</sup>. In these cases, visual acuity does not usually recover with resolution of the edema<sup>16,17</sup>.

One of the limitations of OCTA, is its inability to detect leakage and therefore its inability to differentiate between leaking and non-leaking microaneurysms in DME<sup>10</sup>. However, as treatment of DME currently relies primarily on intravitreal agents and not as much on focal laser<sup>18,19</sup>, the detection of leaking microaneurysms has become of less critical importance.

### 3. “PEVAC-like”, a new DME feature easily visualized by OCTA

Recently, we identified in a diabetic patient, an entity called “perifoveal exudative vascular anomalous like-complex” (PEVAC-like)<sup>21</sup>, previously described in non-diabetic patients as PEVAC<sup>22,23</sup>. The lesion are resistant to anti-VEGF treatment<sup>22</sup> and presents in angiography and OCT<sup>22,24</sup> (Fig.3) as cystoid macular edema (CME) secondary to a perifoveal isolated aneurysm, which appears on OCT as a round, hyperreflective lesion with hyporeflective lumen. On OCTA a flow signal can be observed within the aneurysmal lesion as well as a thick wall. It is important to look for such lesions in diabetic patients,

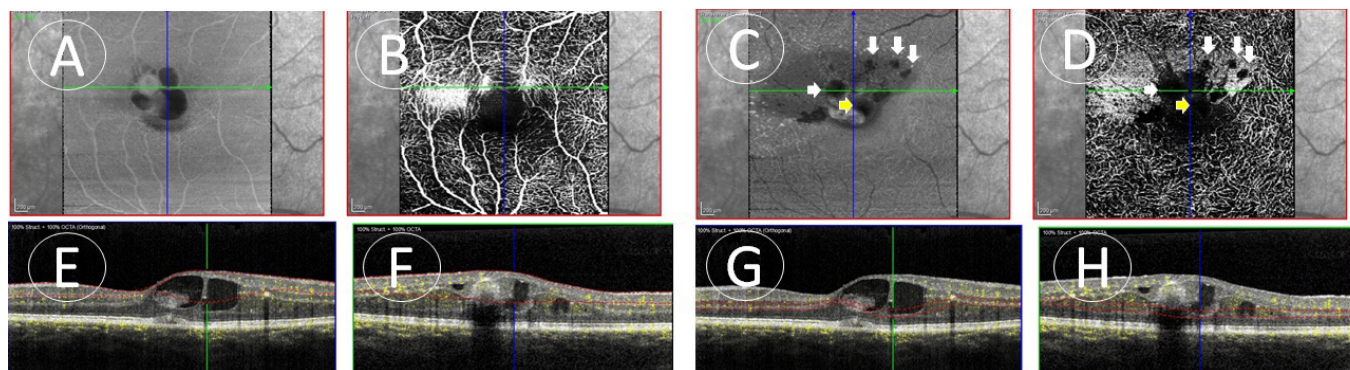


**Figure 1.** Cystoid spaces and absence of network capillary plexus simulating decreased vascular density. Images from Spectralis - Heidelberg. (A): Superficial en face OCTA, showing PEVAC like-lesion and cystoid spaces nearby (B): Superficial capillary plexus showing the PEVAC-like lesion. (C): Deep en face OCTA, showing PEVAC like-lesion and cystoid spaces nearby (yellow arrow); (D): Black round spaces mimicking absence of capillary network, corresponding to cystic spaces and displacement of capillaries (white vertical arrows). The PEVAC-like lesion (white horizontal arrow) and other cystoid spaces are just inside the FAZ and are not identified. (E) and (F), (G) and (H): Structural OCT showing the segmentation slab (dashed red lines) with enough level of accuracy because the anatomical disruption is not significant.

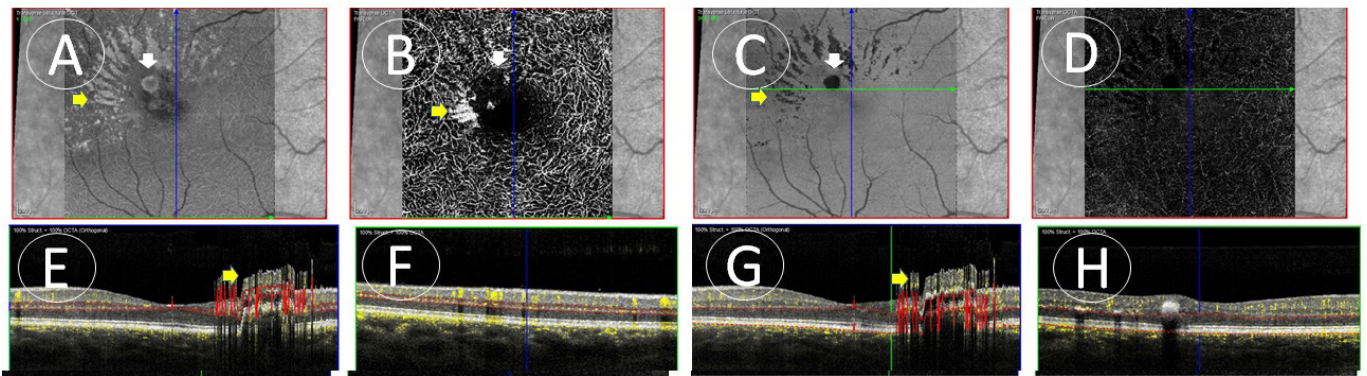


**Figure 2.** Hard Exudates on OCTA en face and on structural OCT. Cross-sectional OCT scans with an OCTA flow overlay. Images from Spectralis - Heidelberg. (A) and (C): Deep and avascular zone en face OCTA, showing the lipoprotein exudates (yellow arrows) and photocoagulated PEVAC-like lesion (white arrow); (B) and (D): Deep capillary plexus and avascular zone; (E) and (G): Shows the reverberation of the signal caused by the hyperreflectivity of the hard exudates. (F) and (H) Cross-sectional OCT scans with an OCTA flow overlay depicted by yellow dots and blots, at variable levels of the retinal layers.

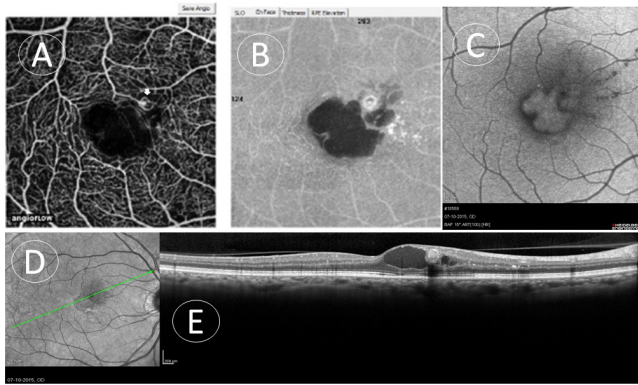


**Figure 3.** PEVAC-like multimodal imaging at baseline: (A): OCTA imaging from Optovue, showing flow signal at the level of the PEVAC like-lesion (white arrow); (B): En face imaging, showing accurately hyperreflective outer ring, corresponding to the wall and the flow inside the lesion. (C): FAF showing enlarged hyperautofluorescent foveal area with hypoautofluorescent halo and an hypoautofluorescent lesion showing macular edema; (D) and (E): IR and structural OCT (Spectralis-Heidelberg) showing parafoveal macrocystic edema and an intraretinal ovoid hyporeflective lesion with hyperreflective walls and posterior shadowing (PEVAC-like lesion).

especially when the DME is resistant to anti-VEGF and if the OCTA has the characteristic aneurismatic lesions. This is usually accompanied by evidence of flow and is located near a large cyst in or outside the foveal area. The lesion is accessible to focal milli-pulse photothermic laser with rapid resolution of cystoid edema.

#### 4. Pre-retinal neovascularization and IRMAs

Pre-retinal neovascularization can be seen as vessels projecting into the vitreous. Intraretinal microvascular abnormalities (IRMA) are seen as abnormal vessels still within the retinal plane<sup>10</sup>.

#### 5. Hard exudates or lipoprotein accumulation

The inability of macrophages activity allows lipoproteins to deposit as hard exudates and as they accumulate within the retinal layers, increasingly distort the layers' boundaries. They appeared as yellow hard exudate or yellow plaques, well depicted in the OCTA *en face*, but as hyperreflective structures it can cause reverberation of the OCT signal. (Fig 2, E and G). These residual lipoprotein exudates contribute to deep capillary network disorganization as they became chronic and confluent in plaques. (Fig.4, C and D) and (Fig.5 D and G).

#### 6. Vascular perfusion / Capillary dropout

Reductions in the deep plexus, have been shown to correlate with disorganization of the retinal inner layers (DRIL) and with decreased visual function<sup>17</sup>. Capillary dropout in the deep capillary plexus imaged by OCTA is also associated with macular photoreceptor disruption on SD-OCT in patients with diabetic retinopathy<sup>27</sup>. In addition, it has been demonstrated that vascular dropout in the choriocapillaris of diabetics, can also be observed on OCTA<sup>28,29</sup>. (Fig.5F)

#### 7. Early findings

OCT angiography is able to detect vascular changes in patients with diabetes but without clinically detectable diabetic retinopathy<sup>10,26,30</sup>. Histopathologic studies reveal that is in DCP that majority of the changes happen early in diabetic retinopathy<sup>31</sup>. On the other hand, cystoid macular edema seems to preferentially occur in regions with absent deep plexus flow<sup>32,17</sup>. Therefore, OCTA can be a good technique to screen early stages of DR.



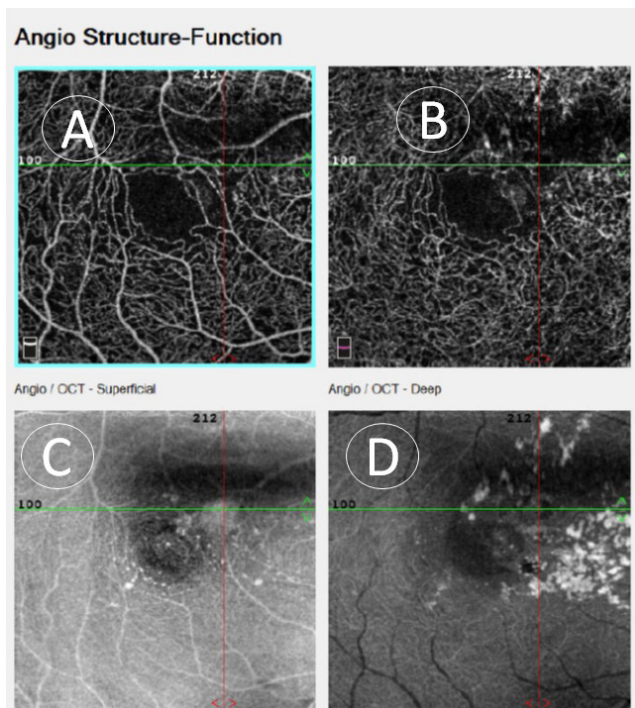


**Figure 4.** Superficial and deep plexus in DME: (A) OCTA, imaging from Optovue, showing the superficial capillaries and a normal, near circle-shaped FAZ (B): Deep capillaries plexus revealing disorganized network (located at 2h circle of the FAZ), where there was cystoid spaces, not totally recovered from the previous bullous retina. (C) and (D): En face OCT, superficial and deep, showing mainly in (D), hyperreflective residual lipoprotein exudates which contributes to deep capillary network disorganization.

## 8. The Foveal Avascular Zone

Enlargement of the foveal avascular zone (FAZ) are visualized in better detail and with greater resolution in OCTA than in FA<sup>7,14</sup>. There is a heterogeneity of the size of the FAZ<sup>33</sup> and confirming studies had shown that, on average, the size of the FAZ tends to increase with increasing severity of diabetic retinopathy and the presence of ischemic maculopathy.<sup>34,35,36,37</sup> Not only the size of the FAZ but also the irregularity of its (Fig: 4 A-B) circle shape, have been shown to correlate with the severity of DR.

## 9. The response to anti-VEGF treatment

The response to anti-VEGF treatment can be anticipated by the presence of macular ischemia, numerous microaneurysms, increased FAZ and decreased vascular density and flow<sup>38</sup> in the deep plexus. Disruption of the deep plexus in OCTA can be correlated with lesions in the photoreceptor layer and outer plexiform layer in structural OCT<sup>38</sup>.

## 10. Future of managing DME in OCTA era

Currently treatment of diabetic macular edema is usually

initiated when vascular damage has already occurred and some vascular changes may not be reversed<sup>10</sup>. The ability to visualize vascular features and correlate them with vision loss may enable us to intervene earlier, in order to prevent irreversible damage to the retina<sup>10</sup>.

## III. UPCOMING OCTA DEVELOPMENTS

### 1. Volume rendering

*En face* imaging not only flattens the volume within the region imaged, but also merges flow information between vessels. Abnormalities of segmentation can lead to either lack of visualization of true flow or incorrect attribution of flow to a specific layer within the retina<sup>39</sup>, especially in pathological tissue.

One method to avoid both problems is to use **volume rendering** of the underlying data. Volume rendering allows visualization of all layers of flow in the retina and permits manipulation of the data in 3 axes of rotation. Volume rendering does not depend on layer segmentation. Retinal structures such as cystoid spaces or tumefactions can be segmented from the structural OCT and integrated with the volume rendered OCTA data, since both are ultimately derived from the structural OCT<sup>40</sup>. This imaging modality has proven useful in evaluating cystoid macular edema due to retinal vascular causes<sup>41</sup> like DME. Examining the relationships between abnormalities in the retina, such as cystoid spaces and vascular anatomy is relatively easy with volume rendering, whereas the same assessment would be very difficult with *en face* imaging. A hybrid approach can be taken in which layers are color-coded for easier interpretation of the images. Volume rendering has not been implemented yet in most commercial instruments<sup>17</sup>.

### 2. Automated metrics of quantitative parameters of the vasculature in diabetics

Vascular density maps have been applied to patients with diabetic retinopathy and have been shown to correlate to the severity of diabetic retinopathy<sup>25</sup>. Other approaches have also been investigated including intercapillary area as well as investigation of the branching patterns of the capillary network<sup>42,43</sup>. The intercapillary area in diabetics shows increased heterogeneity with increasing levels of diabetic retinopathy<sup>44</sup>. On the other hand, cyst and lipoprotein exudates cause a distortion of capillary bed, producing enlargement of the interpapillary space seeming areas of non-perfusion, confounding the features in OCTA.(Fig.5F)

Ultimately, these techniques may provide an objective, automated and quantifiable measure of the progression of retinopathy over time and may be useful adjuncts in the clinical and clinical trial setting<sup>29,45</sup>

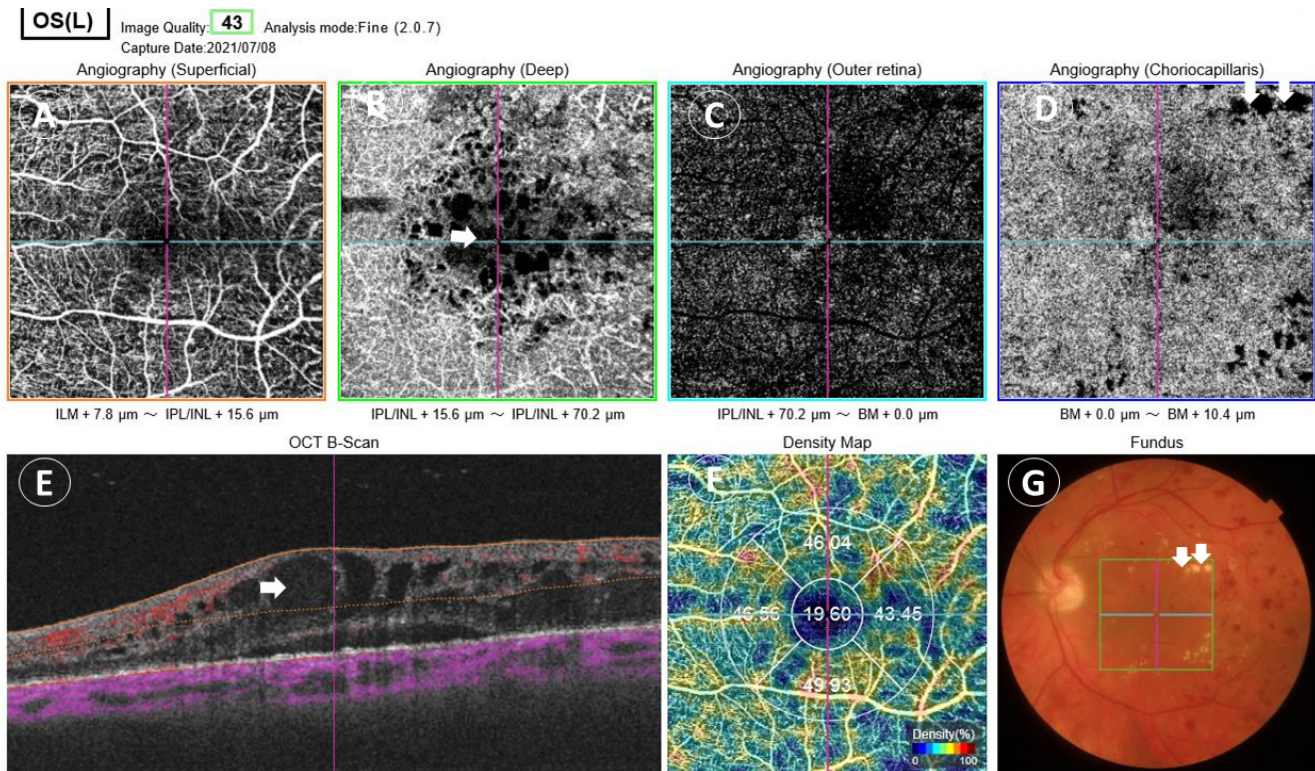


**Figure 5.** Multimodal imaging of OCTA report (OPTOVUE): (A) SCP, (B) DCP, (C) avascular layer and (D) choroidal plexus segmentation; (E) structural OCT with macrocysts and SRF and morphostructural alterations of the retinal layers, (F) a density map of vascular flow with a color scale of vascular density and (G) a color fundus photography where two hard exudate plaques can be seen (white vertical arrows). In the DCP (B) the cystic spaces (horizontal white arrows) can be seen as black spaces (absence of vascular capillaries) which can be interpreted as capillaries dropout. The same black images is seen for the exudate lipoproteic plaques at the level of choroidal layer (white vertical arrows).

### 3. Correlating the OCTA features in diabetic retinopathy with systemic control

Correlation of the OCTA features in diabetic retinopathy with systemic control will be available in the near future. A few early studies have suggested that worse diabetic control may be associated with worse OCTA features<sup>10,46</sup>. In the future, application of “big data” techniques to diabetic eye disease may be able to identify risk factors not only for diabetic retinopathy progression but also, possibly, for systemic morbidity in these patients<sup>10</sup>.

### CONCLUSION

OCTA has distinct advantages over FA in the evaluation of retinal diseases. It provides noninvasive simultaneous 3D structural and blood flow information, allowing for comprehensive evaluation of disease presentation and progression. In addition, the ability to quantify angiographic information allows for objective monitoring of treatment response. Because OCTA is a novel imaging modality, it is still unclear how we should use it in the disease management. With the expected technological improvements in the near future, mainly the automated metrics and volume rendering, will turn OCTA an important tool in standard DME and DR care<sup>39</sup>.

### REFERENCES

1. Simó R, Stitt AW, Gardner TW. Neurodegeneration in diabetic retinopathy: does it really matter? *Diabetologia*. 2018;61(9):1902-1912.
2. Antonetti DA, Klein R, Gardner TW. Diabetic Retinopathy. *N Engl J Med*. 2012;366(13):1227-1239.
3. Hamilton A, Ulbig M, Polkinghorne P. ed. Management of Diabetic Retinopathy. BMJ Books; 1st edition. London;1996.
4. Hagag AM, Gao SS, Jia Y, Huang D. Optical coherence tomography angiography: Technical principles and clinical applications in ophthalmology. *Taiwan J Ophthalmol*. 2017;7(3):115-129.
5. Couturier A, Mané V, Bonnín S, et al. Capillary plexus anomalies in diabetic retinopathy on optical coherence tomography angiography. *Retina*. 2015;35(11):2384-2391.
6. Coscas G, Lupidi M, Coscas F, Chhablani J, Cagini C. Optical Coherence Tomography Angiography in Healthy Subjects and Diabetic Patients. *Ophthalmologica*. 2018;239(2-3):61-73.
7. Ishibazawa A, Nagaoka T, Takahashi A, et al. Optical coherence tomography angiography in diabetic retinopathy: A prospective pilot study. *Am J Ophthalmol*. 2015;160(1):35-44.e1.
8. Parravano M, Costanzo E, Borrelli E, et al. Appearance of cysts and capillary non perfusion areas in diabetic macular edema using two different OCTA devices. *Sci Rep*. 2020;10(1).
9. Pechauer AD, Jia Y, Liu L, Gao SS, Jiang C, Huang D. Optical

- coherence tomography angiography of peripapillary retinal blood flow response to hyperoxia. *Investig Ophthalmol Vis Sci.* 2015;56(5):3287-3291.
10. Spaide RF, Fujimoto JG, Waheed NK, Sadda SR, Staurengi G. Optical coherence tomography angiography. *Prog Retin Eye Res.* 2018;64:1-55.
  11. Zhang M, Wang J, Pechauer AD, et al. Advanced image processing for optical coherence tomographic angiography of macular diseases. *Biomed Opt Express.* 2015;6(12):4661.
  12. Stanga PE, Papayannis A, Tsamis E, et al. New Findings in Diabetic Maculopathy and Proliferative Disease by Swept-Source Optical Coherence Tomography Angiography. *Dev Ophthalmol.* 2016;56:113-121.
  13. Matsunaga DR, Yi JJ, De Koo LO, Ameri H, Puliafito CA, Kashani AH. Optical coherence tomography angiography of diabetic retinopathy in human subjects. *Ophthalmic Surg Lasers Imaging Retin.* 2015;46(8):796-805.
  14. Miwa Y, Murakami T, Suzuma K, et al. Relationship between Functional and Structural Changes in Diabetic Vessels in Optical Coherence Tomography Angiography. *Sci Rep.* 2016;6.
  15. Hasegawa N, Nozaki M, Takase N, Yoshida M, Ogura Y. New insights into microaneurysms in the deep capillary plexus detected by optical coherence tomography angiography in diabetic macular edema. *Investig Ophthalmol Vis Sci.* 2016;57(9):OCT348-OCT355.
  16. Bradley PD, Sim DA, Keane PA, et al. The evaluation of diabetic macular ischemia using optical coherence tomography angiography. *Investig Ophthalmol Vis Sci.* 2016;57(2):626-631.
  17. Spaide RF. Volume-Rendered Optical Coherence Tomography of Diabetic Retinopathy Pilot Study. *Am J Ophthalmol.* 2015;160(6):1200-1210.
  18. Henriques J, Figueira J, Nascimento J, et al. Retinopatia Diabética - orientações clínicas do Grupo de Estudos da Retina de Portugal. *Oftalmol rev SPO.* 2015;39(4 supl. Out-Dez).
  19. Wells JA, Glassman AR, Ayala AR, et al. Aflibercept, bevacizumab, or ranibizumab for diabetic macular edema. *N Engl J Med.* 2015;372(13):1193-1203.
  20. Virgili G, Parravano M, Evans JR, Gordon I, Lucenteforte E. Anti-vascular endothelial growth factor for diabetic macular oedema: A network meta-analysis. *Cochrane Database Syst Rev.* 2017;2017(6).
  21. Henriques J, Pinto F, Rosa PC, et al. Continuous wave milipulse yellow laser treatment for perifoveal exudative vascular anomalous complex-like lesion: A case report. *Eur J Ophthalmol.* 2020 (online ahead of print).
  22. Querques G, Kuhn D, Massamba N, Leveziel N, Querques L, Souied EH. ELECTRONIC CLINICAL CASE Perifoveal exudative vascular anomalous complex Complexe vasculaire exsudatif perifovéal anormal. *J Fr Ophthalmol.* 2011;34.
  23. Ayachit AG, Sacconi R, Ayachit GS, Joshi S, Querques G. Perifoveal exudative vascular anomalous complexlike lesion as a complication of prepapillary arterial loops. *Ophthalmic Surg Lasers Imaging Retin.* 2018;49(12):974-978.
  24. Sacconi R, Freund KB, Yannuzzi LA, et al. The Expanded Spectrum of Perifoveal Exudative Vascular Anomalous Complex. *Am J Ophthalmol.* 2017;184:137-146.
  25. Agemy SA, Sripsema NK, Shah CM, et al. Retinal vascular perfusion density mapping using optical coherence tomography angiography in normals and diabetic retinopathy patients. *Retina.* 2015;35(11):2353-2363.
  26. De Carlo TE, Chin AT, Bonini Filho MA, et al. Detection of microvascular changes in eyes of patients with diabetes but not clinical diabetic retinopathy using optical coherence tomography angiography. *Retina.* 2015;35(11):2364-2370.
  27. Scarinci F, Nesper PL, Fawzi AA. Deep Retinal Capillary Nonperfusion Is Associated with Photoreceptor Disruption in Diabetic Macular Ischemia. *Am J Ophthalmol.* 2016;168:129-138.
  28. Moulton E, Choi W, Waheed NK, et al. Ultrahigh-speed swept-source OCT angiography in exudative AMD. *Ophthalmic Surg Lasers Imaging Retin.* 2014;45(6):496-505.
  29. Choi W, Waheed NK, Moulton EM, et al. Ultrahigh speed swept source optical coherence tomography angiography of retinal and choriocapillaris alterations in diabetic patients with and without retinopathy. *Retina.* 2017;37(1):11-21.
  30. Dimitrova G, Chihara E, Takahashi H, Amano H, Okazaki K. Quantitative retinal optical coherence tomography angiography in patients with diabetes without diabetic retinopathy. *Investig Ophthalmol Vis Sci.* 2017;58(1):190-196.
  31. Moore J, Bagley S, Ireland G, McLeod D, Boulton Me. Three dimensional analysis of microaneurysms in the human diabetic retina. *J Anat.* 1999;194(1):89-100.
  32. Mané V, Dupas B, Gaudric A, et al. Correlation between cystoid spaces in chronic diabetic macular edema and capillary nonperfusion detected by optical coherence tomography angiography. *Retina.* 2016 Dec;36 Suppl 1:S102-S110.
  33. Bresnick GH, Condit R, Syrjala S, Palta M, Groo A, Korth K. Abnormalities of the Foveal Avascular Zone in Diabetic Retinopathy. *Arch Ophthalmol.* 1984;102(9):1286-1293.
  34. Samara WA, Shahlaee A, Adam MK, et al. Quantification of Diabetic Macular Ischemia Using Optical Coherence Tomography Angiography and Its Relationship with Visual Acuity. *Ophthalmology.* 2017;124(2):235-244.
  35. Di G, Weihong Y, Xiao Z, et al. A morphological study of the foveal avascular zone in patients with diabetes mellitus using optical coherence tomography angiography. *Græfe's Arch Clin Exp Ophthalmol.* 2016;254(5):873-879.
  36. Jia Y, Bailey ST, Hwanga TS, et al. Quantitative optical coherence tomography angiography of vascular abnormalities in the living human eye. *Proc Natl Acad Sci U S A.* 2015;112(18):E2395-E2402.
  37. Takase N, Nozaki M, Kato A, Ozeki H, Yoshida M, Ogura Y. Enlargement of foveal avascular zone in diabetic eyes evaluated by en face optical coherence tomography angiography. *Retina.* 2015;35(11):2377-2383.
  38. Lee J, Moon BG, Cho AR, Yoon YH. Optical Coherence Tomography Angiography of DME and Its Association with Anti-VEGF Treatment Response. *Ophthalmology.* 2016;123(11):2368-2375.
  39. Hagag AM, Gao SS, Jia Y, Huang D. Optical coherence tomography angiography: Technical principles and clinical applications in ophthalmology. *Taiwan J Ophthalmol.* 2017;7(3):115-129.
  40. Cabral D, Pereira T, Ledesma-Gil G, et al. Volume rendering of dense B-scan optical coherence tomography angiography to evaluate the connectivity of macular blood flow. *Investig Ophthalmol Vis Sci.* 2020;61(6).
  41. Spaide RF. Volume-rendered angiographic and structural optical

- coherence tomography. *Retina*. 2015;35(11):2181-2187.
42. Cheung N, Donaghue KC, Liew G, et al. Quantitative Assessment of Early Diabetic Retinopathy Using Fractal Analysis. *Diabetes Care*. 2009;32(1):106-110.
  43. Tang FY, Ng DS, Lam A, et al. Determinants of Quantitative Optical Coherence Tomography Angiography Metrics in Patients with Diabetes. *Sci Rep*. 2017;7(1).
  44. Schottenhamml J, Moulton EM, Ploner S, et al. An automatic, intercapillary area-based algorithm for quantifying diabetes-related capillary dropout using optical coherence tomography angiography. *Retina*. 2016 Dec;36 Suppl 1:S93-S101.
  45. Salz DA, De Carlo TE, Adhi M, et al. Select features of diabetic retinopathy on swept-source optical coherence tomographic angiography compared with fluorescein angiography and normal eyes. *JAMA Ophthalmol*. 2016;134(6):644-650.
  46. Bhanushali D, Anegondi N, Gadde SGK, et al. Linking retinal microvasculature features with severity of diabetic retinopathy using optical coherence tomography angiography. *Investig Ophthalmol Vis Sci*. 2016;57(9):519-525.



## 8.3.

# PROLIFERATIVE DIABETIC RETINOPATHY

Bernardete Pessoa, Angelina Meireles  
Centro Hospitalar e Universitário do Porto

In addition to diabetic macular edema (DME) and macular ischemia, proliferative diabetic retinopathy (PDR) is one of the most feared reasons for vision loss due to end stage diabetic retinopathy and related complications as vitreous hemorrhage, tractional retinal detachment, and neovascular glaucoma<sup>1</sup>.

Retinal ischemia is the primary stimulus for neovascularization by upregulated VEGF and other factors, such as inflammatory cytokines and oxidative stress<sup>2</sup>.

### OCTA VERSUS FLUORESCIN ANGIOGRAPHY (FA) IN PDR APPROACH

Although Fluorescein angiography (FA) remains the gold standard for the analyses of the retinal ischemia, neovascularization, particularly of the retinal periphery, detailed features of new vessels and surrounding retinal microvasculature cannot be shown because of fluorescein leakage. In opposition to OCTA, FA is a time-consuming invasive procedure, unrepeatable on the same day or in the short term and can cause severe life-threatening, although extremely rare, complications. Furthermore, does not differentiate whether leakage is from preretinal NV or from other sources and only one eye can be chosen as the early transit eye for characterization<sup>3,4</sup>.

OCTA may be more sensitive than traditional FA in detecting microvascular changes in retinal diseases by enabling high resolution depth-resolved visualization of multiple layers and identification, besides capillary abnormalities (such as microaneurysms and vascular tortuosity), alterations in the shape and size of the foveal avascular zone (FAZ), neovascularization and abnormal retinal vascular changes in PDR eyes<sup>5,6</sup>.

OCTA also enabled differentiation of NV from large vessel vasculitis, and distinguished areas of fibrovascular proliferation with regressed NV from active NV<sup>4</sup>.

Out as main disadvantages of OCTA are the need for visual acuity that allows to fixate on a target, whereas FA does not require fixation, and OCTA have less performance than FA in the presence of vitreous hemorrhage<sup>4</sup>.

Moreover, the quality of the image can be impaired by artifacts induced by segmentation errors due intraretinal edema, when DME is present, and fake deep projections images from superficial vessels. Hypo-reflective

intraretinal cyst on en face OCTA slab can also be misinterpreted as areas of ischemia, a hallmark precursor of PDR stage<sup>5,7</sup>.

OCTA seems to be equivalent or even superior to FA in identifying non-perfused areas (NPA) and in the same field of view, wide field swept-source OCT (SS OCT) could identify areas of NV as well as ultra-wide FA (UWFFA)<sup>5,8-10</sup>.

The field of view for conventional OCTA, which is 3 mm × 3 mm or 6 mm × 6 mm, restricted to the posterior pole is clearly insufficient when compared with conventional FA for PDR disease identification.

However, new scan patterns and image reconstruction methods (montage) have been developed, allowing the inclusion of wider retinal portions, beyond the posterior vascular arcades<sup>5</sup>.

The ultimate technology SS OCT using a narrow bandwidth and longer wavelength tunable (1050 nm) laser, penetrates tissue better allowing wide field (12x 12 mm) image acquisition in seconds due to the higher speed nature of the imaging, as well as improved choroidal visualization. Even though 12 x 12 mm scans limit the resolution of small caliber retinal capillaries, the enhanced resolution of smaller 3x3 mm scans montaged together would prolong scanning time and make it less clinically applicable<sup>8</sup>.

Although the field of view in UWFFA is wider comparing with the ultimate wide-field (WF) SS-OCTA (PLEX® Elite 9000 12x12mm field of view – with five SS-OCTA 12x12mm scans - central, nasal inferior, nasal superior, temporal inferior, and temporal superior) it might be clinically enough useful because most NVs in PDR cases are observed within the retina mid periphery which is covered by OCTA images. A single 12x12mm SS-OCTA centered on the fovea was able to detect at least one area of NV in 90% of PDR eyes and SS-OCTA 12x12mm montages of the posterior pole were able to capture almost all areas of peripheral NV<sup>4,9</sup>.

According to Russel et al study, compared to UWFFA, detection by WF-OCTA had a sensitivity of 0.98 and a specificity of 0.82 for NPA and a sensitivity of 1.0 and specificity of 0.97 for NV detection. NV detected only by UWFFA, but not by OCTA, is rare<sup>4</sup>.

When compared to FA, WF-OCTA demonstrated a sensibility of 92% and a specificity of 99% to differentiate

between IRMA and neovascularization elsewhere (NVE), with a positive and negative predictive value of 96% and 97%, respectively<sup>4,11</sup>.

Comparing SS-OCTA and SD-OCTA, the most recent evidence shows that most areas of NV with a single 12x12mm scan or by using the wider 12x12mm montaged field of view highlights the advantages of SS-OCTA over SD-OCTA, which has a smaller field of view and requires targeted scans of areas with NV (12). Furthermore, the changes in NV seen on FA could be monitored longitudinally using wide field SS-OCTA once the areas of NV have been identified. As OCTA can display capillary networks without dye injection, this technology can be used to monitor neovascularization changes following the treatments and currently assumes also an important role as a predictor and a predictive tool in PDR control<sup>4</sup>.

### OCTA IMAGING PATTERN IN PRE-PDR AND PDR STAGES

In OCTA neovascularization appears as disorganized vessels originating from retina into vitreous which can be located on disk or near to NPAs and intraretinal microvascular abnormalities (IRMAs) (figures 1-3) (2). IRMAs can be diagnosed as dilated retinal vessels without internal limiting membrane (ILM) or posterior hyaloid breach in opposition to neovascularization with expansion into vitreous with ILM breakdown<sup>(13)</sup>. Beyond the identification of DME and other OCT signs of diabetic retinopathy, B-scans that corresponded to en face angiograms provides additional information about whether NV is subhyaloid, growing along the posterior hyaloid, or associated with retinal traction<sup>14,15</sup>. OCTA have also differentiated a sub-type of exuberant vascular proliferation (EVP), as a proliferation of irregular smaller-caliber vessels in more active disease, correlating with more active leakage in FA.

The precise location of NV, above or below ILM, by OCTA have also implications as a predictive biomarker, as an important classification sub-type of NV<sup>9,16,17</sup>.

Compared with above ILM type, the below ILM type is more sensitive to PRP treatment. Hence, the enhance of retinal circulation by PRP treatment has little effects on the above ILM type, attached to the posterior vitreous membrane and growing into the vitreous cavity, and anti-VEGF therapy is pointed out as a better option for those cases<sup>18</sup>.

Another OCTA identified feature of vascular abnormality in some PDR eyes is intraretinal neovascularization, with the appearance of hairpin loops formed by dilated vessels near non-perfusion areas. This tuft of neovascularization might originate from abnormal vessels located in deep retina<sup>19</sup>.

In conclusion, the new advances of OCTA technology towards a high sensibility and specificity detecting and defining different sub-types of pre-PDR and PDR disease, in addition to its potential predictor and predictive biomarker capacity, makes this noninvasive and rapid exam a promising tool for the early diagnoses

and follow-up of the most feared and severe form of diabetic retinopathy.

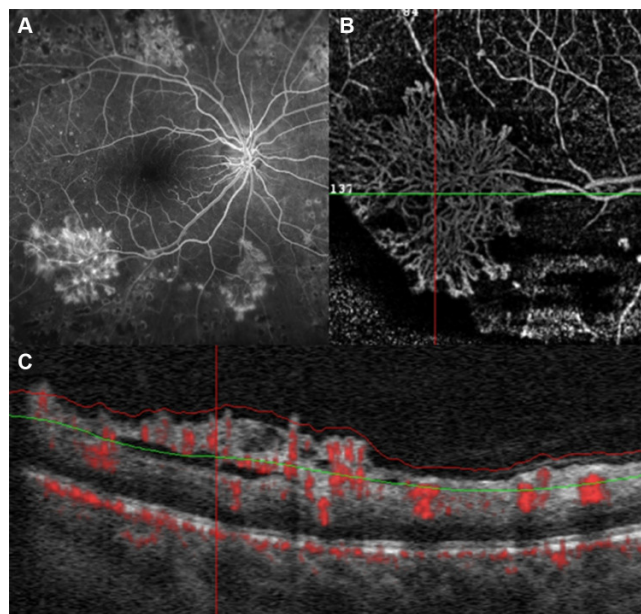


**Figure 1.** A) FA image of an eye with PDR. Note NVE alongside the temporal inferior arcade with a sea fan configuration and leakage. (B) Corresponding OCTA image of the same complex, in which the filamentous irregular new vessels are well outlined and not obscured by fluorescein leakage. (C) OCT B-scan with flow overlay in red showing a flat complex with ILM breaching and flow signal, consistent with active disease.

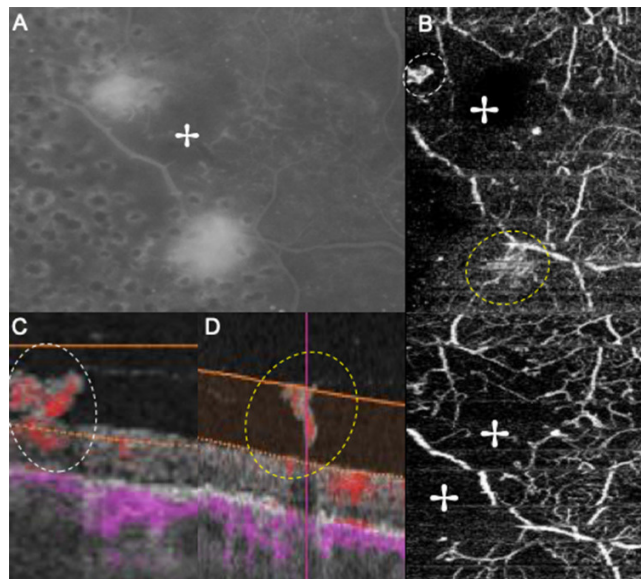


**Figure 2.** Montage showing two NVEs. (A) Late FA image shows leakage associated with both NVEs. (B, top) In OCTA both NVEs appear as vascular loops with irregular new vessels, each one circled by a dashed ellipse. (B, bottom) Areas with absent flow signal adjacent to NVEs (+) are seen, corresponding to the capillary nonperfusion evidenced on FA. (C and D) B-scans of the NVEs show ILM breaching and flow signal, indicating disease activity, in agreement with the FA. Each NVE is circled by a colored dashed ellipse matching the en face image in (B, top).

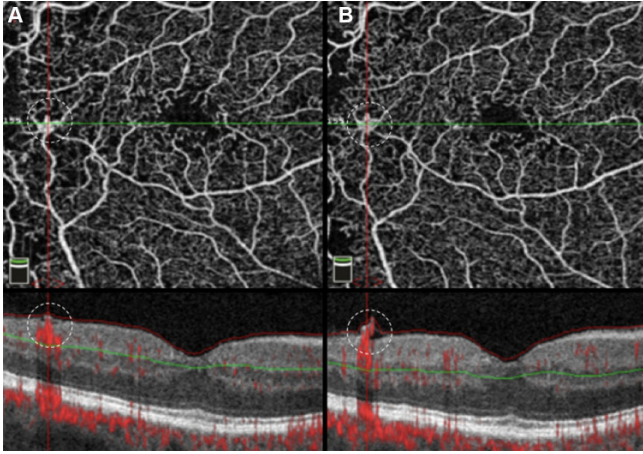


**Figure 3.** Case showing progression of NVE over time. Left images were obtained in an early disease stage. OCTA en face image (A, top) showing a small temporal NVE within the dashed circle. Corresponding OCT B-scan with flow overlay (A, bottom) shows a flat NVE with breaching of the ILM and flow signal (located within the dashed circle). Follow-up OCTA images revealed the same features in the en face OCTA, (B, top; NVE located within the dashed circle) while the corresponding OCT B-scan (B, bottom) revealed NVE progression (situated within the dashed circle), with ILM breaching and new protrusion. Abbreviations: FA, fluorescein angiography; ILM, internal limiting membrane; NVE, neovascularization elsewhere; OCT, optical coherence tomography; OCTA, optical coherence tomography angiography; PDR, proliferative diabetic retinopathy.

Figure 1-3 Source: Vaz-Pereira S et al. Clin Ophthalmol. 2020;14:3351-3362(20). This article is distributed under the terms of the Creative Commons Attribution - Non Commercial (unported, v3.0) License.

## REFERENCES

- Nentwich MM, Ulbig MW. Diabetic retinopathy - ocular complications of diabetes mellitus. World J Diabetes. 2015;6(3):489-99.
- Liu G, Xu D, Wang F. New insights into diabetic retinopathy by OCT angiography. Diabetes Res Clin Pract. 2018;142:243-53.
- Stanga PE, Papayannis A, Tsamis E, Stringa F, Cole T, D'Souza Y, et al. New Findings in Diabetic Maculopathy and Proliferative Disease by Swept-Source Optical Coherence Tomography Angiography. Dev Ophthalmol. 2016;56:113-21.
- Russell JF, Shi Y, Hinkle JW, Scott NL, Fan KC, Lyu C, et al. Longitudinal Wide-Field Swept-Source OCT Angiography of Neovascularization in Proliferative Diabetic Retinopathy after Panretinal Photocoagulation. Ophthalmol Retina. 2019;3(4):350-61.
- Cicinelli MV, Cavalleri M, Brambati M, Lattanzio R, Bandello F. New imaging systems in diabetic retinopathy. Acta Diabetologica. 2019;56(9):981-94.
- Alam M, Zhang Y, Lim JI, Chan RVP, Yang M, Yao X. Quantitative optical coherence tomography angiography features for objective classification and staging of diabetic retinopathy. Retina. 2020;40(2):322-32.
- Spaide RF, Fujimoto JG, Waheed NK. Image artifacts in optical coherence tomography angiography. Retina. 2015;35(11).
- Mustafi D, Saraf SS, Shang Q, Olmos de Koo LC. New developments in angiography for the diagnosis and management of diabetic retinopathy. Diabetes Res Clin Pract. 2020;167:108361.
- Sawada O, Ichiyama Y, Obata S, Ito Y, Kakinoki M, Sawada T, et al. Comparison between wide-angle OCT angiography and ultra-wide field fluorescein angiography for detecting non-perfusion areas and retinal neovascularization in eyes with diabetic retinopathy. Graefes Arch Clin Exp Ophthalmol. 2018;256(7):1275-80.
- Couturier A, Mané V, Bonnin S, Erginay A, Massin P, Gaudric A, et al. Capillary plexus anomalies in diabetic retinopathy on optical coherence tomography angiography. Retina. 2015;35(11):2384-91.
- Arya M, Sorour O, Chaudhri J, Alibhai Y, Waheed NK, Duker JS, et al. Distinguishing intraretinal microvascular abnormalities from retinal neovascularization using optical coherence tomography angiography. Retina. 2020;40(9):1686-95.
- Sambhav K, Grover S, Chalam KV. The application of optical coherence tomography angiography in retinal diseases. Surv Ophthalmol. 2017;62(6):838-66.
- Lee CS, Lee AY, Sim DA, Keane PA, Mehta H, Zarranz-Ventura J, et al. Reevaluating the definition of intraretinal microvascular abnormalities and neovascularization elsewhere in diabetic retinopathy using optical coherence tomography and fluorescein angiography. Am J Ophthalmol. 2015;159(1):101-10.e1.
- Hwang TS, Jia Y, Gao SS, Bailey ST, Lauer AK, Flaxel CJ, et al. Optical coherence tomography angiography features of diabetic retinopathy. Retina. 2015;35(11):2371-6.
- Ishibazawa A, Nagaoka T, Yokota H, Takahashi A, Omae T, Song Y-S, et al. Characteristics of Retinal Neovascularization in Proliferative Diabetic Retinopathy Imaged by Optical Coherence Tomography Angiography. Invest Ophthalmol Vis Sci. 2016;57(14):6247-55.
- Ballman KV. Biomarker: Predictive or Prognostic? J Clin Oncol. 2015;33(33):3968-71.
- Russell JF, Al-Kharsan H, Shi Y, Scott NL, Hinkle JW, Fan KC, et al. Retinal Nonperfusion in Proliferative Diabetic Retinopathy Before and After Panretinal Photocoagulation Assessed by Widefield OCT Angiography. Am J Ophthalmol. 2020;213:177-85.
- Chatziralli IP, Sergentanis TN, Sivaprasad S. Prediction of regression of retinal neovascularisation after panretinal photocoagulation for proliferative diabetic retinopathy. Graefes Arch Clin Exp Ophthalmol. 2016;254(9):1715-21.
- Hwang TS, Zhang M, Bhavsar K, Zhang X, Campbell JP, Lin P, et al. Visualization of 3 Distinct Retinal Plexuses by Projection-Resolved Optical Coherence Tomography Angiography in Diabetic Retinopathy. JAMA Ophthalmol. 2016;134(12):1411-9.
- Vaz-Pereira S, Silva JJ, Freund KB, Engelbert M. Optical Coherence Tomography Angiography Features of Neovascularization in Proliferative Diabetic Retinopathy. Clin Ophthalmol. 2020;14:3351-62.





# JUXTAFOVEAL IDIOPATHIC TELANGIECTASIA

Beatriz O. Lopes,<sup>1</sup> Margarida Brízido,<sup>1</sup> Vanessa Lemos,<sup>1</sup> Margarida Miranda,<sup>1</sup> João Nascimento<sup>1</sup>  
 1 - Hospital Beatriz Ângelo, Loures, Portugal

## INTRODUCTION

Type 2 macular telangiectasia (MacTel 2) is an acquired vascular disease of the macula.<sup>1</sup> It was first described as an idiopathic juxta-retinal telangiectasia (according to the classification system introduced by Gass and Blodi)<sup>2</sup> and later renamed by Yannuzzi *et al.*<sup>3</sup>

MacTel 2 describes an idiopathic macular telangiectasia which is primarily bilateral, occult, and non-exudative.<sup>1,2</sup> It affects both sexes equally, with a predominance in the fifth to seventh decades of life.<sup>4,5</sup>

Its pathophysiology remains poorly understood, however, it is currently believed that MacTel 2 is a neurodegenerative disease of the macula<sup>6</sup>, characterized by Muller cell dysfunction, macular capillary network change and neuronal atrophy.<sup>1,3</sup> Muller cells play an important role in maintaining the structural integrity of the fovea, providing an important nutritional and regulatory support for retinal neuronal and vascular cells.<sup>6,7</sup> Its dysfunction is thought to be responsible for photoreceptor death, dysregulation of inflammatory and angiogenic factors, vascular telangiectasia and subsequent subretinal neovascularization (SRNV).<sup>6,8</sup> The association of this disease with genetic factors, diabetes mellitus and arterial hypertension has also been described.<sup>2</sup>

## CLINICAL CLASSIFICATION

The characteristic findings of MacTel 2 include loss of retinal transparency, retinal crystalline deposits, right-angled venules, intraretinal cystoid spaces, retinal pigment migration, and pigment plaques.<sup>9</sup>

The earliest clinical findings of this entity are the intraretinal crystalline deposits; later, loss of transparency of the parafoveal temporal region becomes apparent, eventually leading to the appearance of right-angled vessels, and hyperplasia and migration of the retinal pigment epithelium (RPE).<sup>1,6</sup>

There are also progressive changes in the juxtafoveal retinal microvasculature, initially at the level of the deep capillary plexus, with subsequent involvement of the superficial capillary plexuses and development of anastomoses between these two plexus, as well as the development of SRNV in the more advanced stages of the disease.<sup>1,10,11</sup>

## MULTIMODAL EVALUATION

**Fluorescein angiography (FA)** has been considered, for many years, the gold standard in the study and evaluation of MacTel 2, typically showing ectasia of the temporal capillaries of the fovea, with late diffuse hyperfluorescence.<sup>4,5</sup> However, FA does not allow the distinction of superficial and deep capillary plexuses changes and may be insufficient to show changes in specific retinal layers and to detect or monitor SRNV.<sup>6</sup>

**Spectral domain optical coherence tomography (SD-OCT)** has offered great insight into the pathogenesis of this disease, by allowing a more detailed assessment of neurodegenerative atrophic changes of the retinal layers in the fovea, including hyporeflective cavitations in the inner and outer retinal layers, internal limiting membrane drupe, atrophy of photoreceptors, disruption of the ellipsoid zone and foveal detachment.<sup>1,10</sup> These findings arise due to neural atrophy and disruption of the foveal structure and appear independent of vascular changes.<sup>12</sup> Unlike other retinal vascular disorders, such as diabetic macular edema and branch retinal vein occlusion, intraretinal hyporeflective spaces and macular leakage on FA are not associated with increased retinal thickening<sup>11</sup> (Figure 1).

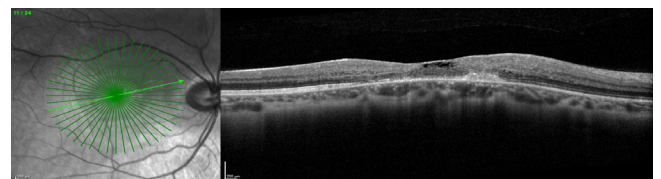


**Figure 1.** Figure 1 - SD-OCT evaluation showing inner retinal hyporeflective cavitations, disruption of the ellipsoid zone and atrophy of photoreceptors in a 27-year-old patient diagnosed with MacTel 2.

Courtesy of Prof. Dr. Rufino Silva

**Blue-light fundus autofluorescence (FAF)**, used as a complementary tool for MacTel 2 diagnosis, shows an increase of relative hyperautofluorescence in the temporal perifoveal area due to macular pigment depletion in early stages, with vascular alterations extending centripetally and a more diffuse, circumferential relative increase

in autofluorescence as the disease progresses. In the late phases, in the presence of RPE atrophy, areas of hypofluorescence are visible, coupled with increased relative hyperautofluorescence.<sup>4</sup>

### OPTICAL COHERENCE TOMOGRAPHY ANGIOGRAPHY (OCT-A) EVALUATION

OCT-A is a new, fast, non-invasive imaging modality that allows detection of high-resolution three-dimensional angiographic information of the retina and choroid, without intravenous dye injection. OCT-A can selectively visualize specific layers: the superficial vascular plexus, the deep vascular plexus, and the outer capillary plexus, contrary to FA. In addition, it has many other advantages over this exam: it is safer, easily repeatable, provides superior image quality, is less affected by the fluorescein leakage that obscures the microvasculature, and provides better imaging through cataracts and segmentation of the retinal and choroidal layers in three dimensions so that the disease process can be better localized.<sup>11</sup>

It completely changed the definition and assessment of this entity, improving the diagnosis of all stages that define the progression of MacTel 2.<sup>10</sup> OCT-A surpasses the diagnosing capability of other exams, by detecting early retinal microvasculature abnormalities mostly in the deep parafoveal temporal capillary plexus, which are within normal limits when evaluated by SD-OCT and are too

thin to be detected by FA.<sup>(1,6)</sup> These microvascular changes may extend circumferentially around the fovea with subsequent involvement of the superficial capillary plexus and posterior development of chorioretinal anastomoses and SRNV in the latter stages of the disease.<sup>6</sup>

Chen *et al.*<sup>1</sup> developed a grading system to classify MacTel 2 severity, based on OCT-A findings seen on *en face* images (Table 1).

Toto *et al.*<sup>4</sup> have created a classification system for MacTel 2 by OCT-A:

- Grade 1: vascular anomalies in the deep and/or superficial plexuses temporal to the fovea
- Grade 2: vascular anomalies in the deep and/or superficial plexuses temporal and nasal to the fovea
- Grade 3: markedly diffuse circumferential vascular anomalies in the deep and superficial plexuses
- Grade 4: neovascularization in the outer retina with any OCT-A signs of Grade 1 to 3

In early nonproliferative MacTel 2, OCT-A images usually demonstrate dilated vessels in the deep retinal capillary plexus that are most pronounced in the region temporal to the fovea. In intermediate, nonproliferative MacTel 2, OCT-A images show multiple, telangiectatic, microaneurysmal-like dilated vessels, residing within the middle retinal layer and extending to the inner and outer retina, with disruption of the ellipsoid zone. In late proliferative or neovascular MacTel 2, OCT-A shows significant alter-

**Table 1.** Staging of idiopathic macular telangiectasia type 2 patients based on optical coherence tomography angiography imaging  
Adapted from *Optical Coherence Tomography Angiography Findings in Type-2 Macular Telangiectasia* by Nalci H *et al.* 2017, *Turk J Ophthalmol.*

Table 1. Staging of idiopathic macular telangiectasia type 2 patients based on optical coherence tomography angiography imaging	
Grade	Findings
1	Normal superficial capillary network
	Telangiectatic changes in the deep capillary network, predominantly temporal of the fovea
2	Mild/moderate telangiectatic changes in the superficial capillary network
	Marked telangiectatic changes in the deep capillary network temporal of the fovea
	Reduced vascular density with capillary closure in the superficial and deep capillary networks
	Irregular capillary size and shape in the perifoveal region of the superficial and deep capillary networks
	Dilated arterioles and right angle venules
3	FAZ irregularity
	Reduced vascular density with increased capillary closure in the superficial and deep capillary networks
	Vascular invasion reaching the RPE layer
	Vascular invasion of the FAZ
	Pigment accumulation causing optical shadowing
	One or more sets of feeding and draining vessels in the superficial and deep layers
4	Abnormal FAZ shape with abnormal shape and dragging of vessels in the perifoveal region
	Visible blood flow through the SRNV formed in the outer retina, RPE, and choroid
5	Marked thinning and reduced vascular density in the outer retina
	Larger vascular diameter but reduced vascular density in the SRNV
	Blood flow visible in the disciform/fibrovascular layer and may advance to the deep choroid

FAZ: Foveal avascular zone, RPE: Retina pigment epithelium, SRNV: Subretinal neovascularization

ations in the juxtafoveal capillary network, with prominent anastomoses. The presence of abnormal vessels corresponds to an area with retinal vascular anastomoses that extends to the outer retina where the ellipsoid zone is disrupted, forming a subretinal fibrovascular plaque.<sup>11</sup> Figures 2 and 3 illustrate typical changes seen in an OCT-A evaluation of a patient diagnosed with MacTel 2, before and after anti-VEGF treatment, respectively.

Subretinal neovascular complexes may not originate solely from retinal vascular structures, as have been previously proposed; in fact, Zhang *et al.*<sup>13</sup> showed that they may also be connected to the choroidal vasculature. According to the literature, other findings described in patients with MacTel 2 include an increased choroidal thickness, which remains controversial. While the role of the choroid in the pathogenesis of the disease is uncertain, it is plausible that Muller cell dysfunction may lead to compensatory choroidal changes. Another explanation may be that the choroidal thickness may increase in response to an increase in the outward production of the vascular endothelial growth factor by RPE.<sup>6</sup> Nunes *et al.*<sup>14</sup> suggested that a thick choroid may be an early manifestation of this entity, which may be a valuable diagnostic clue.

OCT-A also allows quantitative measurements of retinal thickness,<sup>11</sup> as well as vascular density, that seems to be significantly decreased in MacTel 2 patients, especially in the deep plexus.<sup>6, 15</sup> Rarefaction of foveal vessels with increase of the intervascular spaces were another important features described.<sup>4</sup> Changes in vascular density may be explained by capillary network loss and telangiectatic vessels, a reflection of Muller cells degeneration.<sup>1, 6, 15</sup> Enlargement of the foveal avascular zone (FAZ) of deep plexus, also a consequence of the loss of capillary plexus, is another feature of MacTel 2 that could be observed in OCT-A in the earlier stages of the disease.<sup>6, 15</sup>

Determination of the acircularity index of the FAZ has also been described by Giray Ersoz *et al.*<sup>9</sup> The authors concluded that the increase of the acircularity index was associated with a greater severity of the disease.

## CONCLUSION

MacTel 2 affects all microvascular layers of the retina and OCT-A is useful for characterization of this retinal vascular abnormality, providing a better understanding of the pathogenesis and a clear view of disease progression.

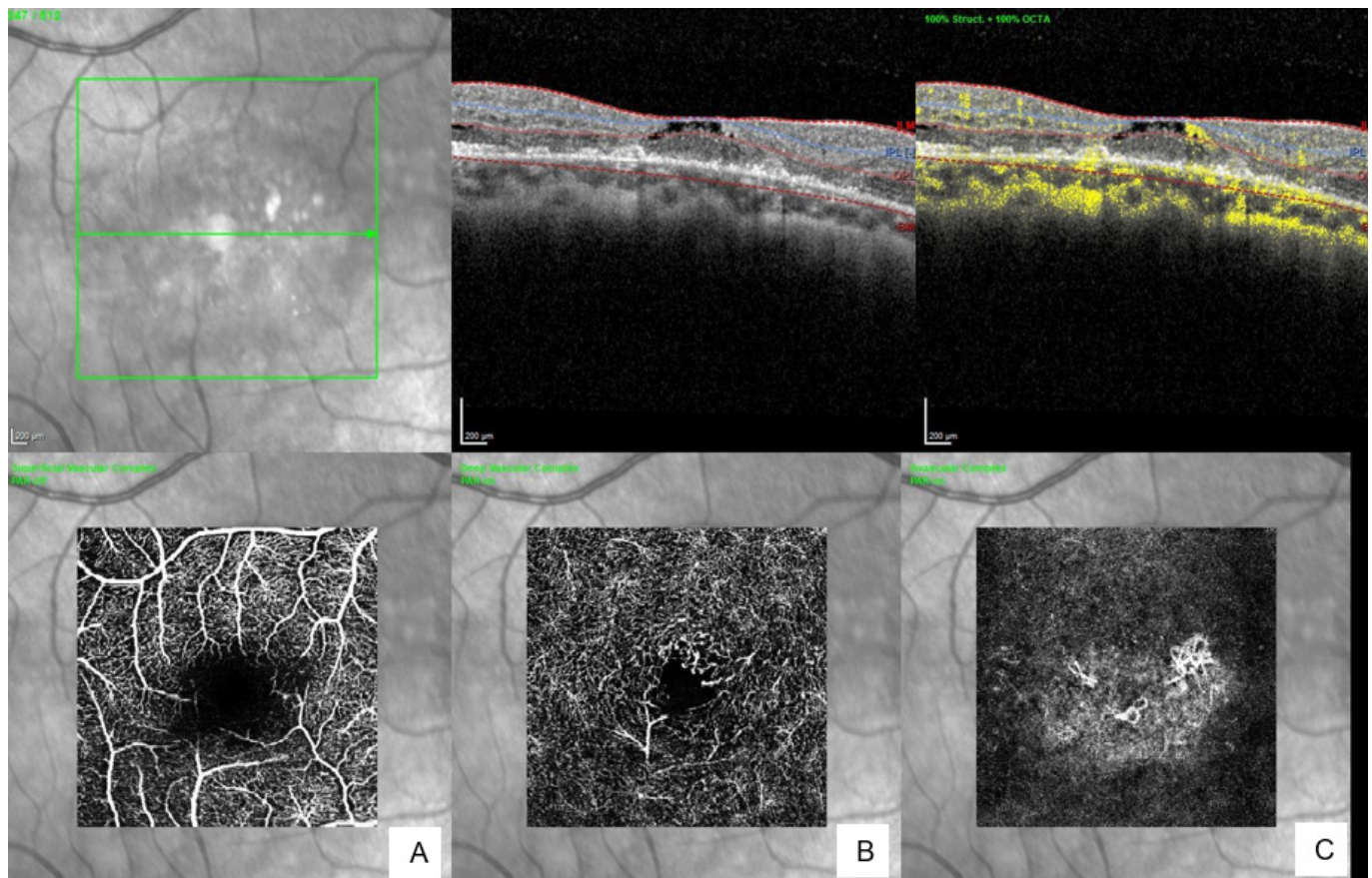


**Figure 2.** OCT-A evaluation showing slightly reduced temporal vascular density in the superficial plexus (A), localized juxtafoveal dilation of the deep plexus (B) and clear vascular invasion of the outer retina by the abnormal vessels (C).

Courtesy of Prof. Dr. Rufino Silva

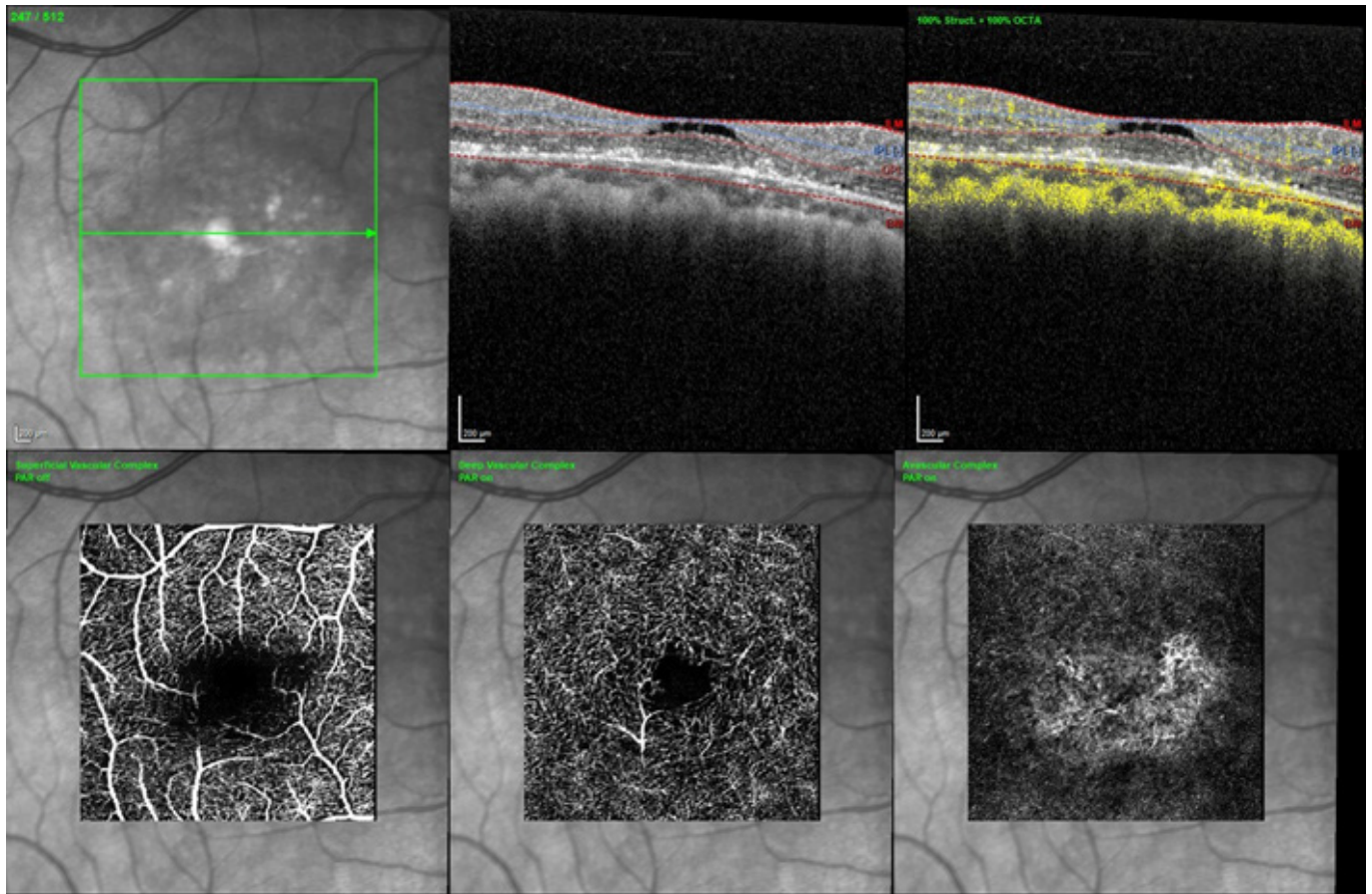


**Figure 3.** Post treatment OCT-A evaluation of the previous patient after anti-VEGF (vascular endothelial growth factor) intravitreal injections, showing clear improvement of the outer retinal neovascularization, despite subtle persistent vascular changes in the superficial and deep plexuses.

Courtesy of Prof. Dr. Rufino Silva

Overall, OCT-A should be integrated into the multimodal imaging evaluation of these patients, as it complements other methods by allowing the detection of early changes. These are important for prompt diagnosis, providing better follow-up and prompt treatment of the neovascular complication.

## REFERENCES

- Nalci H, Sermet F, Demirel S, Ozmert E. Optical Coherence Tomography Angiography Findings in Type-2 Macular Telangiectasia. *Turk J Ophthalmol.* 2017;47(5):279-84.
- Gass JD, Blodi BA. Idiopathic juxtafoveolar retinal telangiectasis. Update of classification and follow-up study. *Ophthalmology.* 1993;100(10):1536-46.
- Yannuzzi LA, Bardal AM, Freund KB, Chen KJ, Eandi CM, Blodi B. Idiopathic macular telangiectasia. *Arch Ophthalmol.* 2006;124(4):450-60.
- Toto L, Di Antonio L, Mastropasqua R, Mattei PA, Carpineto P, Borrelli E, et al. Multimodal Imaging of Macular Telangiectasia Type 2: Focus on Vascular Changes Using Optical Coherence Tomography Angiography. *Invest Ophthalmol Vis Sci.* 2016;57(9):OCT268-76.
- Wu L, Evans T, Arevalo JF. Idiopathic macular telangiectasia type 2 (idiopathic juxtafoveolar retinal telangiectasis type 2A, Mac Tel 2). *Surv Ophthalmol.* 2013;58(6):536-59.
- Dogan B, Erol MK, Akidan M, Suren E, Akar Y. Retinal vascular density evaluated by optical coherence tomography angiography in macular telangiectasia type 2. *Int Ophthalmol.* 2019;39(10):2245-56.
- Unterlauff JD, Eichler W, Kuhne K, Yang XM, Yafai Y, Wiedemann P, et al. Pigment epithelium-derived factor released by Müller glial cells exerts neuroprotective effects on retinal ganglion cells. *Neurochem Res.* 2012;37(7):1524-33.
- Shen W, Fruttiger M, Zhu L, Chung SH, Barnett NL, Kirk JK, et al. Conditional Müller Cell Ablation Causes Independent Neuronal and Vascular Pathologies in a Novel Transgenic Model. *J Neurosci.* 2012;32(45):15715.
- Ersoz MG, Hocaoglu M, Sayman Muslubas I, Arf S, Karacorlu M. Macular Telangiectasia Type 2: Acircularity Index and Quantitative Assessment of Foveal Avascular Zone Using Optical Coherence Tomography Angiography. *Retina.* 2020;40(6):1132-9.
- Villegas VM, Kovach JL. Optical Coherence Tomography Angiography of Macular Telangiectasia Type 2 with Associated Subretinal Neovascular Membrane. *Case Rep Ophthalmol Med.*

- 2017;2017:8186134.
11. Roisman L, Rosenfeld PJ. Optical Coherence Tomography Angiography of Macular Telangiectasia Type 2. *Dev Ophthalmol*. 2016;56:146-58.
  12. Surguch V, Gamulescu MA, Gabel VP. Optical coherence tomography findings in idiopathic juxtafoveal retinal telangiectasis. *Graefes Arch Clin Exp Ophthalmol*. 2007;245(6):783-8.
  13. Zhang Q, Wang RK, Chen CL, Legarreta AD, Durbin MK, An L, et al. Swept Source Optical Coherence Tomography Angiography of Neovascular Macular Telangiectasia Type 2. *Retina*. 2015;35(11):2285-99.
  14. Nunes RP, Goldhardt R, de Amorim Garcia Filho CA, Thorell MR, Abbey AM, Kuriyan AE, et al. Spectral-domain optical coherence tomography measurements of choroidal thickness and outer retinal disruption in macular telangiectasia type 2. *Ophthalmic Surg Lasers Imaging Retina*. 2015;46(2):162-70.
  15. Park YG, Park Y-H. Quantitative analysis of retinal microvascular changes in macular telangiectasia type 2 using optical coherence tomography angiography. *PloS one*. 2020;15(4):e0232255-e.



# INFLAMMATORY RETINAL DISEASES

Sofia Fonseca

Centro Hospitalar de Vila Nova de Gaia/Espinho

Uveitis includes a wide group of inflammatory responses ranging from infectious entities to autoimmune conditions that can target a specific ocular structure or involve the entire eye.<sup>1</sup>

Different types of uveitis often have specific OCT/OCTA findings according to the involved ocular tissues and the kind of inflammatory/infectious process that characterizes them.<sup>2,3</sup>

The retina is a complex structure, with a proper vasculature divided among multiple layers. Uveitis can induce both functional and structural changes to the retina and its vessels during the acute and chronic stages of the inflammatory process. Uveitis is associated with a spectrum of pathologic processes including inflammation, vascular occlusion or leakage, local ischemia, and alteration of cellular mediators. Visually debilitating complications such as macular edema and neovascularization may potentially occur. Also, some inflammatory lesions may be difficult to differentiate from a vascular lesion.<sup>(4)</sup> OCT and OCTA can provide useful information to detect, characterize, and monitor such changes and thereby better manage these diseases.<sup>5</sup> The aim of this chapter is to describe the use of OCTA in patients with inflammatory retinal diseases.

## INFLAMMATORY VASCULITIS

Retinal vasculitis may be a consequence of infectious diseases or inflammatory diseases including systemic lupus erythematosus, Behçet disease, multiple sclerosis, ocular tuberculosis, and sarcoidosis among others. Inflammation of retinal vessels may be a component of almost all types of intermediate and posterior uveitis.<sup>(5)</sup> In active vasculitis, **fundoscopy** reveals focal, multifocal, or diffuse white sheathing of retinal vessels. Perivascular infiltration by inflammatory cells accounts for the pathological vessel sheathing, which is postulated to generate the blurred margins of vessels. Retinal vasculitis may be accompanied by other vascular changes including telangiectasias, vascular anastomosis, microaneurysms, macroaneurysms and optic disc or preretinal neovascularization.<sup>1</sup>

**Fluorescein Angiography (FA)** remains the gold standard imaging modality for the diagnosis and monitoring of retinal vasculitis. Fluorescein can escape

through breaks in blood-retinal barrier, allowing the detection of vascular occlusion or leakage. Dye leakage in posterior uveitis may be helpful for the assessment of the inflammatory activity, but it can be restrictive in the evaluation of adjacent capillary perfusion. In this respect, the use of OCTA has proven advantageous, providing details on microvascular morphology and information about capillary perfusion in both superficial and deep capillary plexus.

Abucham-Neto et al demonstrated that OCTA plays a critical role in the detection of secondary complications of retinal vasculitis that are commonly not detected by FA, including new vessels obscured by retinal hemorrhage, early peripapillary neovascular proliferation, and telangiectasias. Furthermore, the most relevant and repeated finding observed on the OCTA exam was macular capillary dropout. In some cases, ischemic findings were even better demonstrated by OCTA than by FA, including the demonstration of increased FAZ. **OCTA** can demonstrate enlargement and/or irregularity of the foveal avascular zone (FAZ) and capillary remodeling, specifically in patients with involvement of the macula.<sup>6</sup>

With widefield SS-OCTA, Tian et al demonstrated that, qualitatively, on the wide-field OCTA, the deep capillary plexus (DCP) was more frequently involved than the superficial capillary plexus (SCP) in patients with retinal vasculitis and **intermediate uveitis**. This is in line with the findings of previous studies in other diseases. Although wide-field OCTA seems a promising additional tool for the assessment of peripheral retinal ischemia, it currently has limited potential to fully replace wide-field FA. Although the specificity for the detection of capillary non-perfusion on OCTA was high, the sensitivity was rather low.<sup>7</sup>

Additional studies could show that OCTA may be even more sensitive than FA in detecting perifoveal capillary abnormalities, such as hypoperfusion and non-perfusion on the **ocular sarcoidosis** eyes and retinal vasculitis.<sup>6,8</sup> In fact, in ocular sarcoidosis, OCTA showed a higher sensitivity than FA in assessing macular microvascular abnormalities.<sup>8</sup> Also, a recent report illustrated that wide-field OCTA depicts the extensive capillary non-perfusion of the peripheral retina better than FA in some retinal vasculitis cases.<sup>9</sup> Thus, with the progress of OCTA in terms of acquisition time and resolution, wide-field OCTA may



soon become a sensitive and quantitative tool for the direct assessment of peripheral capillary dropout of the individual retinal and choroidal vascular layers.

**Behçet disease (BD)** is a chronic, recurrent, multisystem disease characterized by occlusive and necrotizing vasculitis. The main sight threatening mechanism of BD is retinal vasculitis and its complications. Khairallah et al<sup>10</sup> with the aid of OCTA highlighted the presence of grayish nonperfused/hypoperfused areas mostly involving the DCP in patients with BD vasculitis. Due to dye leakage, FA does not allow FAZ measurement in both eyes; thus, the investigators have to choose one eye. However, OCTA is a very useful tool to evaluate and measure the foveal avascular zone (FAZ). FAZ areas of the BD patients were reported to be significantly larger than in healthy patients. Another common OCTA finding was perifoveolar capillary disruption.<sup>11</sup>

Dye-based angiography poorly visualizes the DCP in contrast to OCTA. Evaluation of deeper vascular components can be useful in more uveitis entities including **Birdshot retinochoroiditis**, which has been shown to be associated with decreased flow density in the DCP.<sup>4</sup>

OCTA can also be important to understand **vasculitis of infectious causes**, like west Nile virus or varicella zoster virus.<sup>12,13</sup> In a case of varicella retinal vasculopathy, OCTA was able to diagnose a unilateral cilioretinal artery occlusion seen as loss of capillary plexuses in both superficial and deep layer analysis.<sup>13</sup>

In conclusion, OCTA is a valuable tool in the diagnosis and follow-up of vasculitis of different etiologies. However, caution should be taken as retinal atrophic alterations, involving the macula and the retinal nerve fibers, may produce projection artifacts on OCTA, indicating nonperfusion/hypoperfusion of both the superficial and deep capillary plexus, where none exists.

#### **Focal retinitis or granulomas of the retina**

OCTA findings in areas of retinitis have been reported in both infectious and non-infectious uveitis. The images usually allow visualization of disruption or absence of the normal capillary plexuses in the affected areas.<sup>5</sup>

In retinochoroiditis caused by *Toxoplasma gondii*, OCTA showed to be a useful diagnostic tool for the non-invasive evaluation of retinal and choroidal vascular networks during acute, relapsing, and quiescent stages (Figure 1). Moreover it can be a promising tool for clinicians to assess treatment efficacy in the follow-up visits, by evaluating restoration of the different vascular networks and visualizing the inversion of progression toward outer retinal and choroidal layers. Besides, it may assess the SCP that seems to be thickened during active stages, and particularly recognize the origin of some hypofluorescent spots seen on fluorescein angiography or indocyanine green angiography, which can correspond to blockage of the flow signal by the clouded retinal pigment epithelium and deep retinal layer structure disruption due to active vitreoretinal inflammation.<sup>14</sup>

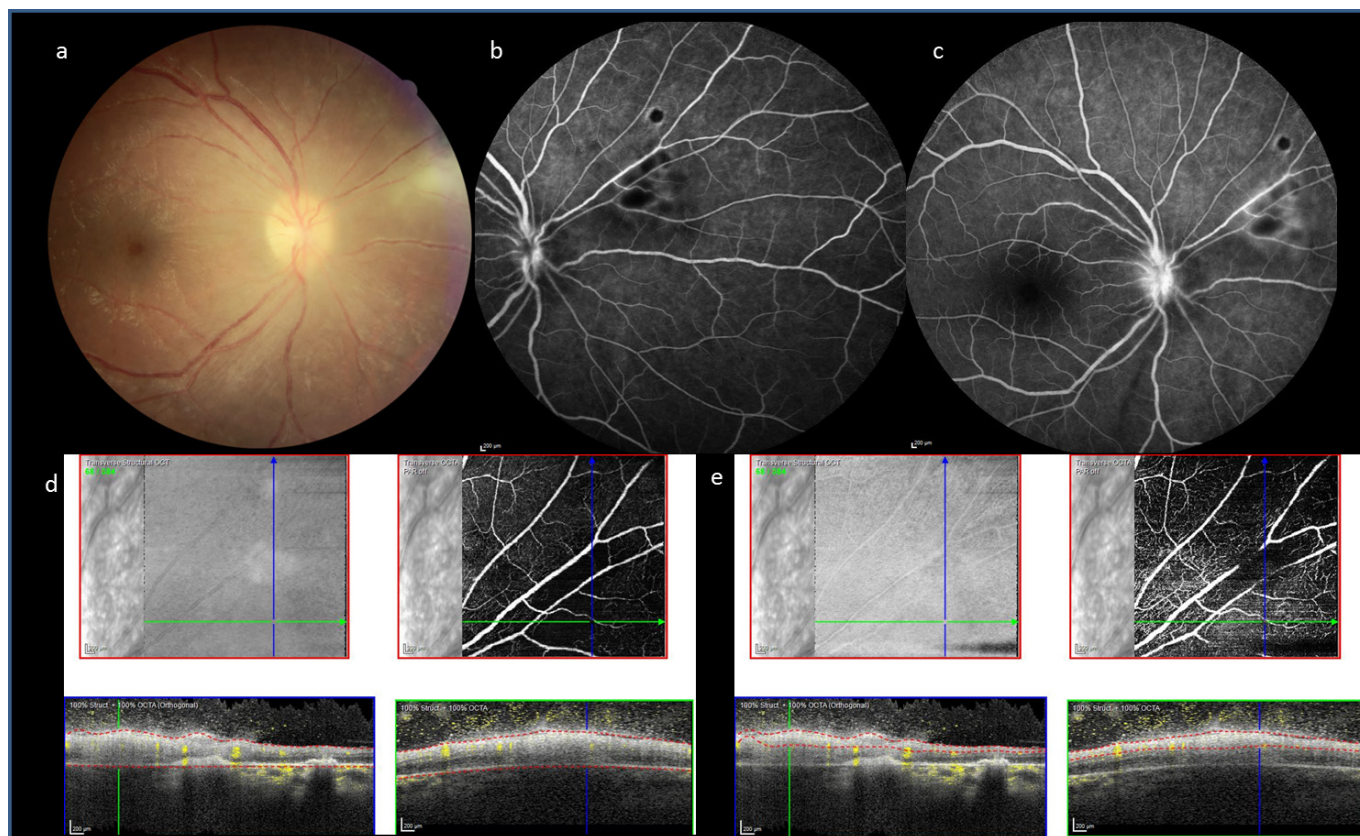


**Figure 1.** a. Active toxoplasmic lesion at nasal retina, adjacent to a pigmented scar. b and c. Hypofluorescent lesion in fluorescein angiography, focal vasculitis. d and e. OCTA images from Heidelberg Engineering's SPECTRALIS OCTA Module, that clearly shows a decorrelation signal, suggestive of reduced blood flow. In the SD-OCTA images is possible to identify vitritis, retinal layers are hiperreflective and unrecognizable at the lesion site.

Intralesional neovascularization can be detected clinically in foci of retinochoroiditis caused by *Bartonella henselae* and confirmed with OCTA. In a case reported by Pichi et al. OCTA highlighted a network of vessels and intralesional microvascular proliferation, not identified with fluorescein angiography.<sup>15</sup> OCT angiography can also be useful in detecting optic disc telangiectatic vessels in cases of neuroretinitis caused by *Bartonella henselae*.<sup>16</sup> Cases of **post fever retinitis** (PFR) have been reported following viral and bacterial infections. Kalhoun et al. described loss of vascularity in the superficial and the deep retinal plexus with the help of OCTA in cases of retinitis post rickettsia fever.<sup>17</sup> Clearly demarcated capillary non perfusion areas were visible at 6 weeks after the resolution of primary retinitis. Other authors have also described retinal perfusion defects with the help of OCTA in cases of PFR such as dengue maculopathy<sup>18-20</sup> and chikungunya retinitis.<sup>21</sup>

### UVEITIC MACULAR EDEMA

One of the most common complications of uveitis is cystoid macular edema (CME). This collection of fluid in the interstitial space in the macular region is hard to evaluate through traditional biomicroscopy, especially in case of media opacity. In contrast, structural OCT easily visualizes and quantifies CME in a non-invasive way and is considered the gold standard technique for the diagnosis and follow up of this condition.

Recent studies using OCTA showed that uveitic macular edema is associated with changes in the density or morphology of DCP. Carrying out a quantitative OCTA analysis, Kim et al. highlighted the presence of distinct areas with impaired retinal perfusion in patients with uveitic macular edema. More specifically, their data revealed remarkably decreased vascular density parameters, including skeleton and vessel density in DCP of uveitic eyes with active CME compared with normal eyes. In addition, ocular inflammation was associated with parafoveal capillary loss in the SCP regardless of the presence of macular edema.<sup>22</sup>

### CONCLUSION

OCTA has been gaining popularity in recent years among retinal and uveitis specialists. It allows to detect and investigate a lesion in a non-invasive way, characterizing its precise spatial extent and to calculate the area and density of vascular flow, as well as flow void areas. It's important to diagnosis and management of uveitis and to understand the pathophysiology of this group of diseases. Nevertheless, it's a new tool and there is limited experience, so further scale studies are required to establish its clinical utility.

### REFERENCES

1. Stephen C, Foster MD, Albert T, Vitale MD. Diagnosis and Treatment of Uveitis. Vol 1. New Delhi: Jaypee Brothers; 2013.
2. Onal S, Tugal-Tutkun I, Neri P, Herbot CP. Optical coherence tomography imaging in uveitis. *Int Ophthalmol*. 2014;34:401-435.
3. Pichi F, Sarraf D, Arepalli S, Lowder CY, Cunningham ET Jr, Neri P et al. The application of optical coherence tomography angiography in uveitis and inflammatory eye diseases. *Prog Retin Eye Res*. 2017;59:178-201.
4. Tranos P, Karasavvidou EM, Gkorou O, Pavesio C. Optical coherence tomography angiography in uveitis. *J Ophthalmic Inflamm Infect*. 2019; 9:21.
5. Invernizzi A, Cozzi M, Staurengi G. Optical coherence tomography and optical coherence tomography angiography in uveitis: A review. *Clin. Experiment. Ophthalmol*. 2019;47:357-371.
6. Abucham-Neto JZ, Torricelli AAM, Lui ACF, Guimarães SN, Nascimento H, Regatieri CV. Comparison between optical coherence tomography angiography and fluorescein angiography findings in retinal vasculitis. *Int J Retina Vitreous* 2018;4:15.
7. Tian M, Tappeneir C, Zinkernagel MS, Wolf S, Munk MR. Swept-source optical coherence tomography angiography reveals vascular changes in intermediate uveitis. *Acta Ophthalmol*. 2019; 97(5):785-791.
8. Cerquaglia A, Iaccheri B, Fiore T, Fruttini D, Belli FB, Khairallah M et al. New Insights On Ocular Sarcoidosis: An Optical Coherence Tomography Angiography Study. *Ocul Immunol Inflamm*. 2018;160:1-10.
9. Marchese A, Miserochi E, Modorati G, Rabiolo A, Poggiali E, Lattanzio R et al. Widefield OCT Angiography of Idiopathic Retinal Vasculitis, Aneurysms, and Neuroretinitis. *Ophthalmol Retina* 2017;1:567-9.
10. Khairallah M, Abroug N, Khochtali S Mahmoud A, Jelliti B, Coscas G et al. Optical coherence tomography angiography in patients with Behçet uveitis. *Retina* 2017; 37(9): 1678-1691
11. Emre S. Guven-Yalmaz S, Ulusoy MO, Ates H. Optical coherence tomography angiography findings in Behçet patients. *Int Ophthalmol*. 2019;39(10):2391-2399.
12. Khairallah M, Kahloun R, Gargouri S Jelliti B, Sellami D, Ben Yahia S et al. Swept-source optical coherence tomography angiography in West Nile Virus chorioretinitis and associated occlusive retinal vasculitis. *Ophthalmic Surg Lasers Imaging Retina*. 2017 Aug 1;48(8):672-675.
13. Khatri A, Timalansa S, Gautam S, Kharel M. Varicella retinal vasculopathy: unilateral cilioretinal artery occlusion despite acyclovir therapy caught using optical coherence tomography-angiography (OCTA-A). *Case Rep Ophthalm Med*. 2019 Jul 17; 2019:5752180.
14. Azar G, Favard C, Salah S, Brézin A, Vasseur V, Mauget-Faysse M. Optical coherence tomography angiography analysis of retinal and choroidal vascular networks during acute, relapsing, and quiescent stages of macular toxoplasma retinochoroiditis. *Biomed Res Int*. 2020:4903735.
15. Pichi F, Srivastava SK, Levinson A, Baynes KM, Traut C, Lowder CY. Afocal chorioretinal bartonella lesion analyzed by optical coherence tomography angiography. *Ophthalmic Surg Lasers*

- Imaging Retina. 2016;47:585-588
16. Ksiaa I, Abroug N, Mahmoud A, Zina S, Hedayatfar A, Attia S et al. Update on Bartonella neuroretinitis. J Curr Ophthalmol. 2019 May 6;31(3):254-261.
  17. Kahloun R, Jelliti B, Ksiaa I Ben Amor H, Zaouali S, Lupidi M et al. Sweptsource optical coherence tomography angiography in Rickettsial retinitis. Retin Cases Brief Rep 2019; 13:34851. 5.
  18. Agarwal A, Choudhary T, Gupta V. Optical coherence tomography angiography features of bilateral retinopathy associated with Chikungunya fever. Indian J Ophthalmol 2018; 66:1425.
  19. Bajgai P, Singh R, Kapil A. Progression of dengue maculopathy on OCTangiography and fundus photography. Ophthalmology 2017;124:1816.
  20. Agarwal A, Aggarwal K, Dogra M, Kumar A, Akella M, Katoch D et al. OCTA Study Group. DengueInduced inflammatory, ischemic foveolitis and outer maculopathy: A sweptsource imaging evaluation. Ophthalmol Retina 2019; 3: 1707.
  21. Aggarwal K, Agarwal A, Katoch D, Sharma M, Gupta V. Optical coherence tomography angiography features of acute macular neuroretinopathy in dengue fever. Indian J Ophthalmol 2017; 65: 12358.
  22. Kim AY, Rodger DC, Shahidzadeh A, Wang RK, Puliafito CA, Kashani AH. Quantifying retinal microvascular changes in uveitis using spectral-domain optical coherence tomography angiography. Am J Ophthalmol. 2016;171:101-112.

11.

# AGE-RELATED MACULAR DEGENERATION (AMD)



# EARLY AND INTERMEDIATE AMD

Rita Flores

Centro Hospitalar Universitário de Lisboa Central

## 1. INTRODUCTION

Age related macular degeneration (AMD) is the leading cause of irreversible blindness in developed countries. The hallmark of the disease is the presence of drusen, yellowish deposits of extracellular debris, usually located between the basal lamina of the retinal pigment epithelium (RPE) and the inner collagenous layer of the Bruch's membrane.<sup>1</sup>

In its early stages, AMD is characterized by the presence of drusen and pigmentary abnormalities resulting from alterations in the retinal pigment epithelium (RPE). In later stages, the disease progress with atrophic or neovascular complications.

The Age Related Eye Disease Study (AREDS) group classifies AMD into three categories, based on the type and severity of fundus lesions, including drusen dimensions and pigmentary changes:

- early AMD, defined as the presence of medium drusen (63 to 125  $\mu\text{m}$ ) with no pigmentary abnormalities;
- intermediate AMD, defined as the presence of large drusen ( $>125 \mu\text{m}$ ) or medium drusen in the presence of pigmentary abnormalities; and
- advanced AMD, characterized by exudative neovascularization (nAMD) and/or geographic atrophy (GA), involving the center of the macula.<sup>2</sup>

Other classification that can be considered is Rotterdam staging system that divides AMD in several stages. Stage 2a, 2b and 3 correspond to early AMD as opposed to advanced disease.

Stage 2a includes large soft drusen ( $>125 \mu\text{m}$ ) or reticular drusen only; stage 2b medium size drusen (63 to 125  $\mu\text{m}$ ) with pigmentary abnormalities and stage 3 large soft drusen ( $>125 \mu\text{m}$ ) or reticular drusen with pigmentary abnormalities.

Although the pathogenesis of AMD is not completely understood, several hypotheses have been proposed since its first description in the late 19th century: an inflammatory disease, a degenerative disease or a result of choroidal hemodynamic disturbances and ischemia. There is a growing body of evidence implicating choroidal and retinal blood flow in the development of drusen, with hypoxia being associated with progression of the disease.<sup>3</sup>

Optical Coherence Tomography angiography with high resolution Spectral Domain OCT (SD-OCT) is a real time non-invasive technology that generates depth-resolved images of the vasculature of the retina and the choroid, that enables the researchers to independently evaluate the vasculature of the inner and outer retina and the choriocapillaris. Other important purpose is to correlate microvascular alterations with structural changes in the retina and RPE.<sup>4</sup>

Swept Source (SS) technology application in OCTA, with its longer wave-length and faster acquisition, provides even better penetration below the RPE and therefore better visualization of the choroid.

## 2. OCTA CHANGES IN EARLY AND INTERMEDIATE AMD

### 2.1. IN THE CHOROID

There is a general reduction in choriocapillaris density in early and intermediate AMD patients, compared with age matched normal controls, with some focal areas of choriocapillaris loss or flow impairment.

Those areas appear as dark patches at choriocapillaris level. Displacement of the larger choroidal vessels can also occur into the space previously occupied by the choriocapillaris. Histopathological studies have demonstrated that areas with increased drusen density seem to correspond to decreased vascular density in choriocapillaris. (Fig. 1)

Drusen and RPE changes cause frequently attenuation shadowing in SD-OCT technology, that can simulate lack of blood flow (Fig. 2), artifact that doesn't occur so frequently with SS-OCT system. These areas of shadowing can be distinguished from areas of decreased perfusion by simultaneously observing *enface* OCTA image and cross sectional OCT intensity image: areas of shadowing will appear dark in both OCT intensity image and angiographic image, whereas areas of decreased flow will appear normal in OCT intensity image but dark in *en face* OCTA image.

Due to the more prevalent attenuation artifacts in SD-OCT, it is much easier to assess loss of choriocapillaris flow on SS-OCTA images than on SD-OCTA images.

Reticular pseudo drusen or subretinal drusenoid deposits (SDD) are a yellow faint interlacing network,

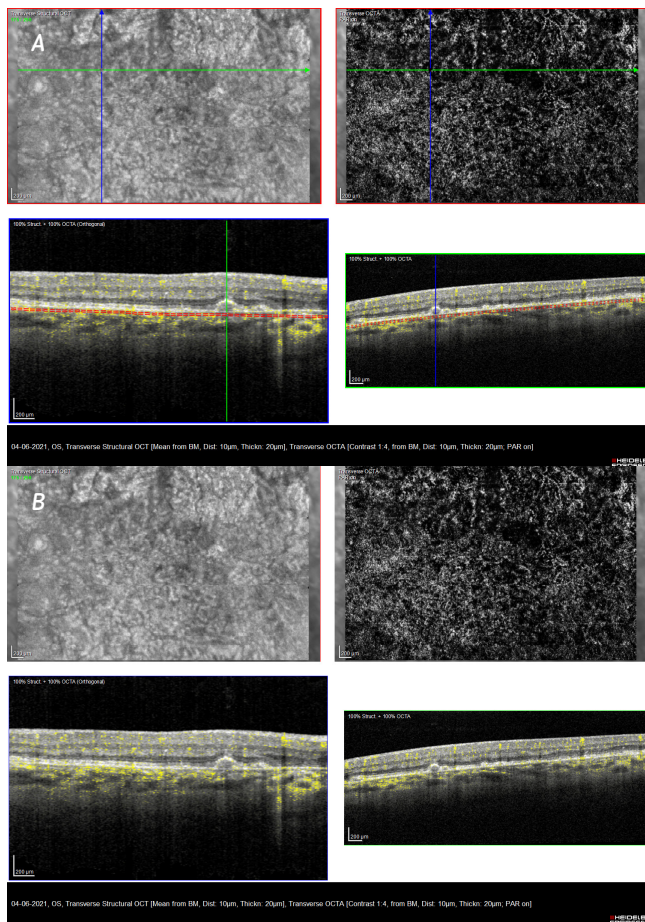


**Figure 1.** Dark patch at choriocapillary level in a drusen area. A: figure with markings. B: figure without markings.

first identified on blue-light fundus photography. Their presence entails a worst prognostic, being associated with a more aggressive disease.

Nesper et al<sup>5</sup> conducted a study to evaluate choriocapillaris non-perfusion in early and intermediate AMD eyes with and without SDD. The authors found that eyes with SDD had significant larger areas of choriocapillaris non-perfusion, compared to eyes without SDD. The extension of those non-perfusion area was strongly correlated with visual acuity.

## 2.2. IN THE RETINA

In a recent study, authors used OCT-A to evaluate the superficial and deep vessel density in patients with early and intermediate AMD. They found a statistically significant difference in both superficial and deep capillary plexus between controls and AMD patients, although no significant differences between early AMD and intermediate AMD patients.<sup>6</sup> (Fig 3)

Further studies published complementary data related to changes in retinal vasculature and ganglion cell layer thickness in intermediate AMD using SD-OCTA.<sup>7</sup> Vascular density was significantly reduced in superficial capillary plexus of AMD eyes compared with normal eyes, particularly in the superior quadrant. A non

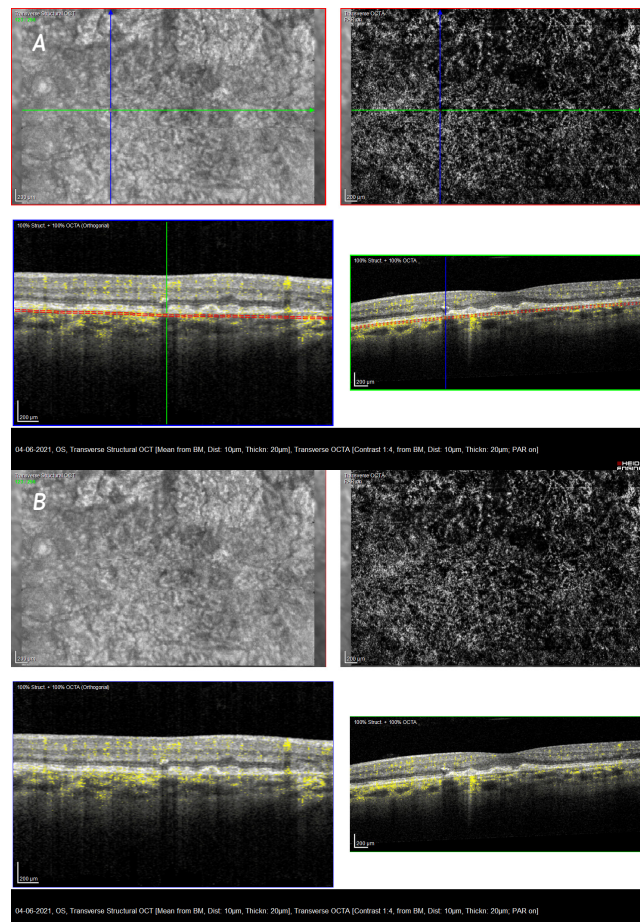


**Figure 2.** Attenuation shadowing in an area of RPE changes. A: figure with marking. B: figure without markings.

significant reduction was also obtained in deep capillary plexus. In the same study, not only the vascular density but also the morphology of the inner retinal vasculature was changed and average ganglion cell layer thickness was also reduced in AMD eyes.

In AMD eyes the evaluation of foveal avascular zone parameters showed no significant changes in AMD.

## CONCLUSION

Current OCTA technology<sup>8</sup> provides vascular imaging in different layers of the retina and the choroid. The faster image collection, non-invasive technique and the independence of external dye for image acquisition are significant benefits, comparing with current FA/ICG images. Yet promising, this technology still needs some improvements regarding the visualization field, acquisition time, reproducibility data and automatic segmentation. Furthermore, OCTA can only provide information concerning vascular flow at a single time point and cannot demonstrate dynamic vascular leakage as is possible with FA or ICG, nor can document flow below a certain threshold. Other important limitations are the artifacts, not only the attenuation ones but also the projection artifacts in which superficial vessels are projected onto deeper layers of the retina and choroid.

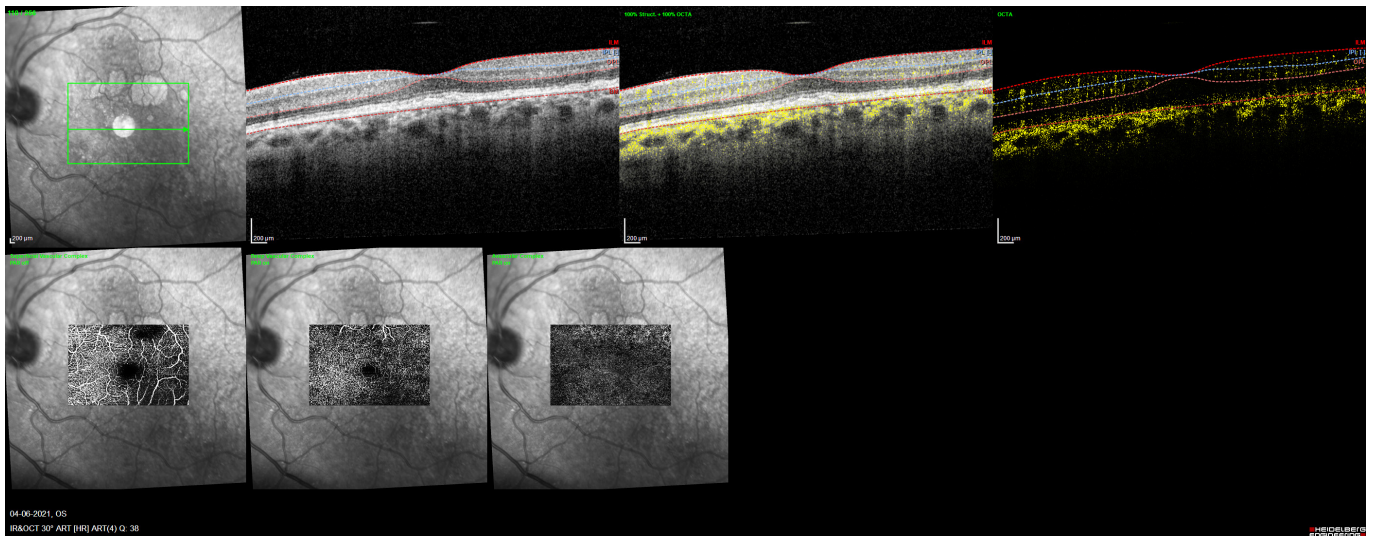


**Figure 3.** Multimodal evaluation and early and intermediate AMD patient

Projection artifacts of the choriocapillaris and choroid can also result from simple attenuation and scattering from the RPE layer.

Understanding OCTA artifacts, complemented with technology improvement and large studies researches will help investigators to better visualize choroid and retinal vasculature and to understand the pathogenesis of the early and intermediate AMD.

Coherence Tomography Angiography Imaging in Age-related Macular Degeneration. *Ophthalmology and Eye Diseases* 2017, Volume 9: 1-7.

## REFERENCES

1. Flores, Rita MD; Carneiro, Angela MD, PhD; Serra, Joana PhD; Gouveia, Nélia PhD; Pereira, Telmo PhD; Mendes, Jorge M. PhD; Coelho, Pedro S. PhD; Tenreiro, Sandra PhD; Seabra, Miguel C. MD, PhD Correlation study between drusen morphology and fundus autofluorescence, *Retina*: March 2021 - Volume 41 - Issue 3 - p 555-562.
2. Ferris FL, 3rd, Wilkinson CP, Bird A, et al.: Clinical classification of age-related macular degeneration. *Ophthalmology* 120:844-851, 2013
3. Remsch, H., Spraul, C., Lang, G. *et al.* Changes of retinal capillary blood flow in age-related maculopathy. *Graefes Arch Clin Exp Ophthalmol* **238**, 960–964 (2000).
4. F. Bandello, E. Souide, G. Querques OCT Angiography in Retinal and Macular Diseases; Karger, Volume 56
5. Nesper PL, Soetikno BT, Fawzi AA. Choriocapillaris Nonperfusion is associated with poor visual acuity in eyes with reticular pseudodrusen. *American Journal of Ophthalmology*. 2017; 174:42-55
6. Toto L, Borrelli E, Di Antonio L, Carpineto P, Mastropasqua R. Retinal vascular plexuses' changes in dry age-related macular degeneration, evaluated by means of optical coherence tomography angiography. *Retina*. 2016 Aug;36(8):1566-72.
7. Trinh M, Kalloniatis M, Nivison-Smith L. Vascular Changes in Intermediate Age-related Macular Degeneration Quantified using Optical Coherence tomography Angiography. *Translational Vision Science & Technology*, August 2019, Vol8, 20.
8. Ma J, Desai R, Nesper P, Gill M, Fawzi A, Skondra D, Optical





11.2.

# NEOVASCULAR AMD



# TYPE 1 NEOVASCULARIZATION

Miguel Amaro

Hospital Vila Franca de Xira, Hospital CUF Coimbra

Exudative AMD is defined as abnormal growth of neovascular tissue from the choriocapillaris through or beneath the retinal pigment epithelium (RPE).<sup>1,2</sup> Gass described three histologic forms of choroidal neovascularization (CNV): type 1 CNV, located beneath RPE monolayer and above the Bruch's membrane is one them and will be describe in this chapter.<sup>3</sup> It's the most frequent phenotype of exudative AMD.<sup>4</sup> While fundus ophthalmoscopy of type 1 CNV shows nonspecific signs such as drusen or pigmentary alterations of RPE, subretinal fluid (SRF), hard exudates, and possibly hemorrhages, multimodal imaging provides an accurate description of the features and extension of the choroidal new vessels.<sup>5</sup> Type 1 CNV corresponds angiographically to occult, ill defined, neovascularization, described as an ill defined lesion in fluorescein angiography (FA).<sup>5,6</sup> The detection of CNV was improved using indocyanine green angiography (ICGA), as demonstrated by Yannuzzi.<sup>7</sup>

As multimodal imaging provides a better understanding of type 1 neovascularization,<sup>8,9</sup> combined FA, ICGA, and Spectral Domain Optical Coherence Tomography (SD-OCT) and Optical Coherence Tomography Angiography (OCTA) play a key role in the diagnosis of type 1 CNV. Our focus will be on OCTA type 1 Choroidal Neovascularization description, more recently called type 1 Macular Neovascularization.

## MORPHOLOGY

Optical coherence tomography angiography (OCTA) is a depth-resolved imaging technique that uses the split spectrum amplitude decorrelation angiography (SSADA) to generate amplitude angiography images. It allows blood flow visualization and thus a quantitative and, to a greater extent, qualitative assessment of newvessels. Type 1 MNV is revealed, in OCTA, by a high flow, well organized vascular network appearing in the outer retinal/choriocapillaris segmentations, with a distinguishable feeder vessel in almost all cases.<sup>10-12</sup>

On OCTA, the neovascular lesion morphology normally corresponds to either “medusa” pattern, in which vessels are radiating in all directions from the center of the lesion (37%), “seafan” pattern, in which vessels are radiating from one side of the lesion (22%), or an ill defined pattern (27%). A long-filamentous-vessel or

a “pruned tree” appearance is seen in 14% with inactive type 1 neovascularization.<sup>8</sup> A dark halo sometimes surrounds the lesion in the choriocapillaris segmentation, which could correspond either to a hypoperfusion of choriocapillaris or a fibrotic tissue.

OCTA facilitated the morphological classification of type 1 lesions, including features characteristic of early, mature, and fibrotic lesions. Kuehlewein et al.<sup>9</sup> evaluated 33 eyes of patients with active or chronic type 1 neovascularization, and 18 (55%) of the lesions were classified as medusa, 7 (21%) as sea-fan, and 8 (24%) as indistinct. There were no significant correlations by OCTA analysis between morphological patterns of neovascularization and the RPE detachment subtype nor with the number of intravitreal anti-VEGF injections received before imaging. Lupidi et al.<sup>13</sup> concluded that medusa or sea-fan shapes represented independent patterns, not passing through a sequential stage. (Fig. 1, 2, 3, 4)

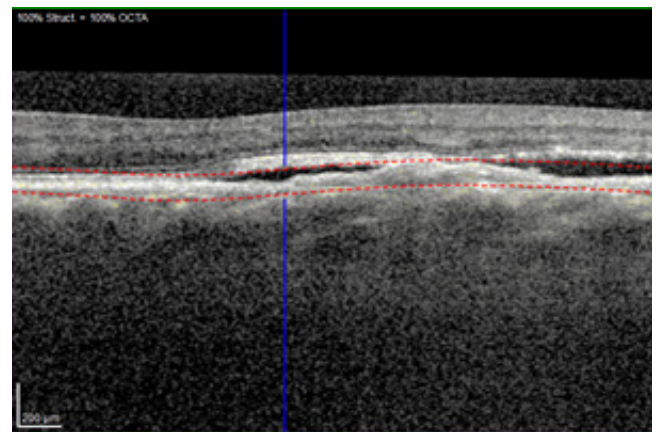


**Figure 1.** PED with retina neurosensorial detachment associated to Type 1 MNV.

However, OCTA may miss important parts of the MNV, as segmentation may not cover the whole neovascular volume, so data must be interpreted with care. Spaide et al.<sup>14</sup> focused, in a recent paper, on the importance of OCTA in understanding the vascular growth patterns and the changes induced by antiangiogenic treatments, observing signs of “abnormalization” of neovessels.

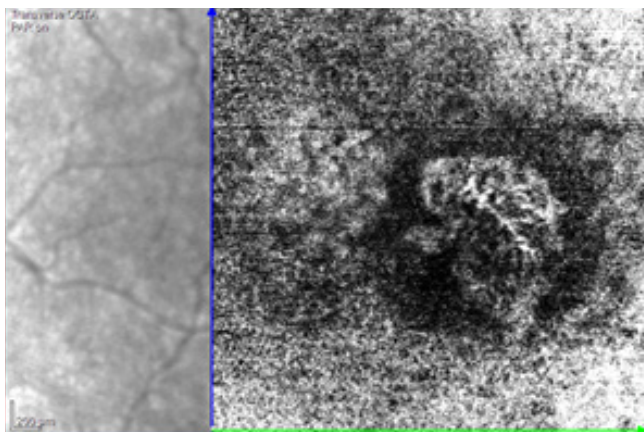


**Figure 2.** En face AngioOCT showing a “Seafan” morphology. A characteristic dark halo surrounds the lesion. Also at the bottom a feeder vessel is visible.

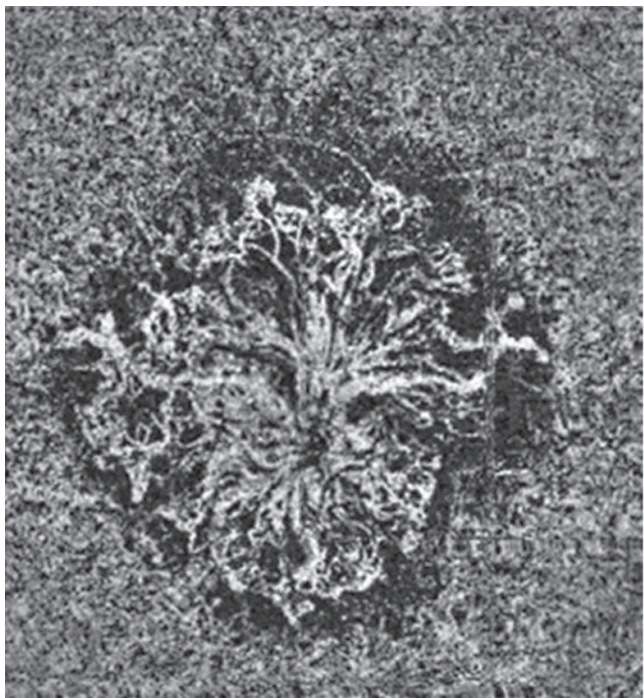


**Figure 3.** En Face AngioOCT with MNV type 1 with Medusa morphology

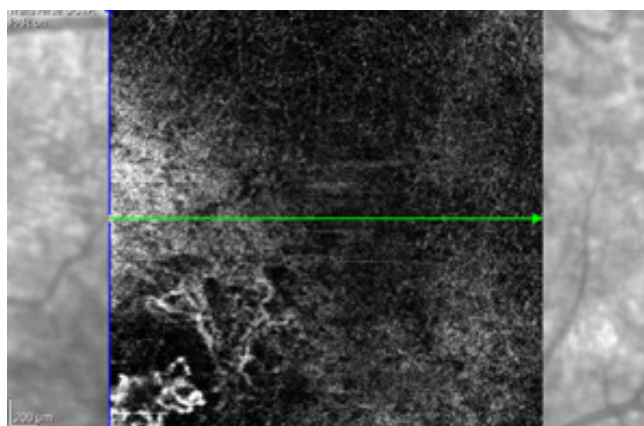


**Figure 4.** En face AngioOCT with MNV1 where a dead tree pattern is observed.

## EVOLUTION

This is a rather interesting concept, contradicting various theories of vascular normalization in eyes receiving intravitreal antiangiogenic injections. Moreover, Kuehlewein et al.<sup>9</sup> investigated the OCTA features of type 1 MNV and they described a neovascular complex, consisting of a feeder vessel and large branching vessels, which is resistant to anti-VEGF therapy.

OCTA reveals a size of the neovascular membrane smaller than both intermediate and late phase of ICG. It is hypothesized either that OCTA underestimate the lesion size, or ICG overestimates the real size of the neovascular complex. It is supported the hypothesis that OCTA could show the actual minimal surface of type 1 MNV, because a non-dye examination is not influenced by phenomenon of leakage. However, it is also possible that attenuation from the RPE generates a smaller lesion area on OCTA images.<sup>15</sup>

Positive evolution is observed in 55% of the patients, consisting of stabilization (20%) and chronicity (35%). Stabilization is considered as long-term remission and an absence of fluid or hemorrhaging for more than 6 months; the neovessels seemed to stop developing, and no activity signals were seen. The clinical appearance shows no exudation or fluid occurrence. Even if there is no exudation, the neovascular area normally is larger at the end of the observation period, growing in a study from 0.68 mm<sup>2</sup> to 1.68 mm<sup>2</sup>.<sup>16</sup>

Chronicity is considered when the neovascularization is consistently responsive to anti-VEGF treatment but requires repetitive reinjections. In these cases, acute disease develops into chronic disease. The neovascularization is often quiescent with consistent and frequent recurrences. The neovascularization area is consistently larger at the end of the observation period, growing from 0.7 mm<sup>2</sup> to 1.4 mm<sup>2</sup>.<sup>16</sup>

Most eyes with chronic evolution have periodic reactivation after treatment, with a periodicity of 50 to 60 days after each intravitreal injection. Before the first injection and between recurrences, it is observed a dark halo around the neovascular complex of approximately 50 microns in diameter. Although the meaning of the dark halo is still controversial<sup>17</sup>, it is hypothesized that is due to blood sequestering by neovascularization reactivation; an increased dark halo means neovascular growth.<sup>18</sup>

The cycles seem to be quite regular. After each treatment, the same main vessels appear to return with increased flow and decreased branch density. The normal cyclic recurrence is extensive and generally global, although it can be localized to a segment of the neovascular complex. In a few cases, acute nonperiodic reactivation occurs independently from treatment. This type of reactivation can take the shape of a shoot, bud, sprout, or outgrowth and may have a specific location: terminal, axillary, lateral, fingerlike, or adventitious. Negative evolution is observed in 45% of the cases, which included fibrosis (18%), atrophy (25%), and hemorrhage or RPE tears (2%).<sup>16</sup>

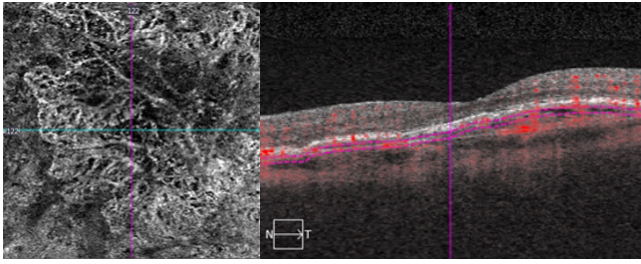


**Figure 5.** En face AngioOCT with MNV1 where a seanfan pattern has matured vessels being converted to a dead tree pattern.

Long-term monitoring of MNV evolution shows that the new vessels become larger, thicker, and straighter. No thin capillaries or fine loops are visible. For any evolution type, the vessel area is larger after treatment than before treatment (Fig.5)

In almost all eyes, after the loading phase of the 3 intravitreal anti-VEGF injections, the disappearance of new vessel ramifications but not of the main trunk can be observed by OCTA. These findings suggest that it is very difficult to predict the prognosis from OCTA findings after 3 loading doses.

Although several factors may play a role in causing vision loss in eyes that undergo long-term anti-VEGF therapy, the mechanism of this process remains poorly understood. One possible reason has been postulated, in which a mature tangled vascular pattern in type 1 lesions was determined to be a resistance factor to macular atrophy.<sup>19</sup> Recently, it was described a high level of macular atrophy development predominantly eccentric to the PED in long-term anti-VEGF therapy for eyes with type 1 NV secondary to AMD.<sup>19</sup> Despite studies reporting results of chorioretinal atrophy and a decrease in BCVA, several other studies have reported a maintained or increased BCVA and OCT morphology improvement.<sup>20</sup>

After each treatment, the same main vessels appear to return with increased flow and decreased branch density. It appears as though some of the main branches are less affected by the treatment. As previously described by Spaide, the onset of a complex pattern after treatment induced a less complex feature, arterialization, to become detectable.<sup>11</sup> This morphological pattern is defined as a “maturation pattern”.

Similarly, there are 3 growth patterns: symmetric growth, asymmetric growth, and finger-like projections.<sup>12</sup> Furthermore, a new entity of NV growth is postulated, “inside the fibrous capsule.” This NV grows in vascular density but not in area. In this specific case, the neovascular complex grows in vascular density inside a fibrous capsule.

The ability of OCTA to assess and quantify neovascularization may highlight activity biomarkers and guide the evaluation, treatment, and monitoring of neovascularization.

In conclusion, OCTA enables accurate information about morphological patterns of the neovascular membrane in patients with choroidal neovascularization. Well or ill-

defined vessel patterns could be seen in eyes with clinically active or inactive choroidal neovascularization. Although filamentous linear vessels on OCTA are associated with disease inactivity, the detection of a branching small-capillary network may not reflect disease activity.

Type 1 MNV evolution can progress to different outcomes: stabilization, chronicity, fibrosis, atrophy, hemorrhage, or RPE tears. Approximately half of the eyes follow a positive evolution, while the other half can become increasingly worse. In the future, we hope that the use of OCTA will help to better define the morphological details in the development of type 1 MNV and develop personalized medicine.

## REFERENCES

1. Bressler NM, Bressler SB, Fine SL. Age-related macular degeneration. *Surv Ophthalmol.* 1988;32:375–413.
2. Gass JD, Norton EW, Justice J Jr. Serous detachment of the retinal pigment epithelium. *Trans Am Acad Ophthalmol Otolaryngol.* 1966;70:990–1015.
3. Gass JD. Biomicroscopic and histopathologic considerations regarding the feasibility of surgical excision of subfoveal neovascular membranes. *Am J Ophthalmol.* 1994;118:285–298.
4. Jung JJ, Chen CY, Mrejen S, et al. The incidence of neovascular subtypes in newly diagnosed neovascular age-related macular degeneration. *Am J Ophthalmol.* 2014;158:769–779.
5. Sandhu SS, Talks SJ. Correlation of optical coherence tomography, with or without additional colour fundus photography, with stereo fundus fluorescein angiography in diagnosing choroidal neovascular membranes. *Br J Ophthalmol.* 2005;89:967–970.
6. Pece A, Sannace C, Menchini U, et al. Fluorescein angiography and indocyanine green angiography for identifying occult choroidal neovascularization in age-related macular degeneration. *Eur J Ophthalmol.* 2005;15:759–763.
7. Yannuzzi LA, Slakter JS, Sorenson JA, Guyer DR, Orlock DA. Digital indocyanine green videoangiography and choroidal neovascularization. *Retina.* 1992;12:191–223.
8. Karacorlu M, Muslubas IS, Serra A, et al. Membrane patterns in eyes with choroidal neovascularization on optical coherence tomography angiography. *Eye.* 2019; 33, 1280–1289.
9. Kuehlewein L, Bansal M, Lenis TL, Iafe NA, Sadda SR, Bonini Filho MA, et al. Optical coherence tomography angiography of type 1 neovascularization in age-related macular degeneration. *Am J Ophthalmol.* 2015;160:739–48.
10. S. D. Adrean, S. Chaili, H. Ramkumar, A. Pirouz, and S. Grant, Consistent long-term therapy of Neovascular age-related macular degeneration managed by 50 or more anti-VEGF injections using a treat-extend-stop protocol, *Ophthalmology*, vol. 125, no. 7, pp. 1047–1053, 2018.
11. R. F. Spaide, Optical coherence tomography angiography signs of vascular abnormalization with antiangiogenic therapy for choroidal neovascularization, *Am J Ophthalmol*, 160, 1, 6–16, 2015.
12. D. Xu, J. P. Dávila, M. Rahimi et al., Long-term progression of type 1 neovascularization in age-related macular degeneration using optical coherence tomography angiography, *Am J*

- Ophthalmol, 187, 10–20, 2018.
13. Lupidi M, Cerquaglia A, Chhablani J, Fiore T, Singh SR, Cardillo Piccolino F, et al. Optical coherence tomography angiography in age-related macular degeneration: the game changer. *Eur J Ophthalmol*. 2018;28:349–57.
  14. Spaide RF. Optical coherence tomography angiography signs of vascular abnormalization with antiangiogenic therapy for choroidal neovascularization. *Am J Ophthalmol*. 2015;160:6–16.
  15. Costanzo E, Miere A, Querques G, Capuano V, Jung C, Souied EH. Type 1 Choroidal Neovascularization Lesion Size: Indocyanine Green Angiography Versus Optical Coherence Tomography Angiography. 2016, 57: OCT 307- OCT313
  16. Rispoli M, Savastano MC, Lumbroso B, Toto L, and Antonio L. Type 1 Choroidal Neovascularization Evolution by Optical Coherence Tomography Angiography: Long-Term Follow-Up. 2020. Article ID 4501395
  17. G. Coscas, M. Lupidi, C. Cagini, and F. Coscas, False-friend ' images on optical coherence tomography angiography: early choroidal neovascularization or artefact?, *Acta Ophthalmol*, 96, 2, 200–202, 2018.
  18. M. Rispoli, M. C. Savastano, and B. Lumbroso, Quantitative vascular density changes in choriocapillaris around CNV after anti-VEGF treatment: dark halo, *Ophthalmic Surg, Lasers & Imaging Reti*, 49, 12, 918–924, 2018.
  19. K. K. Dansingani and K. B. Freund, Optical coherence tomography angiography reveals mature, tangled vascular networks in eyes with neovascular age-related macular degeneration showing resistance to geographic atrophy, *Ophthalmic Surg, Lasers & Imaging Reti*, 46, 9, 907–912, 2015.
  20. J. G. Christenbury, N. Phasukkijwatana, F. Gilani, K. B. Freund, S. Sadda, and D. Sarraf, Progression of macular atrophy in eyes with type 1 neovascularization and age-related macular degeneration receiving long-term intravitreal antivascular endothelial growth factor therapy: an optical coherence tomographic angiography analysis, *Retina*, 38, 7, 1276–1288, 2018

# TYPE 2 NEOVASCULARIZATION

José Roque

IMO - Instituto de Microcirurgia Ocular, Lisboa

Optical Coherence Tomography Angiography (OCT-A) is one of the biggest advances in ophthalmic imaging. It enables a deep assessment of the retinal and choroidal blood flow, sometimes exceeding the levels of detail commonly obtained with dye angiographies. OCT-A allow the visualization of retinal and choroidal vasculature in three dimensions with plexus characterization at different depths, from the internal limiting membrane up to the choroid, without contrast medium or without invasive means. One of the first applications of optical coherence tomography angiography was in detecting the presence of macular neovascularization and establishing its position in relation to the retinal pigmented epithelium and Bruch's membrane.<sup>1</sup> Since the OCT-A acquired images are not masquerade by dye leakage, a clear visualization of the NV network is obtained.

Macular neovascularization (MNV) is an invasion by vascular and associated tissues into the outer retina, subretinal space, or sub-RPE space in varying combinations. The anatomic location of the neovascularization determined by OCT imaging is used to subclassify the vascular component of the disease process.<sup>2</sup> Etiology of macular neovascularization is multifactorial. Alterations in Bruch's membrane, migration of macrophages and production of vascular endothelium growth factor (VEGF), play an important role in the development of this disease.

OCT angiography (OCT-A) has a great ability to show the retinal and choroidal microcirculation in detail. For the purpose of visualizing changes in eyes with MNV or suspected MNV, a segmentation of the outer retina (extending from the outer plexiform layer to Bruch's membrane) and a segmentation of the choriocapillaris (approximately 20  $\mu\text{m}$  thick region just below the RPE) are most useful. Optical coherence tomography angiograms, due to the longer wavelength used by optical coherence tomography, showed a more distinct macular neovascularization vascular pattern than fluorescein angiography, since there is less suffering from light scattering or is less obscured by overlying subretinal haemorrhages or exudation.<sup>1</sup>

MNV can be classified as type 1, type 2, type 3, or mixed lesions. Type 2 MNV, which is the less common form of neovascular AMD, refers to the proliferation of new vessels arising from the choroid into the subretinal space.

Although these vessels traverse the sub-RPE space, the disease process in type 2 macular neovascularization is dominated by the subretinal portion. These lesion types are associated with exudation or haemorrhage directly into the subretinal space.<sup>2</sup>

Histologically type 2 MNV occurs when the neovascular membrane passes through the RPE and is located above the RPE in the subretinal space. It is visualized as a neovascular network that grows from the choroid vasculature and traverses the RPE-Bruch's membrane complex into the subretinal space. Type 2 lesions have the fluorescein angiographic characteristics of early, typically well-defined hyperfluorescence with late leakage - this is related to the angiographic classification of a classic NV.

## TYPE 2 MACULAR NEOVASCULARIZATION AND OCT A FEATURES

Type 2 lesions could be detected by optical coherence tomography angiography, as a well remarked hyper flow lesion in the outer retina, surrounded by a dark halo and assume very typical patterns - vascular changes showed most often well-defined borders towards the surrounding choroidal vessels and larger vessels in the center. The neovascular membrane appears either as a medusa-shaped vascular complex or a glomerulus-shaped lesion in the outer retina. The medusa shaped vascular complex (Fig.1) is characterized by a well-defined oval shape, generally formed by a very dense high-flow network with minimal hypodense structure inside because of the high activity of this kind of choroidal new vessels.<sup>3,4</sup> The glomerulus-shaped lesion (Fig.2), so defined per comparison with the kidney glomerulus, is usually rounded, well defined, and full of a very dense maze of small new vessels, harbouring globular structures of entwined vessels that are separated by hypodense spaces.<sup>3</sup>

Anatomically, the retina is supplied by 2 capillary plexuses: the superficial capillary plexus and the deep capillary plexus. The superficial capillary plexus is located between the internal limiting membrane and the posterior part of the inner plexiform layer, while the deep plexus is situated in the inner nuclear layer. No vascular abnormality is detected in either the superficial or deep retinal capillary layers.

Two automatic segmentations on OCT-A are interesting



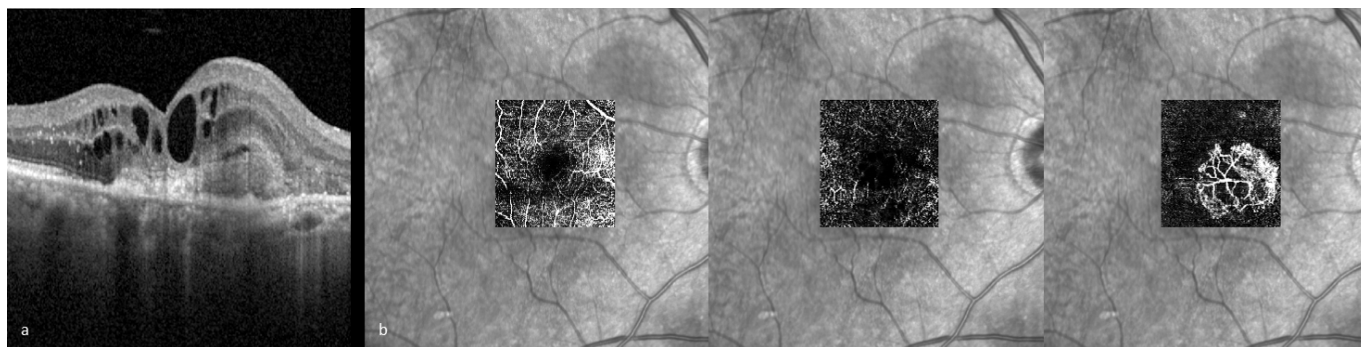


**Figure 1.** Medusa-shaped Type 2 MNV a. Structural OCT b. OCT-A Superficial and deep plexuses, and avascular zone

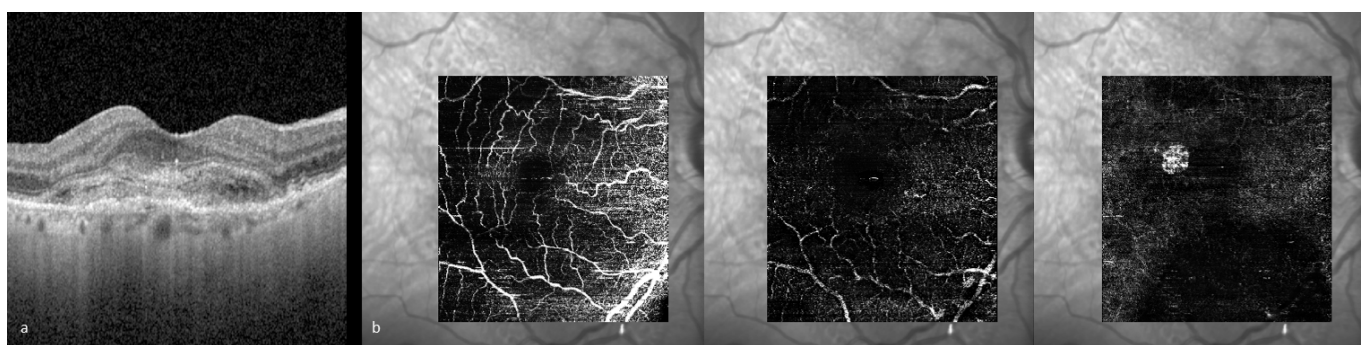


**Figure 2.** Glomerulus-shaped Type 2 MNV a. Structural OCT b. OCT-A Superficial and deep plexuses, and avascular zone.

for study type 2 MNV secondary to AMD. The first, called the “outer retina”, is delimited between the inner nuclear layer and Bruch’s membrane (BM), and the second, called the “choriocapillaris layer” is located under BM. As mentioned, at the pathophysiologic level, type 2 MNV involves choroidal new vessels that cross BM and grow up above the neurosensory retina. This feature allows us to visualize these lesions on the outer retina. One or more central feeder vessels that expand in radial branches and continue deeply into the more profound choroidal layers are visible. It is exceptional to distinguish and recognize the afferent of the efferent branches and, both medusa and glomerulus-shaped lesions, may be connected to a thicker main branch, which seemed continuous from the outer retina into the more profound choroidal layers.<sup>(4)</sup> Glomerulus-shaped or medusa-shaped lesion could also be observed on segmentations performed at the presumed level of the choriocapillaris without any NV lesion at this level revealed on SD-OCT. The significance of this finding is not very clear yet. It is possible that this image may be a projection artifact of the neovascular flow from the outer retina into the choriocapillaris layers.<sup>3</sup>

Furthermore, in most cases, at the choriocapillaris layer, the external borders of the lesion appear as a dark ring or a halo-like shape. The choriocapillaris layer may also demonstrate decreased flow or flow voids adjacent to the NV complex. The dark ring surrounding the neovascular membrane on OCT-A could probably be correlated with a decrease in flow density, explaining the

absence of vasculature visualization. Indeed, OCT-A measures only the linear blood flow. This dark area could present a turbulent motion, impeding the conversion and representation of this flow on a hyperdense frame. This finding may also be observed in the outer retina but is more obvious in the choriocapillaris layers.<sup>3</sup> Additionally, choriocapillaris hypoperfusion may be seen underlying any areas of RPE atrophy.

Karacorlu, M et al<sup>5</sup> evaluated morphologic patterns of neovascular membranes using OCT Angiography. They describe an interesting categorization of morphological patterns of the neovascular membranes. The membrane was identified as “well-defined” if the lesion had a well-defined shape (the vessels branched in all directions from the center of the lesion – medusa - or >90% of the membrane radiated from one side of the lesion - sea-fan) with presence of numerous tiny branching capillaries from the center to the periphery with or without arteriovenous anastomotic loops, or a peripheral arcade of small anastomotic and looping vessels, or was identified as long filamentous if the membrane had a dead-tree or pruned-vascular-tree pattern with long dilated filamentous linear vessels without branching small-capillary networks. Membranes lacking such distinct membrane morphology but with branching small-capillary networks with or without arteriovenous anastomotic loops and the peripheral arcade of small anastomotic and looping vessels were determined to be “ill-defined”. All eyes in study group with type 2 neovascularization had distinct

membrane morphology, well defined, with most lesions identified as sea-fan shapes, or long filamentous. A long-filamentous membrane pattern was seen only in eyes with inactive neovascularization, and the presence of long-filamentous membrane morphology was associated with a significantly longer duration of disease (mean 52.1 months in authors series).

Zhi Zhao et al<sup>6</sup> compared the morphology characteristics of type 1 and 2 MNV in neovascular age-related macular degeneration patients with Optical Coherence Tomography Angiography. They concluded that type 2 MNV was characterized by shorter duration of disease, smaller greatest vascular caliber (GVC), smaller greatest linear dimension (GLD), and smaller flow area and that the duration of the disease correlated with GVC of the MNV. Interestingly these results may have clinical translation. Patients with type 2 MNV tend to exhibit clinical symptoms at an early stage of the disease due to the RPE rupture, so the growth period of these NV is always shorter. Besides, the authors concluded that the duration of the disease correlated with GVC of the MNV, a novel parameter introduced in the study to evaluate NV maturation. NV maturing is an important factor related with the poor response of anti-VEGF treatment. During the natural course of nAMD, neovascular remodelling recruited pericyte coverage, resulting in the enhanced vessel caliber. This leads to an increase in vessel caliber with the NV maturing.<sup>(7,8)</sup> Vessels of mature NV covered with plenty pericytes reduce vascular endothelial cell's sensitivity to VEGF. In this way the authors postulated GVC may be a good imaging quantitative biomarker of the neovascular maturation and duration of disease, as well a potential predictor for the response of anti-VEGF treatment. In this study the authors found that GVC of type 2 MNV was significantly smaller, which confirmed that type 2 MNV was less mature neovascular tissue and may have better response to anti-VEGF treatment.

## CONCLUSIONS

Despite some limitations (good patient cooperation are necessary to obtain good imaging results, “saturation limit”, image acquisition with the retinal cube covering limited areas of the fundus - 3x3 mm or 6x6 mm -, whereas the full posterior pole analysis would be required to explore an area of 12x12 mm, possible artifacts), OCT-A has the potential to be a new imaging method for Type 2 MNV in routine clinical settings with a good sensitivity and specificity.<sup>3</sup> Results from a study by de Carlo et al<sup>9</sup>, reported a sensitivity of 50% and a specificity of 91% for NV detection with OCT-A.

## REFERENCES

1. Lupidi M, Cerquaglia A, Chhablani J, et al. Optical coherence tomography angiography in age-related macular degeneration: The game changer. *European Journal of Ophthalmology*. 2018;28(4):349-357.
2. Spaide RF, Jaffe GJ, Sarraf D, Freund KB, Sadda SR, Staurenghi G, Waheed NK, Chakravarthy U, Rosenfeld PJ, Holz FG, Souied EH, Cohen SY, Querques G, Ohno-Matsui K, Boyer D, Gaudric A, Blodi B, Bauman CR, Li X, Coscas GJ, Brucker A, Singerman L, Luthert P, Schmitz-Valckenberg S, Schmidt-Erfurth U, Grossniklaus HE, Wilson DJ, Guymer R, Yannuzzi LA, Chew EY, Csaky K, Monés JM, Pauleikhoff D, Tadayoni R, Fujimoto J. Consensus Nomenclature for Reporting Neovascular Age-Related Macular Degeneration Data: Consensus on Neovascular Age-Related Macular Degeneration Nomenclature Study Group. *Ophthalmology*. 2020 May;127(5):616-636. Erratum in: *Ophthalmology*. 2020 Oct;127(10):1434-1435.
3. El Ameen A, Cohen SY, Semoun O, Miere A, Srour M, Quaranta-El Maftouhi M, Oubraham H, Blanco-Garavito R, Querques G, Souied EH. Type 2 Neovascularization Secondary to Age-Related Macular Degeneration Imaged by Optical Coherence Tomography Angiography. *Retina*. 2015 Nov;35(11):2212-8.
4. Bandello F, Souied EH, Querques G (eds): *OCT Angiography in Retinal and Macular Diseases*. Dev Ophthalmol. Basel, Karger, 2016, 56, 52–56
5. Karacorlu, M., Sayman Muslubas, I., Arf, S. *et al*. Membrane patterns in eyes with choroidal neovascularization on optical coherence tomography angiography. *Eye* **33**, 1280–1289 (2019).
6. Zhao Z, Yang F, Gong Y, Yu S, Liu H, Wang H, Wang F, Sun X. The Comparison of Morphologic Characteristics of Type 1 and Type 2 Choroidal Neovascularization in Eyes with Neovascular Age-Related Macular Degeneration using Optical Coherence Tomography Angiography. *Ophthalmologica*. 2019;242(3):178-186.
7. Wietecha MS, Cerny WL, DiPietro LA. Mechanisms of vessel regression: toward an understanding of the resolution of angiogenesis. *Curr Top Microbiol Immunol*. 2013; 367: 3–32.
8. Spaide RF. Optical Coherence Tomography Angiography Signs of Vascular Abnormalization With Antiangiogenic Therapy for Choroidal Neovascularization. *Am J Ophthalmol*. 2015; 160(1): 6–16.
9. de Carlo TE, Bonini Filho MA, Chin AT, Adhi M, Ferrara D, Bauman CR, Witkin AJ, Reichel E, Duker JS, Waheed NK. Spectral-domain optical coherence tomography angiography of choroidal neovascularization. *Ophthalmology*. 2015 Jun;122(6):1228-38.



## 11.2.3.

# TYPE 3 NEOVASCULARIZATION

Miguel Lume, João Heitor Marques  
Centro Hospitalar Universitário do Porto

The ability of Optical Coherence Tomography Angiography (OCTA) to visualize the neovascular lesion has enabled a better understanding of the Type 3 Macular Neovascularization (MNV). Traditionally, it has been named Retinal Angiomatous Proliferation (RAP) or Type 3 Choroidal Neovascularization (CNV) as it occurs in eyes with the same phenotypic risk factors and cause the same end-stage findings as CNV in neovascular Age related Macular Disease (nAMD). Nevertheless, these terms should be avoided. Instead, Type 3 MNV more accurately describes this entity as it refers to a downgrowth of vessels from the retinal circulation toward the outer retina and, therefore, this term should be preferred<sup>1</sup>.

Type 3 MNV accounts for 10% of cases of nAMD<sup>2</sup>, having other specificities that should be acknowledged: patients are frequently older and with cardiovascular impairment; there is a high risk of bilateral involvement<sup>3</sup> and a relatively poor prognosis, if left untreated<sup>4</sup>; a thinner choroid is a typical finding and it is often complicated by geographic atrophy<sup>5</sup>; initial lesions tend to be located outside the fovea; finally, although drusen and focal hyperpigmentation complicating soft drusen may lead to Type 3 MNV, more than 90% of eyes with this type of neovascularization have Subretinal Drusenoid Deposits (SDD) (Figure 1) as precursor lesions<sup>6,7</sup>.

### CLINICAL AND DYE-BASED ANGIOGRAPHY FINDINGS

On fundus examination, a typical finding is a small intraretinal hemorrhage which may be accompanied by hard exudates. Occasionally, one can identify a retinal vessel bending 90° into the choroid consisting of a retinal-choroidal anastomosis. SDD are easily visible using fundus autofluorescence and confocal scanning laser ophthalmoscopy but not with Color Fundus Photography (CFP) using standard visible light technology.

Dye-based angiography is useful to identify Type 3 MNV. Fluorescein Angiography (FA) shows a hyperfluorescent lesion that persists on late phase (hot-spot), surrounded by hypofluorescent lesions due to punctate hemorrhages, hard exudates and cystoid macular edema.

More importantly, Indocyanine Green Angiography (ICGA) allows direct visualization of the intraretinal neovascular complex (initial lesion) and of the

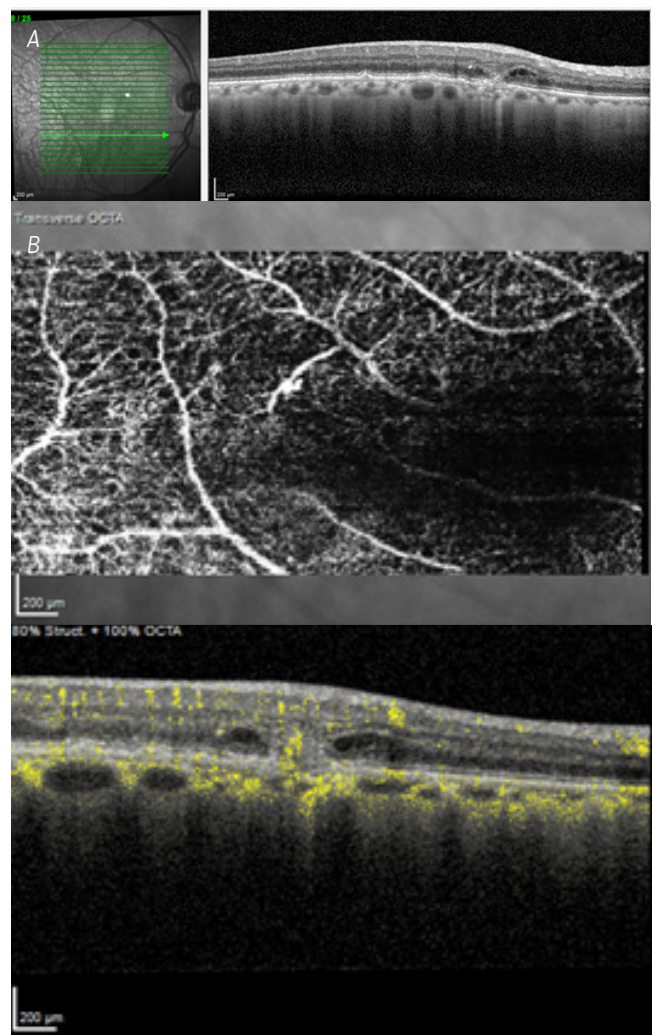


**Figure 1.** a. Patient 1 with early Type 3 MNV: SD-OCT image showing SDD and intraretinal hyper-reflective lesion in the outer retinal layers and protruding to the RPE, which is partially broken. This hyperreflective lesion corresponds to the intraretinal neovascularization. It is also possible to observe small (hyporefective) intraretinal cystoid spaces adjacent to the lesion but there is no PED. b. Patient 1 with early 1 Type 3 MNV: OCT-A c-scan shows high flow lesion descending from the DRCP.

retinal-choroidal anastomosis (advanced lesion), as a hyperfluorescent hot-spot becoming more visible in the late phases in the hypofluorescent surroundings of

intraretinal edema or Pigment Epithelial Detachment (PED) (Figure 2). Typically, its boundaries fade on late phases of the angiogram, a feature that is helpful to distinguish it from Perifoveal Exudative Vascular Anomalous Complex (PEVAC). A feeder vessel with its angulated course dipping down towards the outer retina may be visible in some patients<sup>9</sup>.

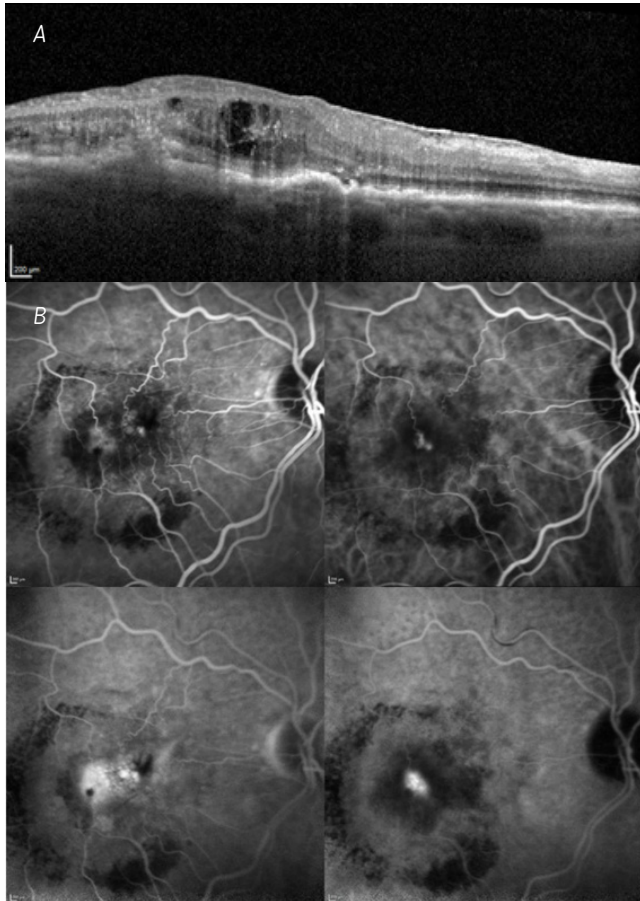


**Figure 2.** a. Patient 2 with advanced Type 3 MNV. A vascularized PED is identifiable. At its peak, a large hyperreflective lesion breaks the PED. It corresponds to the retinal-choroidal anastomosis (RCA). Large cystoid intraretinal spaces can also be seen adjacent to the RCA. b. Patient 2. Early and late phase images of FA and ICGA. One can identify in the midst of hypofluorescent lesions the hyperfluorescent "hot-spot" and its late blurring effect.

## OCT AND OCTA FINDINGS

Optical Coherence Tomography (OCT) is a non-invasive technique allowing high resolution visualization of the retina, choriocapillaris and choroid. It has been shown to have high concordance with ICGA in diagnosing type 3 MNV. Indeed, from patients diagnosed with Type 3 MNV using ICGA, 88.2% were also correspondingly diagnosed using OCT<sup>10</sup>. The typical findings of Type 3 MNV on OCT are a thin choroid (subfoveal choroidal thickness less than 200 $\mu$ m), intraretinal cystoid spaces and the presence of a PED, commonly accompanied

by a continuous hyperreflective lesion representing the vascular anastomosis with or without break of the PED (Figures 3 and 4). The typical PED associated with Type 3 MNV has a gradual slope with no obvious peak and may assume a dome or a trapezoidal shape, differing from the typical PED seen in Polypoidal Choroidal Vasculopathy (PCV), which is narrow with a high peak and associated with the characteristic double layer sign<sup>11</sup>.

OCTA is a useful technique not only to diagnose type 3 MNV, but also to study its pathophysiology and to evaluate the response to anti-VEGF treatment (Figures 5 and 6). The depth-resolved nature of OCTA can pinpoint the location and extension of the neovascular complex to specific retinal or choroidal layers. Miere et al.<sup>12</sup> showed a tuft-shaped high-flow network in the outer retina segmentation and a small clew-like lesion in the choriocapillaris segmentation. Later, it was identified a sub-RPE multilaminar hyperreflectivity ("onion sign") secondary to sub-RPE CNV chronic exudation, supporting the idea of a choroidal origin for Type 3 MNV<sup>13</sup>. Conversely, Bhavsar et al.<sup>14</sup> demonstrated flow in the outer retina contiguous with the deep retinal capillary plexus (DCP) and adjacent to a small PED before the development of a clinically visible lesion which may support the idea of a retinal origin for Type 3 MNV. OCTA has distinctive features depending on which stage Type 3 MNV is<sup>12,15-19</sup>:

**Stage 1** (intraretinal neovascularization). There is an initial intraretinal neovascularization with compensatory angiomatous proliferation of capillaries within the deep retinal layers in the paramacular area. OCT-A shows a telangiectatic high flow lesion descending toward the outer retinal layers.

**Stage 2** (subretinal neovascularization). In stage 2, the intraretinal neovascularization extends further posteriorly into the subretinal space forming subretinal neovascularization. A PED can be seen at this stage (Stage 2b). OCTA shows a high flow lesion extending down and under the retina and it is best visualized in the avascular layer slab.

**Stage 3** (retinal-choroidal anastomosis). The neovascular complex spreads deeper, forming a retinal-choroidal anastomosis with an underlying sub-RPE neovascularization. OCT may show that the hyperreflective lesion extends through the RPE and a PED with heterogeneous hyperreflective material. OCTA C-scan shows abnormal flow in deep retinal, avascular, and choroidal segmentations. Corresponding B-scan images reveal flow penetrating the RPE and extending underneath, sometimes inside the PED.

Nevertheless, there are limitations in using OCTA, as projection artifacts may appear on PED and give a false MNV signal flow<sup>20</sup>. Segmentation confirmation and correlation with structural OCT are mandatory. Also, some studies showed that Spectral Domain OCTA, despite being useful in many cases, was inferior to FA<sup>21</sup> and to Swept Source-OCTA<sup>22</sup> for the detection of the CNV in AMD.

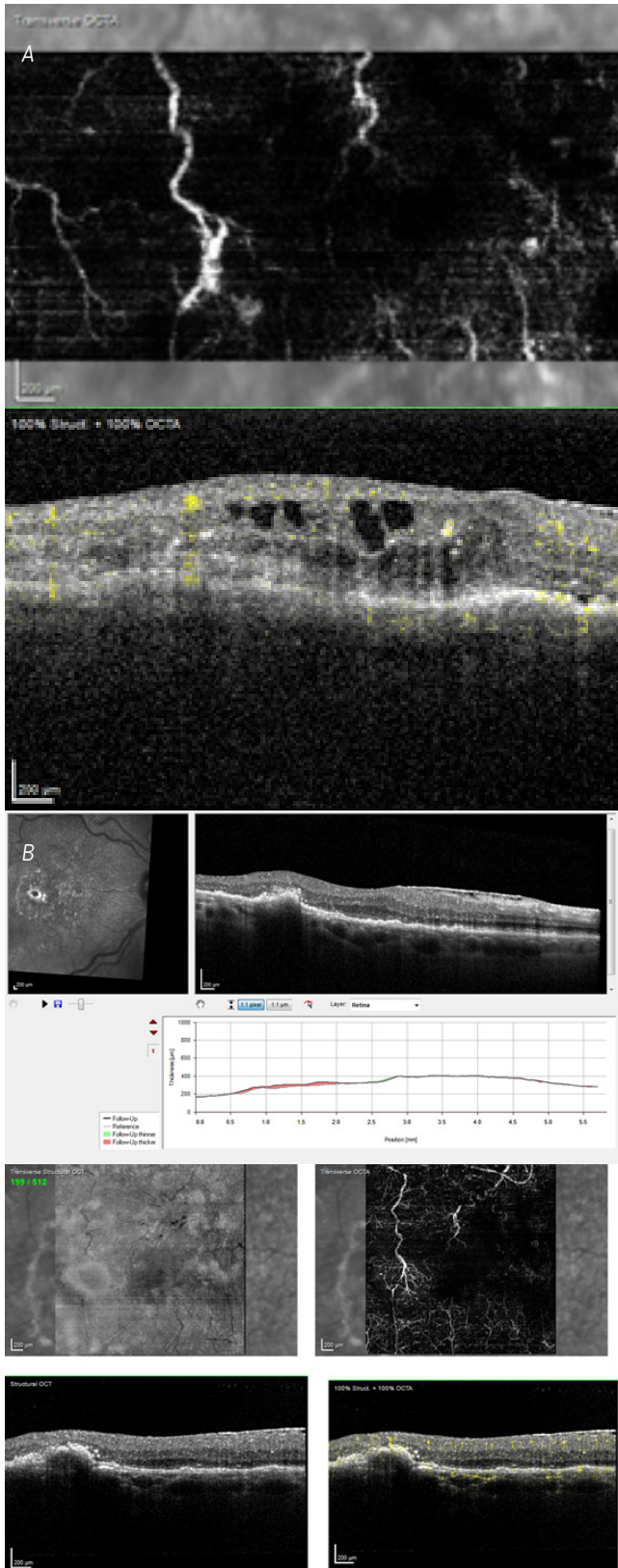


**Figure 3.** a. Patient 3. OCT-A shows a prominent high flow lesion representing the retinal-choroidal anastomosis arising from the DCP. b. Patient 3 after treatment with 3 monthly anti-VEGF injections. On SD-OCT, there's no exudative lesions, but the PED is still present. On OCT-A, the feeder vessel is still visible despite decreased dimension.

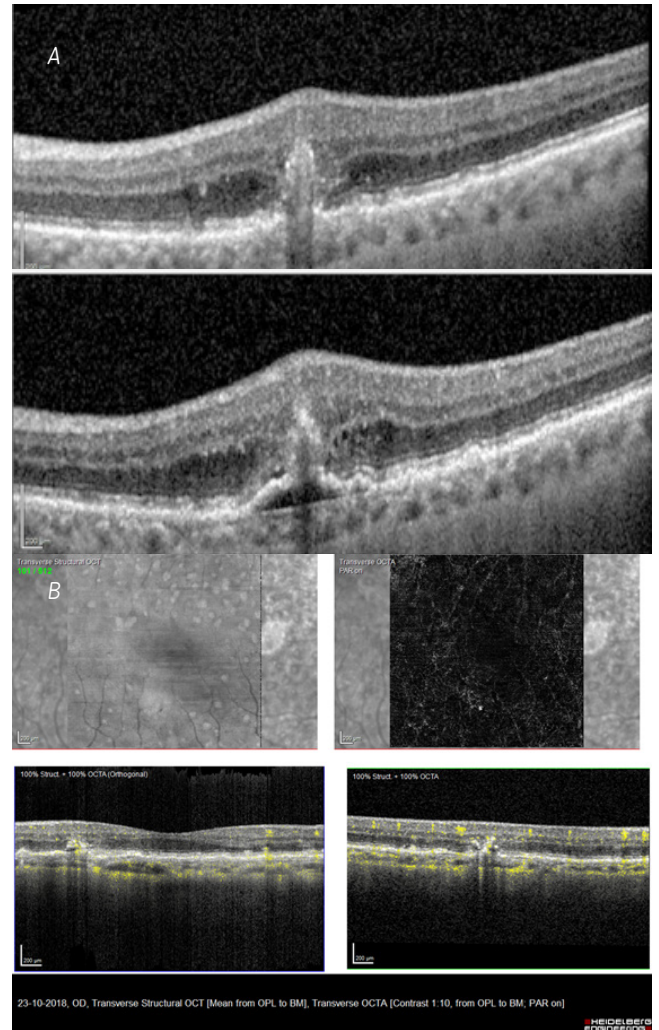


**Figure 4.** a. Patient 4. SD-OCT depicting a stage 2a Type 3 MNV evolving into a stage 2b one month later. b. Patient 4. Transverse OCT-A of the fellow eye showing a small high flow round lesion that corresponds to a nascent intraretinal neovascularization which is also visible on the b-scan as hyperreflective foci and RPE breaking.

Another feature that can be assessed on OCTA is choriocapillaris flow. OCTA shows signal voids in eyes with SDD and drusen<sup>6</sup>. Furthermore, choriocapillaris flow deficit is significantly greater in the peripheral macular regions of eyes with Type 3 MNV, compared to eyes with Type 1/2 CNV and normal control eyes. Additionally, diffuse choriocapillaris flow impairment seems to be more important in eyes with Type 3 MNV than in eyes with Types 1 or 2 CNV, which are more prone to focal deficits instead<sup>23</sup>.

## DIFFERENTIAL DIAGNOSIS

The differential diagnosis of early Type 3 MNV includes macular telangiectasia, PEVAC, diabetic macular edema, arterial macroaneurysm and branch retinal vein occlusion. Advanced Type 3 MNV may be confounded with other types of choroidal neovascularization or may even coexist with Type 1 CNV<sup>24</sup>.

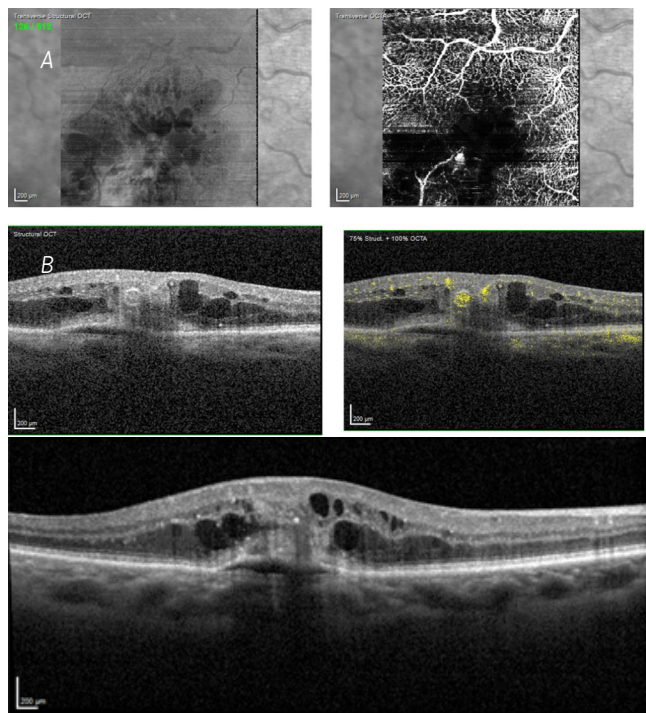


**Figure 5.** a. Patient 5 with large and shallow PED on SD-OCT. A round lesion with hyperreflective boundaries is also noted. On OCT-A this high flow lesion is readily visible. b. Patient 5 with different b-scan showing a large and shallow PED and the hyperreflective lesion connecting the DCP and the sub-RPE space.

**FOLLOW-UP AND TREATMENT MONITORING**

Before the era of anti-VEGFs, Type 3 MNV had a poor visual prognosis<sup>2</sup>. Nowadays, visual outcome is highly dependent on the stage of the disease where treatment starts<sup>25</sup>. Using OCTA, several studies have demonstrated a reduction in intralesional flow following intravitreal anti-VEGF therapy<sup>26, 27</sup>. Phasukkijwatana et al., showed that there was a significant regression of the neovascular lesion area and cystoid macular edema resolution in 17/17 eyes after anti-VEGF therapy, but in 11 eyes large feeder vessels remained unchanged<sup>28</sup>. In other types of AMD-related neovascularization, imaging with OCTA has been shown to have prognostic value during anti-VEGF treatment, namely regarding the morphologic appearance of the MNV<sup>29</sup>. Rather than relying on indirect measures of neovascular activity, OCTA can visualize the MNV and identify changes that precede the onset or recurrence of exudation, which might allow for a more precise anti-VEGF treatment of neovascular AMD<sup>30</sup>. In conclusion, OCTA is a non-invasive technique that can accurately identify early Type 3 MNV lesions and monitor its response to anti-VEGF treatment, allowing a timely diagnosis and improving visual prognosis. These features prove that OCTA is a critical tool in the current multimodal imaging paradigm.

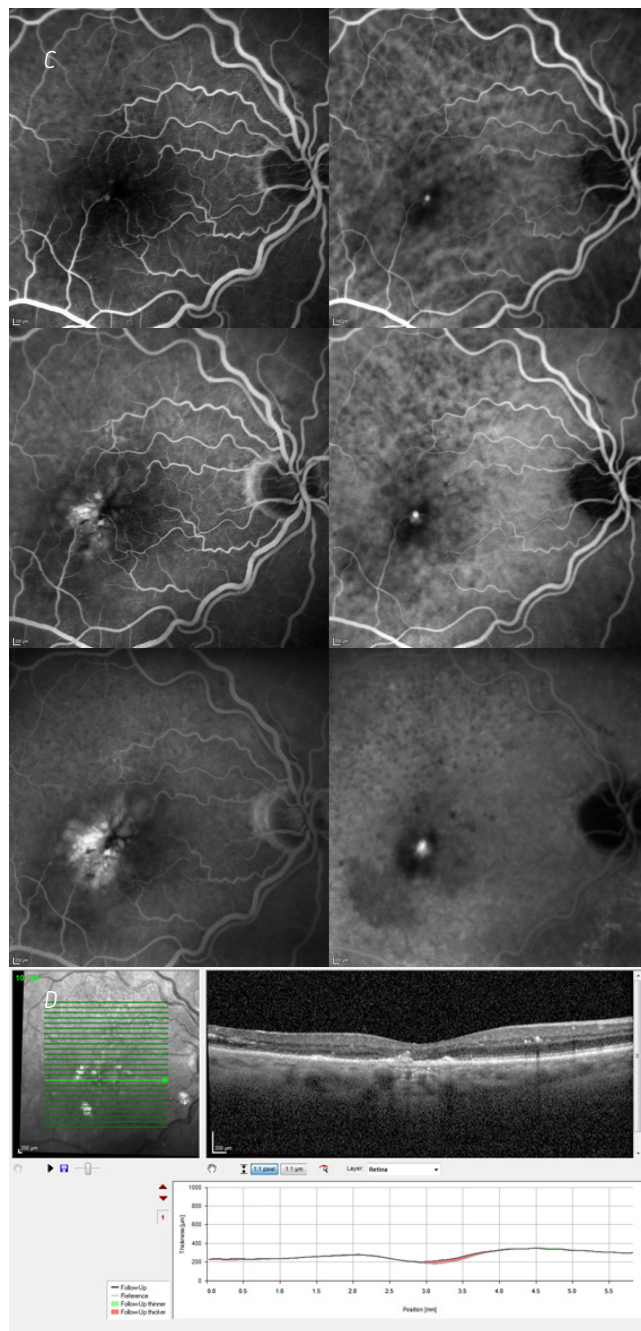


**Figure 5.** c. Patient 5: Early, middle and late phase FA and ICGA showing the hyperfluorescent "hot-spot" lesion. d. Patient 5: OCT after treatment with 3 monthly anti-VEGF injections.

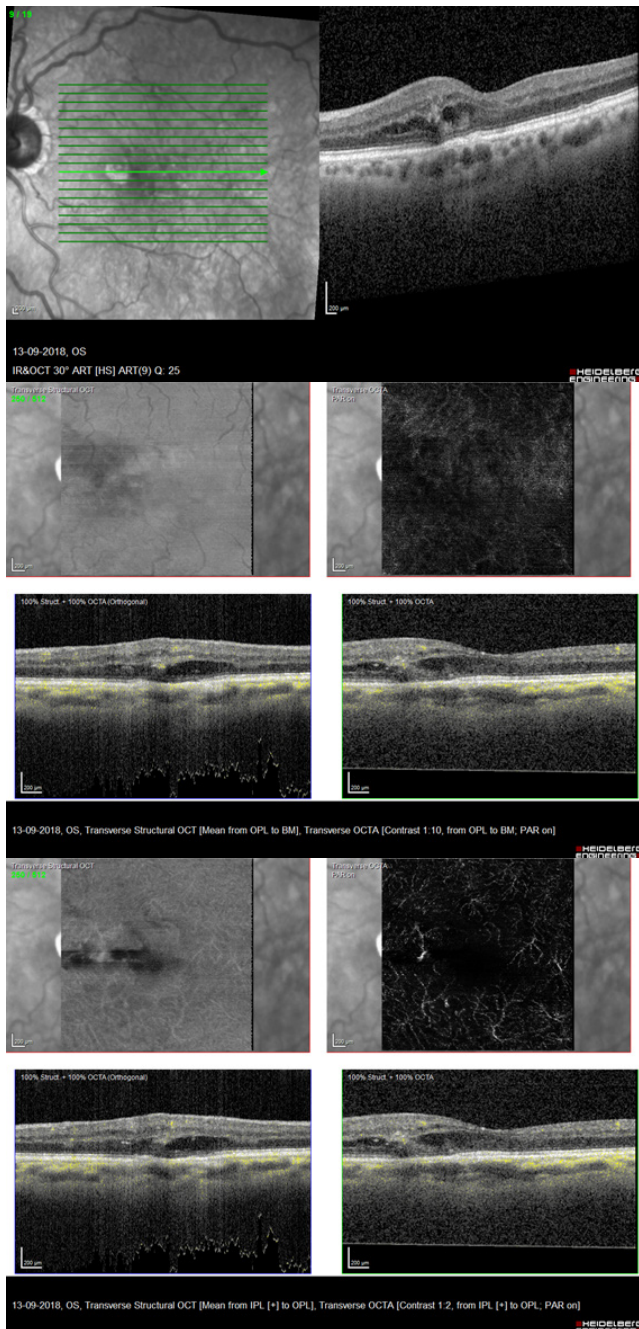


**Figure 6.** a. Patient 6: OCT depicting intraretinal neovascularization as hyperreflective dots surrounded by intraretinal cystoid spaces. b. Patient 6. OCT-A: the avascular slab doesn't detect high-flow lesions. c. Patient 6. OCT-A: the DCP slab clearly shows the nascent intraretinal neovascularization.

## REFERENCES

1. Spaide RF, Jaffe GJ, Sarraf D, et al. Consensus Nomenclature for Reporting Neovascular Age-Related Macular Degeneration Data: Consensus on Neovascular Age-Related Macular Degeneration Nomenclature Study Group. *Ophthalmology*. 2020;127(5):616-636.
2. Scott AW, Bressler SB. Retinal angiomatous proliferation or retinal anastomosis to the lesion. In: *Eye*. Vol 24. Nature Publishing Group; 2010:491-496.
3. Gross NE, Aizman A, Brucker A, Klancnik JM, Yannuzzi LA. Nature and risk of neovascularization in the fellow eye of patients with unilateral retinal angiomatous proliferation. *Retina*. 2005.
4. Yannuzzi LA, Freund KB, Takahashi BS. Review of retinal angiomatous proliferation or type 3 neovascularization. *Retina*. 2008.
5. Kim JH, Kim JR, Kang SW, Kim SJ, Ha HS. Thinner choroid and greater drusen extent in retinal angiomatous proliferation than in typical exudative age-related macular degeneration. *Am J Ophthalmol*. 2013;155(4).
6. Spaide R, Sotaro O, Curcio C. Subretinal Drusenoid Deposits AKA Pseudodrusen *Surv Ophthalmology* 2018;63(6):782-815.
7. Spaide, R. Improving the age-related macular degeneration construct *Retina* 2018;38(5):891-899.
8. Ravera V, Bottoni F, Staurengi G. Retinal angiomatous proliferation diagnosis: a multiimaging approach *Retina* 2016;36(12):2274-2281.
9. Rouvas AA, Papakostas TD, Ntouraki A, Douvali M, Vergados I, Ladas ID. Angiographic and OCT features of retinal angiomatous proliferation. *Eye* 2010;24(11):1633-1643.
10. Kim JH, Chang YS, Kim JW, Lee TG, Kim HS. Diagnosis of type 3 neovascularization based on optical coherence tomography images. *Retina* 2016;36(8):1506-1515.
11. De Salvo G, Vaz-Pereira S, Keane PA, Tufail A, Liew G. Sensitivity and specificity of spectral-domain optical coherence tomography in detecting idiopathic polypoidal choroidal vasculopathy. *Am J Ophthalmol*. 2014;158(6):1228-1238.e1.
12. Miere A, Querques G, Semoun O, El Ameen A, Capuano V, Souied EH. Optical coherence tomography angiography in early type 3 neovascularization. *Retina* 2015;35(11):2236-2241.
13. Miere A, Sacconi R, Amoroso F, Capuano V, Jung C, Bandello F, Souied E, Querques G. Sub-retinal pigment epithelium multilaminar hyperreflectivity at the onset of type 3 macular neovascularization, *Retina*: 2021;41(1):135-143.
14. Bhavsar K V, Jia Y, Wang J, et al. Projection-resolved optical coherence tomography angiography exhibiting early flow prior to clinically observed retinal angiomatous proliferation. *Am J Ophthalmol Case Reports*. 2017;8:53-57.
15. Valler D, Feucht N, Lohmann CP, Ulbig M, Maier M. Diagnostic criteria: OCT angiography for retinal angiomatous proliferation (RAP lesions, type 3 neovascularization). *Ophthalmologie* 2020;117(6):529-537.
16. Nagiel A, Sarraf D, Sadda SR, et al. Type 3 neovascularization: Evolution, association with pigment epithelial detachment, and treatment response as revealed by spectral domain optical coherence tomography. *Retina* 2015;35(4):638-647.
17. Kataoka K, Takeuchi J, Nakano Y, et al. Characteristics and



- Classification of Type 3 Neovascularization With B-Scan Flow Overlay and En Face Flow Images of Optical Coherence Tomography Angiography. *Retina* 2020;40(1):109-120.
18. Querques G, Miere A, Souied EH. Optical Coherence Tomography Angiography Features of Type 3 Neovascularization in Age-Related Macular Degeneration. *Dev Ophthalmol* 2016;56:57-61.
  19. Silva N, Marta A, Baptista P, Furtado M, Lume M. Optical Coherence Tomography Findings (SD-OCT and OCTA) in Early-Stage Type 3 Neovascularization *Case Rep Ophthalmol* 2020;11:493-499.
  20. Zhang A, Zhang Q, Wang RK. Minimizing projection artifacts for accurate presentation of choroidal neovascularization in OCT micro-angiography. *Biomed Opt Express*. 2015;6(10):4130.
  21. Gong J, Yu S, Gong Y, Wang F, Sun X. The Diagnostic Accuracy of Optical Coherence Tomography Angiography for Neovascular Age-Related Macular Degeneration: A Comparison with Fundus Fluorescein Angiography. *J Ophthalmol*. 2016;2016:7521478.
  22. Novais EA, Adhi M, Moulton EM, Louzada RN, Cole ED, Husvogt L, Lee B, Dang S, Regatieri CV, Witkin AJ, Bauman CR, Hornegger J, Jayaraman V, Fujimoto JG, Duker JS, Waheed NK. Choroidal Neovascularization Analyzed on Ultrahigh-Speed Swept-Source Optical Coherence Tomography Angiography Compared to Spectral-Domain Optical Coherence Tomography Angiography. *Am J Ophthalmol*. 2016 Apr;164:80-8.
  23. Corvi F, Cozzi M, Corradetti G, Staurenghi G, Sarraf D, Sadda SVR. Quantitative assessment of choriocapillaris flow deficits in eyes with macular neovascularization. *Graefes Arch Clin Exp Ophthalmol*. January 2021:1-9.
  24. Souied E, Amoroso F Neovascular AMD in Macular Disorders Kim I (Ed) Springer 2020.
  25. Tsai ASH, Cheung N, Gan ATL. Retinal angiomatic proliferation. *Surv Ophthalmol*. 2017;62(4):462-492.
  26. Tan ACS, Dansingani KK, Yannuzzi LA, Sarraf D, Freund KB. Type 3 neovascularization imaged with cross-sectional and en face optical coherence tomography angiography. *Retina*. 2017;37(2):234-246.
  27. Dansingani KK, Naysan J, Freund KB. En face OCT angiography demonstrates flow in early type 3 neovascularization (retinal angiomatic proliferation). *Eye*. 2015;29(5):703-706.
  28. Phasukkijwatana N, Tan ACS, Chen X, Freund KB, Sarraf D. Optical coherence tomography angiography of type 3 neovascularisation in age-related macular degeneration after antiangiogenic therapy. *Br J Ophthalmol*. 2017;101(5):597-602.
  29. Bae K, Kim HJ, Shin YK, Kang SW. Predictors of neovascular activity during neovascular age-related macular degeneration treatment based on optical coherence tomography angiography. *Sci Rep*. 2019;9(1):1-10.
  30. Muakkassa NW, Chin AT, de Carlo T, Klein KA, Bauman CR, Witkin AJ, Duker JS, Waheed NK. Characterizing the effect of anti-vascular endothelial growth factor therapy on treatment-naive choroidal neovascularization using optical coherence tomography angiography. *Retina* 2015 Nov;35(11):2252-9.

# MIXED NEOVASCULARIZATION

Pedro Prata Gomes<sup>1</sup>, Pedro Pereira Neves<sup>2</sup>, Mário Ornelas<sup>2</sup>

<sup>1</sup> - Centro Hospitalar Universitário Lisboa Norte (CHULN) - Hospital de Santa Maria, Lisboa, Portugal

<sup>2</sup> - Centro Hospitalar de Setúbal, EPE, Hospital de São Bernardo, Setúbal, Portugal

In its initial stages, the main feature of age-related macular degeneration (AMD) is the presence of drusen, a cellular polymorphous material located between the retinal pigment epithelium (RPE) and the Bruch's membrane (BM). Patients with early AMD are often asymptomatic, whereas advanced AMD usually presents with progressive central visual loss. In atrophic or "dry" AMD there is geographic atrophy, marked by the loss of certain RPE segments and outer retinal layers<sup>1</sup>. Neovascular or "wet" AMD, on the other hand, is characterized by the presence of choroidal neovascularization (CNV), where abnormal blood vessels originate from the choroid. The prevalence of neovascular AMD subtype is about 15-20%, and it affects approximately 2% of the general population older than 60, with a rapid and progressive course<sup>1</sup>. This neovascularization results from an increase in vascular endothelial growth factor (VEGF) which stimulates vascular growth and leads to BM defects<sup>1</sup>.

The identification and classification of the neovascular net in AMD changed progressively over time, especially with the development of new, non-invasive imaging modalities. Historically, fluorescein angiography (FA) was the only available imaging modality. It classified CNV according to its position in relation to the fovea (extrafoveal, juxtafoveal and subfoveal) and angiographic patterns (classic and occult CNV) (2). Gass was the first to suggest that the neovascular complex location (above or sub RPE) might influence treatment response, and proposed a novel classification which introduced the terms type 1 CNV, where vessels were confined to the sub-RPE space; and type 2 CNV, where vessels were located above the RPE<sup>2</sup>. The development of indocyanine green angiography (ICGA) allowed for the detection and demarcation of occult CNV, providing a more accurate visualization of the choroidal vasculature. This technology was used to first describe polypoidal choroidal vasculopathy (PCV) and retinal angiomatous proliferation (RAP)<sup>2</sup>. Later on, in 1991, optical coherence tomography (OCT) proved to be a quick and non-invasive imaging method, capable of representing the retinal structure with a level of detail inferior to 10µm. OCT allowed for identifying indirect signs of the presence and location of CNV, in addition to monitoring CNV activity<sup>3</sup>. More recently, optical coherence tomography angiography (OCTA) has been used to generate a

noninvasive representation of the retinal and choroidal vascular flow, opening doors to new CNV classifications, patterns and monitorization<sup>3</sup>.

Macular neovascularization in AMD results from the invasive development of vascular and adjacent tissues into the outer retina, subretinal space or sub-RPE space. In 2010, Freund et al.<sup>2</sup> used OCT to describe a novel subclassification of macular neovascularization based on the anatomical location of newly-formed vessels.

Type 1 macular neovascularization: Abnormal vessels originating by choriocapillaris grow into the sub-RPE space, causing remodeling of the feeding and draining vessels of the choroid. Additionally, a varying amount of fibroblasts, myofibroblasts and macrophages lead to the formation of fibrotic tissue. This lesion corresponds to occult neovascularization on FA and is better visualized with ICGA<sup>2,4</sup>.

Type 2 macular neovascularization: Abnormal vessels originating in the choriocapillaris grow into the subretinal space, crossing the RPE. Although the neovascularization is present in the sub-RPE space, the dominant portion is subretinal. In FA, this lesion most frequently corresponds to classic neovascular membranes. Type 2 neovascularization is mostly present in conditions other than AMD<sup>2,4</sup>.

Type 3 macular neovascularization: Abnormal vessels originating in the retinal circulation grow through and beyond the outer retina. Deep capillary plexus vessels supply the lesion, with remodeling to handle flow needs. Intraretinal hemorrhages and cystoid spaces are frequent. FA frequently shows intraretinal leakage and cystoid macular edema<sup>4</sup>.

Mixed macular neovascularization: A reasonable percentage of AMD patients have a mixture of the neovascular subtypes described above, rather than one mechanism alone (12.2 – 16.9% according to Jung et al.<sup>5</sup>). Many type 2 lesions originate from type 1 vessels that penetrate the RPE and some type 3 lesions have concomitant independent type 1 neovascularization. Jung et al.<sup>5</sup> also noted that the anatomical OCT classification described a higher prevalence of mixed neovascularization than the previous FA classification<sup>5</sup>. The initial area and diameter of mixed lesions were significantly larger than type 1, type 2 or type 3 alone<sup>5</sup>. Recently, Coscas et al.<sup>6</sup> used OCTA technology to analyze the response of mixed

type 1 and type 2 neovascularization to intravitreal anti-VEGF injections. The authors identified a substantial reduction in the amount of tiny branching vessels and anastomoses in both neovascular components, associated with the persistence of hyperintense signal from larger trunks<sup>6</sup>. Additionally, they noted a difference in area reduction between the two components (24% reduction in type 2 neovascularization vs 11.2% reduction in type 1 neovascularization), which can in turn be explained by the location of the lesions and proximity of intravitreal drug<sup>6</sup>.

OCTA is a helpful tool to monitor wet AMD, providing information about both functional and morphological aspects in a single OCT scan. It allows for a rapid visualization of the different vascular plexus at various depths, from the internal limiting membrane to the choroid. Additionally, it is possible to identify the correct anatomical position and extension of neovascular membranes, thus more accurately identifying mixed neovascular components. Vessel morphology can be presented on the OCTA en face images both below and above the RPE. Karacorlu et al., classified neovascular membrane patterns: 50% had medusa pattern, 42% sea-fan and 8% long filamentous pattern<sup>7</sup>.

## REFERENCES

1. Lupidi M, Cerquaglia A, Chhablani J, Fiore T, Singh SR, Cardillo Piccolino F, et al. Optical coherence tomography angiography in age-related macular degeneration: The game changer. *European Journal of Ophthalmology*. 2018;28(4):349-57.
2. Freund KB, Zweifel SA, Engelbert M. Do we need a new classification for choroidal neovascularization in age-related macular degeneration? *Retina*. 2010;30(9):1333-49.
3. Sulzbacher F, Pollreisz A, Kaider A, Kickingner S, Sacu S, Schmidt-Erfurth U. Identification and clinical role of choroidal neovascularization characteristics based on optical coherence tomography angiography. *Acta Ophthalmologica*. 2017;95(4):414-20.
4. Spaide RF, Jaffe GJ, Sarraf D, Freund KB, Sadda SR, Staurenghi G, et al. Consensus Nomenclature for Reporting Neovascular Age-Related Macular Degeneration Data. *Ophthalmology*. 2020;127(5):616-36.
5. Jung JJ, Chen CY, Mrejen S, Gallego-Pinazo R, Xu L, Marsiglia M, et al. The incidence of neovascular subtypes in newly diagnosed neovascular age-related macular degeneration. *Am J Ophthalmol*. 2014;158(4):769-79.e2.
6. Coscas G, Lupidi M, Coscas F, Français C, Cagini C, Souied EH. Optical coherence tomography angiography during follow-up: qualitative and quantitative analysis of mixed type I and II choroidal neovascularization after vascular endothelial growth factor trap therapy. *Ophthalmic Res*. 2015;54(2):57-63.
7. Karacorlu M, Sayman Muslubas I, Arf S, Hocaoglu M, Ersoz MG. Membrane patterns in eyes with choroidal neovascularization on optical coherence tomography angiography. *Eye*. 2019;33(8):1280-9.

## 11.2.5.

# NONEXUDATIVE NEOVASCULARIZATION

Ana Maria Cunha<sup>1</sup>, Rodrigo Vilares Morgado<sup>1,2</sup>, Ângela Carneiro<sup>1,2</sup>

1 - Department of Ophthalmology, Centro Hospitalar Universitário de São João

2 - Department of Surgery and Physiology, Faculty of Medicine, University of Porto

## INTRODUCTION

Age-related macular degeneration (AMD) is a degenerative disorder of the macula and the most frequent cause of blindness and moderate to severe vision impairment (MSVI) in high-income countries.<sup>1</sup> Visual impairment typically arises in patients with end-stage disease. Traditionally, late-stage AMD was classified as neovascular AMD and atrophic (non-neovascular) AMD. Despite being usually bilateral, type of disease and disease severity are frequently asymmetric between affected eyes.<sup>2</sup> Neovascular AMD is present when pathologic blood vessels arise from the choroid or the outer retina and extend toward/throughout the outer retina, a process globally known as macular neovascularization (MNV). Often, these vessels are exudative, resulting in leakage of fluid, lipid exudates, or blood and, finally, retinal pigment epithelium (RPE) and outer retinal atrophy with disciform scar formation. Both forms of late AMD (neovascular and atrophic AMD) are responsible for the majority of the cases of visual impairment. The exudation from MNV can be detected clinically by fundoscopic examination, but also through retinal imaging exams as leakage in dye-based angiography, such as fluorescein angiography (FA), hot spot or *plaques* in indocyanine-green angiography (ICGA) and as intraretinal, subretinal or sub-RPE fluid in optical coherence tomography (OCT).

Nevertheless, MNV can be present without exudative features. In the 1970s, two histologic studies in postmortem eyes with AMD first reported the presence of MNV without evidence of overlying hemorrhage or exudation<sup>3, 4</sup>. Posterior histopathologic studies determined that these fibrovascular lesions were located beneath the RPE.<sup>5, 6</sup> Due to this location and the absence of associated exudation, these lesions were not detected with FA or fundoscopic examination but could be depicted in ICGA as focal spots or *plaques* with late staining. Furthermore, these lesions were associated with an increased risk of developing exudative features.<sup>7, 8</sup> However, due to the invasive nature of ICGA, its' low availability, and the absence of therapy for these lesions, this exam was not routinely performed on eyes with nonexudative AMD.

Since its inception, OCTA has also been used to detect

nonexudative MNV.<sup>9-14</sup> Being a faster, less expensive, noninvasive and contrast free retinal imaging exam, it represents a viable tool to monitor eyes with nonexudative AMD, especially in patients with unilateral exudative AMD. With the increased availability of OCTA, several studies have started to investigate the prevalence and natural history of nonexudative MNV.

## PREVALENCE AND NATURAL HISTORY OF NONEXUDATIVE MNV

The prevalence of these lesions has been predominantly documented in fellow eyes of patients with unilateral exudative neovascular AMD. In these eyes, the prevalence of nonexudative neovascular AMD varies from 6.25% to 27%.<sup>15</sup> Most cases of nonexudative MNV are described as “asymptomatic” or “subclinical” since there is no associated significant decrease in best corrected visual acuity (BCVA), except for eyes with concomitant central complete RPE and outer retinal atrophy (cRORA). In fact, BCVA may remain stable in these eyes as long as exudation does not develop.<sup>11</sup> Typical fundoscopic features in these eyes include macular drusen and pigmentary abnormalities with corresponding RPE elevations and intraretinal hyperreflective foci in the OCT.<sup>9, 12, 16</sup> Globally, around 25% of nonexudative MNV lesions will become exudative in up to two years after initial diagnosis<sup>15</sup> and the presence of nonexudative MNV significantly increases the risk of developing exudative AMD, when compared with eyes without any MNV.<sup>11, 14, 16</sup> In eyes that have progressed to exudative AMD, there was a previous increase in the size of the nonexudative vascular network, while eyes with nonexudative MNV that do not progress to exudative AMD typically have a stable size and shape of their vascular network.<sup>11, 16-18</sup> Thus, identifying and following eyes with these lesions may lead to earlier diagnosis and treatment with anti-vascular endothelial growth factor (anti-VEGF) agents if there is conversion to exudative neovascular AMD.

## TOMOGRAPHIC NONEXUDATIVE MNV DIAGNOSIS

Both spectral-domain and swept-source OCTA (SD-OCTA and SS-OCTA, respectively) enable direct visualization of these neovascular complexes while

also confirming the absence of exudative tomographic features (subretinal, intraretinal or sub-RPE fluid). These complexes are typically located beneath the RPE, thus constituting a type 1 neovascular lesion (Figures 1 to 3).<sup>14</sup> <sup>19</sup> Both types of OCTA may also demonstrate conversion to exudative AMD. Since SS-OCTA uses a tunable swept source-laser with a longer center wavelength than the SD-OCTA, enabling imaging deeper into the tissue, it detects the neovascular complexes with higher accuracy, yielding larger MNV areas for the MNV and delivering angiograms with better image quality.<sup>20, 21</sup>

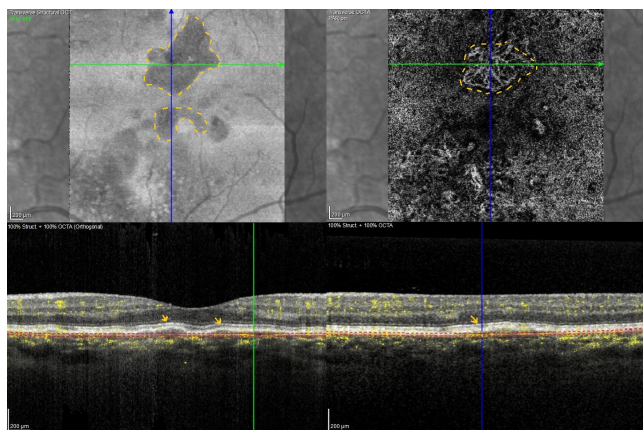


**Figure 1.** SD-OCT and OCTA images of a 64 year-old woman with nonexudative macular neovascularization (NE-MNV). En-face OCT (A) demonstrates a hyporeflective and well circumscribed area (yellow dashed lines). On the corresponding structural OCT B-scans (C, D), an elevation of the retinal pigment epithelium (yellow arrows) can be seen. The OCTA angiogram (B) identifies the NE-MNV plexus, as a well circumscribed, “lacy-wheel”-shaped lesion, with hyperintense signal (yellow dashed lines).

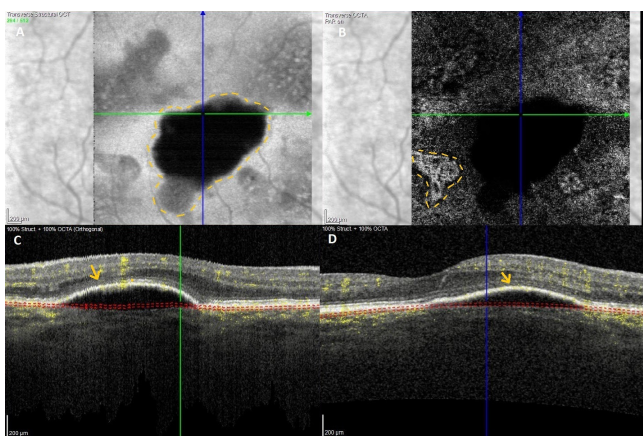


**Figure 2.** SSD-OCT and OCTA images of a 73 year-old man with nonexudative macular neovascularization (NE-MNV). Structural OCT B-scans (C, D) highlight a nonhomogeneous retinal pigment epithelium detachment (yellow arrows) that corresponds to a dark, well-defined area (yellow dashed lines) in the En-face (A) OCT scan and an area of low signal on the OCTA angiogram (B). The OCTA angiogram (B) demonstrates the presence of an NE-MNV plexus in close proximity to the aforementioned low signal area (yellow dashed lines).

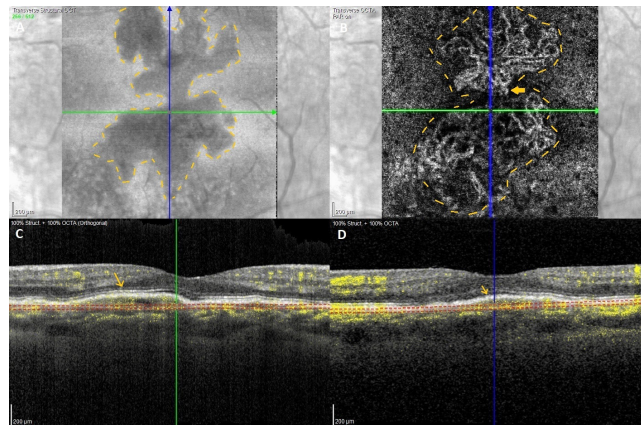


**Figure 3.** SD-OCT and OCTA images of a 68 year-old woman with nonexudative macular neovascularization (NE-MNV). En-face OCT (A) demonstrates a nonhomogeneous, well defined area (yellow dashed lines) that corresponds to the heterogeneous sub-RPE tissue seen on the OCT B-scan (yellow arrows at C and D). OCTA angiogram (B) segmented at the avascular complex area and centered on the foveal avascular zone highlights a NE-MNV complex with dead tree-like branches (yellow dashed lines), that appears to possess a slightly deeper feeding branch located in the choroid (yellow arrows).

### NONEXUDATIVE NEOVASCULARIZATION AND LATE ATROPHIC AMD

Nonexudative MNV may exist not only in eyes with intermediate AMD but also in eyes with macular atrophy. The rate of atrophy progression seems to be lower in eyes with both nonexudative MNV and cRORA compared to eyes with cRORA alone.<sup>18</sup> Moreover, when these lesions coexist, the nonexudative MNV lesion tends to be located in an adjacent area, in which there is no progression of atrophy. There is also typically a sharp demarcation in the SD-OCT images between the areas of cRORA and areas without any atrophy, with enhanced choroidal signal in the former, due to loss of the RPE.<sup>17</sup>

### TO TREAT OR NOT TO TREAT?

The management of nonexudative MNV is currently under discussion. Whether these subclinical lesions should be treated prophylactically with intravitreal injections of anti-VEGF to prevent the onset of exudation has been a topic of debate. A single-masked, sham-controlled, randomized clinical trial has been performed to evaluate intravitreal aflibercept injection (IAI) as prophylaxis against the conversion to exudative AMD in high-risk eyes. The rates of conversion were not lower in the IAI group compared with the sham treatment group at month 24.<sup>22</sup>

Moreover, even if lesion growth is present, there is no additional benefit in treatment with anti-VEGF agents before exudative disease develops. These lesions may persist for several years without decreasing visual acuity and may provide nutritional support to overlying RPE and photoreceptors.<sup>14, 23</sup> Nonexudative MNV does not

appear to be responsible for the deterioration of visual function until conversion to exudative neovascular AMD occurs. Furthermore, OCTA studies have shown that some MNV lesions do not disappear after anti-VEGF therapy, which suggests that these lesions are mature and do not respond to repeated injections.<sup>24</sup>

Nevertheless, an early detection of exudative MNV produces better anti-VEGF treatment outcomes. Thus, we advocate close clinical follow up, with regular structural OCT and OCTA exams and home monitoring with an Amsler grid, without treatment, until exudation develops. More randomized clinical trials are still necessary to support these recommendations.

## FUTURE DIRECTIONS OF INVESTIGATION

In summary, nonexudative MNV in AMD is a subclinical condition that usually occurs in eyes with good visual acuity.

One of the main priorities of future research is to better understand the pathophysiology of conversion to exudative lesions. It is important to understand why there is an enlargement of some nonexudative lesions and its role in the development of exudative disease. Moreover, it is critical to identify other imaging and biochemical biomarkers that can predict the risk of exudative conversion. By identifying these predictors, existent technology, such as the OCTA, will be even more helpful in stratifying the follow-up and eventually treatment of eyes with AMD.

Another important cornerstone of future research is to develop a treatment that can stabilize nonexudative MNV lesions and prevent conversion to exudative disease without increasing the development or progression of macular atrophy, which already occurs with anti-VEGF therapy.<sup>24, 25</sup> Molecules such as angiopoietin-1, platelet-derived growth factor or transforming growth factor beta, which are also important in the pathophysiology of AMD, may become new important treatment targets for the benefit of eyes with nonexudative MNV.<sup>26</sup>

## REFERENCES

1. Bourne RRA, Jonas JB, Bron AM, et al. Prevalence and causes of vision loss in high-income countries and in Eastern and Central Europe in 2015: magnitude, temporal trends and projections. *British Journal of Ophthalmology*. 2018;102(5):575.
2. Gangnon RE, Lee KE, Klein BEK, Iyengar SK, Sivakumaran TA, Klein R. Severity of age-related macular degeneration in 1 eye and the incidence and progression of age-related macular degeneration in the fellow eye: the Beaver Dam Eye Study. *JAMA Ophthalmol*. 2015;133(2):125-132.
3. Green WR, Key SN, 3rd. Senile macular degeneration: a histopathologic study. *Trans Am Ophthalmol Soc*. 1977;75:180-254.
4. Sarks SH. New vessel formation beneath the retinal pigment epithelium in senile eyes. *Br J Ophthalmol*. 1973;57(12):951-65.
5. Spraul CW, Grossniklaus HE. Characteristics of Drusen and Bruch's membrane in postmortem eyes with age-related macular degeneration. *Arch Ophthalmol*. 1997;115(2):267-73.
6. Green WR, McDonnell PJ, Yeo JH. Pathologic features of senile macular degeneration. *Ophthalmology*. 1985;92(5):615-27.
7. Schneider U, Gelissen F, Inhoffen W, Kreissig I. Indocyanine green angiographic findings in fellow eyes of patients with unilateral occult neovascular age-related macular degeneration. *Int Ophthalmol*. 1997;21(2):79-85.
8. Hanutsaha P, Guyer DR, Yannuzzi LA, et al. Indocyanine-green videoangiography of drusen as a possible predictive indicator of exudative maculopathy. *Ophthalmology*. 1998;105(9):1632-6.
9. Roisman L, Zhang Q, Wang RK, et al. Optical Coherence Tomography Angiography of Asymptomatic Neovascularization in Intermediate Age-Related Macular Degeneration. *Ophthalmology*. Jun 2016;123(6):1309-19.
10. Carnevali A, Cicinelli MV, Capuano V, et al. Optical Coherence Tomography Angiography: A Useful Tool for Diagnosis of Treatment-Naïve Quiescent Choroidal Neovascularization. *Am J Ophthalmol*. 2016;169:189-198.
11. Bailey ST, Thaware O, Wang J, et al. Detection of Nonexudative Choroidal Neovascularization and Progression to Exudative Choroidal Neovascularization Using OCT Angiography. *Ophthalmol Retina*. 2019;3(8):629-636.
12. Yanagi Y, Mohla A, Lee WK, et al. Prevalence and Risk Factors for Nonexudative Neovascularization in Fellow Eyes of Patients With Unilateral Age-Related Macular Degeneration and Polypoidal Choroidal Vasculopathy. *Invest Ophthalmol Vis Sci*. 2017;58(9):3488-3495.
13. Choi W, Moulton EM, Waheed NK, et al. Ultrahigh-Speed, Swept-Source Optical Coherence Tomography Angiography in Nonexudative Age-Related Macular Degeneration with Geographic Atrophy. *Ophthalmology*. 2015;122(12):2532-44.
14. de Oliveira Dias JR, Zhang Q, Garcia JMB, et al. Natural History of Subclinical Neovascularization in Nonexudative Age-Related Macular Degeneration Using Swept-Source OCT Angiography. *Ophthalmology*. 2018;125(2):255-266.
15. Laiginhas R, Yang J, Rosenfeld PJ, Falcão M. Nonexudative Macular Neovascularization - A Systematic Review of Prevalence, Natural History, and Recent Insights from OCT Angiography. *Ophthalmol Retina*. 2020;4(7):651-661.
16. Yanagi Y, Mohla A, Lee SY, et al. Incidence of Fellow Eye Involvement in Patients With Unilateral Exudative Age-Related Macular Degeneration. *JAMA Ophthalmol*. 2018;136(8):905-911.
17. Capuano V, Miere A, Querques L, et al. Treatment-Naïve Quiescent Choroidal Neovascularization in Geographic Atrophy Secondary to Nonexudative Age-Related Macular Degeneration. *Am J Ophthalmol*. 2017;182:45-55.
18. Heiferman MJ, Fawzi AA. Progression of subclinical choroidal neovascularization in age-related macular degeneration. *PLoS One*. 2019;14(6):e0217805.
19. Treister AD, Nesper PL, Fayed AE, Gill MK, Mirza RG, Fawzi AA. Prevalence of Subclinical CNV and Choriocapillaris Nonperfusion in Fellow Eyes of Unilateral Exudative AMD on OCT Angiography. *Transl Vis Sci Technol*. 2018;7(5):19.
20. Novais EA, Adhi M, Moulton EM, et al. Choroidal Neovascularization Analyzed on Ultrahigh-Speed Swept-Source Optical Coherence Tomography Angiography Compared to Spectral-Domain Optical Coherence Tomography Angiography. *Am J Ophthalmol*. 2016;164:80-8.

21. Miller AR, Roisman L, Zhang Q, et al. Comparison Between Spectral-Domain and Swept-Source Optical Coherence Tomography Angiographic Imaging of Choroidal Neovascularization. *Invest Ophthalmol Vis Sci.* 2017;58(3):1499-1505.
22. Heier JS, Brown DM, Shah SP, et al. Intravitreal aflibercept injection vs sham as prophylaxis against conversion to exudative age-related macular degeneration in high-risk eyes: a randomized clinical trial. *JAMA Ophthalmol.* 2021;139(5):542-547.
23. Yang J, Zhang Q, Motulsky EH, et al. Two-Year Risk of Exudation in Eyes with Nonexudative Age-Related Macular Degeneration and Subclinical Neovascularization Detected with Swept Source Optical Coherence Tomography Angiography. *Am J Ophthalmol.* 2019;208:1-11.
24. Gemenetzi M, Lotery AJ, Patel PJ. Risk of geographic atrophy in age-related macular degeneration patients treated with intravitreal anti-VEGF agents. *Eye (Lond).* 2017;31(1):1-9.
25. Nassisi M, Baghdasaryan E, Borrelli E, Ip M, Sadda SR. Choriocapillaris flow impairment surrounding geographic atrophy correlates with disease progression. *PLoS one.* 2019;14(2):e0212563-e0212563.
26. Cabral T, Mello LGM, Lima LH, et al. Retinal and choroidal angiogenesis: a review of new targets. *Int J Retina Vitreous.* 2017;3:31.

# FIBROTIC NEOVASCULARIZATION

João Romano<sup>1</sup>, Nuno Oliveira<sup>1</sup>

<sup>1</sup> - Centro Hospitalar de Leiria, EPE, Leiria, Portugal

## INTRODUCTION

Macular fibrosis is the end stage in the natural history of exudative age-related macular degeneration (AMD), the late result of aberrant angiogenesis involving the macula<sup>1,2</sup>. A neovascular membrane originating from the choroid or retina develops and, if left untreated, progresses to a fibrovascular structure that eventually ends in a fibrotic scar. This phenomenon leads to photoreceptors and retinal pigment epithelium (RPE) destruction, resulting in permanent alteration in the macular morphology and irreversible vision loss<sup>3-5</sup>. Retinal glial cells have been pointed as the origin of macular fibrosis, but other cell types, including vascular endothelial cells, RPE, macrophages, glial cells and fibroblast-like cells may contribute to macular fibrosis<sup>6,7</sup>.

Although anti-vascular endothelial growth factor (VEGF) treatment generally stabilizes or improves visual acuity, scar formation is not avoided in a significant proportion of cases. According to the Comparison of AMD Treatment Trials<sup>5,8</sup>, some baseline characteristics could predict the development of fibrosis in treatment-naïve eyes with exudative AMD. The choroidal neovascularization (CNV) subtype, as determined by fluorescein angiography (FA) at baseline was an important risk factor. Fibrotic scars were least likely to develop in eyes with occult CNV or retinal angiomatous proliferation (RAP), but the risk increased significantly in the presence of predominantly classic CNV. Similarly, Bloch and associates<sup>9</sup> and a post hoc analysis of the Harbor trial<sup>10</sup> showed an increased risk of scarring in case of Type 2 CNV. It was hypothesized that intravitreal anti-VEGF treatment decreases scar formation in purely occult lesions by confining the CNV to the sub-RPE space, thereby stopping progression to classic CNV<sup>5</sup>.

## OCT ANGIOGRAPHY

Multimodal imaging evaluation allows a broader characterization of macular fibrosis. On color photographs, fibrosis is demonstrated by a well-demarcated, elevated mound of whitish or yellowish material within or under the retina (Figure 1). It is possible to identify an early hypofluorescent lesion in FA, with progressive staining and a late-phase aspect of a hyperfluorescent plaque without leakage, in case

of inactivity of the CNV, while on spectral-domain optical coherence tomography, fibrosis appears as a compact, homogenous subretinal hyperreflective lesion, with variable degrees of loss of the RPE and outer retina<sup>11,12</sup>. In addition, optical coherence tomography angiography (OCTA) has the ability to detect a perfused vascular network within the fibrotic scar, as well as capillary architectural changes<sup>11-16</sup>. Taking into account the involvement of the central retina and low vision associated, these patients have difficulty in maintaining fixation, increasing motion and projection artifacts, making it difficult to perform the exam and interpret the collected images.

Considering the relatively recent OCTA technology, associated with the specificity of this late AMD complication, the literature on this topic is scarce. Miere and colleagues<sup>11</sup> compared active and inactive fibrotic neovascular lesions in patients with exudative AMD and identified a neovascular network (Figure 1) within the fibrotic scar in 93.8% of the studied eyes. Three major neovascular network patterns were also described: a pruned vascular tree, a tangled network, and a vascular loop. These patterns appear either independently or combined and maybe be grouped in two different phenotypes: dead tree phenotype, including lesions with a main pruned vascular tree pattern and the blossoming tree phenotype, when tangled network and vascular loop patterns prevail. The pruned vascular tree pattern was the most frequent pattern identified and was distinguished by the presence of a central feeder vessel, which was a larger caliber vessel from where the other vascular trunks emerged. It was characterized by an irregular and filamentous flow and thin capillaries were not visible. The remaining patterns presented a characteristic high flow. The tangled pattern presenting an interlacing vascular network, while the vascular loop appeared as a convoluted network. There was no statistically significant association between the vascular pattern on OCTA images and disease activity, except for the tangled network, which appeared to be associated with inactive fibrotic CNV.

Thus, while the presence of major vascular trunks with irregular flow was the main feature of the dead tree phenotype, the blossoming tree phenotype was more tortuous, with abundant anastomoses and higher flow.



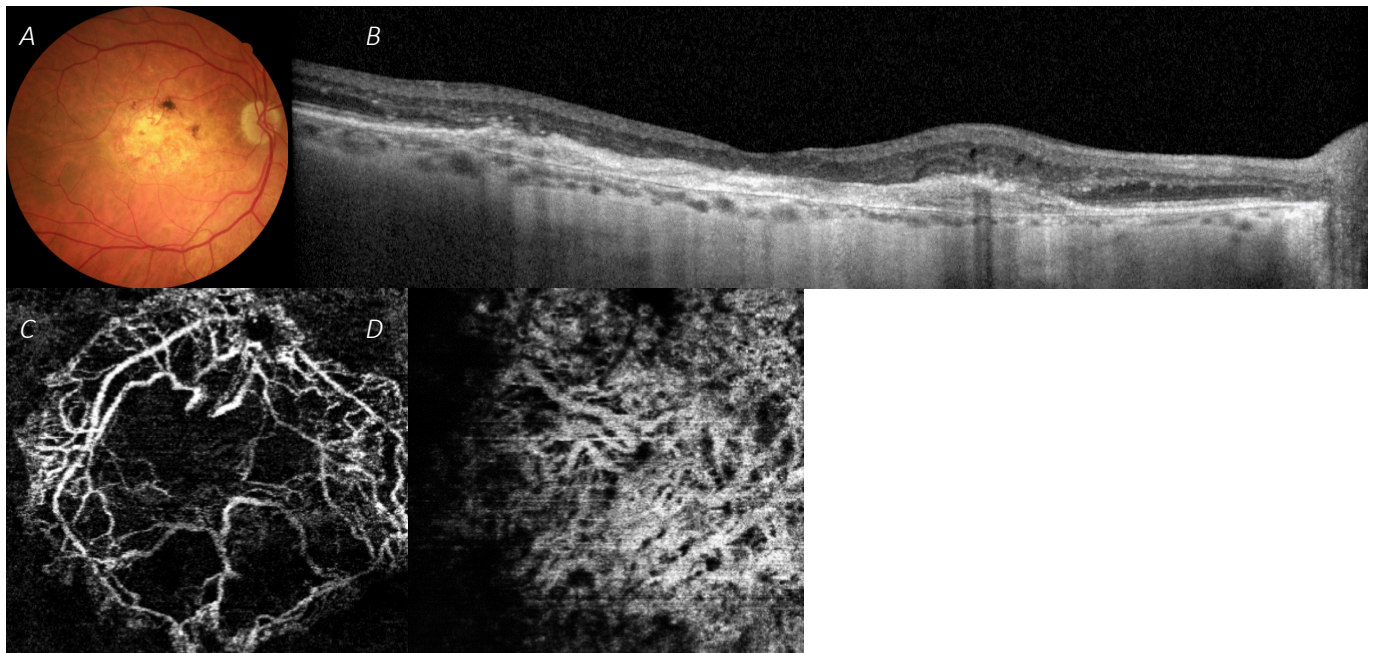


**Figure 1.** Imaging of a previously treated Type 3 neovascular choroidal membrane that evolved into a fibrotic membrane. A. Color fundus photography demonstrates a yellowish central macular lesion. It is also possible to identify retinal vessels connecting to the macular scar. B. Optical coherence tomography (structural OCT) shows a hyperreflective subretinal lesion, with extensive atrophy of the outer retinal layers and the RPE. C. Optical coherence tomography angiography (OCTA) of a disorganized neovascular network composed of slightly tortuous large caliber vessels associated with tangled network areas in its most peripheral area. D. OCTA image of choroidal vessels underneath the neovascular network.

Spaide<sup>17</sup> theorized that the higher flow observed in the remaining patent vessels could be secondary to an increased vascular resistance. This increased flow could provide a stimulus for arteriogenesis, with consequent maturation of neovascular complex and enlargement of the vascular caliber.

Furthermore, two types of dark lesion were also identified<sup>11</sup>: flow void and dark halos. The first had a diffuse lack of signal in the segmentation corresponding to the fibrotic scar, while the second was present in the choriocapillaris segmentation, surrounding the vascular network and possibly corresponding to a non-perfusion zone. The two types of dark areas, were not statistically correlated with disease activity.

Otherwise, Balaskas et al identified a neovascular complex in 67% of the fibrotic lesions<sup>13</sup>. In most cases, a specific pattern was not characterized, but some consistent features were identified, namely the presence of larger caliber vessels in a tangled, disorganized pattern. In all cases, there was an abrupt disruption of the neovascular complex edges and peripheral arcades where not identified. Flow was detected in some portions of the subretinal fibrotic tissue being absent elsewhere.

Besides morphological features that characterize fibrotic neovascular membranes, recent studies tried to identify quantitative OCTA biomarkers for choroidal neovascular activity in AMD. Parameters including blood flow area,

perfusion density (PD), fractal dimension (FD), and lacunarity (LAC) were used to differentiate quiescent, active and inactive phases of the disease<sup>18-20</sup>. However, they showed conflicting results<sup>18,19</sup>. PD is defined as the total area of perfused vasculature per unit area<sup>20</sup>. FD is a statistical descriptor of space-filling patterns. It represents the degree of pattern complexity of a vascular network, where higher values indicate increased pattern complexity. Otherwise, LAC is calculated through a mathematical formula and measures the non-uniformity of a vascular lesion. Higher values correspond to superior heterogeneity of the lesion, while lower values reflect a homogenous vascular structure<sup>20,21</sup>.

Coscas et al compared active exudative AMD with inactive previously treated fibrotic lesions and reported that the latter presented lower mean vessel density, but higher blood flow area, FD and LAC<sup>19</sup>. In fact, the model including area and FD had the best discriminative ability between both groups. On the other hand, Al-Sheikh et al previously studied the FD of neovascular networks and reported a higher mean FD in active exudative AMD when compared with inactive previously treated lesions<sup>18</sup>. The lesion area and vessel density were not statistically significantly different between both groups.

Serra and colleagues recently compared quantitative OCTA parameters between quiescent and previously treated inactive Type 1 neovascularization in AMD<sup>20</sup>.

Inactive CNVs presented statistically significant higher LAC and lower FD. LAC showed the best discrimination ability, followed by FD, suggesting that this parameters may be useful to distinguish quiescent from inactive Type 1 CNVs.

## REFERENCES

1. Stevens TS, Bressler NM, Maguire MG, Bressler SB, Fine SL, Alexander J, et al. Occult choroidal neovascularization in age-related macular degeneration. A natural history study. *Arch Ophthalmol.* 1997;115(3):345-50.
2. Viola F, Massacesi A, Orzalesi N, Ratiglia R, Staurengi G. Retinal angiomatous proliferation: natural history and progression of visual loss. *Retina.* 2009;29(6):732-9.
3. Pauleikhoff D. neovascular age-related macular degeneration: Natural History and Treatment Outcomes. *Retina.* 2005;25(8):1065-84.
4. Wong TY, Chakravarthy U, Klein R, Mitchell P, Zlateva G, Buggage R, et al. The natural history and prognosis of neovascular age-related macular degeneration: a systematic review of the literature and meta-analysis. *Ophthalmology.* 2008;115(1):116-26.
5. Daniel E, Toth CA, Grunwald JE, Jaffe GJ, Martin DF, Fine SL, et al. Risk of scar in the comparison of age-related macular degeneration treatments trials. *Ophthalmology.* 2014;121(3):656-66.
6. Little K, Ma JH, Yang N, Chen M, Xu H. Myofibroblasts in macular fibrosis secondary to neovascular age-related macular degeneration - the potential sources and molecular cues for their recruitment and activation. *EBioMedicine.* 2018;38:283-91.
7. Grossniklaus HE, Green WR, Group ftSSTR. Histopathologic and Ultrastructural Findings of Surgically Excised Choroidal Neovascularization. *Archives of Ophthalmology.* 1998;116(6):745-9.
8. Daniel E, Pan W, Ying GS, Kim BJ, Grunwald JE, Ferris FL, 3rd, et al. Development and Course of Scars in the Comparison of Age-Related Macular Degeneration Treatments Trials. *Ophthalmology.* 2018;125(7):1037-46.
9. Bloch SB, Lund-Andersen H, Sander B, Larsen M. Subfoveal fibrosis in eyes with neovascular age-related macular degeneration treated with intravitreal ranibizumab. *Am J Ophthalmol.* 2013;156(1):116-24.e1.
10. Adrean SD, Morgenthien E, Ghanekar A, Ali FS. Subretinal Fibrosis in HARBOR Varies by Choroidal Neovascularization Subtype. *Ophthalmol Retina.* 2020;4(7):752-4.
11. Miere A, Semoun O, Cohen SY, El Ameen A, Srouf M, Jung C, et al. Optical coherence tomography angiography features of subretinal fibrosis in age-related macular degeneration. *Retina.* 2015;35(11):2275-84.
12. Souied EH, Miere A, Cohen SY, Semoun O, Querques G. Optical Coherence Tomography Angiography of Fibrosis in Age-Related Macular Degeneration. *Dev Ophthalmol.* 2016;56:86-90.
13. Balaskas K, Ali ZC, Saddik T, Gemenetzi M, Patel P, Aslam TM. Swept-source optical coherence tomography angiography features of sub-retinal fibrosis in neovascular age-related macular degeneration. *Clin Exp Ophthalmol.* 2019;47(2):233-9.
14. Schneider EW, Fowler SC. Optical coherence tomography angiography in the management of age-related macular degeneration. *Curr Opin Ophthalmol.* 2018;29(3):217-25.
15. Iafe NA, Phasukkijwatana N, Sarraf D. Optical Coherence Tomography Angiography of Type 1 Neovascularization in Age-Related Macular Degeneration. *Dev Ophthalmol.* 2016;56:45-51.
16. Souied EH, Addou-Regnard M, Ohayon A, Semoun O, Querques G, Blanco-Garavito R, et al. Spectral-Domain Optical Coherence Tomography Analysis of Fibrotic Lesions in Neovascular Age-Related Macular Degeneration. *Am J Ophthalmol.* 2020;214:151-71.
17. Spaide RF. Optical Coherence Tomography Angiography Signs of Vascular Abnormalization With Antiangiogenic Therapy for Choroidal Neovascularization. *Am J Ophthalmol.* 2015;160(1):6-16.
18. Al-Sheikh M, Iafe NA, Phasukkijwatana N, Sadda SR, Sarraf D. Biomarkers of neovascular activity in age-related macular degeneration using optical coherence tomography angiography. *Retina.* 2018;38(2):220-30.
19. Coscas F, Cabral D, Pereira T, Geraldes C, Narotamo H, Miere A, et al. Quantitative optical coherence tomography angiography biomarkers for neovascular age-related macular degeneration in remission. *PLoS One.* 2018;13(10):e0205513.
20. Serra R, Coscas F, Pinna A, Cabral D, Coscas G, Souied EH. Quantitative optical coherence tomography angiography features of inactive macular neovascularization in age-related macular degeneration. *Retina.* 2021;41(1):93-102.
21. Smith TG, Jr., Lange GD, Marks WB. Fractal methods and results in cellular morphology--dimensions, lacunarity and multifractals. *J Neurosci Methods.* 1996;69(2):123-36.



# ANTI-VEGF TREATMENT AND FOLLOW UP

Manuel Falcão<sup>1,2</sup>, Carolina Madeira<sup>1,3</sup>, Rita Laiginhas<sup>3,4,5</sup>, Mengxi Shen<sup>4</sup>, Philip J. Rosenfeld<sup>4</sup>

1 - Department of Ophthalmology, Centro Hospitalar Universitário São João

2 - Department of Surgery and Physiology of the Faculty of Medicine of the University of Porto

3 - Faculty of Medicine of the University of Porto

4 - Department of Ophthalmology, Bascom Palmer Eye Institute, University of Miami Miller School of Medicine, Miami, Florida

5 - Centro Hospitalar Entre Douro e Vouga, Santa Maria da Feira

## 1. THE IMPACT OF OCTA IN THE TREATMENT AND FOLLOW-UP OF EXUDATIVE MACULAR NEOVASCULARIZATION?

At the turn of the millennium optical coherence tomography (OCT) began its use in clinical ophthalmology. It rapidly became the major imaging modality for diagnosing and managing age-related macular degeneration (AMD) as it allows fast, risk-free, three-dimensional imaging of the retina.

Prior to OCT, the diagnosis of exudative AMD relied on clinical observation and the presence of leakage on fluorescein angiography (FA). OCT images can be viewed as cross-sectional B-scans or as *en face* maps and are easily repeated at every visit allowing characterization and quantification of retinal edema and response to treatments. Simultaneously, as OCT technology evolved, intravitreal injections with anti-vascular endothelial growth factors (anti-VEGF), which led to great improvements in the visual acuity results of exudative retinal diseases, were being introduced. Both events led to a paradigm shift in current clinical practices.

Treating patients with exudative neovascular AMD depends on the use of intravitreal anti-VEGF agents. Even though the initial clinical trials with anti-VEGF agents relied on monthly injections, most treatment regimens in clinical practice are based on symptoms and evidence of fluid on structural OCT B-scans<sup>1</sup> with retina specialists treating patients using either a “treat and extend” (TAE) or a “*pro re nata*” (PRN) treatment strategy. The main objective of both treatment modalities is to keep the macula “dry”, i.e. no fluid on OCT B-scans. This has led to a decline in the use of FA in clinical practice.

A new imaging modality known as OCT-Angiography (OCTA) has been growing in popularity. OCTA has revolutionized the diagnosis of neovascular AMD as this imaging modality can detect macular neovascular complexes without the need of intravenous dyes even when exudation is absent. The OCTA angiogram by

itself does not show the presence/absence of exudation; the presence of exudation is based on structural OCT B-scans. The use of both imaging modalities distinguishes exudative from nonexudative macular neovascularization (MNV).

These images can be obtained in every-day clinical practice and allow a better understanding of both the pathophysiology of the MNV as well as its transformation to exudative disease. Non-exudative MNV was initially described in the 1970's with indocyanine green angiography. OCTA allows the screening of patients with intermediate AMD for the presence of nonexudative complexes and monitor their evolution. To date, the presence of nonexudative MNV is the only factor that has been consistently shown to predict exudation.<sup>2</sup> Other OCTA parameters including MNV size, vessel area density and vessel skeleton density changes over time have failed to reliably predict the onset of exudation from these nonexudative lesions<sup>3</sup> and, as a result, current recommendations for these lesions include close clinical follow-up to detect exudation as soon as it develops.

Once exudation occurs, treatment with intravitreal anti-VEGF therapy and follow-up with OCT B-scans is mandatory. Even though this strategy is able to treat exudation in most cases there are still several unmet needs in which, potentially, OCTA may help. These needs include predicting when non-exudative disease may start exudating, predicting treatment intervals, determining which patients may stop treatment and further understanding the complex relationship between the progression of outer retinal atrophy, atrophy of the retinal pigment epithelium, the MNV and the use anti-VEGF therapy.

## 2. TECHNICAL CONSIDERATION WHEN FOLLOWING PATIENTS WITH NEOVASCULAR AMD DURING TREATMENT

OCTA allows for a detailed characterization and detection of MNV as the vessel structure can be observed and it is not obscured by dye leakage or dye staining of drusen.

OCTA can detect and quantify the presence of very small branches that are obscured by the leakage from dye angiographies. The response to therapy of these vessels over time can be observed and quantified. As visualization of the MNV is dependent on the device, direct comparisons of OCT angiograms from different devices during follow-up evaluations may be difficult to interpret accurately.<sup>4, 5</sup> Currently two types of OCTA instruments are used in the clinical practice: spectral domain (SD-OCTA) and swept source (SS-OCTA). SS-OCTA is better at providing high quality images of MNV<sup>6, 7</sup> and may be advantageous in the presence of macular hemorrhage or vitreous opacities due to its longer wavelength and increased light penetration through blood, some media opacities and into the choroid.<sup>8</sup>

Widefield SS-OCTA is another important advance. Its use is relevant in following extensive or multifocal neovascular lesions, and in eyes with peripapillary MNV, that may go unnoticed in a routine 6x6mm central macular scan.

It is also important to highlight that the “angio flow OCTA” should be viewed together with the structural OCT as it offers advantages. This is very important in the presence of hyper-reflective material that may produce an artefactual flow image but also appears bright on the structural scan as well. Usually, when the signal is bright on both the *en face* flow and structure image, the flow signal should be interpreted with caution.

Several parameters have been evaluated in research such as the size, branching and volume of the MNV, the choriocapillaris flow, and the choroidal structure and vascularity. These parameters may guide treatment decisions in the future, but there is currently no robust evidence that they may be useful in clinical practice.

### 3. HISTORY OF MACULAR NEOVASCULARIZATION WITH ANTI-VEGF TREATMENT

Knowledge regarding the response of MNV to anti-VEGF is still evolving. Recent studies have shown that the effects of treatment on abnormal vasculature can vary and may be different depending on the type of MNV. Responses to therapy vary between cases in which the MNV may become undetectable on OCTA to cases in which the MNV grew despite treatment. OCTA only became available when clinical trials with monthly anti-VEGF dosing were over. However, evaluation of the MNV with FA in the MARINA trial showed that the mean area of MNV did not decrease despite monthly intravitreal ranibizumab.<sup>9</sup> Therefore, it is not expected that OCTA will show, in most cases, a complete regression of the neovascular complexes. Since then, treatment has evolved to increasing injection intervals over time. As a result, there are no studies using OCTA in which a monthly suppression of intra-ocular VEGF has occurred. Both TAE and PRN treatment regimens allow for a window of opportunity for VEGF levels to

increase and this may have an effect on the behaviour of MNV over time. For instance, it is theoretically possible for MNV to grow in size without further exudation and thus without further need for treatment (Figure 1). The implications of this are unknown.

In type 1 and 2 MNV, the majority of studies have shown a significant decrease of the size of the MNV complex, represented as blood flow area, after the first treatments followed by a regrowth of the lesion.<sup>10-13</sup> Several studies have shown that the initial inhibition of intravitreal VEGF leads to the pruning of the smaller branches of the neovascular “tree”. Larger branches usually remain stable despite anti-VEGF treatment. However, as intravitreal levels of anti-VEGF diminish, re-proliferation of the small pruned vessels may occur.<sup>14</sup> Furthermore, the re-proliferation of vessels appear to be similar to the vessels that disappeared after treatment.<sup>15</sup> The small branches are probably immature vessels that respond to anti-VEGF therapy while larger vessels are more mature, surrounded by pericytes and resistant to anti-VEGF.<sup>14</sup> Also it is possible that the vessels are never really pruned back, but the blood flow through these vessel is diminished below the level of detection when using OCTA and their re-appearance reflects a return of flow to these small vessels. Most likely, it is these smaller immature vessels that are responsible for the exudation.

Comparing type 1 and 2 MNV, the latter seem to significantly regress more after the initial anti-VEGF treatment.<sup>11, 12, 16</sup> The reasons for the different responses remain unknown being possible that the anti-VEGF concentrations reached under the retinal pigment epithelium are less than in the sub-retinal space or the type 1 MNV represent more mature vessels.<sup>11</sup>

Type 3 MNV behaviour after treatment remains controversial. Lesion regression in OCTA has been reported in 29–49% of cases.<sup>17, 18</sup> One comprehensive study of type 3 MNV suggested that after treatment the neovascular complex does not completely regress and may recur.<sup>19</sup>

Some long-term follow-up studies of patients receiving anti-VEGF therapy have shown low rates of complete regression of the MNV on OCTA.<sup>10, 20</sup> One study compared patients under a treat-extend-stop protocol (patients who were able to stop treatment) versus a TAE protocol that needed persistent therapy. Two thirds of patients that were able to stop treatment did not have a MNV detectable on OCTA whilst in the other group the MNV was still observed in all cases.<sup>20</sup>

In addition to lesion size or complete lesion regression, other quantitative data that has been analysed include a reduction of the fractal dimension and branching terminal vessels after treatment. However, vessel density and lacunarity seem to remain unchanged.<sup>10-13, 20</sup>

Several OCTA biomarkers associated with an anti-VEGF treatment response have been identified. A closed-circuit pattern of MNV, the presence of a peripheral loop, capillary fringe, lower baseline fractal dimension,

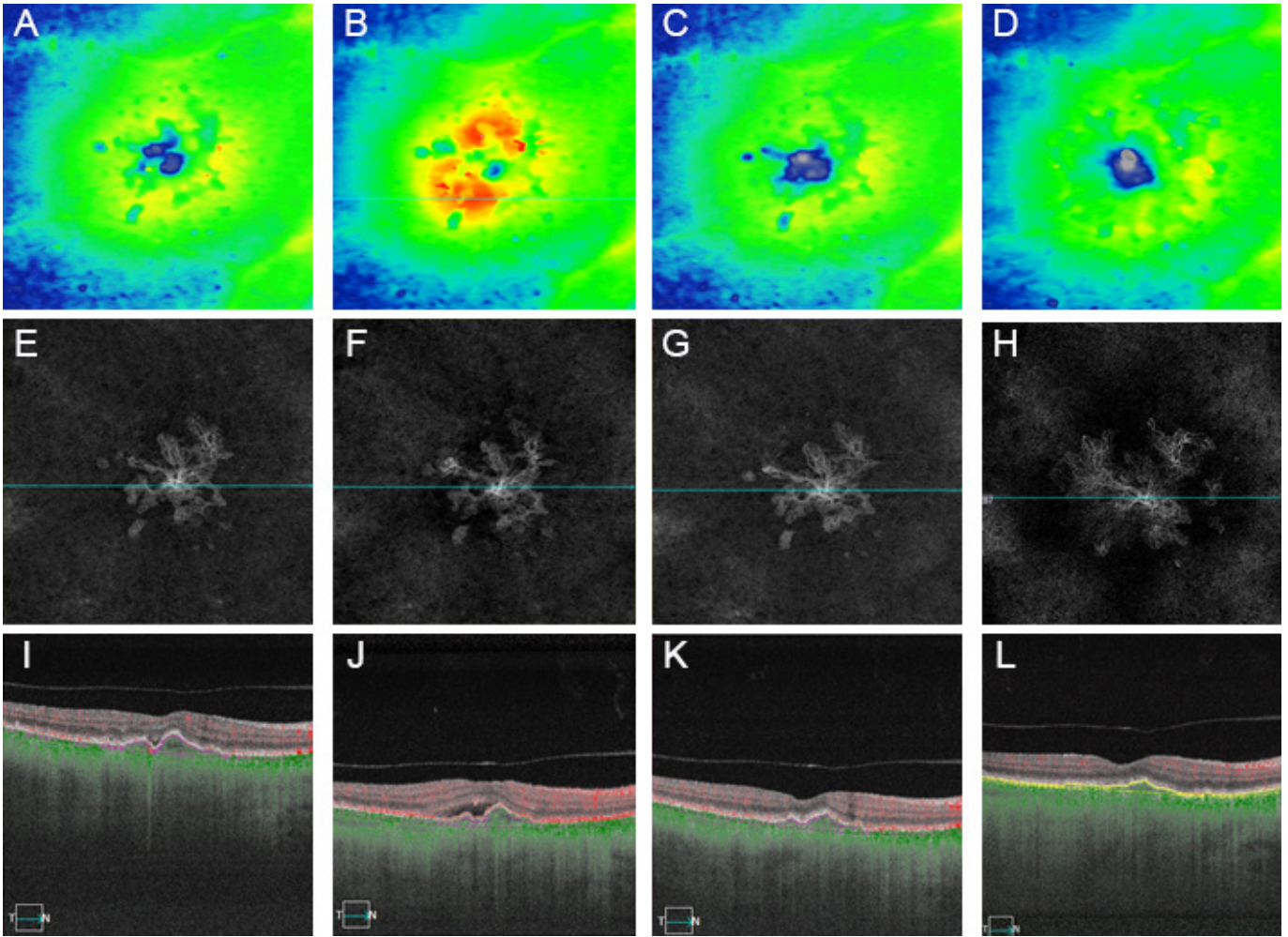


**Figure 1.** Swept source optical coherence tomography angiography (SS-OCTA, PLEX® Elite 9000, Carl Zeiss Meditec, Dublin, CA) imaging from a type 1 macular neovascular lesion due to age-related macular degeneration (AMD) treated with aflibercept following a treat and extend approach – Courtesy of Dr. Philip J. Rosenfeld. (A-D) Retinal thickness map. (E-H) En face angiograms derived from the RPE-RPEfit slab. (I-L) B-scans corresponding to the blue line in panels E-H. At the first visit (A, E, I), a non-exudative type 1 macular neovascular lesion was detected (the neovascular lesion can be appreciated in panel E, corresponding to a double layer sign on panel I). After 11 months of follow-up (B, F, J), exudative conversion was noted (increased retinal thickness in panel B, and subretinal fluid in panel J). Treatment was started, and, after five monthly aflibercept injections (C, G, K), the fluid regressed (decreased retinal thickness in panel C, no fluid on panel K) and the macular neovascular lesion remained stable (panel G). In the next three years (D, H, L), only one additional aflibercept injection was needed and the vision remained stable (20/25). Despite absent exudation (D, L), the growth of the lesion can be observed (H).

and a lower surface area have been associated with sustained exudation and a greater need for anti-VEGF injections.<sup>10, 20</sup>

#### 4. CURRENT STATUS

Currently, no OCTA parameter has shown to have any advantage compared with OCT B-scans for the management of neovascular exudative AMD in routine clinical practice. However, it is anticipated that the greatest impact of OCTA imaging will be the development of biomarkers that will help distinguish between clinically active and inactive lesions so as to guide the use of antiangiogenic treatment in routine clinical practice. In addition to identifying nonexudative MNV, OCTA may

offer other clinical and research insights that will improve outcomes and address unmet needs in our patients with AMD in the future.

#### REFERENCES

1. Fleckenstein M, Keenan TDL, Guymer RH, Chakravarthy U, Schmitz-Valckenberg S, Klaver CC, et al. Age-related macular degeneration. *Nat Rev Dis Primers*. 2021;7(1):31.
2. Laiginhas R, Yang J, Rosenfeld PJ, Falcao M. Nonexudative Macular Neovascularization - A Systematic Review of Prevalence, Natural History, and Recent Insights from OCT Angiography. *Ophthalmol Retina*. 2020;4(7):651-61.
3. Shen M, Zhang Q, Yang J, Zhou H, Chu Z, Zhou X, et al. Swept-Source OCT Angiographic Characteristics of Treatment-Naive

- Nonexudative Macular Neovascularization in AMD Prior to Exudation. *Invest Ophthalmol Vis Sci.* 2021;62(6):14.
4. Mastropasqua R, Evangelista F, Amodè F, D'Aloisio R, Pinto F, Doronzo E, et al. Optical Coherence Tomography Angiography in Macular Neovascularization: A Comparison Between Different OCTA Devices. *Transl Vis Sci Technol.* 2020;9(11):6.
  5. Corvi F, Cozzi M, Barbolini E, Nizza D, Belotti M, Staurengi G, et al. Comparison between Several Optical Coherence Tomography Angiography Devices and Indocyanine Green Angiography of Choroidal Neovascularization. *Retina.* 2020;40(5):873-80.
  6. Novais EA, Adhi M, Moulton EM, Louzada RN, Cole ED, Husvogt L, et al. Choroidal Neovascularization Analyzed on Ultrahigh-Speed Swept-Source Optical Coherence Tomography Angiography Compared to Spectral-Domain Optical Coherence Tomography Angiography. *Am J Ophthalmol.* 2016;164:80-8.
  7. Miller AR, Roisman L, Zhang Q, Zheng F, Rafael de Oliveira Dias J, Yehoshua Z, et al. Comparison Between Spectral-Domain and Swept-Source Optical Coherence Tomography Angiographic Imaging of Choroidal Neovascularization. *Invest Ophthalmol Vis Sci.* 2017;58(3):1499-505.
  8. Zhang Q, Zheng F, Motulsky EH, Gregori G, Chu Z, Chen CL, et al. A Novel Strategy for Quantifying Choriocapillaris Flow Voids Using Swept-Source OCT Angiography. *Invest Ophthalmol Vis Sci.* 2018;59(1):203-11.
  9. Kaiser PK, Blodi BA, Shapiro H, Acharya NR, Group MS. Angiographic and optical coherence tomographic results of the MARINA study of ranibizumab in neovascular age-related macular degeneration. *Ophthalmology.* 2007;114(10):1868-75.
  10. Cabral D, Coscas F, Pereira T, Francais C, Geraldes C, Laiginhas R, et al. Quantitative Optical Coherence Tomography Angiography Biomarkers in a Treat-and-Extend Dosing Regimen in Neovascular Age-Related Macular Degeneration. *Transl Vis Sci Technol.*
  11. Kim JM, Cho HJ, Kim Y, Jung SH, Lee DW, Kim JW. Responses of Types 1 and 2 Neovascularization in Age-Related Macular Degeneration to Anti-Vascular Endothelial Growth Factor Treatment: Optical Coherence Tomography Angiography Analysis. *Semin Ophthalmol.* 2019;34(3):168-76
  12. Levine ES, Custo Greig E, Mendonca LSM, Gulati S, Despotovic IN, Alibhai AY, et al. The long-term effects of anti-vascular endothelial growth factor therapy on the optical coherence tomography angiographic appearance of neovascularization in age-related macular degeneration. *Int J Retina Vitreous.* 2020;6:39
  13. Tew TB, Lai TT, Hsieh YT, Ho TC, Yang CM, Yang CH. Comparison of different morphologies of choroidal neovascularization evaluated by ocular coherence tomography angiography in age-related macular degeneration. *Clin Exp Ophthalmol.* 2020;48(7):927-37
  14. Spaide RF. Optical Coherence Tomography Angiography Signs of Vascular Abnormalization With Antiangiogenic Therapy for Choroidal Neovascularization. *Am J Ophthalmol.* 2015;160(1):6-16.
  15. Huang D, Jia Y, Rispoli M, Tan O, Lumbroso B. Optical Coherence Tomography Angiography of Time Course of Choroidal Neovascularization in Response to Anti-Angiogenic Treatment. *Retina.* 2015;35(11):2260-4.
  16. McClintic SM, Gao S, Wang J, Hagag A, Lauer AK, Flaxel CJ, et al. Quantitative Evaluation of Choroidal Neovascularization under Pro Re Nata Anti-Vascular Endothelial Growth Factor Therapy with OCT Angiography. *Ophthalmol Retina.* 2018;2(9):931-41
  17. Miere A, Querques G, Semoun O, Amoroso F, Zambrowski O, Chapron T, et al. Optical Coherence Tomography Angiography Changes in Early Type 3 Neovascularization after Anti-Vascular Endothelial Growth Factor Treatment. *Retina.* 2017;37(10):1873-9.
  18. Phasukkijwatana N, Tan ACS, Chen X, Freund KB, Sarraf D. Optical coherence tomography angiography of type 3 neovascularisation in age-related macular degeneration after antiangiogenic therapy. *Br J Ophthalmol.* 2017;101(5):597-602.
  19. Spaide RF. New Proposal for the Pathophysiology of Type 3 Neovascularization as Based on Multimodal Imaging Findings. *Retina.* 2019;39(8):1451-64.
  20. Bae K, Kim HJ, Shin YK, Kang SW. Predictors of neovascular activity during neovascular age-related macular degeneration treatment based on optical coherence tomography angiography. *Sci Rep.* 2019;9(1):19240

# GEOGRAPHIC ATROPHY

Maria da Luz Cachulo<sup>1,2,3</sup>, Cláudia Farinha<sup>1,2,3</sup>, João Pedro Marques<sup>1,2,3</sup>, Mário Soares<sup>2</sup>, Isabel Pires<sup>1,2,3</sup>, Rufino Silva<sup>1,2,3,4</sup>

1- University of Coimbra, Coimbra Institute of Clinical and Biomedical Research (ICBR), Faculty of Medicine, Coimbra, Portugal

2- Ophthalmology Department, Centro Hospitalar e Universitário de Coimbra (CHUC), Portugal

3- Association for Innovation and Biomedical Research on Light and Image (AIBILI), Coimbra, Portugal

4- Coimbra Medical Space, Coimbra, Portugal

## INTRODUCTION

Geographic atrophy (GA) represents the nonexudative late stage of age-related macular degeneration (AMD), the leading cause of visual impairment and irreversible visual loss in developed countries.<sup>1</sup> Approximately 20% of AMD patients with severe visual acuity loss present with GA for which no evidence-based proven therapy has been established for treatment or prevention.<sup>2</sup>

GA is characterized by progressive loss of outer retinal layers including photoreceptors (PR) and the retinal pigment epithelium (RPE), which can also be accompanied by loss or rarefaction of the underlying choriocapillaris (CC) during disease progression.<sup>3</sup> As all three layers are functionally interdependent, the exact pathophysiology of GA is still a topic of intense research. Specifically, the initial site of disease impact, the sequence of alterations affecting the PR/RPE/CC complex, as well as the interactions between affected tissue components.<sup>4</sup> Clinically, GA has traditionally been defined on color fundus photographs (CFP) as one or multiple sharply delineated circular or oval areas of depigmentation, thinning of underlying tissue and increased visibility of large choroidal blood vessels at the posterior pole. The size requirement for GA varies across studies, ranging from 1/8 to 1/4 of a disc area (corresponding roughly to 175  $\mu\text{m}$  and 430  $\mu\text{m}$  in diameter, respectively) on CFPs.<sup>3</sup> The term “geographic areas of atrophy” was introduced for the first time by Gass in 1970 to describe atrophic retinal lesions in several contexts such as “senile macular choroidal degeneration”, “central areolar choroidal sclerosis” and “serpiginous peripapillar choroiditis”.<sup>5</sup> Nowadays, the advances in genetics and multimodal imaging have allowed more precise differential diagnosis of mimicking diseases, leading to the consensus of using the term “GA” exclusively in the context of AMD.<sup>6</sup> Ophthalmoscopy or CFP were for many years the gold standard to diagnosis and monitoring progression of GA.<sup>3</sup> However, they are limited in the identification of certain features of dry AMD, such as subretinal drusenoid deposits and morphological alterations of the RPE adjacent to GA.

The wide spectrum of phenotypic variations of GA lead to the development of an optical coherence tomography (OCT)-based classification, which in combination with fundus autofluorescence (FAF), is currently the gold standard for the assessment of GA and its progression. This multimodal approach offers improved detection rate and demarcation of the lesion boundaries due to higher contrast, compared to CFP.<sup>7</sup> Thus, based on modern spectral-domain or swept-source OCT findings, the Classification of Atrophy Meetings (CAM) program recently proposed a consensus terminology for staging retinal atrophy associated with AMD: complete RPE and outer retinal layer atrophy (cRORA), incomplete RPE and outer retinal layer atrophy (iRORA), complete outer retinal layer atrophy (cORA), and incomplete outer retinal layer atrophy (iORA).

Classical GA or cRORA is characterized by atrophy of the outer nuclear layer, external limiting membrane (ELM), ellipsoide zone (EZ), photoreceptors, retinal pigment epithelium (RPE) and choriocapillaris (CC) for which OCT criteria include: (1) a region of hyper-transmission into the choroid of at least 250  $\mu\text{m}$  in diameter, (2) a zone of attenuation or disruption of the RPE at least 250  $\mu\text{m}$  in diameter, (3) evidence of overlying photoreceptor degeneration, and iv) absence of scrolled RPE or other signs of an RPE tear (Fig. 1).<sup>8</sup> The term nascent GA refers to iRORA which is defined on OCT by the following criteria: (1) a region of signal hyper-transmission into the choroid and (2) a corresponding zone of attenuation or disruption of the RPE, with or without persistence of basal laminar deposits (BLamD), and (3) evidence of overlying photoreceptor degeneration, i.e., subsidence of the inner nuclear layer (INL) and outer plexiform (OPL), presence of a hypo-reflective wedge in the Henle fiber layer (HFL), thinning of the outer nuclear layer (ONL), disruption of the external limiting membrane (ELM), or disintegration of the ellipsoid zone (EZ), and when these criteria do not meet the definition of cRORA. Nascent GA was identified as a form of intermediate AMD with high-risk characteristics for progression to GA (cRORA) (Fig. 2).<sup>9</sup> Recently, novel imaging modalities and genetic testing



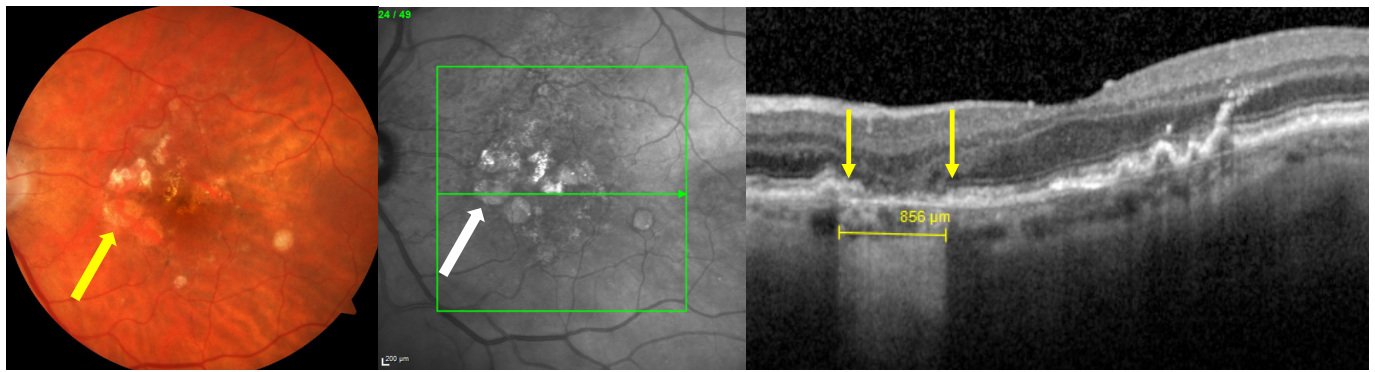


**Figure 1.** Color fundus photography (CFP), infra-red (IR) images and spectral domain optical coherence tomography (SD-OCT) scan of an eye with an area of complete retinal pigment epithelium and outer retinal layer atrophy (cRORA). The area of cRORA is identified on CFP and IR images with a yellow and white thick arrow, respectively. On SD-OCT, cRORA lesion is characterized by a) a region of hyper-transmission into de choroid greater than 250  $\mu\text{m}$  in diameter (identified with the straight yellow parenthesis); b) the attenuation/interruption of retinal pigment epithelium and outer retinal layers, particularly the ellipsoide zone and external limiting membrane, bounded by the two thin yellow arrows and c) the atrophy/thinning of outer nuclear layer.

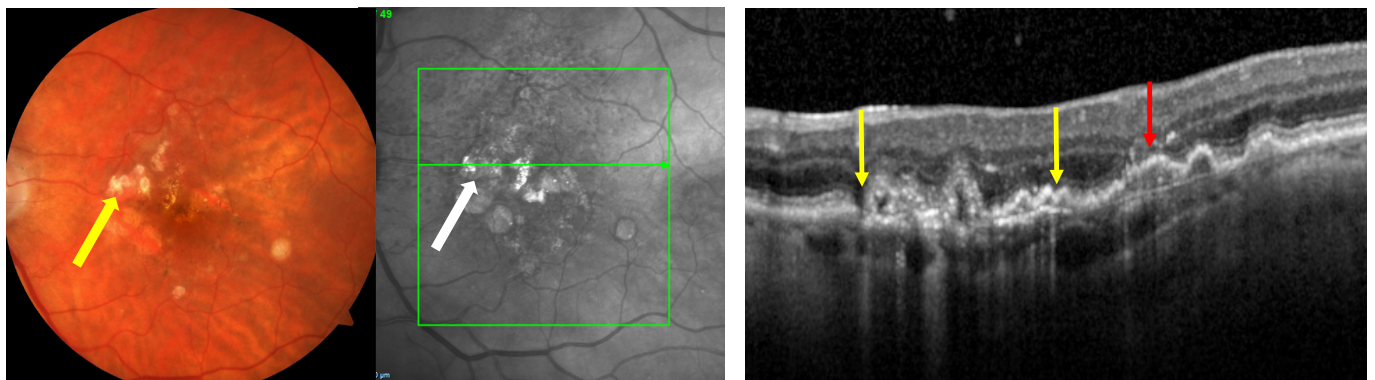


**Figure 2.** Color fundus photography (CFP), infra-red (IR) images and spectral domain optical coherence tomography (SD-OCT) scan of the same eye with a different area of incomplete retinal pigment epithelium and outer retinal layer atrophy (iRORA). The area of iRORA is identified in CFP and IR images with a yellow and white thick arrow, respectively. On SD-OCT, iRORA lesion is characterized by a) a region of non-homogeneous hyper-transmission signal into de choroid (identified with the straight yellow parenthesis) b) the interruption of retinal pigment epithelium and outer retinal layers, bounded by the two thin yellow arrows and c) the subsidence of the inner nuclear layer (INL) and outer plexiform (OPL) identified in the image with a red arrow.

have been introduced to study retinal diseases including GA associated with AMD. In this context, OCT-angiography (OCT-A) plays a prominent role.

### OCT - ANGIOGRAPHY IN GEOGRAPHIC ATROPHY

The interrelationship between CC and RPE is the basis for debate in GA pathophysiology, concerning the point of disease onset. Multiple studies have shown the involvement of choroidal vasculature in AMD pathogenesis, and the question of whether alterations of CC precede and cause atrophy, or arise as a consequence of the morphological retinal changes, remains a controversial topic.<sup>10–15</sup>

Histopathologic studies have investigated the role of CC and RPE in the development and progression of GA

with differing results regarding the onset of pathogenesis of GA. While some studies describe the primary impact appearing to be at the level of the RPE, other results indicate CC breakdown, preceding RPE degeneration and even so far as to classify GA as a vascular disease.<sup>14,16–20</sup>

Fluorescein angiography (FA) and indocyanine green angiography (ICGA) are invasive methods used for visualization of CC and choroid. However, FA and ICGA only provide two-dimensional images and therefore do not allow for the segmentation of specific retinal or choroidal layers. Optical coherence tomography is a fast-evolving technology and offers multiple imaging modalities for monitoring disease progression and associated structural changes in AMD. A recent advancement in the field of OCT for ocular posterior pole component visualization is the ability to image blood vessels non-invasively, without

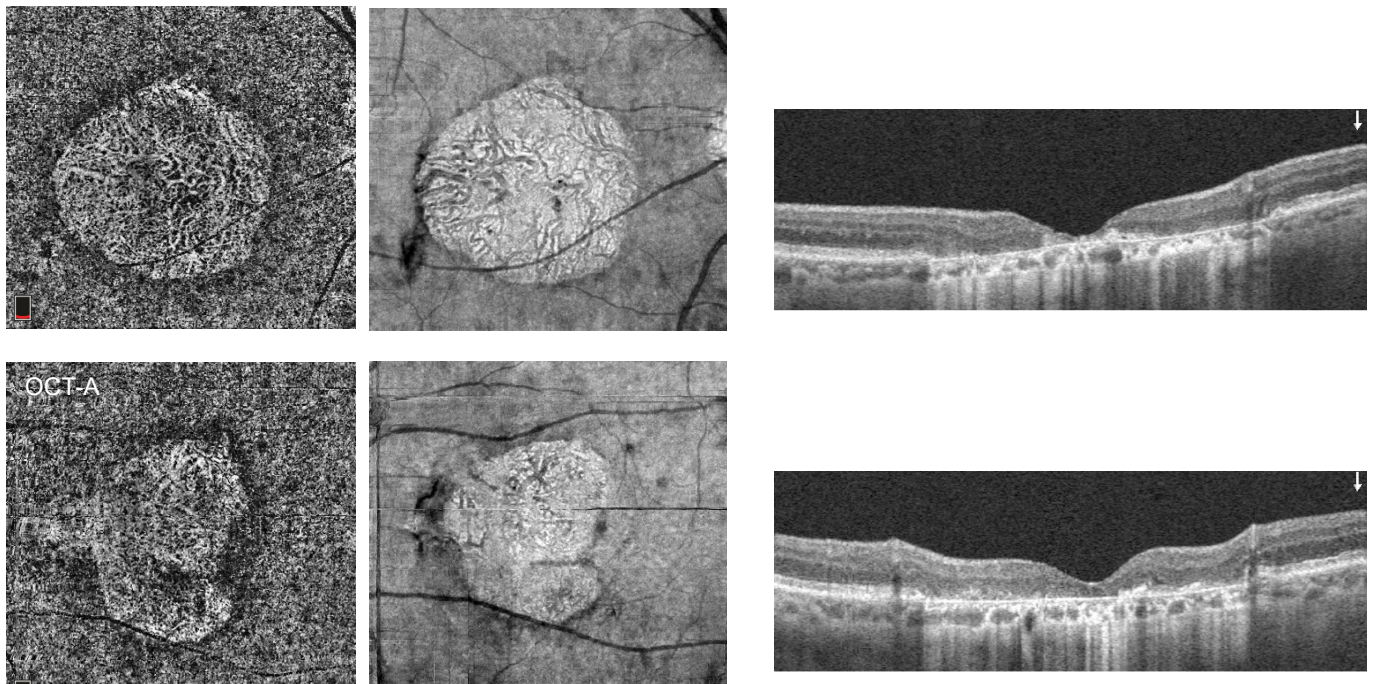


**Figure 3.** Optical coherence tomography angiography (OCT-A) choriocapillaris slab, infrared reflection (IR) images and the respective structural spectral domain optical coherence tomography (SD-OCT) of the right (on the top of the image) and left eye (on the bottom of the image) of the same patient with geographic atrophy GA. In the OCT-A image both eyes revealed loss of the dense choriocapillaris flow signal with uncovered mid- and large vessels in the atrophic area as well as a choriocapillaris rarefaction that exceeds over the area of the atrophy.

the need of dye injection. OCT Angiography allows for imaging of the choriocapillaris layer, given the three-dimensional slab-based of flow signal. Visualization of the PR/RPE/CC complex with these novel multimodal imaging techniques may allow better understanding of the pathophysiology of GA. Using OCT-A, different studies demonstrated a generalized reduction in choroidal vessel density, particularly affecting the choriocapillaris flow signal in the early stages of AMD.<sup>21–25</sup> Several authors also reported a reduction of choriocapillaris flow signal up to total loss in areas of GA with presence of larger choroidal vessels adjacent to the Bruch's membrane<sup>24,26,27</sup> and this reduction normally exceed the area of RPE atrophy detected by fundus autofluorescence imaging. It is consistently reported that patients with GA have a more expressive flow signal attenuation when compared with controls inside and outside GA areas. Additionally, the surrounding area was showed to have a significantly higher flow impairment compared to eccentric areas of the same eye. These findings indicate that choriocapillaris may be affected before the development of cRORA/GA.<sup>24,27–30</sup> More recently, OCT-A evaluation revealed that not only the reduced choriocapillaris flow signal expands outside the area of atrophy, but also the surrounding flow signal attenuation is correlated with disease progression and therefore could be considered as a prognostic factor of GA progression rate.<sup>31</sup> Several authors demonstrated that eyes with more signal attenuation around the GA margin showed a significantly higher progression of the

disease.<sup>32–34</sup> Additionally, the areas of the GA margin with more intense choriocapillaris flow signal impairment were those which demonstrate to expand faster when compared to the remaining areas of the GA margin in the same eye.<sup>30</sup> OCT Angiography could also allow to distinguish eyes with GA from mimicking diseases such as late-onset Stargardt disease, as in the latter there is significantly less flow signal deficits outside the area of atrophy and, in contrast, more pronounced choriocapillaris flow signal attenuation inside the atrophic area.<sup>31</sup> The authors of a study comparing the choroidal flow signal in late-onset Stargardt disease and GA concluded that using only OCT-A data, late-onset Stargardt disease and GA patients could be distinguished with 65,0% and 92,3% of sensitivity and specificity, respectively.<sup>24</sup>

OCT Angiography imaging is also reported to improve visualization of quiescent or subclinical macular neovascularization (MNV) that could develop in eyes with GA.<sup>35,36</sup> Currently, some studies reported that this type of MNV may play a protective role in GA progression, as it can have a potential nutritive effect on the RPE and neurosensory retina in the context of choriocapillaris attenuation consistently observed in eyes with GA.<sup>36–38</sup>

### TAKE-HOME MESSAGES

1. OCT Angiography has been improving visualization of vascular alterations associated with GA, which provides further insights into the pathophysiology of the

disease and helps to define and evaluate risk factors for development and progression, to differentiate from mimicking diseases, and to establish new therapeutic strategies.

2. OCT-A analysis revealed that quiescent MNVs might have a protective effect on GA progression, which poses questions about the beneficial effect of early or intense treatment of this type of MNV in this specific context.

## REFERENCES

1. Wong WL, Su X, Li X, Cheung CMG, Klein R, Cheng CY, et al. Global prevalence of age-related macular degeneration and disease burden projection for 2020 and 2040: A systematic review and meta-analysis. *The Lancet Global Health*. 2014;2(2).
2. Holz FG, Sadda SR, Busbee B, Chew EY, Mitchell P, Tufail A, et al. Efficacy and Safety of Lampalizumab for Geographic Atrophy Due to Age-Related Macular Degeneration. *JAMA Ophthalmology*. 2018 1;136(6).
3. Schmitz-Valckenberg S. The Journey of “Geographic Atrophy” through Past, Present, and Future. *Ophthalmologica*. 2017;237(1).
4. Hecht A, Pollreis A, Sayegh R, Told R, Baratsits M, Baumann B, et al. Relationship between morphological and vascular alterations in geographic atrophy using a multimodal imaging approach. *Acta Ophthalmologica*. 2020 17;98(6).
5. Gass JD. *Stereoscopic Atlas of Macular Diseases*. First. St Louis: CV Mosby; 170AD.
6. Saksens NTM, Fleckenstein M, Schmitz-Valckenberg S, Holz FG, den Hollander AI, Keunen JEE, et al. Macular dystrophies mimicking age-related macular degeneration. *Progress in Retinal and Eye Research*. 2014;39.
7. Domalpally A, Danis R, Agrón E, Blodi B, Clemons T, Chew E. Evaluation of Geographic Atrophy from Color Photographs and Fundus Autofluorescence Images. *Ophthalmology*. 2016;123(11).
8. Sadda SR, Guymer R, Holz FG, Schmitz-Valckenberg S, Curcio CA, Bird AC, et al. Consensus Definition for Atrophy Associated with Age-Related Macular Degeneration on OCT. *Ophthalmology*. 2018;125(4).
9. Guymer RH, Rosenfeld PJ, Curcio CA, Holz FG, Staurengli G, Freund KB, et al. Incomplete Retinal Pigment Epithelial and Outer Retinal Atrophy in Age-Related Macular Degeneration. *Ophthalmology*. 2020;127(3).
10. Maguire P, Vine AK. Geographic Atrophy of the Retinal Pigment Epithelium. *American Journal of Ophthalmology*. 1986;102(5).
11. Schatz H, McDonald HR. Atrophic Macular Degeneration. *Ophthalmology*. 1989;96(10).
12. McLeod DS, Grebe R, Bhutto I, Merges C, Baba T, Luty GA. Relationship between RPE and Choriocapillaris in Age-Related Macular Degeneration. *Investigative Ophthalmology & Visual Science*. 2009 1;50(10).
13. Bhutto I, Luty G. Understanding age-related macular degeneration (AMD): Relationships between the photoreceptor/retinal pigment epithelium/Bruch’s membrane/choriocapillaris complex. *Molecular Aspects of Medicine*. 2012;33(4).
14. Biesemeier A, Taubitz T, Julien S, Yoeruek E, Schraermeyer U. Choriocapillaris breakdown precedes retinal degeneration in age-related macular degeneration. *Neurobiology of Aging*. 2014;35(11).
15. Clark SJ, McHarg S, Tilakaratna V, Brace N, Bishop PN. Bruch’s Membrane Compartmentalizes Complement Regulation in the Eye with Implications for Therapeutic Design in Age-Related Macular Degeneration. *Frontiers in Immunology*. 2017 19;8.
16. McLeod DS. Quantifying changes in RPE and choroidal vasculature in eyes with age-related macular degeneration. *Invest Ophthalmol Vis Sci*. 2002;43(6):1986–93.
17. McLeod DS, Grebe R, Bhutto I, Merges C, Baba T, Luty GA. Relationship between RPE and Choriocapillaris in Age-Related Macular Degeneration. *Investigative Ophthalmology & Visual Science*. 2009 1;50(10).
18. Mullins RF, Khanna A, Schoo DP, Tucker BA, Sohn EH, Drack A v., et al. Is Age-Related Macular Degeneration a Microvascular Disease? In 2014.
19. Mullins RF, Johnson MN, Faidley EA, Skeic JM, Huang J. Choriocapillaris Vascular Dropout Related to Density of Drusen in Human Eyes with Early Age-Related Macular Degeneration. *Investigative Ophthalmology & Visual Science*. 2011 21;52(3).
20. Bird AC, Phillips RL, Hageman GS. Geographic Atrophy. *JAMA Ophthalmology*. 2014 1;132(3).
21. Nesper PL, Soetikno BT, Fawzi AA. Choriocapillaris Nonperfusion is Associated With Poor Visual Acuity in Eyes With Reticular Pseudodrusen. *American Journal of Ophthalmology*. 2017 ;174.
22. Cicinelli MV, Rabiolo A, Sacconi R, Carnevali A, Querques L, Bandello F, et al. Optical coherence tomography angiography in dry age-related macular degeneration. *Survey of Ophthalmology*. 2018 ;63(2).
23. Lane M, Moulton EM, Novais EA, Louzada RN, Cole ED, Lee B, et al. Visualizing the Choriocapillaris Under Drusen: Comparing 1050-nm Swept-Source Versus 840-nm Spectral-Domain Optical Coherence Tomography Angiography. *Investigative Ophthalmology & Visual Science*. 2016 17;57(9).
24. Müller PL, Pfau M, Möller PT, Nadal J, Schmid M, Lindner M, et al. Choroidal Flow Signal in Late-Onset Stargardt Disease and Age-Related Macular Degeneration: An OCT-Angiography Study. *Investigative Ophthalmology & Visual Science*. 2018 21;59(4).
25. Spaide RF. Choriocapillaris Flow Features Follow a Power Law Distribution: Implications for Characterization and Mechanisms of Disease Progression. *American Journal of Ophthalmology*. 2016;170.
26. Sacconi R, Corbelli E, Carnevali A, Querques L, Bandello F, Querques G. Optical coherence tomography angiography in geographic atrophy. *Retina*. 2018;38(12).
27. Choi W, Moulton EM, Waheed NK, Adhi M, Lee B, Lu CD, et al. Ultrahigh-Speed, Swept-Source Optical Coherence Tomography Angiography in Nonexudative Age-Related Macular Degeneration with Geographic Atrophy. *Ophthalmology*. 2015;122(12).
28. Sacconi R, Corbelli E, Querques L, Bandello F, Querques G. A Review of Current and Future Management of Geographic Atrophy. *Ophthalmology and Therapy*. 2017 8;6(1).
29. Qin J, Rinella N, Zhang Q, Zhou H, Wong J, Deiner M, et al. OCT Angiography and Cone Photoreceptor Imaging in

- Geographic Atrophy. *Investigative Ophthalmology & Visual Science*. 2018 Dec 20;59(15).
30. Sacconi R, Corbelli E, Borrelli E, Capone L, Carnevali A, Gelormini F, et al. Choriocapillaris flow impairment could predict the enlargement of geographic atrophy lesion. *British Journal of Ophthalmology*. 2021;105(1).
  31. Müller PL, Pfau M, Schmitz-Valckenberg S, Fleckenstein M, Holz FG. OCT-Angiography in Geographic Atrophy. *Ophthalmologica*. 2020 7;
  32. Thulliez M, Zhang Q, Shi Y, Zhou H, Chu Z, de Sistiernes L, et al. Correlations between Choriocapillaris Flow Deficits around Geographic Atrophy and Enlargement Rates Based on Swept-Source OCT Imaging. *Ophthalmology Retina*. 2019;3(6).
  33. Alagorie AR, Nassisi M, Verma A, Nittala M, Corradetti G, Velaga S, et al. Relationship between proximity of choriocapillaris flow deficits and enlargement rate of geographic atrophy. *Graefe's Archive for Clinical and Experimental Ophthalmology*. 2020 11;258(5).
  34. Nassisi M, Baghdasaryan E, Borrelli E, Ip M, Sadda SR. Choriocapillaris flow impairment surrounding geographic atrophy correlates with disease progression. *PLOS ONE*. 2019 22;14(2).
  35. Carnevali A, Cicinelli MV, Capuano V, Corvi F, Mazzaferro A, Querques L, et al. Optical Coherence Tomography Angiography: A Useful Tool for Diagnosis of Treatment-Naïve Quiescent Choroidal Neovascularization. *Am J Ophthalmol*. 2016;169.
  36. Laiginhas R, Yang J, Rosenfeld PJ, Falcão M. Nonexudative Macular Neovascularization – A Systematic Review of Prevalence, Natural History, and Recent Insights from OCT Angiography. *Ophthalmology Retina*. 2020;4(7).
  37. Christenbury JG, Phasukkijwatana N, Gilani F, Freund KB, Sadda S, Sarraf D. Progression of macular atrophy in eyes with type 1 neovascularization and age-related macular degeneration receiving long-term intravitreal anti-vascular endothelial growth factor therapy. *Retina*. 2018;38(7).
  38. Capuano V, Miere A, Querques L, Sacconi R, Carnevali A, Amoroso F, et al. Treatment-Naïve Quiescent Choroidal Neovascularization in Geographic Atrophy Secondary to Nonexudative Age-Related Macular Degeneration. *Am J Ophthalmol*. 2017;182.



12.

# PACHYCHOROID RELATED DISEASES



# PACHYCHOROID DISEASES OF THE MACULA

Luís Mendonça

Serviço de Oftalmologia do Hospital de Braga

## INTRODUCTION

Pachychoroid is a relatively novel and evolving concept describing a phenotype characterized by attenuation of the choriocapillaris overlying dilated choroidal blood vessels, and associated with progressive retinal pigment epithelium dysfunction and possible neovascularization. The emphasis in defining pachychoroid-related disorders has shifted away from simply an abnormally thick choroid (*pachychoroid*) toward a detailed morphological definition of a pathologic state (*pachychoroid disease*) with functional implications. Several clinical manifestations have been described within the pachychoroid disease spectrum, including *central serous chorioretinopathy* (CSC), *pachychoroid pigment epitheliopathy* (PPE), *pachychoroid neovasculopathy* (PNV), *polypoidal choroidal vasculopathy/aneurysmal type 1 neovascularization* (PCV/AT1), *focal choroidal excavation* (FCE), *peripapillary pachychoroid syndrome* (PPS). These conditions all exhibit common characteristic choroidal alterations and are believed to represent different manifestations of a common pathogenic process.<sup>1</sup>

Hyperpermeable and dilated choroidal vessels have been observed using indocyanine green angiography (ICGA) in eyes with CSC and PCV/AT1.<sup>2</sup> With the advent of enhanced-depth imaging optical coherence tomography (EDI-OCT) and subsequently swept-source optical coherence tomography (SS-OCT), increased choroidal thickness was also described.<sup>3,4</sup> The terms pachychoroid and, subsequently, pachychoroid disease were introduced to describe a phenotype characterized by focal or diffuse increase in choroidal thickness, accounted for by dilated choroidal vessels in Haller's layer (*pachyvessels*), accompanied by thinning of the choriocapillaris and Sattler's layer with/without retinal pigment epithelium (RPE) abnormalities overlying the pachyvessels.<sup>5</sup> While a thick choroid is frequently seen, choroidal thickness *per se* is not the most important criterion for defining the pachychoroid disease phenotype. Instead, the presence of characteristic morphologic changes which implicate structural and functional choroidal alteration as key pathophysiologic mechanism is essential to diagnose pachychoroid disease.<sup>1,6</sup>

## OCT ANGIOGRAPHY

Technological advances during the last few decades have improved our understanding of the disease spectrum.

The primary role of the choroid has been highlighted in studies using ICGA and OCT, showing choroidal vascular congestion and hyperpermeability.<sup>4,7</sup> More recently, optical coherence tomography angiography (OCTA) has allowed for the noninvasive assessment of retinal and choroidal microvasculature. Analysis of the decorrelation signal makes it possible to visualize blood flow within the retinal layers and deeper, at the choriocapillaris level. Moreover, *en face* reconstruction, provides high-definition vascular mapping images. OCTA has been used for the qualitative and quantitative analysis of CC in healthy and pathologic eyes. A review of the major contribution of OCTA on the understanding of the pachychoroid continuum will follow, focusing on PPE and PNV. CSC and PCV/AT1 will be the subject of the following chapters.

## INNER CHOROIDAL BLOW FLOW IMPAIRMENT

In pachychoroid disease, the spatial distribution of RPE changes, neurosensory detachment, and neovascularization seem to correlate with the localized choroidal thickening attributable to dilatation of Haller's layer vessels and thinning of the choriocapillaris and Sattler's layers. Quantification of choriocapillaris flow characteristics with OCTA has been addressed by several investigators. Some have searched for functional changes at the level of the innermost part of the choriocapillaris, with a working hypothesis that a reduction in flow signal might be related anatomically to structural sequelae (Fig. 1).<sup>12-16</sup>

Gal-Or *et al.* found a higher prevalence of inner choroidal flow signal attenuation zones in pachychoroid eyes than in normal controls, and most (68%) of these zones were related anatomically to pachyvessels. Although the mechanisms by which choriocapillaris flow characteristics can contribute to structural sequelae remain elusive, and the determination of whether they are precursors to choriocapillaris thinning would require longitudinal analysis, it is possible that they represent zones of inner choroidal ischemia.<sup>12</sup> Similarly, other studies have suggested the idea of a primary choroidopathy, where microvascular flow deficits may constitute one of the underlying subclinical changes preceding pachychoroid spectrum disorders.<sup>14</sup>

Baek *et al.* analyzed vascular density and signal void



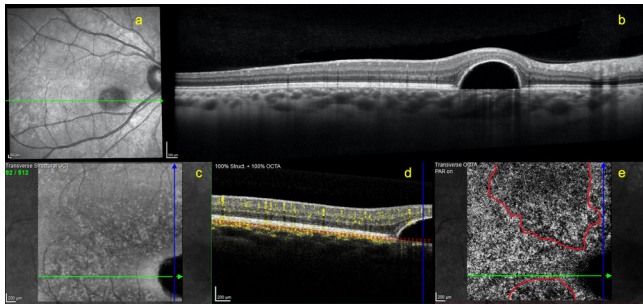


**Figure 1.** Multimodal imaging of a 52-year-old male patient with PPE; a–b: structural OCT B-scan through serous PED with underlying pachyvessels and choriocapillaris and Sattler's layer thinning; c: structural en-face OCT; d: autosegmented slab boundary of the choriocapillaris; e: en-face OCTA of the autosegmented slab showing areas of flow signal attenuation (red line). (Courtesy of Susana Penas)

area in the choriocapillaris of eyes with earlier stages of pachychoroid spectrum (uncomplicated pachychoroid and PPE) compared to age-matched eyes of normal controls. Choriocapillaris vascular density was significantly lower in eyes with PPE compared with controls. The number, the total area and the average size of signal voids was the highest in the PPE group followed by the pachychoroid without epitheliopathy and then controls. 89% signal void area colocalized with pachyvessels, and the average size of the signal void was higher if it was colocalized with pachyvessel. The area of flow impairment in the choriocapillaris was increased in eyes with pachychoroid and even greater when epitheliopathy was present. Pachyvessel was associated with choriocapillaris flow impairment by location and size.<sup>16</sup>

Sakurada *et al.* explored the relationship between choroidal vascular hyperpermeability on ICGA, choroidal thickness on SS-OCT, and choriocapillaris blood flow using OCTA, in eyes with PPE. Reduced choriocapillaris flow density, increased choroidal thickness, and choroidal vascular hyperpermeability appear to colocalize in eyes with PPE. Their results suggest that, although the presence of choroidal thickening, vascular hyperpermeability, and dilated Haller's vessels in eyes with pachychoroid disease may relate to increased outer choroidal blood flow and vascular congestion, in areas of vascular hyperpermeability, there appears to be ischemia affecting the inner choroid, RPE, and outer retina due to reduced choriocapillaris blood vascularity. Even though a definite causal role of pachyvessels in inducing reduced choriocapillaris blood flow was not possible, one could speculate that if pachyvessels occurs before vascular hyperpermeability, then vascular hyperpermeability represents staining because of ischemia resulting from compression of choriocapillaris, rather than dye leakage related to choroidal vascular congestion. Dilated Haller's blood vessels and increased hydrostatic pressure from vascular congestion would secondarily compress the inner choroid reducing choriocapillaris blood flow. A longitudinal study showing the sequence

of morphological changes seen in eyes with PPE would be necessary to resolve this causal relationship.<sup>17</sup>

More recently, Spaide *et al.* analyzed the vascular branching characteristics of the choriocapillaris in eyes with pachychoroid as compared with normal controls with OCTA, using frame-averaging methods. Choriocapillaris vascular morphology was different among eyes displaying pathologic manifestations in the context of pachychoroid as compared with uncomplicated pachychoroid or normal eyes. The choriocapillaris vessel branch number was less in eyes with pachychoroid disease as defined by a history of CSC or peripapillary pachychoroid syndrome as compared with either normal eyes or those with uncomplicated pachychoroid. These same eyes showed an increase in capillary branch length, slightly wider capillaries, and decreased fractal dimension (“branching complexity”) as compared with pachychoroid without disease or normal eyes. Among all of these parameters, there was no statistically significant difference between the uncomplicated pachychoroid and the normal eyes. In conclusion, disease in the pachychoroid spectrum should be more likely related to choriocapillaris vascular parameters than to choroidal thickness *per se*. Microvascular damage from breakdown of the choroid blood pressure control systems may precede disease expression in the pachychoroid spectrum.<sup>6</sup>

In addition to the impairment of choriocapillaris blood flow, thinning of outer nuclear layer (ONL) has also been observed in eyes with pachychoroid disease. Interestingly, the ONL was thinner in eyes with PPE than in eyes with uncomplicated pachychoroid in one study, suggesting that degeneration of photoreceptors and/or RPE may also occur, even in the absence of subretinal fluid.<sup>18</sup> Later on, Lee *et al.* described a distinctive focal disruption of the ellipsoid zone/interdigitation zone in eyes with PPE, with a stable clinical course, and possibly as a result of regression of characteristic RPE elevations or drusenoid lesions, recently named pachydrusen.<sup>19,20</sup> These outer retinal atrophic changes were identified early on the pachychoroid continuum and could be an expression of inner choroid/RPE disturbances driven by ischemia.

## TYPE 1 NEOVASCULARIZATION

Type 1 neovascularization is defined by the presence of a vascularized pigment epithelial detachment (PED). Diagnosis of active neovascularization relies on cross-sectional optical coherence tomography (OCT) to image the PED and fluorescein angiography to demonstrate “poorly defined” stippled hyperfluorescence with late leakage and/or staining at the site of the PED.

Although type 1 neovascularization is a well-recognized complication of chronic CSC, it can also arise in pachychoroid eyes that have not yet manifested frank subretinal fluid.<sup>4</sup> The term “pachychoroid neovascularopathy” (PNV) was adopted to acknowledge that neovascularization can occur in pachychoroid eyes even in the absence of neurosensory detachment

(i.e., on a background of pachychoroid pigment epitheliopathy).<sup>21,23</sup> Recent studies using EDI-OCT and SS-OCT have also demonstrated that the choroids of eyes harboring aneurysmal (polypoidal) lesions within Type 1 neovascular complexes (PCV) often exhibit pachychoroid characteristics.<sup>24</sup> These were subsequently renamed Aneurysmal Type 1 Neovascularization (PCV/AT1)<sup>25</sup> and will be further discussed in a following chapter.

## PACHYCHOROID NEOVASCULOPATHY

PNV is a type 1 choroidal neovascularization, overlying focal areas of choroidal thickening and dilated choroidal vessels. It can develop in patients affected by pachychoroid pigment epitheliopathy or chronic central serous chorioretinopathy. The absence of drusen, the presence of pachydrusen, younger age of onset and choroidal thickening distinguish it from neovascular age-related macular degeneration (AMD).<sup>23</sup>

Type 1 neovascularization can be highlighted noninvasively with optical coherence tomography angiography (OCTA), which shows an entangled vascular network between RPE and Bruch's membrane, with well-defined margins and irregular shapes (Fig. 2).<sup>26</sup>

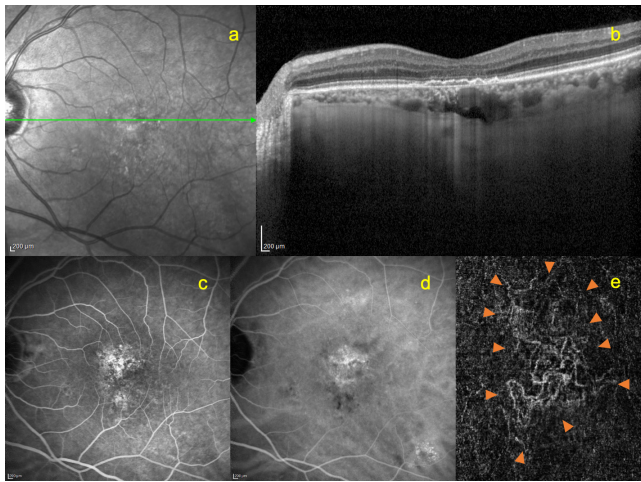


**Figure 2.** Multimodal imaging of a 64-year-old male patient with PNV; a-b: structural OCT B-scan through flat irregular PED with underlying pachyvessels and choriocapillaris and Sattler's layer thinning; c: late-phase FA; d: mid-late phase ICGA; e: en-face OCTA of an autosegmented slab through the avascular outer retina showing an entangled vascular network with irregular shape (orange arrowheads). (Courtesy of Susana Penas)

According to several studies, OCTA may detect choroidal neovascularization more frequently than the combination of OCT, FA and ICGA.<sup>21,27,28</sup> Dansingani *et al.* found that shallow irregular PED in eyes with pachychoroid features were shown to harbor neovascular tissue in 95% of a consecutive cohort, compared to 41% diagnosed with dye angiography.<sup>21</sup> In a series of consecutive patients with flat irregular PED and chronic CSC, OCTA detected

the presence of choroidal neovascularization in 35.6% of cases, while using the combination of SD-OCT, FA and ICGA, neovascularization was detected in only 25% of flat irregular PED. All hyperreflective flat irregular PED on OCT were avascular on OCTA while they were at least partially hyperreflective when associated with neovascularization.<sup>27</sup>

OCTA has also been used to show that neovascularization can be associated with the type of PED on structural OCT in patients with CSC. Accordingly, neovascularization was found more often in flat irregular PED compared to focal PED (43% vs 10%).<sup>28</sup> It is also shown that quiescent type 1 neovascularization can be present in up to 11% of eyes with previous diagnosis of PNV.<sup>29</sup> Changes in retinal capillary plexus have also been shown in PNV. OCTA was used to demonstrate that superficial and deep vascular densities of the macular region were lower in the patients with PNV compared with the control group. In the patients with PNV, the macular region showed signs of inner retinal capillary dropout, which might be caused by choroidal ischemia.<sup>30</sup>

## REFERENCES

- Cheung CMG, Lee WK, Koizumi H, Dansingani K, Lai TYY, Freund KB. Pachychoroid disease. *Eye*. 2018 Jul 10;33(1):14–33.
- Guyon DR, Yannuzzi LA, Slakter JS, Sorenson JA, Hope-Ross M, Orlock DR. Digital Indocyanine-green Videoangiography of Occult Choroidal Neovascularization. *Ophthalmology*. 1994;101(10):1727–37.
- Ferrara D, Mohler KJ, Waheed N, Adhi M, Liu JJ, Grulkowski I, et al. En Face Enhanced-Depth Swept-Source Optical Coherence Tomography Features of Chronic Central Serous Chorioretinopathy. *Ophthalmology*. 2014;121(3):719–26.
- Dansingani KK, Balaratnasingam C, Naysan J, Freund KB. En Face Imaging Of Pachychoroid Spectrum Disorders With Swept-Source Optical Coherence Tomography. *Retina*. 2016 Mar;36(3):499–516.
- Warrow DJ, Hoang QV, Freund KB. Pachychoroid Pigment Epitheliopathy. *Retina*. 2013 Jun;
- Spaide RF, Ledesma-Gil G. Choriocapillaris Vascular Parameters In Normal Eyes And Those With Pachychoroid With And Without Disease. *Retina*. 2021;41(4):679–85.
- Guyon DR, Yannuzzi LA, Slakter JS, Sorenson JA, Ho A, Orlock D. Digital Indocyanine Green Videoangiography of Central Serous Chorioretinopathy. *Arch Ophthalmol*. 1994;112(8):1057–62.
- Matsumoto H, Hoshino J, Mukai R, Nakamura K, Kikuchi Y, Kishi S, et al. Vortex Vein Anastomosis at the Watershed in Pachychoroid Spectrum Diseases. *Ophthalmol Retin*. 2020;4(9):938–45.
- Spaide RF, Ledesma-Gil G, Cheung CMG. Intervortex Venous Anastomosis In Pachychoroid-Related Disorders. *Retina*. 2021;41(5):997–1004.
- Hoshino J, Matsumoto H, Mukai R, Nakamura K, Arai Y, Kikuchi Y, et al. Variation of vortex veins at the horizontal watershed in normal eyes. *Graefes' Archive Clin Exp Ophthalmol*. 2021;1–6.
- Ersoz MG, Arf S, Hocaoglu M, Muslubas IS, Karacorlu M. Indocyanine Green Angiography Of Pachychoroid Pigment

- Epitheliopathy. *Retina*. 2018;38(9):1668–74.
12. Gal-Or O, Dansingani KK, Sebrow D, Dolz-Marco R, Freund KB. Inner Choroidal Flow Signal Attenuation In Pachychoroid Disease. *Retina*. 2018;38(10):1984–92.
  13. Chan SY, Wang Q, Wei WB, Jonas JB. Optical Coherence Tomographic Angiography In Central Serous Chorioretinopathy. *Retina*. 2016;36(11):2051–8.
  14. Rochepeau C, Kodjikian L, Garcia M-A, Coulon C, Burillon C, Denis P, et al. Optical Coherence Tomography Angiography Quantitative Assessment of Choriocapillaris Blood Flow in Central Serous Chorioretinopathy. *Am J Ophthalmol*. 2018;194:26–34.
  15. Yun C, Huh J, Ahn SM, Lee B, Kim JT, Hwang S-Y, et al. Choriocapillaris flow features and choroidal vasculature in the fellow eyes of patients with acute central serous chorioretinopathy. *Graefes Archive Clin Exp Ophthalmol*. 2019;257(1):57–70.
  16. Baek J, Kook L, Lee WK. Choriocapillaris Flow Impairments in Association with Pachyvessel in Early Stages of Pachychoroid. *Sci Rep-uk*. 2019;9(1):5565.
  17. Sakurada Y, Fragiotta S, Leong BCS, Parikh R, Hussnain SA, Freund KB. Relationship Between Choroidal Vascular Hyperpermeability, Choriocapillaris Flow Density, And Choroidal Thickness In Eyes With Pachychoroid Pigment Epitheliopathy. *Retina*. 2020;40(4):657–62.
  18. Ersoz MG, Karacorlu M, Arf S, Hocaoglu M, Muslubas IS. Outer Nuclear Layer Thinning In Pachychoroid Pigment Epitheliopathy. *Retina*. 2018;38(5):957–61.
  19. Lee JH, Kim JY, Jung BJ, Lee WK. Focal Disruptions In Ellipsoid Zone And Interdigitation Zone On Spectral-Domain Optical Coherence Tomography In Pachychoroid Pigment Epitheliopathy. *Retina*. 2018;Publish Ahead of Print(NA):NA;
  20. Spaide RF. Disease Expression In Nonexudative Age-Related Macular Degeneration Varies With Choroidal Thickness. *Retina*. 2018 Apr;38(4):708–16.
  21. Dansingani KK, Balaratnasingam C, Klufas MA, Sarraf D, Freund KB. Optical Coherence Tomography Angiography of Shallow Irregular Pigment Epithelial Detachments In Pachychoroid Spectrum Disease. *American Journal of Ophthalmology*. 2015 Dec;160(6):1243-1254.e2.
  22. Sato T, Kishi S, Watanabe G, Matsumoto H, Mukai R. Tomographic Features Of Branching Vascular Networks In Polypoidal Choroidal Vasculopathy. *Retina*. 2007 Jun;27(5):589–94.
  23. Pang CE, Freund KB. Pachychoroid neovascularopathy. *Retina*. 2015 Jan;35(1):1–9.
  24. FRCOphth CMGC, MD TYYL, MD PR, MD S-JC, MD YC, MD KBF, et al. Polypoidal Choroidal Vasculopathy Definition, Pathogenesis, Diagnosis, and Management. *Ophthalmology*. 2018 Jan 9;125(5):1–17.
  25. FRCOphth CMGC, FRCOphth TYYL, Ophth KTMMm, MD PR, MD S-JC, PhD JEKM, et al. Polypoidal Choroidal Vasculopathy Consensus Nomenclature and NoneIndocyanine Green Angiograph Diagnostic Criteria from the Asia-Pacific Ocular Imaging Society PCV Workgroup. *Ophthalmology*. 2021 Mar 1;128(3):443–52.
  26. Azar G, Wolff B, Maugeat-Fajsse M, Rispoli M, Savastano M-C, Lumbroso B. Pachychoroid neovascularopathy: aspect on optical coherence tomography angiography. *Acta ophthalmologica [Internet]*. 2016 Sep 6;1–7.
  27. Bousquet E, Bonnin S, Mrejen S, Krivosic V, Tadayoni R, Gaudric A. Optical Coherence Tomography Angiography Of Flat Irregular Pigment Epithelium Detachment In Chronic Central Serous Chorioretinopathy. *Retina*. 2018;38(3):629–38.
  28. Hwang H, Kim JY, Kim KT, Chae JB, Kim DY. Flat Irregular Pigment Epithelium Detachment In Central Serous Chorioretinopathy: A Form of Pachychoroid Neovascularopathy? *Retina*. 2020;40(9):1724–33.
  29. Carnevali A, Capuano V, Sacconi R, Querques L, Marchese A, Rabiolo A, et al. OCT Angiography of Treatment-Naïve Quiescent Choroidal Neovascularization in Pachychoroid Neovascularopathy. *Ophthalmol Retina*. 2017;1(4):328–32.
  30. Shen C, Zhang J, Tian J, Liu Y, Zhao H. Optical coherence tomography angiography for visualization of retinal capillary plexuses in pachychoroid neovascularopathy. *Can J Ophthalmology*. 2021;56(2):105–11.

## 12.1.

# CENTRAL SEROUS CHORIORETINOPATHY

Susana Penas

Centro Hospitalar e Universitário de São João, Porto

Central serous chorioretinopathy (CSC) is a macular disorder characterized by the presence of sub-retinal fluid (SRF), eventually associated with retinal pigment epithelium (RPE) detachments<sup>1,2</sup>. It is far more common among male patients, and has been associated with stress/anxiety (personality type A) and steroids (endogenous or exogenous)<sup>3</sup>. It is usually a self-limited condition, with spontaneous resolution of the fluid and recovery to normal or near-normal visual acuity, eventually leaving mild visual complaints, but occasionally patients develop chronic or recurrent forms of disease<sup>4</sup>, that might threaten the visual function<sup>5,6</sup>.

Recent imaging data brought to light the important role of the choroid in the pathogenesis of CSC<sup>7</sup>. CSC has been included in the pachychoroid spectrum of diseases<sup>8</sup>, presenting abnormally thick choroids on the optical coherence tomography (OCT), with documented hyperpermeability on the indocyanine-green angiography (ICGA), in both the affected and unaffected eyes<sup>1,2</sup>.

The OCT angiography (OCTA) advent has led to new groundbreaking insights in the study of the vascular circulation in both retinal and choroidal diseases<sup>9</sup>. Its use in CSC revealed important data on the pathogenesis of this chorioretinal disorder.

## ACUTE AND CHRONIC CSC

Microvascular flow deficits have been reported in the choroid of CSC patients. Although flow void areas are physiologic findings in the aging choriocapillaris, some authors reported a significantly greater total average flow signal void area in CSC patients than in healthy controls<sup>10</sup>. Furthermore, some other authors related these flow void areas with the underlying choroidal structure, concluding that the mean flow void area of the choriocapillaris over the vascular bed was larger than over the stromal bed in CSC patients<sup>11</sup>. They therefore hypothesized that in the areas of compressed choriocapillaris, over the large choroidal vessels (pachyvessels), the blood flow might be impaired, leading to focal ischemia. They also suggest that this narrow choriocapillaris might suffer directly from barotrauma and shear stress, induced by the large underlying choroidal vessels, secondary to an impaired venous return<sup>11</sup>. In fact, CSC patients have presented a delay in the choriocapillaris flow that might result from a congestion of the vortex veins<sup>12</sup> and/or inter-vortex venous anastomosis (Figure 1)<sup>13,14</sup>.

OCTA angiography has also shown significant changes in the choriocapillaris flow pattern in chronic CSC patients.

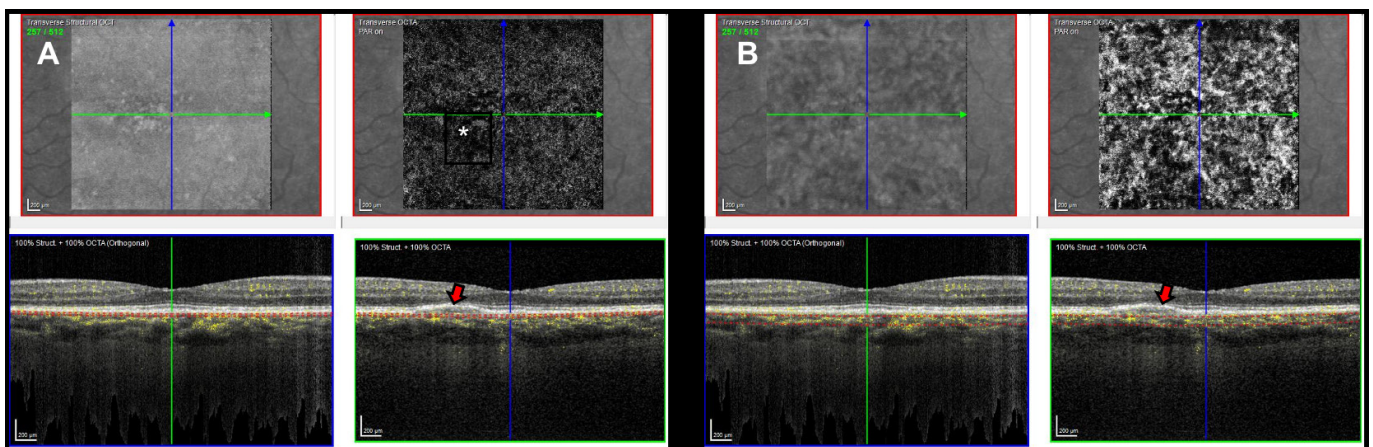


**Figure 1.** Optical coherence tomography angiography (OCTA) of the fellow eye of a 56-year-old female patient with central serous chorioretinopathy (CSC). Transverse OCTA at the choriocapillaris level (A) shows some flow voids and a relatively hypoperfused area (asterisk) that corresponds to the flat, regular pigment epithelium detachment (red arrow). Some enlarged choroidal vessels are present at the OCTA imaging of deeper choroidal layers (B), also visible in the structural OCT.

Teussink et al. performed a comparison between FA and ICGA findings with OCTA in chronic CSC<sup>15</sup>. They found that abnormalities on late-phase ICGA and FA collocate with those on OCTA. They also described an aberrant choriocapillaris flow in these patients, presenting areas of hypoperfusion with hyperperfusion in the surrounding area. The hot spots visible on ICGA were located near hypoperfused spots on OCTA and retinal areas with current or former subretinal fluid were co-localized with these flow abnormalities<sup>15</sup>. They suggested that a reduced blood perfusion in the choriocapillaris may be surrounded by a reactive hyperperfusion, raising the hydrostatic pressure within the fenestrated choriocapillaris, leading to SRF leakage and serous neuroretinal detachment. They also concluded that these flow abnormalities were not dependent of disease activity nor treatment.

Nicoló et al. compared CSC and controls using a swept-source OCTA (SS OCTA), allowing a better visualization of deeper choroidal vessels<sup>16</sup>. They concluded that the choroidal vascular flow area is larger in CSC eyes, as well as in unaffected fellow eyes, than in age-matched healthy control eyes. In addition, they also detected some differential internal choroidal flow, presenting a significantly lower flow area in the choriocapillaris than in deeper choroidal levels. This different spatial distribution of the vascular flow within the choroid in CSC eyes might be secondary to a compensatory regulation mechanism of the choroid. These authors hypothesized that following a vasodilatation of part of the choroid, a relative vasoconstriction of the choriocapillaris might occur in the attempt to compensate to the limited autoregulatory capacity of the choroid<sup>16</sup>.

Nevertheless, care must be taken when analyzing choroidal OCTA images in CSC patients with significant sub-retinal fluid, PED or pigment clumps, because these findings can induce significant shadowing artifacts on the deeper layers, simulating choroidal hypoperfusion or ischemia (Figure 2).

After CSC treatment, with both photodynamic therapy (PDT) or micropulse laser, a significant reduction of the flow deficit areas in the choriocapillaris has been documented. Nevertheless, PDT showed a more powerful effect in the choriocapillaris recovery, as well as a significant reduction of the mean central choroidal volume (Figure 2)<sup>17</sup>.

### CHOROIDAL NEOVASCULARIZATION

The occurrence of choroidal neovascularization (CNV) during the course of chronic CSC has been widely reported. Fung et al. detected this complication in 27 eyes of 22 patients over a 15-year period of clinical follow-up<sup>18</sup>. CNV in chronic CSC should be classified as pachychoroid neovasculopathy or neovascularization associated to pachychoroid, which is defined as type 1 neovascularization, associated with choroidal thickening and /or choroidal dilated vessels, in the absence of characteristic age-related macular degeneration (AMD) or degenerative changes<sup>19</sup>. Hage et al. reported CNV

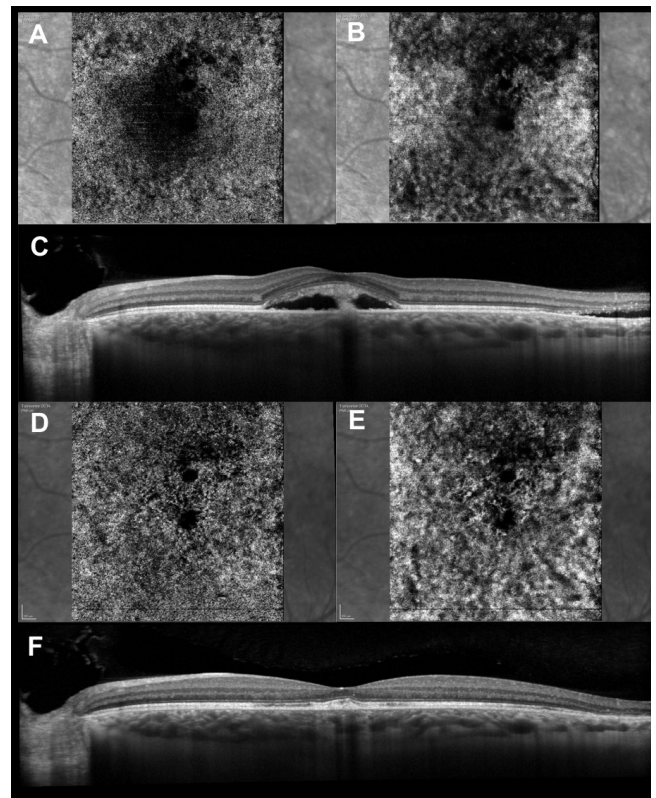


**Figure 2.** Optical coherence tomography angiography (OCTA) imaging of the eye of a 52-year-old male patient with active recurrent central serous chorioretinopathy (CSC). The sub-retinal fluid (SRF) visible on the structural OCT (C) partially obscures the choriocapillaris (A) and middle choroidal vasculature (B). One-month after photodynamic therapy (PDT), the SRF disappeared (F) allowing a better visualization of both choroidal vascular layers (D, E), as well as some flow voids and shadowing artifacts due to pigment clumps. The choroidal thickness decreased after PDT (F).

in 10 of 53 eyes with flat irregular pigment epithelium detachments (PED) in chronic CSC patients, when submitted to a multimodal imaging including structural SD-OCT, FA and ICGA<sup>20, 21</sup>. Nevertheless, it remains a clinical challenge to differentiate a low-grade activity type 1 CNV from an avascular flat irregular PED in chronic CSC patients. The lack of accurate criteria to allow this differentiation sometimes renders the decision-making process more complex. Usually, the presence of a hyperreflective solid or lamellar material underneath the PED is suggestive of CNV<sup>20</sup>. Furthermore, fundus examination can contribute with some suspicious signs like hemorrhages and hard exudation, although these can also be present in long-course chronic CSC. FA and ICGA frequently are unable to make a differential diagnosis since the angiographic findings induced by widespread RPE changes and atrophy can be easily confounded with CNV.

More recently, OCTA proved to be able to detect CNV in chronic CSC, not visible with other imaging techniques, even with dye-based angiographies<sup>22</sup>. OCTA outweighs the classic angiography performance in these

due to the absence of leakage effect and the ability to independently segment both the retinal and choroidal vascular plexuses<sup>23</sup>. El Maftouhi et al. identified CNV in all the patients with irregular undulating PED, confirming its neovascular content, and in none of the patients with flat linear PED<sup>22</sup>. The ability to detect early and quiescent CNV via OCTA is crucial for a good management of chronic CSC patients, even if they don't need immediate treatment for their neovascularization. In fact, the occurrence of type 1 CNV in CSC patients is not synonymous to prompt anti-VEGF treatment, and this decision should be based on a recent loss of visual acuity and signs of CNV activity (Figure 3)<sup>20, 23</sup>. Furthermore, OCTA has allowed a more precise characterization of CNV in CSC. Sacconi et al. described a different CNV appearance in comparison to age-related

macular degeneration (AMD), typically presenting large-caliber vessels with a paucity of capillaries within the lesions even at baseline (Figure 3)<sup>23</sup>. The structural differences in CNV from CSC and AMD could be explained by a distinct genesis of these two pathologies. The prolonged presence of a PED in chronic CSC might result in a disruption of the Bruch's membrane and subsequent stimulation of neovascularization<sup>18</sup>. Differently from AMD, CNV secondary to CSC results from a long-standing growth of neovessels, eventually playing a "compensatory" role in chronic photoreceptor and RPE suffering<sup>23</sup>. These same authors also reported a different response to CNV treatment in CSC. CNV in CSC showed less changes one month after treatment in comparison to AMD. In both half-fluence photodynamic therapy (PDT) and aflibercept groups, the vessel density

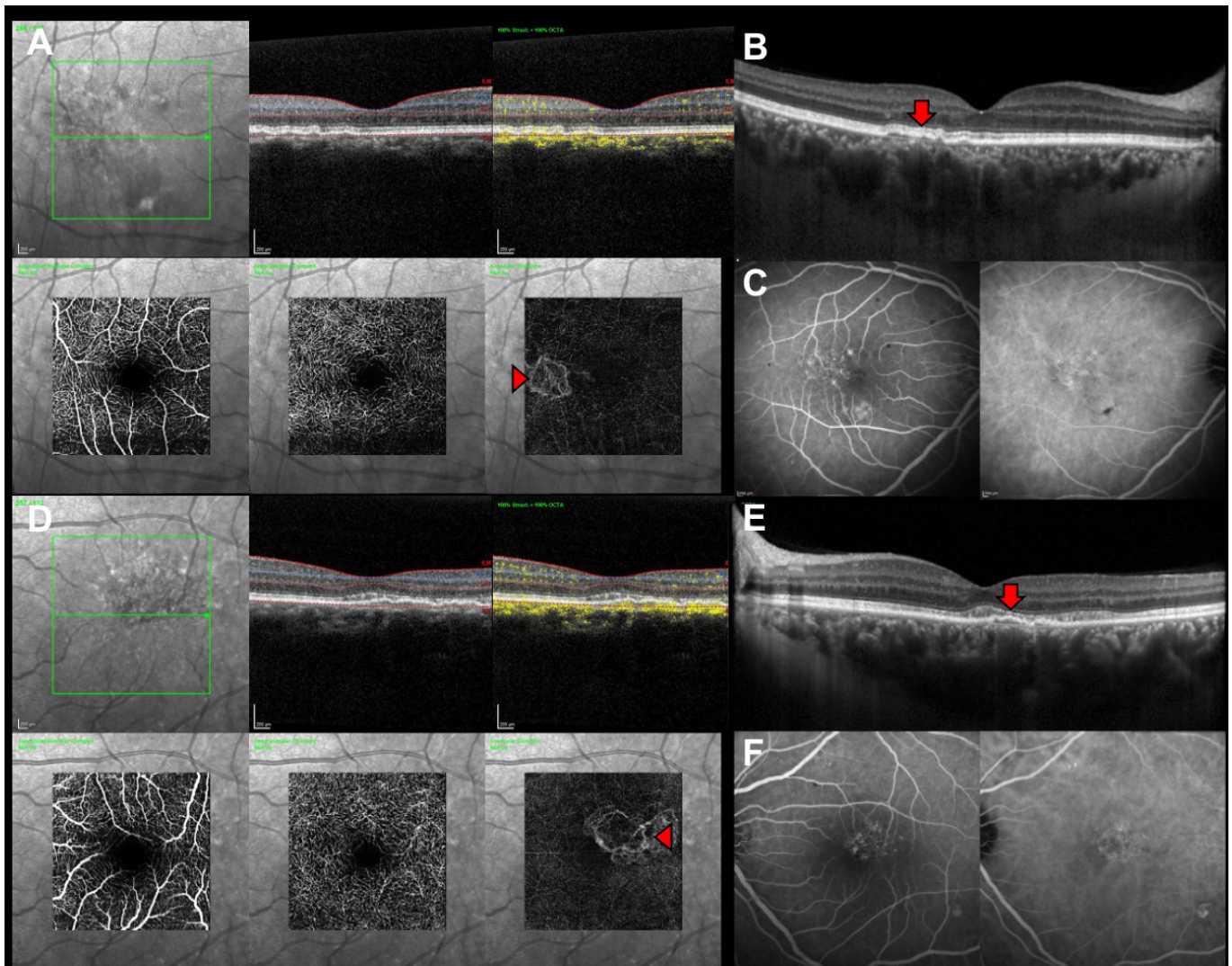


**Figure 3.** Optical coherence tomography angiography (OCTA) imaging of both eyes of a 46-year-old male patient with spontaneously resolved central serous chorioretinopathy (CSC) in his left eye (D). He was asymptomatic on the right eye (A) and sub-retinal fluid was never detected. Structural OCT presented shallow irregular undulating pigment epithelium detachments (red arrows), with no intra or sub-retinal fluid. Fluorescein and indocyanine green angiograms presented late mild stippled leakage (C,F), but no obvious signs of choroidal neovascularization (CNV). OCTA detected a quiescent bilateral juxtafoveal CNV (red arrow-heads). Typically, CNV in CSC presents large-caliber vessels with a paucity of capillaries.

(VD) did not significantly change, although a slight reduction in CNV area was observed. All patients presented a favorable clinical response<sup>23</sup>. These authors speculate that arteriogenesis could be the main generator of CNV in CSC. In fact, Spaide speculated that two distinct mechanisms were implicated in CNV genesis: the angiogenesis, characterized by new-vessels proliferation and highly VEGF-dependent, and the arteriogenesis, characterized by the dilation of preexisting channels and not highly VEGF-dependent<sup>24</sup>. The expansion of the trunk and large branches (arteriogenesis) seems to be the main mechanism of CNV in CSC, whereas the growth and branching of vascular sprouts (angiogenesis) is the main process of CNV in AMD (Figure 3)<sup>23</sup>.

The conversion of CSC to polypoid choroidal neovascularization (PCV) has been documented<sup>25</sup>. Some authors suggested that PCV might more likely be a secondary manifestation than a primary pathology of the choroid, resulting from the chronic exudation and RPE changes characteristic of chronic CSC<sup>26</sup>. It has been assumed that PCV and CSC, both from the pachychoroid spectrum of diseases, share a common pathogenesis.

## REFERENCES

- 1- Daruich, A., A. Matet, A. Dirani, E. Bousquet, M. Zhao, N. Farman, et al. Central serous chorioretinopathy: Recent findings and new physiopathology hypothesis. *Prog Retin Eye Res.* 2015; 48: 82-118.
- 2- Kaye, R., S. Chandra, J. Sheth, C. J. F. Boon, S. Sivaprasad and A. Lotery. Central serous chorioretinopathy: An update on risk factors, pathophysiology and imaging modalities. *Prog Retin Eye Res.* 2020; 79:100865.
- 3- Yannuzzi, L. A. Type A behavior and central serous chorioretinopathy. *Retina.* 2012; 32 Suppl 1: 709.
- 4- Penas, S., A. F. Costa, J. Araujo, P. Faria, E. Brandao, A. Rocha-Sousa, et al. Chronicity and Recurrence as Prognostic Factors in Central Serous Chorioretinopathy after Half-Dose Photodynamic Therapy. *J Clin Exp Ophthalmol.* 2016; 07.
- 5- Castro-Correia, J., M. F. Coutinho, V. Rosas and J. Maia. Long-term follow-up of central serous retinopathy in 150 patients. *Doc Ophthalmol.* 1992; 81(4): 379-386.
- 6- Loo, R. H., I. U. Scott, H. W. Flynn, Jr., J. D. Gass, T. G. Murray, M. L. Lewis, et al. Factors associated with reduced visual acuity during long-term follow-up of patients with idiopathic central serous chorioretinopathy. *Retina.* 2002; 22(1): 19-24.
- 7- Prunte, C. and J. Flammer. Choroidal capillary and venous congestion in central serous chorioretinopathy." *Am J Ophthalmol.* 1996; 121(1): 26-34
- 8- Cheung, C. M. G., W. K. Lee, H. Koizumi, K. Dansingani, T. Y. Y. Lai and K. B. Freund. Pachychoroid disease. *Eye.* 2018; 10;33(1):14-33.
- 9- Borrelli, E., D. Sarraf, K. B. Freund and S. R. Sadda. OCT angiography and evaluation of the choroid and choroidal vascular disorders. *Prog Retin Eye Res.* 2018; 67: 30-55.
- 10- Rochepeau C, Kodjikian L, Garcia MA, Mathis T. Optical Coherence Tomography Angiography Quantitative Assessment of Choriocapillaris Blood Flow in Central Serous Chorioretinopathy. *Am J Ophthalmol.* 2019;201:82-83.
- 11- Yun C, Huh J, Ahn SM, Lee B, Kim JT, Hwang SY, et al. Choriocapillaris flow features and choroidal vasculature in the fellow eyes of patients with acute central serous chorioretinopathy. *Graefes Arch Clin Exp Ophthalmol.* 2019;257(1):57-70.
- 12- Kishi S, Matsumoto H, Sonoda S, Hiroe T, Sakamoto T, Akiyama H. Geographic filling delay of the choriocapillaris in the region of dilated asymmetric vortex veins in central serous chorioretinopathy. *PLoS One.* 2018 9;13(11):e0206646.
- 13- Spaide RF, Ledesma-Gil G, Gemmy Cheung CM. Intervortex venous anastomosis in pachychoroid-related disorders. *Retina.* 2021 1;41(5):997-1004.
- 14- Spaide RF, Gemmy Cheung CM, Matsumoto H, Kishi S, Boon CJF, van Dijk EHC, et al. Venous overload choroidopathy: A hypothetical framework for central serous chorioretinopathy and allied disorders. *Prog Retin Eye Res.* 2021 21:100973. (Epub ahead of print).
- 15- Teussink MM, Breukink MB, van Grinsven MJ, Hoyng CB, Klevering BJ, Boon CJ, et al. OCT Angiography Compared to Fluorescein and Indocyanine Green Angiography in Chronic Central Serous Chorioretinopathy. *Invest Ophthalmol Vis Sci.* 2015;56(9):5229-37.
- 16- Nicolò M, Rosa R, Musetti D, Musolino M, Saccheggiani M, Traverso CE. Choroidal Vascular Flow Area in Central Serous Chorioretinopathy Using Swept-Source Optical Coherence Tomography Angiography. *Invest Ophthalmol Vis Sci.* 2017 1;58(4):2002-2010.
- 17- Ho M, Lai FHP, Ng DSC, Iu LPL, Chen LJ, Mak ACY, et al. Analysis of choriocapillaris perfusion and choroidal layer changes in patients with chronic central serous chorioretinopathy randomised to micropulse laser or photodynamic therapy. *Br J Ophthalmol.* 2021;105(4):555-560.
- 18- Fung, A. T., L. A. Yannuzzi and K. B. Freund. Type 1 (sub-retinal pigment epithelial) neovascularization in central serous chorioretinopathy masquerading as neovascular age-related macular degeneration. *Retina.* 2012; 32(9): 1829-1837.
- 19- Pang, C. E. and K. B. Freund. Pachychoroid neovascularopathy. *Retina.* 2015; 35(1): 1-9
- 20- Hage, R., S. Mrejen, V. Krivosic, G. Quentel, R. Tadayoni and A. Gaudric. Flat irregular retinal pigment epithelium detachments in chronic central serous chorioretinopathy and choroidal neovascularization. *Am J Ophthalmol.* 2015; 159(5): 890-903. e893.
- 21- Bousquet E, Bonnin S, Mrejen S, Krivosic V, Tadayoni R, Gaudric A. Optical coherence tomography angiography of flat irregular pigment epithelium detachment in chronic central serous chorioretinopathy. *Retina.* 2018;38:629-38.
- 22- Quaranta-El Maftouhi, M., A. El Maftouhi and C. M. Eandi. Chronic central serous chorioretinopathy imaged by optical coherence tomographic angiography. *Am J Ophthalmol.* 2015;160(3): 581-587.e581
- 23- Sacconi R, Tomasso L, Corbelli E, Carnevali A, Querques L, Casati S, et al. Early response to the treatment of choroidal neovascularization complicating central serous chorioretinopathy: a OCT-angiography study. *Eye (Lond).* 2019;33(11):1809-1817.
- 24- Spaide RF. Optical coherence tomography angiography signs of vascular abnormalization with antiangiogenic therapy for choroidal neovascularization. *Am J Ophthalmol.* 2015;160:

- 6–16.
- 25 - Yang LH, Jonas JB, Wei WB. Conversion of central serous chorioretinopathy to polypoidal choroidal vasculopathy. *Acta Ophthalmol.* 2015;93(6):e512-4.
- 26 - Ahuja RM, Downes SM, Stanga PE, Koh AH, Vingerling JR, Bird AC. Polypoidal choroidal vasculopathy and central serous chorioretinopathy. *Ophthalmology.* 2001;108(6):1009-10.





## 12.2.

# POLIPOYDAL CHOROIDAL VASCULOPATHY

Rufino Silva<sup>1,2,3,4</sup>, Jorge Simão<sup>2,3</sup>, Cláudia Farinha<sup>1,2,3</sup>, João Pedro Marques<sup>1,2</sup>, Maria Luz Cachulo<sup>1,2</sup>

1- University of Coimbra, Coimbra Institute for Clinical and Biomedical Research (iCBR), Faculty of Medicine, Coimbra, Portugal;

2- Ophthalmology Department, Centro Hospitalar e Universitário de Coimbra (CHUC), Portugal;

3- Association for Innovation and Biomedical Research on Light and Image (AIBILI), Coimbra, Portugal.

4- Coimbra Medical Space, Coimbra, Portugal

## INTRODUCTION

Polypoidal choroidal vasculopathy (PCV) was described for the first time in 1982<sup>1</sup> and is characterized by the presence of polyp-like dilations and an abnormal branching vascular network<sup>2,3</sup>. Different terms were proposed in the past to designate this disorder, namely “posterior uveal bleeding syndrome”<sup>24</sup> and “multiple recurrent retinal pigment epithelium detachments in black women”<sup>25</sup>. More recently, the term aneurysmal type 1 neovascularization was adopted<sup>6</sup>. In spite of the unquestionable presence of aneurysmal vascular dilations or tangled vessels and branching vascular networks, the disease is most widely known as Polypoidal Choroidal Vasculopathy (PCV)<sup>7-10</sup>. It is considered to be a primary abnormality of inner choroidal vessels. The affected vessels tend to bulge causing aneurysmatic protrusions or tangled vessels, due to the defective lining secondary to minimal pericytes and thinned out endothelial cells<sup>11</sup>. Hyperpermeability and hemorrhage due to stasis of a dilated venule and an arteriole involved by sclerosis at the site where they cross in the inner choroid might cause oedema and degeneration of the tissue<sup>12</sup>. Voluminous accumulation of blood cells and fibrin might generate elevation of tissue pressure sufficient to displace the weak ended lesion anteriorly. The result suggests that the polypoidal vessels in this case represent abnormalities in the inner choroidal vasculature<sup>12</sup>. The diagnosis is based on the presence of polyps on indocyanine-green angiography (ICGA), which remains the goldstandard. However, Optical Coherent Tomography (OCT) and Optical Coherent Tomography Angiography (OCTA) together have a high sensitivity and specificity for the diagnosis of PCV<sup>13,14</sup>. The primary abnormality involves the choroidal circulation and the characteristic lesion is an inner choroidal vascular network of vessels ending, in the great majority of cases, in an aneurysmal dilatation. Clinically, a reddish orange, spheroid, polyp-like structure may be observed. Genetic variants associated with PCV do not appear to translate across ethnic lines<sup>15-18</sup>. The natural course of the disease often follows a remitting-relapsing course with chronic, multiple, recurrent serosanguineous detachments of the retinal pigment epithelium and neurosensory retina with long-term preservation of good vision in many cases(6). A more

recent knowledge has expanded the spectrum of PCV allowing us a clear characterization of PCV as a distinct subtype of exudative age-related macular degeneration (AMD), but can also be identified in other diseases<sup>13,16,19</sup>. Caucasian populations with PCV may express genotypic and phenotypic characteristics that are closer to AMD characteristics than Asian patients<sup>13,16,19,20</sup>. The best treatment is neither well defined nor unanimous. The 12-month results of the EVEREST II trial<sup>21-23</sup> showed that combination therapy was superior to ranibizumab monotherapy in best-corrected visual acuity (BCVA) gains and complete polyp regression while requiring fewer injections. The PLANET study<sup>7,8</sup> a 2-year randomized clinical trial (RCT) designed to evaluate the efficacy and safety of treatment with intravitreal aflibercept injection in PCV by comparing intravitreal Aflibercept monotherapy with Aflibercept plus rescue photodynamic therapy (PDT), showed that functional and anatomical outcomes of intravitreal Aflibercept monotherapy were noninferior to intravitreal Aflibercept plus rescue PDT. The ATLANTIC study<sup>24</sup> demonstrated the efficacy and safety of Aflibercept monotherapy at 12 months in a treat and extend regimen with no additional benefit of PDT.

## DIAGNOSIS OF POLIPOYDAL CHOROIDAL VASCULOPATHY

PCV is becoming increasingly recognized and diagnosed. In Asia, 20% to 50% of patients with serosanguineous maculopathy are diagnosed with PCV(13,21). It has also been previously reported in 4% to 14% of Caucasian patients<sup>21,25</sup> and over 21.5% of patients who had neovascular AMD resistant to anti-vascular endothelial growth factor (VEGF) therapy were actually PCV(26) presumed to be choroidal neovascularisation, previously treated with  $\geq 8$  intravitreal injections of ranibizumab 0.5 mg (Lucentis; Novartis AG, Basel, Switzerland). The diagnosis of PCV can often be missed due to the infrequent use of ICGA. PCV differs from nAMD in clinical presentation, response to anti-VEGF therapy, and treatment paradigms<sup>6,20,27</sup>. The distinction between PCV and nAMD is thus clinically important in clinical practice.

ICGA is the gold standard exam for the diagnosis

of PCV. The Everest study defined the criteria for the diagnosis in 2012 and these criteria are still a reference<sup>21,28,29</sup>. They include the presence early focal sub-retinal hyperfluorescence on ICGA (Fig.1) and at least one of the following six diagnostic criteria: (1) nodular appearance of polyp(s) on stereoscopic examination, (2) hypofluorescent halo around nodule(s), (3) presence of a branching vascular network, (4) pulsation of polyp(s) on dynamic ICGA, (5) orange sub-retinal nodules on color fundus photography, or (6) massive sub-macular hemorrhage ( $\geq 4$  disc areas in size). These criteria are based on ICGA and in the presence of early focal sub-RPE hyperfluorescence. However, ICGA is invasive, expensive, time-consuming, not widely available, and rarely may cause life-threatening allergic reactions. Structural OCT and OCTA complemented with color fundus photography have been reported as highly specific and sensitive for the diagnosis of PCV with or without fluorescein angiography<sup>30-33</sup>.

### STRUCTURAL OCT FINDINGS IN PCV

When used alone or with other imaging modalities, structural OCT has become a useful tool for the screening and diagnosis of PCV. Multiple, sharply peaked pigment epithelial detachments (PEDs) with an associated “double layer sign” in OCT B-scans are typical features<sup>27,34,35</sup>. Polyps are defined by an inverted “U-shaped” elevation of the retinal pigment epithelium (RPE) with heterogeneous internal reflectivity<sup>36</sup> (Fig. 1 and Fig.2). The PCV polyps are usually observed as a

notch in the PED or immediately attached to the elevated RPE<sup>14,36</sup>. The BVN has a characteristic appearance with a “double-layer sign” that is visualized as two parallel hyperreflective lines on OCT<sup>14,36</sup>. En face OCT features also can help in diagnosing polypoidal lesions, revealing the presence of dilated vascular structures with hyperreflective borders and polypoidal vascular dilations.<sup>36-38</sup>

### OCTA FOR THE DIAGNOSIS OF PCV

OCTA has been reported to be more accurate than structural OCT for the diagnosis of PCV<sup>39-43</sup>. However, most of these studies have used en face spectral-domain OCTA imaging, which is capable of detecting BVNs in a high percentage of the cases, but the detection of the polypoidal lesions is more variable ranging from 17%-92.3%<sup>32,39,40,42</sup>. In fact, OCTA can detect flow with a velocity as low as 0.2~0.3 mm/s using a 70k-Hz A-scan within seconds<sup>44,45</sup>. In contrast, ICGA takes at least 5 minutes to identify polyps from the first 30 seconds of video recorded by a confocal scanning laser ophthalmoscope in the filling phase of the polyps, and 5 minutes to picture hyperfluorescent polyps in the early phase<sup>45,46</sup>. The absence of a flow signal in OCTA in polyps revealed by ICGA has been described to represent 7 to 50% of the lesions<sup>47,48</sup> and may indicate slow, turbulent or compromised filling of blood flow from choroidal vessels<sup>21,45,48</sup>. OCTA manual segmentation is fundamental for detecting each polypoidal lesion and decrease the rate of undetected polyps<sup>48</sup>.

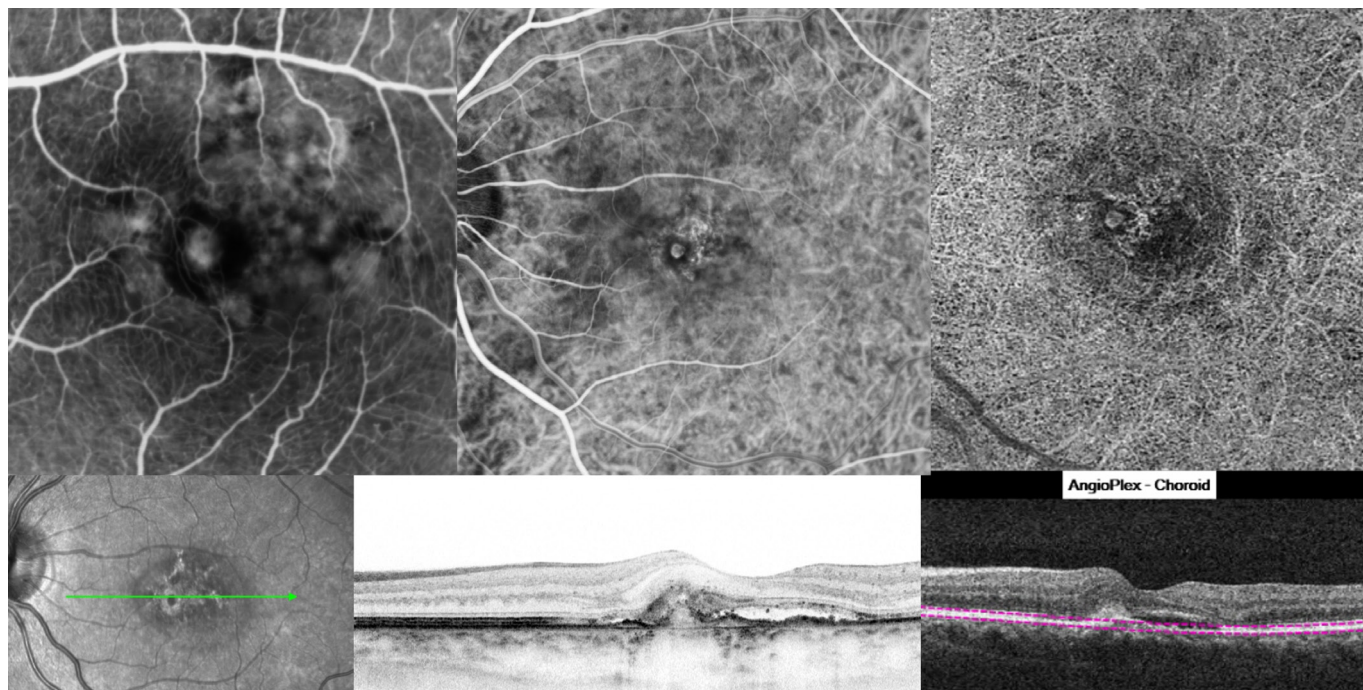


**Figure 1.** PCV lesion in FA, ICGA, OCTA and SD-OCT. In this case the polyp component is seen in both ICGA and OCT-A as a round hypersignal structure with flow, surrounded by a hyposignal halo. The BVN is best appreciated in en face OCTA. The SD-OCT shows the peaked RPE elevation typical for the underlying presence of polyps and the double layer sign representing the BVN, along with subretinal fluid.

Cross-sectional OCTA is more sensitive than en face OCTA in detecting flow signal in polyps. A cross-sectional study combined SD-OCT and OCTA to differentiate treatment-naïve eyes with PCV, choroidal neovascularization, and retinal angiomatous proliferation and compared with the diagnosis based on fluorescein angiography and indocyanine green angiography<sup>49</sup>. Spectral domain OCT signs used to diagnose PCV included presence of two out of three of any RPE detachment (pigment epithelial detachment/double-layer sign), notched or narrow-peaked pigment epithelial detachment, or round subretinal RPE structure. OCTA signs used to diagnose PCV included presence of a localized subretinal pigment epithelium hyperflow signal in the cross-sectional OCTA and/or presence of a focal hyperflow sign in the en face OCTA outer retina slab (Fig.2). Combination of OCT and OCTA achieved 82.6% sensitivity and 100.0% specificity for differentiating PCV from choroidal neovascularization/retinal angiomatous proliferation. Compared with spectral-domain OCTA, swept-source OCTA (SS-OCTA) uses a longer wavelength of light that penetrates better through the RPE, has a faster scanning speed that allows for denser raster scans for a given field

of view and is safer. Higher laser energy can be used, resulting in images with a better signal-to-noise ratio<sup>33</sup> and a better detection of blood flow for neovascular lesions beneath the RPE<sup>50–52</sup>. Cheung and associates<sup>53</sup> used SS-OCTA to evaluate PCV, and the sensitivities and specificities for detection of BVNs and polyps were compared with indocyanine green angiography. SS-OCTA had a sensitivity and specificity of 83.0% and 57.1% for vascular networks, and 40.5% and 66.7% for polyps, respectively. This is however inferior to the cross-sectional approach with SD-OCT and OCTA<sup>49</sup>.

In almost all the studies, both ICGA and SS-OCTA images were evaluated side-by-side rather than graded independently, and the results were compared. But to determine whether SD-OCTA or SS-OCTA can replace ICGA for PCV diagnosis, images need to be independently classified and only then compared. In a recent study<sup>33</sup> polypoidal lesions were independently identified in all eyes using both modalities, and there was agreement on the number of polypoidal lesions in 55% of eyes. In 39% of the eyes, SS-OCTA graders identified a greater number of polypoidal lesions, only in 6% ICGA graders identified more lesions. There was

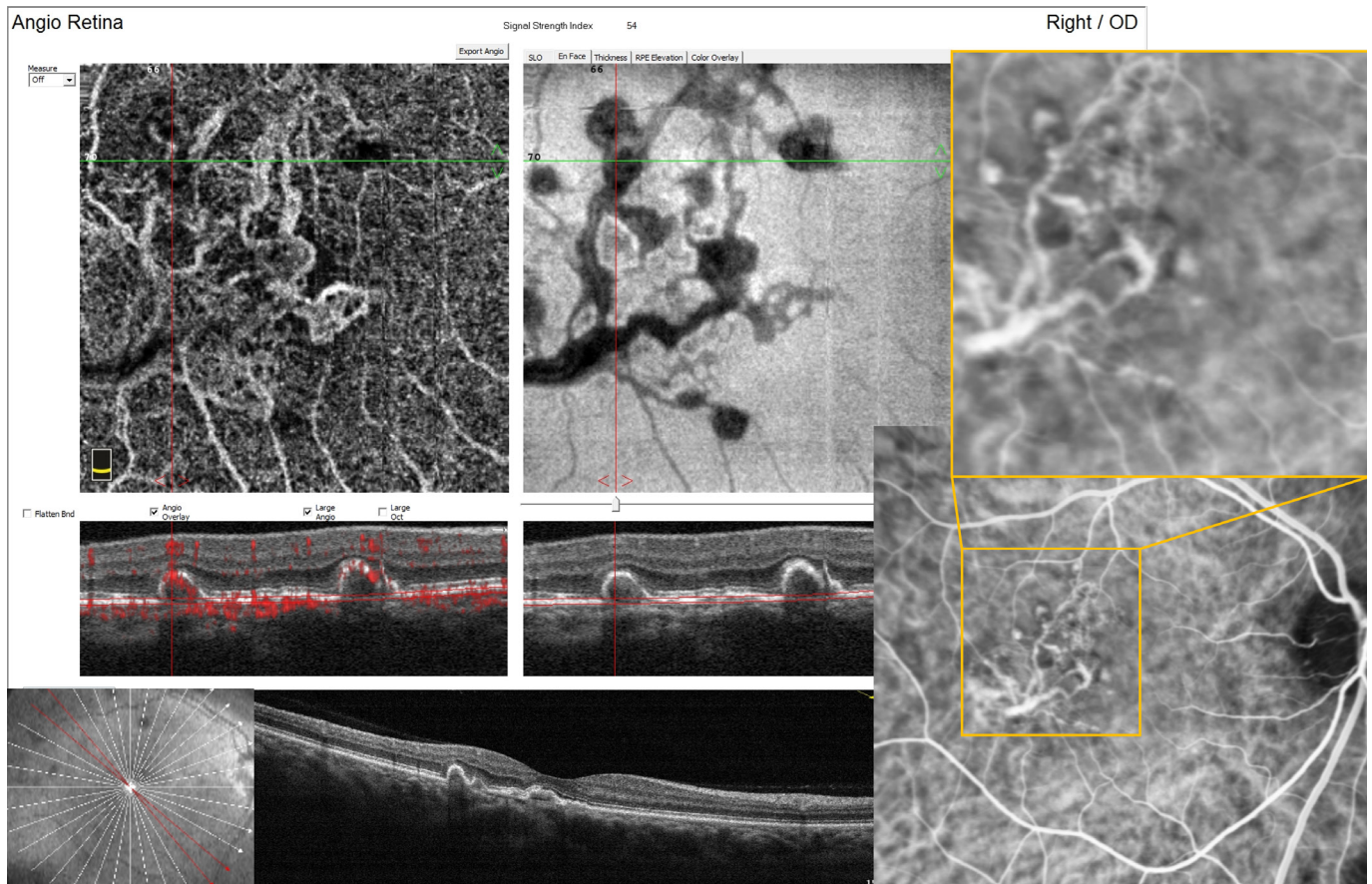


**Figure 2.** Macular PCV lesion in OCTA and ICGA. OCTA en face image in the left shows the BVN with more detail compared to ICGA, however the polyps are devoid of flow in the choriocapillaris slab (where the BVN is best seen), and appear as rounded hyposignal structures; in the B-scan image with super-imposed flow (below, in the left) one can appreciate the presence of flow (in red) in the top of the peaked RPE elevations corresponding to polyps. En face structural OCT (above, in the center) shows very nicely the BVN and polyps of the PCV lesion in close correspondence with the PCV lesion observed in ICGA.

no significant difference in the lesion area measurements. ICGA misdiagnosed as focal PCV lesions some areas of atrophy and a low-lying serous retinal pigment epithelial detachment, erroneously identified as part of the BVN. SS-OCTA imaging correctly diagnosed the focal areas of atrophy and the serous retinal pigment epithelial detachment. The lesion with the largest difference in area measurements resulted from focal areas of atrophy, misdiagnosed as polypoidal lesions on ICGA, and a low-lying serous retinal pigment epithelial detachment erroneously identified as part of the BVN by ICGA graders. Using manual segmentation in the SS-OCTA improves identification of type 2 neovascularization that can be missed with ICGA, and the presence of tangled vessels that can appear as small ICGA hypercyanescent rings when the dye fades<sup>33,54</sup>. According to this small study<sup>33</sup>, which warrants further investigation, SS-OCTA imaging is comparable to ICGA for the diagnosis of treatment-naïve PCV and may even be better than ICGA in correctly identifying polypoidal lesions and BVNs in naïve PCV. Considering the difficulty of accessing the ICGA, the side effects and costs, the fact that some ICGA findings may be misidentified as PCV lesions, the Everest Criteria for PCV should be revised with the inclusion of SS / SD-OCTA en face and cross-sectional imaging.

### TAKE-HOME MESSAGES

- ICG is still the gold standard for PCV diagnosis
- The structural signs of SD-OCT used to diagnose PCV included the presence of RPE detachment / double-layer sign, notched or narrow-peaked RPE detachment, or round subretinal pigment epithelium structure.
- OCTA signs used to diagnose PCV included the presence of a localized hyperflow sign from the subretinal pigment epithelium in the cross-sectional OCTA and/or the presence of a focal hyperflow sign in the en face OCTA.
- Structural SD/SS-OCT and transverse SD-OCTA findings demonstrated a sensitivity greater than 80% and a specificity near 100% to differentiate PCV from choroidal neovascularization/retinal angioma-tous proliferation.

### REFERENCES

1. Yannuzzi LA, Sorenson J, Spaide RF, Lipson B. Idiopathic polypoidal choroidal vasculopathy (IPCV). *Retina*. 1990;10(1):1–8.
2. Yannuzzi LA, Ciardella A, Spaide RF, Rabb M, Bailey Freund K, Orlock DA. The expanding clinical spectrum of idiopathic polypoidal choroidal vasculopathy. *Arch Ophthalmol*. 1997;115(4):478–85.
3. Koh AHC, Chen LJ, Chen SJ, Chen Y, Giridhar A, Iida T, et al. Polypoidal choroidal vasculopathy: Evidence-Based Guidelines for Clinical Diagnosis and Treatment. 33, *Retina*; 2013. 686–716.
4. Kleiner RC, Brucker AJ, Johnston RL. The posterior uveal bleeding syndrome. *Retina*. 1990;10(1):9–17.
5. Stern RM, Nicholas Zakov Z, Zegarra H, Gutman FA. Multiple recurrent serosanguineous retinal pigment epithelial detachments in black women. *Am J Ophthalmol*. 1985;100(4):560–9.
6. Dansingani KK, Gal-Or O, Sadda SR, Yannuzzi LA, Freund KB. Understanding aneurysmal type 1 neovascularization (polypoidal choroidal vasculopathy): a lesson in the taxonomy of ‘expanded spectra’ – a review. 46, *Clinical and Experimental Ophthalmology*. Blackwell Publishing; 2018. p. 189–200.
7. Lee WK, Iida T, Ogura Y, Chen SJ, Wong TY, Mitchell P, et al. Efficacy and safety of intravitreal aflibercept for polypoidal choroidal vasculopathy in the PLANET study a randomized clinical trial. *JAMA Ophthalmol*. 2018 Jul 1;136(7):786–93.
8. Wong TY, Ogura Y, Lee WK, Iida T, Chen SJ, Mitchell P, et al. Efficacy and Safety of Intravitreal Aflibercept for Polypoidal Choroidal Vasculopathy: Two-Year Results of the Aflibercept in Polypoidal Choroidal Vasculopathy Study. *Am J Ophthalmol*. 2019 Aug 1;204:80–9.
9. Leal S, Silva R, Figueira J, Cachulo ML, Pires I, De Abreu JRF, et al. Photodynamic therapy with verteporfin in polypoidal choroidal vasculopathy: Results after 3 years of follow-up. *Retina*. 2010;30(8):1197–205.
10. Silva RM, Figueira J, Cachulo ML, Duarte L, Faria de Abreu JR, Cunha-Vaz JG. Polypoidal choroidal vasculopathy and photodynamic therapy with verteporfin. *Graefes Arch Clin Exp Ophthalmol*. 2005;243(10).
11. Lafaut Ba, Aisenbrey S, Van Den Broecke C, Bartz-Schmidt K-U, Heimann K. Polypoidal choroidal vasculopathy pattern in age-related macular degeneration. *Retina*. 2000;20(6):650.
12. Okubo A, Sameshima M, Uemura A, Kanda S, Ohba N. Clinicopathological correlation of polypoidal choroidal vasculopathy revealed by ultrastructural study. *Br J Ophthalmol*. 2002;86(10):1093–8.
13. Cheung CMG, Lai TYY, Ruamviboonsuk P, Chen SJ, Chen Y, Freund KB, et al. Polypoidal Choroidal Vasculopathy: Definition, Pathogenesis, Diagnosis, and Management. Vol. 125, *Ophthalmology*. 2018. 708–24.
14. De Salvo G, Vaz-Pereira S, Keane PA, Tufail A, Liew G. Sensitivity and specificity of spectral-domain optical coherence tomography in detecting idiopathic polypoidal choroidal vasculopathy. *Am J Ophthalmol*. 2014;158(6):1228–1238.e1. /
15. Gotoh N, Yamada R, Nakanishi H, Saito M, Iida T, Matsuda F, et al. Correlation between CFH Y402H and HTRA1 rs11200638 genotype to typical exudative age-related macular degeneration and polypoidal choroidal vasculopathy phenotype in the Japanese population. *Clin Exp Ophthalmol*. 2008;36(5):437–42.
16. Jordan-Yu JMN, Teo KYC, Fan Q, Gana JC, Leopando AK, Nunes S, et al. Phenotypic And Genetic Variations Between Asian And Caucasian Polypoidal Choroidal Vasculopathy Eyes. *Br J Ophthalmol*. 2020;(in press).
17. Honda S, Matsumiya W, Negi A. Polypoidal choroidal vasculopathy: Clinical features and genetic predisposition [Internet]. Vol. 231, *Ophthalmologica*. Ophthalmologica; 2014 [cited 2020 Nov 22]. p. 59–74. Available from: <https://pubmed.ncbi.nlm.nih.gov/24280967/>
18. Zhang X, Wen F, Zuo C, Li M, Chen H, Wu K. Association of genetic variation on chromosome 9p21 with polypoidal choroidal

- vasculopathy and neovascular age-related macular degeneration. *Investig Ophthalmol Vis Sci*. 2011 Oct 1;52(11):8063–7.
19. Wong CW, Yanagi Y, Lee WK, Ogura Y, Yeo I, Wong TY, et al. Age-related macular degeneration and polypoidal choroidal vasculopathy in Asians. Vol. 53, *Progress in Retinal and Eye Research*. Elsevier Ltd; 2016. 107–39.
  20. Mitchell P, Liew G, Gopinath B, Wong TY. Age-related macular degeneration. Vol. 392, *The Lancet*. Lancet Publishing Group; 2018. p. 1147–59.
  21. Koh A, Lee WK, Chen LJ, Chen SJ, Hashad Y, Kim H, et al. Everest study: Efficacy and safety of verteporfin photodynamic therapy in combination with ranibizumab or alone versus ranibizumab monotherapy in patients with symptomatic macular polypoidal choroidal vasculopathy. *Retina*. 2012 Sep;32(8):1453–64.
  22. Lim TH, Lai TYY, Takahashi K, Wong TY, Chen LJ, Ruamviboonsuk P, et al. Comparison of Ranibizumab with or without Verteporfin Photodynamic Therapy for Polypoidal Choroidal Vasculopathy: The EVEREST II Randomized Clinical Trial. *JAMA Ophthalmol*. 2020;138(9):935–42.
  23. Koh A, Lai TYY, Takahashi K, Wong TY, Chen LJ, Ruamviboonsuk P, et al. Efficacy and safety of ranibizumab with or without verteporfin photodynamic therapy for polypoidal choroidal vasculopathy: A randomized clinical trial. *JAMA Ophthalmol*. 2017 1;135(11):1206–13.
  24. Marques JP, Bernardes J, Geada S, Soares M, Teixeira D, Farinha C, et al. Non-exudative macular neovascularization in pseudoxanthoma elasticum. *Graefes Arch Clin Exp Ophthalmol*. 2020;
  25. Hatz K, Prunte C. Polypoidal choroidal vasculopathy in Caucasian patients with presumed neovascular age-related macular degeneration and poor ranibizumab response. *Br J Ophthalmol*. 2014;98(2):188–94.
  26. Hatz K, Prunte C. Polypoidal choroidal vasculopathy in Caucasian patients with presumed neovascular age-related macular degeneration and poor ranibizumab response. *Br J Ophthalmol*. 2014;98(2):188–94.
  27. Liu R, Li J, Li Z, Yu S, Yang Y, Yan H, et al. Distinguishing polypoidal choroidal vasculopathy from typical neovascular age-related macular degeneration based on spectral domain optical coherence tomography. *Retina*. 2016;36(4):778–86.
  28. Tan CS, Ngo WK, Lim LW, Tan NW, Lim TH. EVEREST study report 3: diagnostic challenges of polypoidal choroidal vasculopathy. Lessons learnt from screening failures in the EVEREST study. *Graefes Arch Clin Exp Ophthalmol*. 2016;254(10):1923–30.
  29. Tan CS, Ngo WK, Chen JP, Tan NW, Lim TH, Koh A, et al. EVEREST study report 2: Imaging and grading protocol, and baseline characteristics of a randomised controlled trial of polypoidal choroidal vasculopathy. *Br J Ophthalmol*. 2015 May 1;99(5):624–8.
  30. Chaikitmongkol V, Khunsongkiet P, Patikulasila D, Ratanasukon M, Watanachai N, Jumroendararasame C, et al. Color Fundus Photography, Optical Coherence Tomography, and Fluorescein Angiography in Diagnosing Polypoidal Choroidal Vasculopathy. *Am J Ophthalmol*. 2018 1;192:77–83.
  31. Chaikitmongkol V, Kong J, Khunsongkiet P, Patikulasila D, Sachdeva M, Chavengsakongkram P, et al. Sensitivity and Specificity of Potential Diagnostic Features Detected Using Fundus Photography, Optical Coherence Tomography, and Fluorescein Angiography for Polypoidal Choroidal Vasculopathy. In: *JAMA Ophthalmology*. American Medical Association; 2019. 661–7.
  32. Cheung CMG, Kim JE. Diagnosing Polypoidal Choroidal Vasculopathy Without Indocyanine Green Angiography. 137, *JAMA Ophthalmology*. 2019. 667–8.
  33. Kim K, Yang J, Feuer W, Gregori G, Kim ES, Rosenfeld PJ, et al. A Comparison Study of Polypoidal Choroidal Vasculopathy Imaged with Indocyanine Green Angiography and Swept-Source Optical Coherence Tomography Angiography. *Am J Ophthalmol* [Internet]. 2020 Sep 1 [cited 2021 May 30];217:240–51.
  34. Sengupta S, Surti R, Vasavada D. Sensitivity and Specificity of Spectral-Domain Optical Coherence Tomography in Detecting Idiopathic Polypoidal Choroidal Vasculopathy. *Am J Ophthalmol*. 2015;160(1):203–4.
  35. De Salvo G, Vaz-Pereira S, Keane PA, Tufail A, Liew G. Sensitivity and specificity of spectral-domain optical coherence tomography in detecting idiopathic polypoidal choroidal vasculopathy. *Am J Ophthalmol*. 2014 1;158(6):1228–1238.e1.
  36. Kokame GT, Shantha JG, Hirai K, Ayabe J. En Face Spectral-Domain Optical Coherence Tomography for the Diagnosis and Evaluation of Polypoidal Choroidal Vasculopathy. *Ophthalmic Surgery, Lasers Imaging Retin*. 2016;47(8):737–44.
  37. Simonett JM, Chan EW, Chou J, Skondra D, Colon D, Chee CK, et al. Quantitative analysis of en face spectral-domain optical coherence tomography imaging in polypoidal choroidal vasculopathy. In: *Ophthalmic Surgery Lasers and Imaging Retina*. Slack Incorporated; 2017. 126–33.
  38. Semoun O, Coscas F, Coscas G, Lalloum F, Srour M, Souied EH. En face enhanced depth imaging optical coherence tomography of polypoidal choroidal vasculopathy. *Br J Ophthalmol*. 2016 1;100(8):1028–34.
  39. Tanaka K, Mori R, Kawamura A, Nakashizuka H, Wakatsuki Y, Yuzawa M. Comparison of OCT angiography and indocyanine green angiographic findings with subtypes of polypoidal choroidal vasculopathy. *Br J Ophthalmol*. 2017;101(1):51–5.
  40. Tomiyasu T, Nozaki M, Yoshida M, Ogura Y. Characteristics of polypoidal choroidal vasculopathy evaluated by optical coherence tomography angiography. *Investig Ophthalmol Vis Sci*. 2016;57(9):OCT324–30.
  41. Takayama K, Ito Y, Kaneko H, Kataoka K, Sugita T, Maruko R, et al. Comparison of indocyanine green angiography and optical coherence tomographic angiography in polypoidal choroidal vasculopathy. *Eye*. 2017 1;31(1):45–52.
  42. Srour M, Querques G, Souied EH. Optical Coherence Tomography Angiography of Idiopathic Polypoidal Choroidal Vasculopathy. *Dev Ophthalmol*. 2016;56:71–6.
  43. Wang Y, Yang J, Li B, Yuan M, Chen Y. Detection Rate and Diagnostic Value of Optical Coherence Tomography Angiography in the Diagnosis of Polypoidal Choroidal Vasculopathy: A Systematic Review and Meta-Analysis. *J Ophthalmol*. 2019;2019:6837601.
  44. Tokayer J, Jia Y, Dhalla A-H, Huang D, Huang D, Swanson EA, et al. Medical and biological imaging; (170.4470) *Ophthalmology*; (999.999) Blood flow. *Arch Ophthalmol*. 1991;254(5035):114–6.

45. Miura M, Muramatsu D, Hong YJ, Yasuno Y, Iwasaki T, Goto H. Noninvasive vascular imaging of polypoidal choroidal vasculopathy by Doppler optical coherence tomography. *Investig Ophthalmol Vis Sci*. 2015;56(5):3179–86.
46. Bo Q, Yan Q, Shen M, Song M, Sun M, Yu Y, et al. Appearance of Polypoidal Lesions in Patients with Polypoidal Choroidal Vasculopathy Using Swept-Source Optical Coherence Tomographic Angiography. *JAMA Ophthalmol*. 2019 1;137(6):642–50.
47. Inoue M, Balaratnasingam C, Freund KB. Optical coherence tomography angiography of polypoidal choroidal vasculopathy and polypoidal choroidal neovascularization. *Retina*. 2015 27;35(11):2265–74.
48. Chang C-J, Huang Y-M, Hsieh M-H, Li A-F, Chenid S-J. Flow signal change in polyps after anti-vascular endothelial growth factor therapy. 2020.
49. Cheung CMG, Yanagi Y, Akiba M, Tan A, Mathur R, Chan CM, et al. Improved detection and diagnosis of polypoidal choroidal vasculopathy using a combination of optical coherence tomography and optical coherence tomography angiography. *Retina*. 2019;39(9):1655–63.
50. Miller AR, Roisman L, Zhang Q, Zheng F, Rafael de Oliveira Dias J, Yehoshua Z, et al. Comparison between spectral-domain and swept-source optical coherence tomography angiographic imaging of choroidal neovascularization. *Investig Ophthalmol Vis Sci*. 2017;58(3):1499–505.
51. Novais EA, Adhi M, Moulton EM, Louzada RN, Cole ED, Husvogt L, et al. Choroidal Neovascularization Analyzed on Ultrahigh-Speed Swept-Source Optical Coherence Tomography Angiography Compared to Spectral-Domain Optical Coherence Tomography Angiography. *Am J Ophthalmol*. 2016 1;164:80–8.
52. Cicinelli MV, Cavalleri M, Consorte AC, Rabiolo A, Sacconi R, Bandello F, et al. Swept-source and spectral domain optical coherence tomography angiography versus dye angiography in the measurement of type 1 neovascularization. *Retina*. 2020 1;40(3):499–506.
53. Cheung CMG, Yanagi Y, Mohla A, Lee SY, Mathur R, Chan CM, et al. Characterization and differentiation of polypoidal choroidal vasculopathy using swept source optical coherence tomography angiography. *Retina*. 2017;37(8):1464–74.
54. Yuzawa M, Mori R, Kawamura A. The origins of polypoidal choroidal vasculopathy. *Br J Ophthalmol*. 2005;89(5):602–7.

# HIGH MYOPIA

Fernanda Vaz, Maria Picoto  
Hospital de Egas Moniz, CHLO

## INTRODUCTION

Yannuzzi *et al* defined high myopia as a condition in which the spherical equivalent refractive error of an eye is  $\geq 6.00$  negative dioptres and the ocular accommodation is relaxed<sup>1</sup>.

Pathological myopia is the categorical term for the adverse complications of myopia, defined as an excessive axial elongation associated with myopia that leads to structural changes in the posterior segment of the eye (including posterior staphyloma, myopic maculopathy, and high myopia-associated optic neuropathy), eventually leading to the loss visual acuity<sup>1</sup>.

High myopia and pathological myopia are major causes of legal blindness and low vision worldwide, affecting particularly youngsters, increasing in prevalence over the last decades<sup>2-4</sup>. The natural course of high myopia is variable and the development of pathological myopia is not fully understood. When the macula is involved, a dramatic reduction in the visual acuity may eventually occur. Therefore, it is of outmost importance to determine macular changes associated with high myopia<sup>2-5</sup>. Optical coherence tomography (OCT) and OCT-angiography (OCTA) are essential tools for their identification and follow-up<sup>5</sup>.

OCTA findings in retinal microvasculature are important to elucidate the pathophysiological mechanisms of high myopia, to assist the discovery of novel treatment modalities and protective measures to prevent myopic retinopathy<sup>2,6</sup>.

## RETINA

According to recent reports in the literature, high myopia is associated with reduced vascular densities of the macular superficial (SCP) and deep capillary plexus (DCP). Li *et al* found that both the superficial (SVD) and deep retinal vascular densities (DVD) were significantly decreased in the myopic group, and were negatively correlated with the axial lengths (AL) in the myopic eye<sup>6</sup>. Ucak and colleagues compared high myopic eyes with a control group and determined a significant decrease in the SVD and DVD in the former, which was significantly associated with an elongation in AL and a decrease in the retinal nerve fiber layer (RNFL) and ganglion cell layer (GCL) thicknesses.

Moreover, a significant positive correlation between visual acuity and either SVD or DVD was found. They also noted that the superficial or deep foveal avascular zones (FAZ) were not significantly different between the two cohorts<sup>2</sup>. Yang *et al* reported retinal microvascular network alterations in highly myopic eyes, which correlated with AL elongation<sup>7</sup>.

Fan *et al* compared the OCTA findings of three groups: a control group, a moderate myopic group and a high myopic group. They reported that both the SVD and DVD were decreased in the myopic groups. The SVD and DVD were reported to be associated with AL, and the SVD was also associated with the GCL thickness. Conversely, the vessel density (VD) in the optic disc region had no difference between groups, and it was not associated with AL, spherical equivalent, or RNFL thickness<sup>8</sup>. Qu *et al* noted that although there was no significant differences in the retinal blood flow velocities of patients with moderate or high myopia compared with the healthy controls, both SVD and DVD were significantly lower in the myopic groups compared with controls<sup>9</sup>. Milani *et al* determined that the FAZ was similar between the myopic and control eyes, but the SVD was significantly lower. They also reported a significant correlation between the SVD and retinal thickness<sup>10</sup>. Al-Sheikh *et al*, measured vessel complexity on both the SCP and DCP and found a statistically lower complexity in myopic eyes compared with controls<sup>11</sup>.

These findings are consistent with previous studies using other techniques. Shimada *et al* reported decreased retinal blood flow, mainly due to the narrowing of the retinal vessel diameter in eyes with high myopia using laser Doppler velocimetry. They also reported that the speed of the blood flow within the vessel was unchanged in myopic eyes<sup>12</sup>.

## CHORIOCAPILLARIS

Previous studies using different imaging modalities have demonstrated reduced choriocapillaris perfusion in high myopia, alongside with reduced retinal perfusion.

Devarajan *et al* studied specific layers of the choroid in highly myopic young adults and examined their association with levels of myopia. They found that eyes with extreme myopia had thinner vascular layers and more vessel branching compared with high myopia<sup>13</sup>.



Al-Sheikh *et al*, demonstrated an increase in the total and average area of flow voids in the choroid circulation and a lower choroidal thickness in myopic eyes compared to the control group<sup>11</sup>.

### CHOROIDAL NEOVASCULARIZATION

Myopic choroidal neovascularization (CNV) is a common complication associated with high myopia, affecting 5% to 11% of patients with this condition<sup>14</sup>. It is the most frequent etiology of CNV before the fifth decade of life<sup>15</sup>. CNV lesions in high myopia are characterized by considerably less retinal edema, subretinal fluid and pigment epithelial detachments, compared with CNV associated with AMD. Furthermore, myopic CNV are usually smaller in size and have a less need for anti-VEGF therapy. These suggest that the development of CNV in myopia may share some signaling pathways with CNV seen in AMD, but with different root causes and pathogenical mechanisms (Figure 1)<sup>4</sup>.

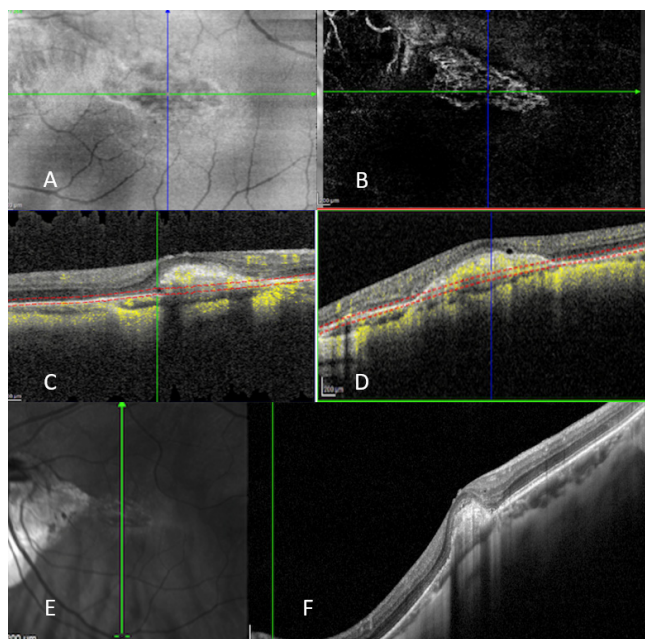


**Figure 1.** Typical OCT-A and OCT-B in a 55-year-old woman with active mCNV (SE: -10D). A-D Organized interlaced neovascular pattern with numerous tiny capillaries and loops, bordered by a dark halo in OCTA. E-F OCT B-scan confirm the lesion is an active mCNV by the dome shaped hyperreflective elevation above the RPE with fuzzy borders associated with discrete retinal changes

Fluorescein angiography (FA) is considered to be the gold standard for detecting myopic CNV and assessing its activity<sup>16</sup>. However, FA is an invasive procedure and results in varying degrees of patient discomfort, including anaphylactic reactions<sup>17</sup>. OCTA has the advantage of not requiring any dye injection and allowing better and more detailed visualization of the vascular networks without being blurred by dye leakage. OCTA showed a

good sensitivity for myopic CNV detection (90%-94%) comparing with FA's (95%)<sup>14,18-20</sup>. Some studies showed a good specificity (93.75%) as well<sup>19,21</sup>.

The ability of OCTA in detecting myopic NVC seems to be even better than in wAMD. This can be explained by the location and size of CNVs. Myopic CNV are usually Type 2 (or "classic" on FA), and therefore located above the RPE. Therefore, the vascular network can be obtained more clearly by OCTA<sup>19</sup>.

Since OCTA reflects the blood flow, it can easily detect active CNVs, whereas it may not detect simple CNV membranes without blood flow (inactive CNVs). Usually there is a good visualization of the myopic neovascular membrane with the 30- $\mu$ m manual segmentation, underneath the Bruch's membrane<sup>18</sup>. Querques *et al* described some morphological findings considered to be biomarkers of activity in myopic CNV on OCTA. According to this study, myopic CNVs appeared as irregular in shape, with poorly defined margins, and without a visible core. In most cases the neovascular network appeared to be mainly interlacing in active myopic CNVs, while in inactive CNVs it appeared to be mainly tangled<sup>21</sup>. In recent works, it was suggested the use of other morphological aspects as biomarkers of activity for myopic CNV. The most frequent appearance of active myopic CNV in OCTA was the pattern of medusa or sea fan (Figure 2). Branching and multiple anastomoses or loops were also very frequent in active CNVs. Conversely, a choroid dark halo (as opposed to wAMD), had low specificity for diagnosing active myopic CNVs<sup>22</sup>.

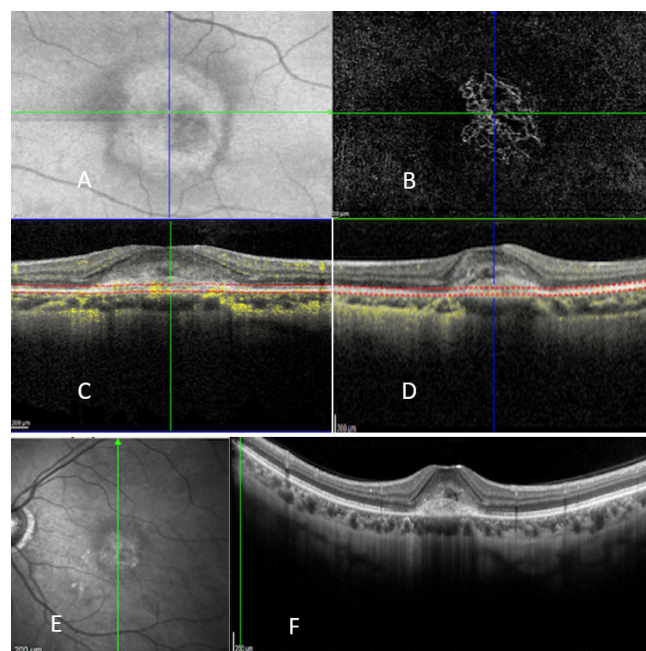


**Figure 2.** Composite OCT images in a 30-year-old woman with active mCNV (SE: -8D). A-D Typical medusa-shaped neovascular network with numerous tiny anastomoses in OCTA. E-F OCT B confirms the lesion as an active mNVC by the fuzzy shape around the hyperreflective NVC and the presence of some intraretinal fluid.

In highly myopic patients especially if a staphyloma is present, or in eyes with high AL with impaired fixation, the performance of the OCTA in image acquisition may be decreased, generating segmentation errors and artifacts<sup>23</sup>. These shortcomings can be surpassed by manually correcting the segmentation and by optimizing the focus<sup>18</sup>.

Garcia-Layana and associates reported that in pathologic myopia with CNV, the sensitivity of OCT B-scans for the detection of CNV activity during treatment was 97.0%. A combination of OCTA and OCT B-scans would be adequate for monitoring the activity of moderate-sized myopic CNV<sup>24</sup>.

## CONCLUSION

OCTA technology has the potential to be a significant adjunct to traditional multimodal imaging assessment for studying the macula in high myopic eyes, particularly when choroidal neovascularization develops. Increasing wide spread use require increased speeds of image capture in the next future. OCTA technology is a valuable tool in detecting myopic CNV and also in predicting the evolution of the lesion, using some morphologic aspects as biomarkers of activity (Figure 3). Additionally, functional flow image and the corresponding B-scan refine the detection rate of myopic CNV. Perhaps in the future this noninvasive technique will replace the role of FA in detecting CNV in high myopic eyes.

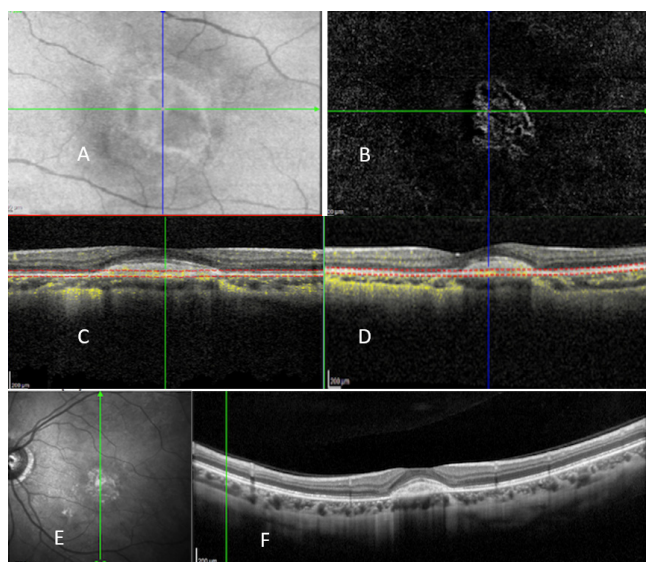


**Figure 3.** Composite images of the patient presented on fig. 2 after anti-vegf intra-vitreous treatment. A-D. OCT A shows apparent reduction of size and vessel density. E-F SD-OCT B-scan shows a decrease of CNV size and confirms the inactive nature of the lesion by the welldefined boundary around the hyperreflective CNV

## REFERENCES

- 1- Flitcroft DI, He M, Jonas JB et al. IMI – Defining and Classifying Myopia: A Proposed Set of Standards for Clinical and Epidemiologic Studies. *Invest Ophthalmol Vis Sci.* 2019; 60: M20-M30
- 2- Ucak T, Icel E, Yilmaz H et al. Alterations in optical coherence tomography angiography findings in patients with high myopia. *Eye.* 2020; 24; 34:1129–1135
- 3- <https://aapos.org/glossary/progressive-high-myopia>
- 4- Ohno-Matsui K, Ishibashi T. Pathologic Myopia, Choroidal Vascular/Bruch's Membrane Disease, section 3. In Schachat AP, editor. *Ryan's Retina*, 6th Edition. Elsevier; 2018. P 1423-1437.
- 5- Ng DSC 1, Cheung CYL, Luk FO et al. Advances of optical coherence tomography in myopia and pathologic myopia. *Eye.* 2016; 30:901–916
- 6- Li M 1, Yang Y 2, Jiang H et al. Retinal Microvascular Network and Microcirculation Assessments in High Myopia, *Am J Ophthalmology.* 2017;174:56-67
- 7- Yang Y, Wang J, Jiang H et al. Retinal microvasculature alteration in high myopia. *Investig Ophthalmol Vis Sci.* 2016;57:6020–6030.
- 8- Fan H, Chen HY, Ma HJ et al. Reduced macular vascular density in myopic eyes. *Chin Med J.* 2017; 20;130:445–451
- 9- Qu D, Lin Y, Jiang H, Shao Y, Shi Y, Airen S, et al. Retinal nerve fiber layer (RNFL) integrity and its relations to retinal microvasculature and microcirculation in myopic eyes. *Eye Vis.* 2018;5:25.
- 10- Milani P, Montesano G, Rossetti L, Bergamini F, Pece A. Vessel density, retinal thickness, and choriocapillaris vascular flow in myopic eyes on OCT angiography. *Graefes Arch Clin Exp Ophthalmol.* 2018;256:1419–27.
- 11- Al-Sheikh M, Phasukkijwatana N, Dolz-Marco R, et al. Quantitative OCT angiography of the retinal microvasculature and the choriocapillaris in myopic eyes. *Invest Ophthalmol Vis Sci.* 2017;58:2063–2069.
- 12- Shimada N, Ohno-Matsui K, Harino S, et al. Reduction of retinal blood flow in high myopia. *Graefes Arch Clin Exp Ophthalmol.* 2004;242 (4):284–288.
- 13- Devarajan K Sim R, Chua J et al. Optical coherence tomography angiography for the assessment of choroidal vasculature in high myopia. *Br Journal of Ophthalmology.* 2020; 104(7):917-923.
- 14- Cheng Y, Ying L, Huang X, Qu Y. Application of optical coherence tomography angiography to assess anti-vascular endothelial growth factor therapy in myopic choroidal neovascularization. *Retina.* 2019; 39:712–718
- 15- Cohen SY, Laroche A, Leguen Y, et al. Etiology of choroidal neovascularization in young patients. *Ophthalmology.* 1996; 103:1241–1244.
- 16- Ohno-Matsui K, Ikuno Y, Lai TYY, Gemmy Cheung CM. Diagnosis and treatment guideline for myopic choroidal neovascularization due to pathologic myopia. *Prog Retin Eye Res.* 2018;63:92–106
- 17- Kwiterovich KA, Maguire MG, Murphy RP, et al. Frequency of adverse systemic reactions after fluorescein angiography. Results of a prospective study. *Ophthalmology* 1991;98(7): 1139–1142.
- 18- Bruyère E, Miere a, Cohen SY, et al. Neovascularization

- secondary to high myopia imaged by optical coherence tomography angiography. *Retina*. 2017; 37:2095–2101.
- 19- Miyata M, Ooto S, Hata M, et al. Detection of Myopic Choroidal Neovascularization Using Optical Coherence Tomography Angiography, *Am J Ophthalmol* 2016;165:108-14.
  - 20- Iacono P, Battaglia PM, Papayannis A, et al. Fluorescein angiography and spectral-domain optical coherence tomography for monitoring anti-VEGF therapy in myopic choroidal neovascularization. *Ophthalmic Res* 2014;52:25–31
  - 21- Querques L, Giuffre C, Corvi F et al. Optical coherence tomography angiography of myopic choroidal neovascularization. *Br J Ophthalmol* 2017;101:609–615.
  - 22- Li S, Sun L, Zhao X, Huang S, et al. Assessing the activity of myopic choroidal neovascularisation Comparison Between Optical Coherence Tomography Angiography and and Dye Angiography. *Retina* 2020 40:1757–1764.
  - 23- Spaide RF, Fujimoto JG, Waheed NK. Image artifacts in optical coherence tomography angiography. *Retina* 2015; 35:2163–2180.
  - 24- Garcia-Layana A, Salinas-Alaman A, Maldonado MJ, Sainz-Gomez C, Fernandez-Hortelano A. Optical coherence tomography to monitor photodynamic therapy in pathological myopia. *Br J Ophthalmol* 2006;90(5):555–558.

# OTHER DISEASES ASSOCIATED WITH CHOROIDAL NEOVASCULARIZATION

Margarida Marques<sup>1</sup>, Maria Elisa Luís<sup>2</sup>

1- Assistente Graduada de Oftalmologia do Centro Hospitalar Universitário de Lisboa Central

2- Assistente Hospitalar de Oftalmologia do Centro Hospitalar Universitário de Lisboa Central

## ANGIOID STREAKS

Angioid streaks were first described in 1889 by Doyne and named by Knapp because of their similarity to blood vessels.<sup>1</sup> They represent Bruch's membrane dehiscences, caused by excess calcification of Bruch's elastic layer.<sup>1,2</sup> The streaks are irregular, linear, reddish lesions that typically radiate outward from the optic disc.<sup>2</sup>

Several pathologies have been described in association with angioid streaks, namely: pseudoxanthoma elasticum, sickle cell disease and Paget disease. Other associations include optic nerve head drusen, abetalipoproteinemia and Ehlers–Danlos syndrome. They may also be idiopathic.<sup>3</sup> Peripapillary or macular neovascularization is one of the main complications of angioid streaks, and occurs in approximately 42–84% of the cases.<sup>4</sup> Sometimes, recognition of neovascularization secondary to angioid streaks can be difficult using conventional imaging technology, as visualization of hyperintense leaking membrane can be masked by the hyperfluorescent streaks on fluorescein angiography (FA).<sup>5</sup>

Optical coherence tomography angiography (OCT-A) is a useful and sensitive tool for identifying the presence of neovascularization, its activity, and its spatial relationship with Bruch's membrane. Angioid streaks are detectable on OCT-A as hyporeflective branching lines in choriocapillaris segmentation or choriocapillary rarefaction, with artefacts projected in the outer retina portion.<sup>6,7</sup>

More recently, El Matri *et al.* described the presence of an irregular deep vascular network/plexus as a risk factor for active neovascularization.<sup>7,8</sup> This irregular vascular network was detected on OCT-A as a peripapillary or macular hyperelective, tangled capillary-like lesion, filling spaces between the streaks in the outer retina and choriocapillaris segmentation. Concerning the studies previously mentioned, one patient developed an active neovascularization emerging from the irregular deep vascular network. In agreement with El Matri *et al.*, Corbelli *et al.* also described the same irregular network in retinal areas affected with angioid streaks, using OCT-A

technology.<sup>6</sup> In both studies, these findings corresponded, on structural OCT, to flat and irregular retinal pigment epithelium (RPE) detachments with hyperreflective deposits above the Bruch's membrane, and without intraretinal or subretinal fluid. The authors hypothesized that these networks represented the development of fibrovascular tissue over the Bruch's breaks.<sup>6</sup> Although El Matri *et al.* considered it as a non-exudative/quiescent neovascularization, so an initial phase of neovascular physiopathology, Corbelli *et al.* advocated that the irregular deep vascular network and the choroidal neovascularization are two different pathological entities. Other characteristic described on OCT-A in eyes with angioid streaks was the presence of regions of rarefaction of choriocapillaries.<sup>7</sup> Authors theorized that these areas corresponded to RPE fenestrations and choriocapillaries atrophy over the Bruch's ruptures.<sup>7</sup>

Concerning the angioid streaks-associated neovascularization *per se*, their tangled arrangement closely follows and/or arise from the choroid, particularly from areas of Bruch's membrane disruption. This is really a choroidal neovascularization. Type 1/occult and 2/classic neovascularization have been described, although type 2 is the most common presenting subtype.<sup>9,10</sup> With the latter type, structural OCT shows more frequently a hyperreflective tissue with fibrin exudates between the RPE and neurosensory retina; in contrast with type 1 neovascularization in which only moderately hyperreflective tissue was detected.<sup>9</sup> Also, type 1 neovascularization demonstrated a lower incidence of exudation and a better visual acuity than type 2.<sup>9,10</sup> Polypoidal choroidal vasculopathy was also described in association with angioid streaks.<sup>9,11</sup>

OCT-A characteristics of angioid streaks-associated neovascularization revealed more commonly an irregular, poorly defined, loose, tangled morphology with long filamentous linear vessels *vs.* an interlacing, dense, cobweb or sea-fan shape pattern with several anastomoses and loops.<sup>6</sup> The interlacing/sea-fan morphology, which is similar to that observed in neovascular age-related macular degeneration (nAMD), appears to be

associated more frequently with active and exudative features.<sup>5,6,12</sup> Additionally, Chapron *et al.* found that neovascular membrane surrounded by a dark halo, in the choriocapillaris segmentation, was statistically correlated with anti-VEGF therapy in the last 6 months, and that angioid streaks-associated neovascularization tend to be larger than AMD or myopia-related neovascularization.<sup>5</sup>

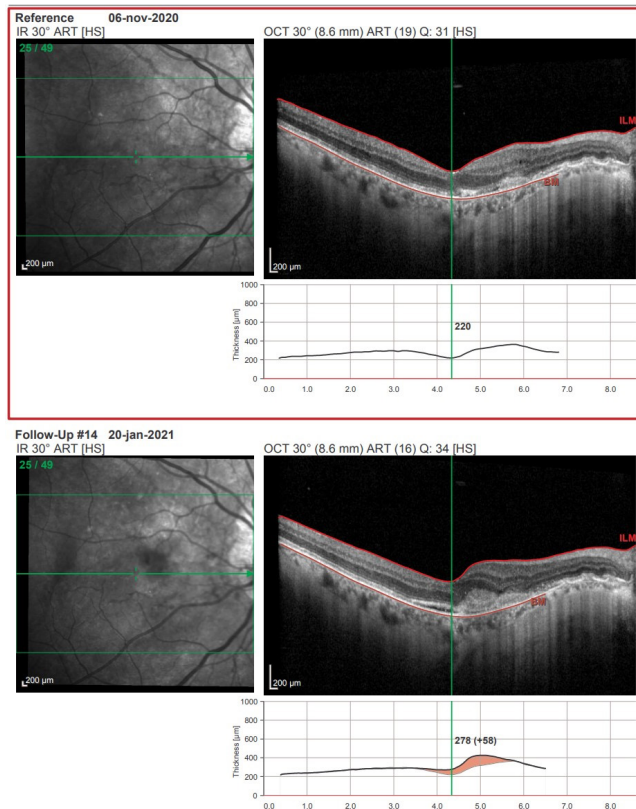


**Figure 1:** Comparative structural OCT B-scan of the right eye of patient with angioid streaks. Upper image: Infrared fundus image showing angioid streaks extending through the macula. Disruption of the RPE-Bruch membrane with atrophy and backscattering effect. Bottom image: Infrared fundus image showing angioid streaks extending through the macula. Corresponding OCT image showing partially preserved foveal depression and hyperelective subretinal lesion with subretinal fluid related to neovascular growing. (Cortesy of Rita Flores)

### CHOROIDAL RUPTURES

Choroidal rupture is defined as a break in the RPE, Bruch's membrane and choriocapillaris that follows a blunt traumatic event.<sup>13</sup> Neovascularization is a common complication associated with traumatic choroidal rupture.<sup>14</sup> Analogous to angioid streaks, recognition of neovascular complex using fluorescein angiography can be challenging as choroidal ruptures appear hyperfluorescent in mid and late phases of FA, due to staining.<sup>14</sup> Traumatic choroidal ruptures appear in the OCT-A as a linear and regular choriocapillaris rarefaction or a

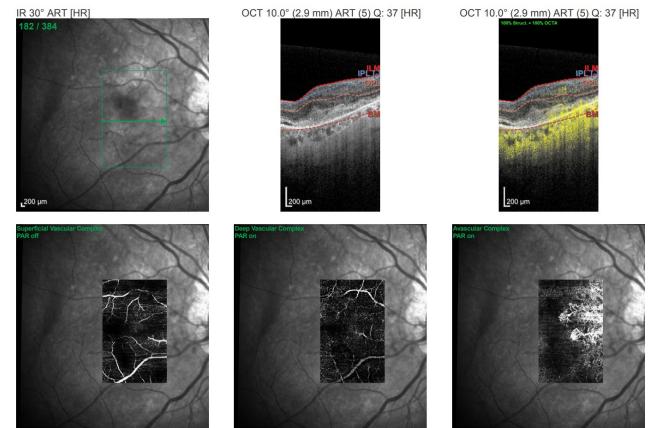


**Figure 2:** Infrared fundus image, OCT B-scan and OCT-A corresponding to the right eye of a patient with angioid streaks, mentioned in Figure 1 bottom image. Perifoveal-involving, irregular, tangled neovascular network, assessed in the choriocapillaris segmentation (avascular complex). Neovascular lesion extends along the primary RPE-Bruch membrane defect. In conclusion, OCT-A associated with other multimodal imaging seems to be useful in detecting specific precursors and/or predictors of peripapillary or macular neovascularization in asymptomatic eyes with angioid streaks. However, more studies are needed to validate these biomarkers. (Cortesy of Rita Flores)

vascular network interruption/hypointense structure in the area corresponding to the rupture.<sup>14-16</sup> Similar to angioid streaks, OCT-A characteristics, concerning choroidal rupture-associated neovascularization, reveals more commonly an hyperintense, irregular but well defined tangled morphology differently from the sea-fan shape pattern found in neovascular AMD.<sup>15,16</sup> Another interesting characteristic observed by Preziosa *et al.* is that neovascular tissue is located alongside and/or crosses the choroidal break with no correlation with the shape of Bruch's rupture, which contrasts with angioid streaks-associated neovascularization where it follows the path of the streaks.<sup>9,10,15</sup> In conclusion, OCT-A can be helpful to detect neovascular complications earlier and to follow its progression. Future prospective studies using OCT-A and larger sample sizes are needed in order to establish predictors of activity, progression and prognosis.

### REFERENCES

1. Soubrane G, Massamba N, Akin I, Risard-Gasiorowski S. Angioid Streaks. In: *Encyclopedia of Ophthalmology*. Berlin, Heidelberg: Springer Berlin Heidelberg; 2014:1-8.
2. Clarkson JG, Altman RD. Angioid streaks. *Surv Ophthalmol*. 1982;26(5):235-246.
3. Trempe C. The Relation of Angioid Streaks to Systemic Disease. *Arch Ophthalmol*. 1972;88(5):580-580.
4. Lim JI, Bressler NM, Marsh MJ, Bressler SB. Laser Treatment of

- Choroidal Neovascularization in Patients With Angioid Streaks. *Am J Ophthalmol*. 1993;116(4):414-423.
5. Chapron T, Mimoun G, Miere A, et al. Optical coherence tomography angiography features of choroidal neovascularization secondary to angioid streaks. *Eye*. 2019;33(3):385-391.
  6. Corbelli E, Carnevali A, Marchese A, et al. Optical coherence tomography angiography features of angioid streaks. *Retina*. 2018;38(11):2128-2136.
  7. El Matri K, Falfoul Y, Chebil A, Amoroso F, Bouraoui R, El Matri L. Irregular vascular network identified with OCT-A in angioid streaks: A probable predictor of active choroidal neovascularization (case series). *Eur J Ophthalmol*. December 2020.
  8. El Matri K, Falfoul Y, Hassairi A, Chebil A, Ammari M, El Matri L. OCT Angiography in angioid streaks without neovascular complications. *Acta Ophthalmol*. 2017;95.
  9. Nakagawa S, Yamashiro K, Tsujikawa A, et al. The time course changes of choroidal neovascularization in angioid streaks. *Retina*. 2013;33(4):825-833.
  10. Gal-Or O, Balaratnasingam C, Freund KB. Optical coherence tomography angiography findings of choroidal neovascularization in pseudoxanthoma elasticum. *Int J Retin Vitre*. 2015;1(1):1-5.
  11. Baillif-Gostoli S, Quaranta-El Maftouhi M, Mauget-Fajÿsse M. Polypoidal choroidal vasculopathy in a patient with angioid streaks secondary to pseudoxanthoma elasticum. *Graefes Arch Clin Exp Ophthalmol*. 2010;248(12):1845-1848.
  12. Mazzaferro A, Corbelli E, Cicinelli MV, et al. OCT-Angiography features of choroidal neovascularization secondary to angioid streaks. *Invest Ophthalmol Vis Sci*. 2016;57(12):1647.
  13. Lupidi M, Muzi A, Castellucci G, et al. The choroidal rupture: current concepts and insights. *Surv Ophthalmol*. February 2021.
  14. Pierro L, Giuffrè C, Rabiolo A, Gagliardi M, Arrigo A, Bandello F. Multimodal imaging in a patient with traumatic choroidal ruptures. *Eur J Ophthalmol*. 2017;27(6):e175-e178.
  15. Preziosa C, Corvi F, Pellegrini M, Bochicchio S, Rosar AP, Staurenghi G. Optical Coherence Tomography Angiography Findings in a Case of Choroidal Neovascularization Secondary To Traumatic Choroidal Rupture. *Retin Cases Brief Rep*. 2020;14(4):339-342.
  16. Lorusso M, Micelli Ferrari L, Nikolopoulou E, Micelli Ferrari T. Optical Coherence Tomography Angiography Evolution of Choroidal Neovascular Membrane in Choroidal Rupture Managed by Intravitreal Bevacizumab. *Case Rep Ophthalmol Med*. 2019;2019:1-4.



# MACULAR DYSTROPHIES

Pedro Nuno Pereira<sup>1</sup>, João Pedro Marques<sup>1,2,3,4</sup>

<sup>1</sup>- Ophthalmology Unit, Centro de Responsabilidade Integrado de Oftalmologia (CRIO), Centro Hospitalar e Universitário de Coimbra (CHUC)

<sup>2</sup>- University Clinic of Ophthalmology, Faculty of Medicine, University of Coimbra (FMUC), Coimbra, Portugal

<sup>3</sup>- Clinical Academic Center of Coimbra (CACC), Coimbra, Portugal

<sup>4</sup>- Coimbra Institute for Clinical and Biomedical Research (ICBR), Faculty of Medicine, University of Coimbra (FMUC), University of Coimbra, Coimbra, Portugal

## INTRODUCTION

Inherited retinal dystrophies (IRDs) represent a genetically and phenotypically heterogeneous group of rare eye diseases. Despite the low prevalence (~1:4000), IRDs are the leading cause of irreversible visual impairment and blindness among children and young adults in developed countries, thus creating a significant socioeconomic impact. Deep phenotyping by means of multimodal retinal imaging is extremely useful for diagnosis, monitoring and identifying biomarkers associated with functional outcomes. With the recent approval of the first gene therapy drug and several gene therapies in clinical trial stage, the role of deep phenotyping and genotyping in IRDs cannot be overemphasized.<sup>1</sup>

Macular dystrophies are a heterogeneous subgroup of IRDs characterized by bilateral, relatively symmetrical macular abnormalities that significantly impair central visual function. Substantial progress in recent years allowed to improve knowledge of the underlying molecular mechanisms and pathophysiology of these rare diseases.

Optical coherence tomography angiography (OCTA) offers a non-invasive method to study both retinal and choroidal circulation in patients with suspected or confirmed IRDs. The majority of IRDs involve degeneration of the outer retinal layers and retinal pigment epithelium (RPE), as well as changes in retinal vessels and choriocapillaris.<sup>2,3</sup> The temporal relationship between retinal degeneration and vascular atrophy, however, has been difficult to determine using current clinical imaging techniques. OCTA could be useful in this regard by permitting assessment of the retinal and choroidal vasculature and quantification of capillary density, without injecting contrast products such as fluorescein or indocyanine green dyes. Furthermore, in combination with structural *en face* OCT, degeneration of the retina and RPE may be compared to retinal and choroidal vascular changes. Since macular dystrophies are IRDs with a macula-predominant phenotype, OCTA is a valuable technique to complement other imaging modalities aiming to better characterize vascular changes in the retina and choroid of these patients.

## STARGARDT DISEASE

Stargardt disease (STGD), the most common hereditary

macular dystrophy, results from autosomal recessive mutations in *ABCA4* gene.<sup>4</sup> Patients typically develop macular atrophy resulting in central vision loss, classically presenting in the first two decades of life, although a subset of patients may present in the fourth or fifth decades (late-onset STGD).<sup>5</sup>

The most striking changes in STGD are in the posterior pole, with variable centrifugal expansion. Typical changes include a mottled pattern of yellowish, pisci or punctiform, isolated or confluent lesions named flecks, which translate the deposition of lipofuscin in the RPE. Central atrophy and peripapillary sparing are two other common features.

OCTA in STGD demonstrates preserved superficial retinal vessels with a range of choroidal atrophy. Thickness of the retinal and choroidal layers is reduced in patients with STGD as opposed to healthy controls.<sup>6</sup> Younger patients with a recent onset of symptoms are more likely to have a central region of reduced choriocapillaris perfusion and hyper-intense deep choroid. These patients may present lesions that disrupt RPE integrity and block the reflectivity of choroidal flow. On the other hand, those with more advanced disease show complete loss of choriocapillaris in the macula, such that the deep choroidal vessels are readily visualized (Figures 1-2). These changes correlate with the hypocyanescence on indocyanine green angiography frequently visualized in patients with STGD, representing selective choriocapillaris loss.<sup>7</sup>

According to *Pellegrin et al*, macular atrophy in STGD differs from age-related macular degeneration (AMD)-associated geographic atrophy (GA) as residual choriocapillaris lobules are seen at the margins of the atrophic area, whereas in GA choriocapillaris are globally rarefied with absence of focal damage within the margins of atrophy.<sup>8</sup> The opportunity to non-invasively evaluate choriocapillaris over time with OCTA may provide a better understanding of the pathogenesis of STGD, thus identifying imaging biomarkers and outcome measures for future genetic therapies and monitoring therapeutic response.

## X-LINKED RETINOSCHISIS

X-Linked retinoschisis (XLRS) is the most common form of juvenile-onset vitreoretinal degeneration



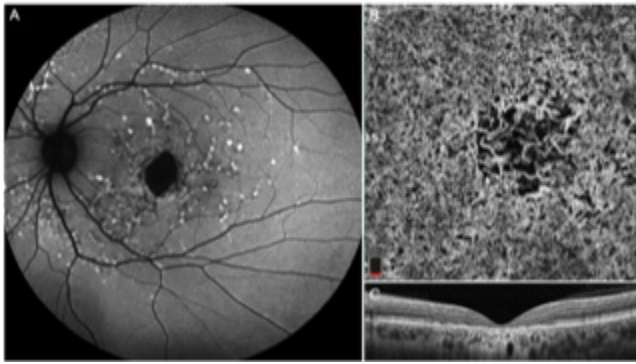


**Figure 1.** Multimodal retinal imaging in a case of STGD (A) On Fundus Autofluorescence, the hypoautofluorescent pisciform lesions correspond to atrophic flecks. The more recent flecks are hyperautofluorescent and represent lipofuscin accumulation in areas at risk of becoming atrophic. The flecks spare the peripapillary region, a common finding in STGD. A central hypoautofluorescent area represents macular atrophy. In advanced cases, OCTA shows increased intercapillary space, remodeling of the foveal avascular zone and the absence of choriocapillaris in the area of atrophy, as shown in (B). Spectral domain optical coherence tomography depicts central retinal thinning with atrophy of the outer retinal layers (C).

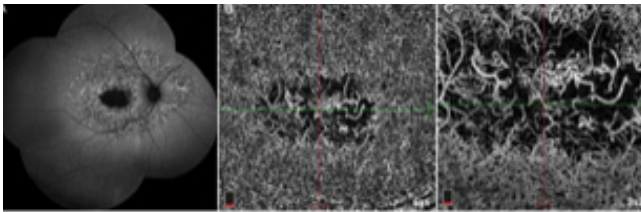


**Figure 2.** (A) Fundus autofluorescence highlights numerous flecks in the posterior pole, along with a central hypoautofluorescent zone corresponding to macular atrophy. Note the peripapillary sparing. (B) and (C) correspond to an optical coherence tomography angiography (OCTA) scan of the choriocapillaris (6x6 and 3x3 mm, respectively). The choriocapillaris slab of OCTA depicts a central area of choriocapillaris loss where the deep choroidal vessels are seen.

in males.<sup>9</sup> The presence of “spoke-wheel” folds in the macula (macular schisis) is the hallmark feature of XLRS. Peripheral retinal changes are observed in approximately 50% of males, including schisis (with inner or outer retinal holes), metallic sheen, pigmentary changes, white spiculations, neovascularization and vitreous veils. An increased risk of vitreous hemorrhage or rhegmatogenous retinal detachment (RRD) has been reported for patients with peripheral retinoschisis.<sup>10</sup> The advent of macular atrophy is a frequent cause of decreased visual acuity in older adults.

The identification of macular schisis can be truly challenging on clinical examination, making multimodal imaging essential. Splitting of the outer and inner retinal layers can be readily identified by structural OCT and

enface OCTA scans (Figure 3). A spoke-wheel appearance consisting of concentric areas of low- and high- signal intensity can be observed in fundus autofluorescence (FAF) images. However, in the rare cases where a normal/near macular OCT is seen, peripheral changes may be the only clue to the clinical diagnosis. Ultra-wide field imaging with fluorescein angiography or OCTA may be extremely helpful in identifying less common vascular abnormalities such as neovascularization and vascular sheathing.<sup>11</sup>

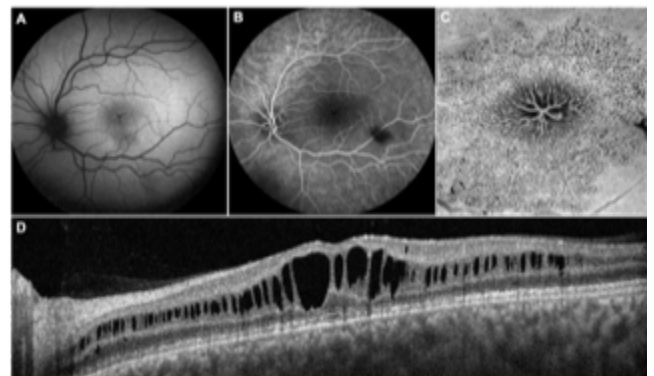


**Figure 3.** Multimodal retinal imaging in a patient with XLRS. (A) The spoke-wheel is noticed on fundus autofluorescence. (B) On Fluorescein angiography, there is no leakage nor hyperfluorescence associated with retinal splitting or cystic-like spaces. (C) Enface optical coherence tomography enables the best visualization of distribution and characterization of schisis. (D) Optical coherence tomography scan shows multiple pseudo-cystic changes and inner retinal splitting involving retinal layers.

## BEST DISEASE

Best Disease (BD) is an autosomal dominant condition associated with disease-causing variants in *BEST1*, and the second most common macular dystrophy. Stage 1 (early stage) disease is characterized by a normal fundus or minimal RPE changes (pre-vitelliform).<sup>12</sup> A single, bilateral and symmetrical egg-yolk-like lesion (vitelliform) at the fovea corresponds to the classical appearance of stage 2 BD. This lesion may start to undergo resorption, progressing to a “pseudohypopyon” (stage 3). The subretinal yellow material gravitates inferiorly within the lesion. Stages 1 and 2 are usually associated with preserved visual acuity. Reduced visual acuity is observed from stage 3 onwards. In stage 4 (vitelliruptive) a breakdown of the subretinal material ensues. End-stage BD (Stage 5) is characterized by either sub-RPE fibrosis, atrophy or choroidal neovascularization (CNV)<sup>13</sup>. Despite the classification of fundus appearance into stages, there is rarely predictable progression from one stage to the other.

The vitelliform lesion is hyperautofluorescent on FAF imaging and is characterized by the presence of

subretinal hyperreflective material on OCT.<sup>14</sup> Subretinal fluid is a frequent finding which waxes and wanes over time. The fibrosis that establishes in advanced BD has been reported as resembling a “circus tent” due to its exaggerated height and height-to base ratio.<sup>15</sup> OCTA studies suggest this fibrosis to have a neovascular origin.<sup>16</sup> OCTA is particularly useful for the non-invasive detection of CNV in vitelliform disorders including BD (Figure 4), where fluorescein angiography can be very difficult to interpret.<sup>9</sup>

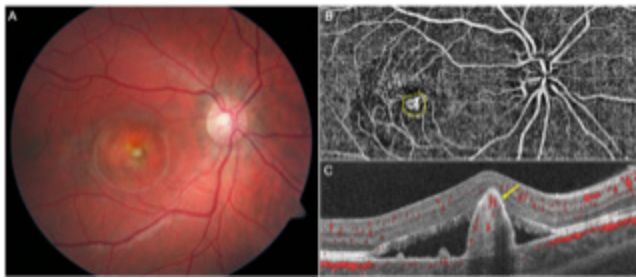


**Figure 4.** Best disease, stage 5. (A) color fundus photography; (B-C) OCTA and OCT scan, respectively, revealing active choroidal neovascularization with flow under the RPE (yellow arrow).

### IMAGING CHOROIDAL NEOVASCULARIZATION IN INHERITED RETINAL DYSTROPHIES

IRDs have multiple complications, one of which is CNV. For many years, fluorescein ( $\pm$  indocyanine green) angiography was the gold standard for the detection of CNV in these patients. However, the invasive nature of the procedure, difficulties in interpretation in the specific case of IRDs (early hyperfluorescence may be more difficult to isolate, while late leakage is difficult to discern from staining in later frames) and the refinement of OCT and OCTA technology, led to a significant decrease in the number of angiographies performed.

The automated segmentation of OCTA allows to delineate angiographic flow in the outer retina despite a possibly distorted architecture, thereby clearly highlighting the CNV net. Furthermore, OCTA is capable of quantifying the area of the neovascular lesion, which may be useful in monitoring progression and response to therapy.<sup>17,18</sup>

Detection of CNV by OCTA has proved important in vitelliform dystrophies such as BD or adult-onset foveomacular vitelliform dystrophy (AOFVD).<sup>19</sup> In the particular setting of vitelliform lesions, intense staining patterns are usually seen on FA, which may obscure CNV detection with this method.<sup>20</sup>

OCTA showed a sensitivity of 80%, and a specificity of 100%, in a study investigating cases of AOFVD-associated CNV.<sup>21</sup>

Sorsby Fundus Dystrophy, a rare autosomal dominant macular dystrophy, is another example where CNV can be captured with OCTA, without the need for dye-dependent angiography systems.<sup>18</sup>

The widespread use of OCTA led to a recent increase in

the identification of asymptomatic, non-exudative CNV in several retinal conditions, including Pseudoxanthoma Elasticum (PXE)-related retinopathy (Figure 5).<sup>22</sup>

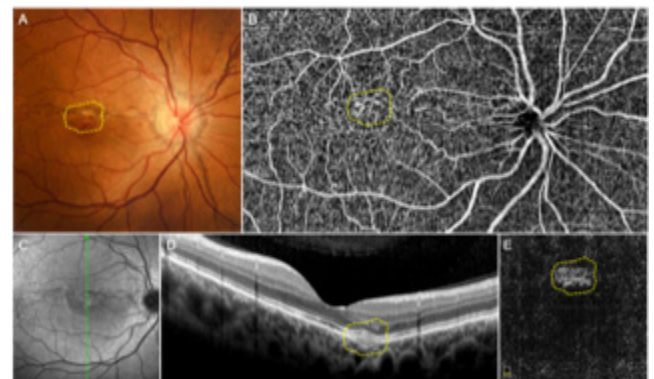


**Figure 5.** Several images of the ocular features of PXE-related retinopathy. (A) Color fundus photography showing angioid streaks and peau d'orange maculopathy. (B) On OCTA scan, a small extrafoveal neovascular net is seen (yellow dotted line). (C) Infra-red imaging demonstrating the topographic association between an angioid streak and the neovascular complex. (D) A vertical OCT scan showing a focal choroidal excavation (yellow dotted line) in association with the neovascular complex (double layer sign). No signs of activity are observed (non-exudative macular neovascularization). (E) Outer retina slab of OCTA highlighting the neovascular complex.

### CONCLUSION

In summary, there is almost unlimited potential for OCTA to aid in the evaluation of patients with macular dystrophies. The inclusion of OCTA in the deep phenotyping of these patients may help clear up the interplay between blood flow and retinal changes in IRDs.

### REFERENCES

1. Pennesi ME. Retinal gene therapy : current progress and future prospects. 2015;10(3):281-299.
2. Michaelides M, Hunt DM, Moore AT. The genetics of inherited macular dystrophies. 2003;641-651.
3. Yeoh J, Rahman W, Chen F, Webster AR, Moore AT. Choroidal imaging in inherited retinal disease using the technique of enhanced depth imaging optical coherence tomography. 2010;1719-1728.
4. Molday RS. ATP-binding cassette transporter ABCA4 : Molecular properties and role in vision and macular degeneration. 2007;507-517.
5. Ganzfeld T. Stargardt's. 2015;5-7.
6. Adhi M, Read SP, Ferrara D, Weber M, Duker JAYS, Waheed NK. Morphology and Vascular Layers of the Choroid in Stargardt Disease Analyzed Using Spectral-Domain Optical Coherence Tomography. *Am J Ophthalmol.* 2015;1-10.
7. Giani A, Pellegrini M, Carini E, Peroglio Deiro A, Bottoni F, Staurenghi G. The dark atrophy with indocyanine green

- angiography in stargardt disease. *Investig Ophthalmol Vis Sci*. 2012;53(7):3999-4004.
8. Pellegrini M, Acquistapace A, Oldani M, et al. Dark Atrophy: An Optical Coherence Tomography Angiography Study. *Ophthalmology*. 2016;123(9):1879-1886.
  9. Rahman N, Georgiou M, Khan KN, Michaelides M. Macular dystrophies : clinical and imaging features , molecular genetics and therapeutic options. 2019:1-10.
  10. Fahim AT, Ali N, Blachley T, Michaelides M. Peripheral fundus findings in X-linked retinoschisis. 2017:1555-1559.
  11. Modalities I. Juvenile X-Linked Retinoschisis : A Comparison of Imaging Modalities and Review of Angiographic. :1-3.
  12. Petrukhin K, Koisti MJ, Bakall B, et al. Identification of the gene responsible for best macular dystrophy. *Nat Genet*. 1998;19(3):241-247.
  13. Livingstone MS, Hubel DH. Psychophysical evidence for separate channels for the perception of form, color, movement, and depth. *J Neurosci*. 1987;7(11):3416-3468.
  14. Ferrara DC, Costa RA, Tsang S, Calucci D, Jorge R, Freund KB. Multimodal fundus imaging in Best vitelliform macular dystrophy. 2010:1377-1386.
  15. Kumar V. Fibrotic pillar leads to focal choroidal excavation in Best vitelliform dystrophy. 2018.
  16. Shahzad R, Abdul M, Siddiqui R, Ed F. Choroidal neovascularization secondary to Best vitelliform macular dystrophy detected by optical coherence tomography angiography. *J AAPOS*. 2016.
  17. Jia Y, Bailey ST, Wilson DJ, et al. Quantitative optical coherence tomography angiography of choroidal neovascularization in age-related macular degeneration. *Ophthalmology*. 2014;121(7):1435-1444.
  18. Kuehlewein L, Sadda SR, Sarraf D. OCT angiography and sequential quantitative analysis of type 2 neovascularization after ranibizumab therapy. *Eye*. 2015;29(7):932-935.
  19. Chowers I, Tiosano L, Audo I, Grunin M, Boon CJF. Adult-onset foveomacular vitelliform dystrophy: A fresh perspective. *Prog Retin Eye Res*. 2015;47:64-85.
  20. Sodi A, Murro V, Caporossi O, et al. Long-Term Results of Photodynamic Therapy for Choroidal Neovascularization in Pediatric Patients with Best Vitelliform Macular Dystrophy. *Ophthalmic Genet*. 2015;36(2):168-174.
  21. Lupidi M, Coscas G, Cagini C, Coscas F. Optical coherence tomography angiography of a choroidal neovascularization in adult onset foveomacular vitelliform dystrophy: Pearls and pitfalls. *Investig Ophthalmol Vis Sci*. 2015;56(13):7638-7645.
  22. Marques JP, Bernardes J, Geada S, et al. Non-exudative macular neovascularization in pseudoxanthoma elasticum. *Graefes Arch Clin Exp Ophthalmol*. 2021;259(4):873-882.

# VITELLIFORM DYSTROPHIES

Cláudia Farinha, MD<sup>1,2,3</sup>

1- Ophthalmology Department, Coimbra Hospital and University Centre (CHUC), Coimbra, Portugal

2- Association for Innovation and Biomedical Research on Light and Image (AIBILI), Coimbra, Portugal

3- Faculty of Medicine, University of Coimbra (FMUC), Coimbra, Portugal

The vitelliform macular dystrophies (VMD) are a complex group of inherited clinical entities that share the common feature of vitelliform material deposition between the neuroretina and the retinal pigment epithelium (RPE). They are both genetically and phenotypically heterogeneous, meaning that mutations in the same gene can present with different phenotypes, even in patients from the same family; and similar phenotypes can be caused by mutations in different genes. Besides, both penetrance and expressivity may vary considerably. The onset of the disease is broad, ranging from childhood until middle age, and conversion between phenotypes during follow-up is also possible, as casually observed in the pattern dystrophies. All this considered, accurate diagnosis can be challenging in some cases. Complete clinical and familiar history together with multimodal imaging examination is essential. Electroretinography/electrooculography, as well as genetic sequencing, are many times fundamental to achieve a definite diagnosis<sup>1</sup>. The most common is Best vitelliform macular dystrophy (autosomal dominant, BEST1 gene), while Autosomal Recessive Bestrophinopathy (also BEST1) is less frequent. Another important group are the Pattern Dystrophies, characterized by various patterns of pigment deposition within the macula, they are usually autosomal dominant and present later in life. Based on the pattern of the pigment distribution they are classified into 5 categories: 1. Adult-onset Foveomacular Vitelliform Dystrophy (AOFVD); 2. Butterfly-shaped Pigment Dystrophy; 3. Reticular Dystrophy; 4. Multifocal Pattern Dystrophy Simulating Stargardt's Disease; 5. Fundus Pulverulentus.

## OPTICAL COHERENCE TOMOGRAPHY ANGIOGRAPHY IN VITELLIFORM MACULAR DYSTROPHIES

Multimodal Imaging is currently the mainstay in the diagnosis and phenotypic characterization of Vitelliform Macular Dystrophies. This usually comprises color fundus photography, fundus autofluorescence, infra-red imaging, and optical coherence tomography (Figure 1). The emergence of complications such as choroidal neovascularization (CNV), traditionally requires invasive dye-based exams such as fluorescein angiography (FA) and indocyanine green angiography (ICGA) to detect the abnormal neovascular network. However, due to the nature of the

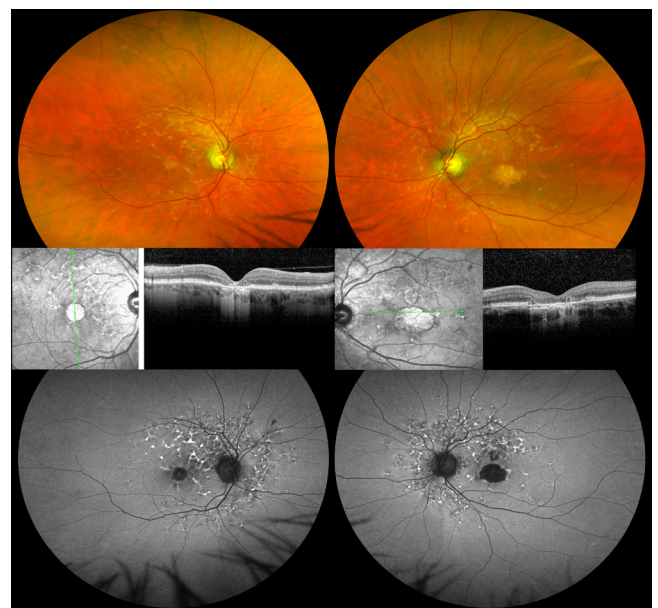


**Figure 1:** Multimodal Imaging of a patient with Pattern Reticular Dystrophy, including wide-field color fundus photography and autofluorescence, near infra-red imaging, and SD-OCT. The vitelliform material has disappeared at this stage, with the development of macular atrophy in both eyes.

vitelliform material and associated subretinal fluid, a definite identification is sometimes difficult<sup>2</sup>. Lipofuscin dye staining and pooling in the vitelliform lesion, as well as retinal pigment atrophic changes and proliferation can obscure the accurate diagnosis of the CNV. Optical Coherence Tomography Angiography (OCTA) in this setting may be particularly useful, as the neovascular network can be readily identified without the masking effect seen in the FA<sup>2</sup>. In addition, changes in the CNV morphology in response to therapy can be easily assessed in a noninvasive and repeatable way through follow-up.

Apart from its role in identifying CNV secondary to VMD, studies also explored the retinal and choriocapillaris microvascular changes with OCTA. In Best Disease (BD) patients had patchy and/or diffuse loss of capillary density in both superficial and deep capillary plexuses and in the choriocapillaris, when comparing to healthy controls. Besides, significant correlations between the deep capillary plexus vessel density and best-corrected

visual acuity were found with disease stage. Similar findings of decreased flow densities measured by OCTA in the superficial and deep retinal vascular layers in patients with AOFVD were also reported<sup>3-6</sup>.

### OCTA in the detection of CNV secondary to VMD

Currently, available OCTA devices provide detailed 3-dimensional volumes of the retinal and choroidal vasculatures that can be analyzed layer-by-layer in both en-face or cross-sectional display. Furthermore, OCTA allows for simultaneous co-localization of blood flow with microstructural changes in conventional OCT B-scans. Some platforms give automated quantitative data of flow (angio-analytics), but these should still be interpreted with caution, as they are dependent on segmentation accuracy, artifacts, and metrics are not interchangeable between devices<sup>7,8</sup>. More recently, OCTA has become an essential and widely used tool for the noninvasive diagnosis and monitoring of CNV.

Compared to conventional dye-based angiography the primary limitation of OCTA is the absence of dynamic information such as filling speed and pooling or leakage, however, in the context of VMD this can be an advantage, considering the limitations of FA in CNV detection in this setting<sup>6</sup>. Besides, the en face OCTA can show the neovascular membrane morphology with detail, and collections of sub and intra-retinal fluid in structural B-scans suggesting CNV activity (Figures 2 and 3). Several studies have shown that this technology may be used to characterize with accuracy the neovascular network and to better follow up the disease progression. The ability to provide direct visualization of the neovascular membrane in VMD may strongly impact treatment decisions<sup>6,9</sup>.

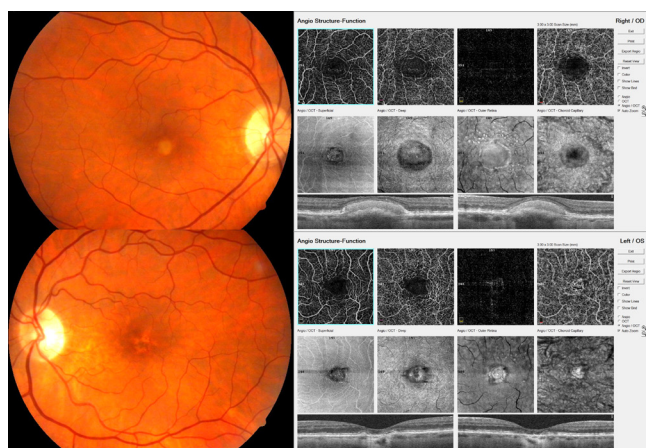


**Figure 2.** Woman with AOVMD, 69yo. In the right eye de vitelliform material is seen in the B-scan, along with RPE irregularity, and the en face OCTA does not show any neovascular lesion. In the left eye (bottom row) there is atrophy of the RPE in the fovea, which can appear as a pseudoflow image in the choriocapillaris slab in the OCTA.

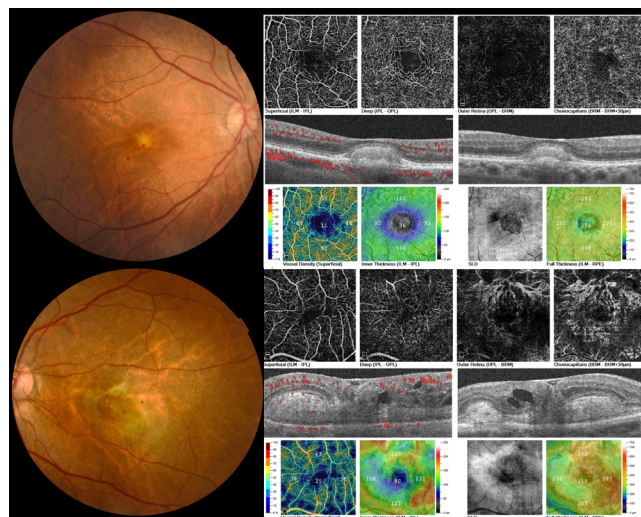


**Figure 3.** AOVMD patient (female, 86yo). Central vitelliform lesion in the right eye and type 2 VMD-CNV in the left eye. The morphology and complexity of the CNV are rapidly recognized in the outer retina and choriocapillaris slabs of the en face OCTA, obviating the need for invasive dye-based angiography.

Choroidal neovascularization is traditionally regarded as an uncommon complication of Best Disease and has been considered a hallmark of end-stage disease. OCTA already proved to be of value in its diagnosis, and even has revealed that CNV may develop in earlier stages and even be the presenting sign<sup>4,5,10</sup>. In this regard, Parodi *et al.*<sup>5</sup> suggested that the CNV identified by OCTA in the vitelliform and pseudohypopyon stages of BD may be distinct from the CNV associated with the vitelliruptive and atrophic stages. In their study, only eyes in the former stages showed exudative changes, and treatment with anti-VEGF led to stabilization of lesion size with improvement in visual acuity. Thus, they proposed that in BD two CNV sub-forms can be found: exudative CNV is rare and develops in the early stages of the disease, with bleeding and fluid formation; and non-exudative CNV, which develops very commonly in the advanced stage of BD, without any exudative manifestation<sup>5</sup>. While the former present with higher perfusion and more vascular disorganization in OCTA, the latter may develop more slowly, stimulated by the trophic demand of the outer retina. Importantly, these reports show a greater prevalence of CNV (up to 39%) compared with prior studies based on traditional imaging (2–9%). Non-exudative CNV was identified in 96% of eyes in stages vitelliruptive and atrophic/cicatrical. Considering that it is difficult to detect non-exudative CNV on FA/ICGA due to staining of the vitelliform lesion, OCTA provides a more accurate diagnosis<sup>5</sup>. Arrigo *et al.*<sup>11</sup> also explored quantitative OCTA features, namely CNV vessel tortuosity in BD, and showed that a cut-off could be used in stratifying the morpho-functional features of the vascular network, with possible impact on treatment decisions and prognosis.

## OCTA during anti-VEGF treatment

Treatment-naïve exudative CNV in VMD is characterized by a well-defined complex with numerous tiny internal anastomotic vessels and vascular loops at the termini of the lesion, signs associated with active lesions as previously described<sup>12</sup>. These fine, arborizing vessels, regress during treatment with anti-VEGF, while the central and more mature trunks containing pericyte-protected endothelial cells may prevail and are typical of more chronic lesions<sup>10,13</sup>. This vascular remodeling of CNV with therapy may be followed by a re proliferation (re-opening or new vessels), and there is a cyclic pattern with regression phases alternating with progression phases (Figure 4). Both qualitative and quantitative OCTA parameters might increase before the exudative signs reappear, rendering OCTA as a very useful tool in treatment regimen individualization<sup>10</sup>. The area of CNV can also be measured by OCTA, and its change with treatment quantified in some devices<sup>10,12</sup>.

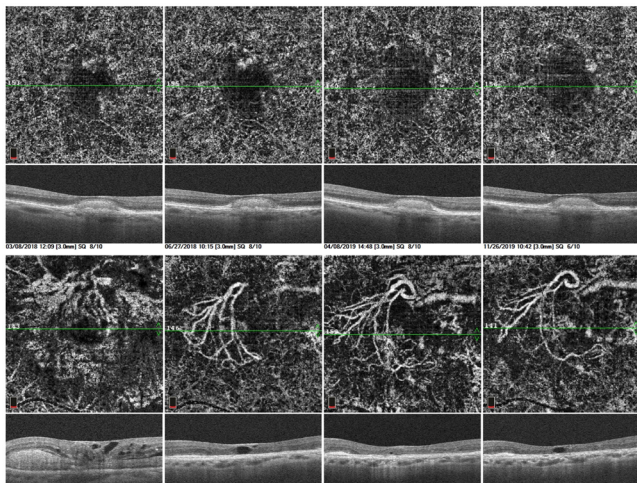


**Figure 4.** ADVM patient (female, 86yo). Follow-up analysis of the first two years of anti-VEGF treatment in the left eye for VMD-CNV. In the upper row, the right eye has a stable vitelliform lesion, with deposition of relatively homogenous material between the neuroretina and the RPE, there is irregularity of the RPE, however, the choriocapillaris OCTA slab does not reveal any neovascular network, neither there is intraretinal or subretinal fluid in the sequential B-scans.

In the bottom row, the type 2 CNV in the left eye is clearly visible in both structural B-scan and en face OCTA. In the OCTA image, the intricate pattern of neovessels with terminal loops and arcades is very typical of an active lesion. During follow-up, there is rarefaction of peripheral immature neovessels and persistence of the larger and more mature central trunks.

When deciding to start treatment, OCTA may also be useful, since previous reports validated anti-VEGF treatment for exudative CNV, whereas the stability displayed by non-exudative CNV in late atrophic/

cicatricial stages (no exudative features and no changes in quantitative OCTA vascular parameters), suggests that anti-VEGF is probably unnecessary, and may even be harmful at this point by potentially accelerating atrophy, with consequent visual loss<sup>5</sup>.

## Final considerations

Altogether, the advantages of OCTA in VMD are leading to a decrease in conventional invasive angiography, even when CNV is suspected. The fact that OCTA is non-invasive, allows frequent imaging of the patients during treatment in complete safety, and the comprehensive layer-by-layer analysis is useful both in diagnosis and prognosis. Limitations of OCTA are mainly related to the presence of segmentation artifacts, which might be more evident in patients with disrupted macular anatomy, such as in macular dystrophies. Projection artifacts from the overlying retinal vessels to the surface of the vitelliform subretinal material may be a source of pseudoflow signal and might be misinterpreted as CNV with consequent needless initiation of anti-VEGF therapy, or misinterpretation of response to therapy<sup>4,14</sup>.

In summary, the OCTA is now considered an excellent imaging option in VMD patients, especially when a CNV is suspected, and provides further insight on the pathophysiology of these entities, revealing that CNV might be more frequent than previously thought, especially in the advanced stages of the disease.

## REFERENCES

1. Rahman N, Georgiou M, Khan KN, Michaelides M. Macular dystrophies: clinical and imaging features, molecular genetics and therapeutic options. *Br J Ophthalmol.* 2020;104(4):451-460.
2. Stattin M, Ahmed D, Glittenberg C, Krebs I, Ansari-Shahrezaei S. Optical Coherence Tomography Angiography for the Detection of Secondary Choroidal Neovascularization in Vitelliform Macular Dystrophy. *Retin Cases Br Reports.* 2020;14(1):49-52.
3. Treder M, Laueremann JL, Alnawaiseh M, Heiduschka P, Eter N. Quantitative changes in flow density in patients with adult-onset foveomacular vitelliform dystrophy: an OCT angiography study. *Graefes Arch Clin Exp Ophthalmol.* 2018;256(1):23-28.
4. Qaseem Y, German O, Cicinelli MV, Mirza RG. The Role of Optical Coherence Tomography Angiography (OCTA) in Detecting Choroidal Neovascularization in Different Stages of Best Macular Dystrophy: A Case Series. *Medicina (Kaunas).* 2021;57(3):213.
5. Parodi MB, Arrigo A, Bandello F. Optical Coherence Tomography Angiography Quantitative Assessment of Macular Neovascularization in Best Vitelliform Macular Dystrophy. *Invest Ophthalmol Vis Sci.* 2020 3;61(6):61.
6. Ong SS, Patel TP, Singh MS. Optical Coherence Tomography Angiography Imaging in Inherited Retinal Diseases. *J Clin Med.* 2019 28;8(12):2078.
7. Tan ACS, Tan GS, Denniston AK, Keane PA, Ang M, Milea D, Chakravarthy U, Cheung CMG. An overview of the clinical applications of optical coherence tomography angiography. *Eye*

- (Lond). 2018;32(2):262-286.
8. de Carlo TE, Romano A, Waheed NK, Duker JS. A review of optical coherence tomography angiography (OCTA). *Int J Retina Vitreous*. 2015;1:5.
  9. Sulzbacher F, Pollreisz A, Kaider A, Kicking S, Sacu S, Schmidt-Erfurth U; Vienna Eye Study Center. Identification and clinical role of choroidal neovascularization characteristics based on optical coherence tomography angiography. *Acta Ophthalmol*. 2017;95(4):414-420.
  10. Murro V, Mucciolo DP, Giorgio D, Sodi A, Passerini I, Cipollini F, Virgili G, Giansanti F. Optical coherence tomography angiography cyclic remodeling of CNV in patients affected by Best macular dystrophy. *Ophthalmic Genet*. 2020;41(5):440-447.
  11. Arrigo A, Bordato A, Aragona E, Amato A, Viganò C, Bandello F, Battaglia Parodi M. Macular neovascularization in AMD, CSC and best vitelliform macular dystrophy: quantitative OCTA detects distinct clinical entities. *Eye (Lond)*. 2021. doi: 10.1038/s41433-021-01396-2. *Epub ahead of print*.
  12. Coscas GJ, Lupidi M, Coscas F, Cagini C, Souied EH. Optical coherence tomography angiography versus traditional multimodal imaging in assessing the activity of exudative age-related macular degeneration: A New Diagnostic Challenge. *Retina*. 2015;35(11):2219-28.
  13. Al-Sheikh M, Iafe NA, Phasukkijwatana N, Sadda SR, Sarraf D. Biomarkers of neovascular activity in age-related macular degeneration using optical coherence tomography angiography. *Retina*. 2018;38(2):220-230.
  14. Moussa M, Leila M, Moussa O, Hashem AO. Customized Slab-Segmentation Method for Projection-Artifact Elimination in Best Vitelliform Macular Dystrophy: A Swept-Source Optical Coherence Tomography Angiography Study. *Clin Ophthalmol*. 2021;15:825-834.

# 17. CHOROIDITIS

Maria João Furtado, Rita Vieira  
Centro Hospitalar Universitário do Porto

The choroid is a densely vascularized, high flow structure, with multiple functions. The complex nature of the choroidal anatomy limits *in-vivo* imaging<sup>1</sup>. Choroiditis refers to inflammatory pathology of the choroid, occurring in the setting of posterior uveitis or panuveitis<sup>2</sup>. It may present as diffuse, focal or multifocal and has different etiologies, including infectious and non-infectious<sup>2,3</sup>. Dye angiography has been the gold standard for clinical assessment of uveitis and indocyanine green angiography (ICGA) definitely contributed to a better understanding of choroiditis<sup>4</sup>.

The emergence of the non-invasive OCT angiography (OCTA) in the latest few years brought a new perspective of the retinal and choroidal vasculature, offering a three-dimensional detail of the posterior segment microvasculature. OCTA creates a depth-resolved vascular network contrast image, from the difference between static and non-static tissue, overcoming some limitations of classic angiography in the choroidal evaluation<sup>1,5,6,7</sup>. The conventional classification of choroiditis into choriocapillaritis and stromal choroiditis is ICGA based<sup>8</sup>. However, new perspectives are emerging on this issue with significant contribution of OCTA imaging. OCTA is becoming a key tool for investigating the choriocapillaris (CC)<sup>9,10,11</sup>. Imaging of deeper choroidal layers is still limited, mainly due to significant artifacts and scattering by the RPE and the CC<sup>7,12,13</sup>.

The previously called “White Dot Syndromes” are a group of inflammatory chorioretinopathies (Table 1) of unknown etiology which have a characteristic appearance of multiple yellow-white lesions involving the outer retinal layers, retinal pigment epithelium (RPE), CC and deep choroid<sup>14</sup>. Along this chapter, the OCTA findings in the most common primary inflammatory chorioretinopathies will be presented due to the potential great impact of this imaging tool in the approach of these disorders<sup>1</sup>.

## OCTA FINDINGS IN PRIMARY INFLAMMATORY CHORIORETINOPATHIES

Multiple Evanescent White Dot Syndrome (MEWDS) is an acute, idiopathic, usually self-limited condition that typically affects young myopic women. There is still debate about the pathophysiology of MEWDS.

**Table 1-** ICGA based classification of primary inflammatory chorioretinopathies

PRIMARY CHORIOCAPILLARITIS	PRIMARY STROMAL CHOROIDITIS
MEWDS	
APMPPE	Birdshot Retinochoroiditis
MFC/PIC	Sympathetic Ophthalmia
Serpiginous Choroiditis	VKH Disease
Rare entities: AZOOR, AMN...	

While it has been traditionally classified as a primary choriocapillaritis, new perspectives are emerging. Recent multimodal imaging studies proposed an alternative pathogenesis, as no changes at the CC level were found in different series of MEWDS patients in OCTA scans<sup>6,15,16,17</sup>. Pichi et al suggested that MEWDS could be a primary photoreceptoritis considering the universal changes present on structural OCT at the outer retina level, in particular affecting the outer segments of photoreceptors and ellipsoid zone<sup>15</sup>. Zicarelli et al also showed no flow impairment at the CC level on OCTA scans but their findings suggested the primary insult in MEWDS involved the RPE with secondary damage to the photoreceptors<sup>17</sup>. In conclusion, OCTA provided evidence that MEWDS is primarily an inflammation of the photoreceptors and/ or the RPE and the CC may not be affected, as well as the retinal vascular plexa, at any timepoint of the disease (Figure 1)<sup>7</sup>.

Acute posterior multifocal placoid pigment epitheliopathy (APMPPE) is an uncommon inflammatory condition that generally affects young healthy adults, between the second and fourth decades, who present with transient acute central or paracentral vision loss related to multiple yellow creamy deep placoid lesions, located in the posterior pole<sup>3,6</sup>. Though a debate still exists about the exact sequence of events, the prevailing perspective about APMPPE has been that the primary insult occurs in the inner choroid, resulting in multifocal CC



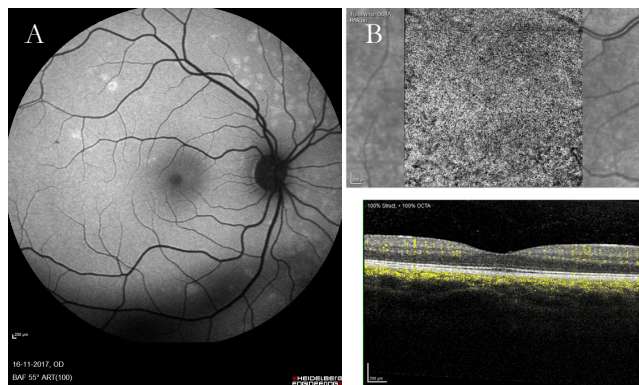


**Figure 1.** MEWDS. A. Fundus autofluorescence, with hyperautofluorescent lesions predominantly on the nasal retina, reflecting RPE and photoreceptors damage. B. OCTA scan of the CC on the central macula, with no significant flow changes

hypoperfusion with secondary outer retinal changes. The CC reduced flow is demonstrated by indocyanine green angiography (ICGA) and OCTA, with an almost perfect overlap between one another (Figure 2)<sup>1,18</sup>. Multimodal imaging approach of APMPE, including OCTA, suggested a possible sequence of events from the primary insult to the resolution of the lesions, in four consecutive phases: choroidal, chorioretinal, transitional and resolution<sup>18</sup>. Phase 1, or choroidal, is characterized by CC hypoperfusion detected through OCTA and confirmed in ICGA. This CC flow voids appear larger than the corresponding area of outer retina disruption on SD-OCT. Despite permanent outer retinal changes, CC perfusion tends to be reestablished and this could explain the good prognosis of this disease, even without treatment<sup>18,19</sup>.

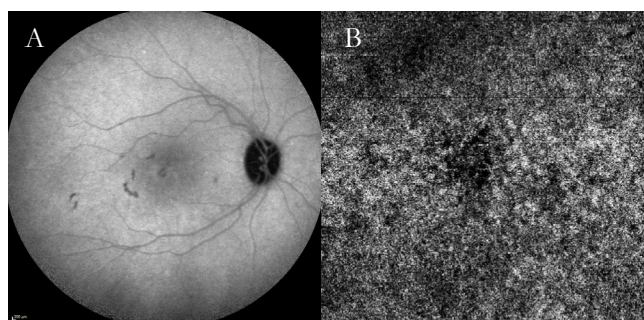


**Figure 2.** APMPE. A. ICGA, late phase, showing foveal and other macular hypofluorescent lesions. B. OCTA en face scan of the CC, showing a central flow void signal (blue circle), overlapping the central ICGA dark area.

Serpiginous choroiditis (SC) is a primary choriocapillaris and commonly occurs as a chronic, relapsing, bilateral, asymmetric disease, progressing in a centrifugal and phased manner around the optic disc. Recurrent inflammatory bouts lead to irreversible chorioretinal scarring. Overlapping phenotypes of SC have been described. Serpiginous-like choroiditis is associated

with *Mycobacterium tuberculosis* infection. No differences could be seen between these phenotypes in multimodal imaging, including OCTA<sup>3</sup>. Active SC lesions appear as non-perfused areas of the CC on OCTA, corresponding to hypofluorescent lesions on ICGA. OCTA of inactive lesions demonstrates only partial reperfusion of the CC (Figure 3)<sup>12,13</sup>. Concerning deeper choroidal layers, OCTA imaging is still challenging. A conversion from a “black-on-white” effect to a “white-on-black” has been reported in the Haller’s layer below the atrophic regions. This effect remains to be explained<sup>12,13,20</sup>.

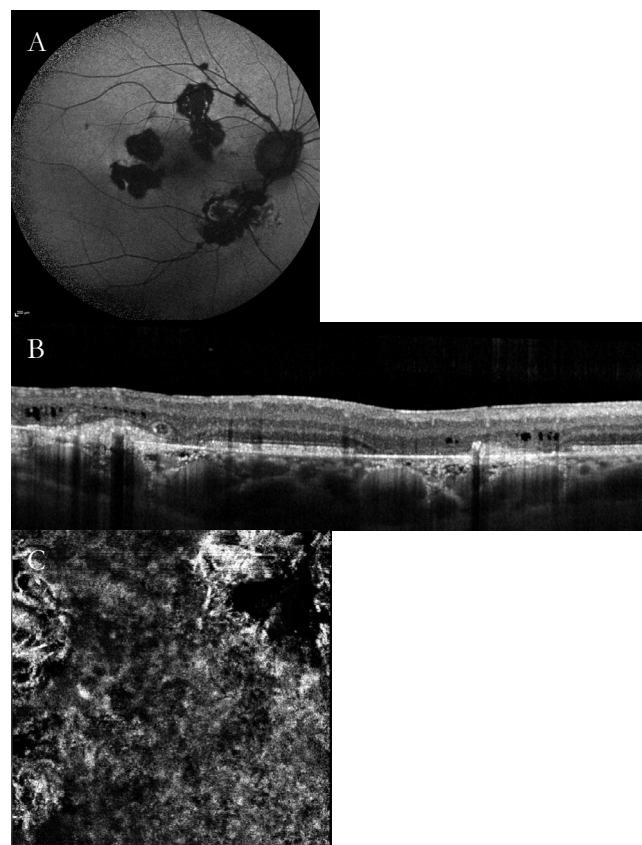


**Figure 3.** Serpiginous like Choroiditis. A. Fundus autofluorescence showing hypoautofluorescent lesions with ameboid contour and with associated hyperautofluorescent areas in the inferior lesion. B. SD-OCT transverse scan (orange line). C. central CC OCTA en face scan - post-acute phase; note CC multifocal flow voids (blue circles) and some shadowing from inflammatory lesions (red arrows)

Multifocal Choroiditis (MFC) and Punctate Inner Choroidopathy (PIC) belong to a group of chorioretinal inflammatory disorders that usually present with recurrent episodes of intraocular inflammation and affect more frequently young myopic females. Considering that MFC and PIC target the same structures in the same phenotypic manner and, when active, are treated the same way, there seems to be limited clinical utility in trying to differentiate them<sup>21</sup>. The main sites involved in the inflammatory process appear to be the subretinal pigment epithelium and outer retinal spaces and both

entities share mechanisms of vision loss such as direct inflammatory damage of the RPE and outer retina, scarring and inflammatory choroidal neovascularization (iCNV). MFC/PIC are the most frequent cause of iCNV. The majority of iCNV are well-defined classic lesions on FA and on OCT appear as hyperreflective type 2 lesions<sup>22,23,24,25</sup>. The differential diagnosis between a purely inflammatory MFC/PIC lesion *versus* iCNV is challenging. OCTA may detect neovascular flow, overcoming the limitations of dye angiography and OCT (Figure 4). However, OCTA alone is not yet sufficient to determine the exudative *status* of iCNV<sup>24,25,26</sup>.

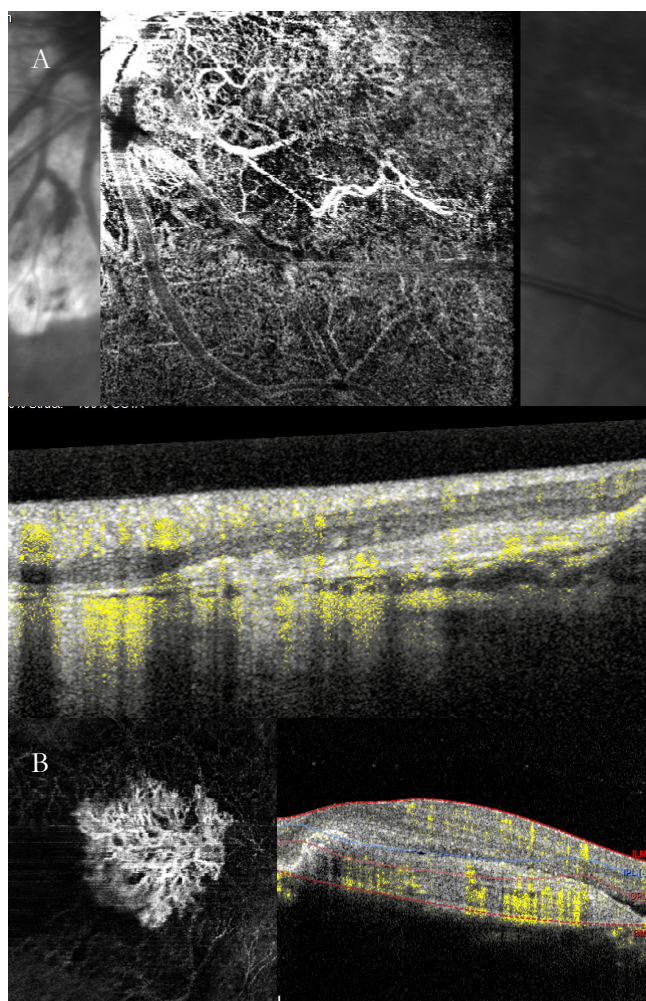


**Figure 4.** PIC. A. OCTA scan showing a neovascular lesion (iCNV) in the avascular layer, corresponding to the hyperreflective mixed lesion type in the OCT transverse scan (note the color coded flow signal). B. Another patient with a florid iCNV, complicating a PIC inflammatory lesion.

Results from one of the largest cohorts of eyes with MFC and OCTA showed a much higher rate of neovascular flow in MFC lesions (83%) than previously reported. Additionally, a high rate of neovascular flow was found in subretinal (91%) and mixed (100%) lesions, while purely subRPE lesions did not demonstrate neovascular flow on OCTA (Figure 5). These observations suggests

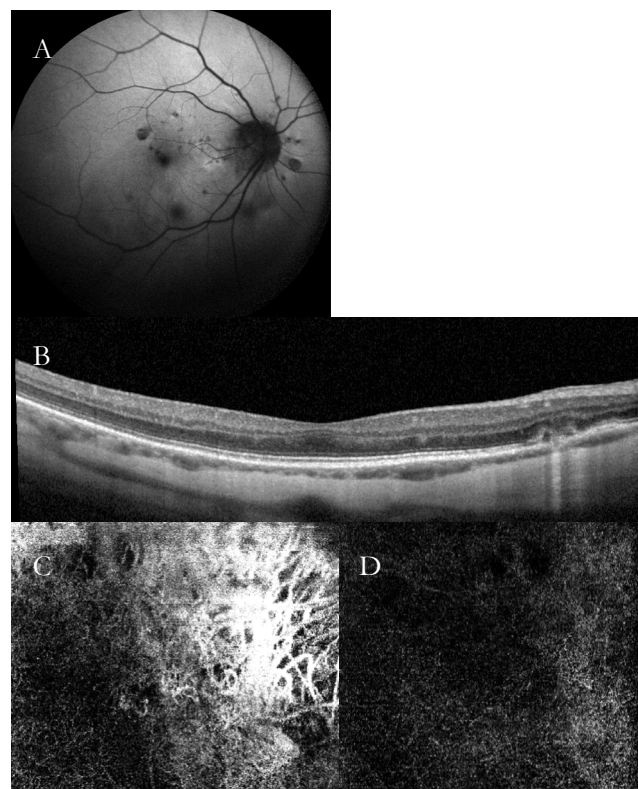


**Figure 5.** PIC. The patient had no symptoms and no inflammatory activity for more than 4 years. A. Note the small hyperautofluorescence temporal to the optic disc (red arrow). B. OCT scan reveals disruption of RPE and outer retinal layers, with some hyperreflective material in the outer retina. C. Small neovascular lesion on the OCTA scan of the avascular layer. D. The neovascular lesion regressed after anti-VEGF treatment

that development of neovascularization in MFC is intrinsically linked to the loss of integrity of the RPE. Breaches in the RPE may provide a conduit for pathologic angiogenesis<sup>27</sup>. There are conflicting results in the literature concerning the effect on the size and pattern of the iCNV after anti-VEGF treatment, but a decrease in lesion size and vascular complexity may result<sup>27,28</sup>.

Birdshot retinochoroiditis (BSRC) is traditionally classified as a stromal choroiditis. It presents as a chronic, bilateral uveitis that progresses with parallel, independent, retinal inflammation and stromal choroiditis. It has a strong association to HLA A-29, being present in almost 100% of all cases. Macular edema is a common complication, as well as progressive choroidal atrophy<sup>29</sup>.

Distinct retinal vascular changes have been recently described through OCTA, such as abnormal telangiectatic vessels, capillary loops, increased intercapillary spaces with a reduction in the vascular density in superficial and deep capillary plexus<sup>29,30</sup>. Vessel density of the retinal capillary plexuses may be a promising imaging biomarker for disease severity<sup>31</sup>. Typically, in the early stages of the disease, CC flow seems to be unaffected, favoring the hypothesis of choroidal infiltrates to be partial thickness lesions. With progression of choroidal atrophy to the

inner choroidal layers in the late stages of the disease, CC flow is reduced and the yellow atrophic lesions will appear co-localized with CC flow voids<sup>29</sup>. SS-OCTA allowed visualization of early BSRC lesions present on ICGA, suggesting that acute lesions originate in the Haller's layer, and in the absence of treatment, damage extends up into the inner choroid and ultimately to the RPE and retina<sup>32</sup>. A recent work highlighted the pathologic flow loss in >50% of eyes with BSRC, even in those with normal visual acuity. Different patterns of CC flow voids were present, relating BSRC eyes with abnormal vision with lower subfoveal CC density, when compared to eyes with normal vision, suggesting that compromised flow in the CC may contribute to decreased VA<sup>33</sup>.

OCTA findings in other stromal choroiditis are still not fully characterized. CC assessment of granulomatous choroiditis in the setting of Vogt-Koyanagi-Harada disease (VKH) and Sympathetic ophthalmia (SO) showed multiple dark foci corresponding to CC flow voids, reflecting possible ischemic changes, induced by damage in deeper layers<sup>34,35,36</sup>.

In conclusion, OCTA evaluation of choroidal inflammatory diseases provides new insights on the pathophysiology of these entities and will possibly lead to new classification proposals and treatment options. It is essential to be aware and recognize image artifacts and efforts are still needed to improve image quality, in particular of the deep choroidal layers.

## REFERENCES

- Borrelli E, Sarraf D, Freund B, Sadda S. OCT angiography and evaluation of the choroid and choroidal vascular disorders. *Progress in Retinal and Eye Research* 2018; 67:30-55.
- Jabs D, Nussenblatt R, Rosenbaum J. Standardization of Uveitis Nomenclature (SUN) Working Group. *Am J Ophthalmol* 2005;140(3):509-516.
- Invernizzi A, Cozzi M, Staurenghi G. Optical coherence tomography and optical coherence tomography angiography in uveitis: A review. *Clin Experiment Ophthalmol* 2019; 47:357-371.
- Yannuzzi L, Sorenson J, Guyer D, Slakter J, Chang B, Orlock D. Indocyanine green videoangiography: current status. *Eur J Ophthalmol* 1994;4(2):69-81.
- Pichi F, Sarraf D, Morara M, Mazumdar S, Neri P, Gupta V. Pearls and pitfalls of optical coherence tomography angiography in the multimodal evaluation of uveitis. *J Ophthalmic Inflamm Infect* 2017; 7:20.
- Pichi F, Sarraf D, Arepalli S et al. The application of optical coherence tomography angiography in uveitis and inflammatory eye diseases. *Progress in Retinal and Eye Research* 2017; 59:178-201.
- Spaide R, Fujimoto J, Waheed N et al. Optical coherence tomography angiography. *Prog Retin Eye Res* 2018; 64:1-55.
- Herbort C. Primary stromal choroiditis. *Acta Ophthalmol* 2017;95.
- Dingerkus V, Munk M, Brinkmann M et al. Optical coherence tomography angiography (OCTA) as a new diagnostic tool in uveitis. *Journal of Ophthalmic Inflammation and Infection* 2019; 9:10.
- Al-Sheikh M, Falavarjani K, Pfau M, et al. Quantitative features of the choriocapillaris in healthy individuals using swept-source optical coherence tomography angiography. *Ophthalmic Surg Lasers Imaging Retina* 2017;48: 623-631.
- Wang Q, Chan S, Yang J et al. Vascular density in retina and choriocapillaris as measured by optical coherence tomography angiography. *Am J Ophthalmol* 2016; 168:95-109.
- Macedo S, Pohlmann D, Lenglinger M, Pleyer U, Jousseaume A, Winterhalter S. *BMC Ophthalmology* 2020; 20:258;
- Montorio D, Giuffrè C, Miserocchi E, Modorati G, Sacconi R, Mercuri S, Querques L, Querques G, Bandello F. Swept-source optical coherence tomography angiography in serpiginous choroiditis. *Br J Ophthalmol* 2018;102(7):991-995.
- Herbort C, Papadia M, Mantovani A. Classification of Choroiditis based on Inflammatory lesion process rather than on fundus appearance: enhanced comprehension through the ICGA concepts of the iceberg and jelly-fish effects. *Klin Monbch Augenheilkd* 2012; 229(4):306-313.
- Pichi F, Srivastava SK, Chexal S, et al. En face optical coherence tomography and optical coherence tomography angiography of multiple evanescent white dot syndrome. *Retina* 2016; 36:S178-S188.
- Yannuzzi L, Miller A, Gregori G, Davis J, Rosenfeld P. Swept-source OCT angiography shows sparing of the choriocapillaris in multiple evanescent white dot syndrome. *OSLI Retina* 2017; 48:69-74.
- Zicarelli F, Mantovani A, Preziosa C, Staurenghi G. Multimodal imaging of Multiple Evanescent White Dot Syndrome: A new interpretation. *Ocular Immunology & Inflammation*, 2019; 0(00): 1-7.
- Burke T, Chu C, Salvatore S, Bailey C et al. Application of OCT-angiography to characterise the evolution of chorioretinal lesions in acute posterior multifocal placoid pigment epitheliopathy. *Eye* 2017; 31:1399-1408.
- Klufas M, Phasukkijwatana N, Iafe N et al. Optical coherence tomography angiography reveals choriocapillaris flow reduction in placoid chorioretinitis. *Ophthalmol Retin* 2017; 1:77-91.
- Desai R, Nesper P, Goldstein D et al. OCT angiography imaging in serpiginous choroidopathy. *Ophthalmol Retina* 2018; 2:351-9.
- Spaide RF et al. Redefining Multifocal Choroiditis and Panuveitis and Punctate Inner Choroidopathy through multimodal imaging. *Retina* 2013; 33:1315-1324.
- Agarwal A, Invernizzi A, Singh RB, et al. An update on inflammatory choroidal neovascularization: epidemiology, multimodal imaging, and management. *J Ophthalmic Inflamm Infect* 2018; 8:13.
- Cunningham ET, Pichi F, Dolz-Marco R et al. Inflammatory Choroidal Neovascularization. *Ocular Immunology & Inflammation* 2020; 28(1): 2-6.
- Levison AL, Baynes KM, Lowder CY, Kaiser PK, Srivastava SK. Choroidal neovascularisation on optical coherence tomography angiography in punctate inner choroidopathy and multifocal choroiditis. *Br J Ophthalmol* 2017; 101:616-622.
- Cheng L, Chen X, Weng S, et al. Spectral-domain optical coherence tomography angiography findings in multifocal choroiditis with active lesions. *Am J Ophthalmol* 2016;169:145-

- 161.
26. Astroz P, Miere A, Mrejen S et al. Optical Coherence Tomography Angiography to distinguish Choroidal Neovascularization from macular Inflammatory lesions in Multifocal Choroiditis. *Retina* 2018; 38:299–309.
  27. Zahid S, Chen K, Jung J et al. Optical Coherence Tomography Angiography of chorioretinal lesions due to Idiopathic Multifocal Choroiditis. *Retina* 2017; 37:1451–1463.
  28. Baumal C, De Carlo T, Waheed N et al. Sequential Optical Coherence Tomographic Angiography for Diagnosis and Treatment of Choroidal Neovascularization in Multifocal Choroiditis. *JAMA Ophthalmol* 2015; 133: 8-9.
  29. De Carlo TE, Bonini Filho MA, Adhi M et al. Retinal and Choroidal vasculature in birdshot chorioretinopathy analyzed using spectral domain optical coherence tomography. *Retina* 2015;35(11):2392-2399.
  30. Pohlmann D, Macedo S, Stübiger N et al. Multimodal Imaging in Birdshot Retinochoroiditis. *Ocular Immunology & Inflammation*, 2017; 25(5):626-637.
  31. Roberts P, Nester P, Goldstein D et al. Retinal capillary density in patients with Birdshot Chorioretinopathy. *Retina* 2018; 38(2):387-394.
  32. Pepple K, Chu Z, Weinstein J et al. Use of En Face Swept-Source Optical Coherence Tomography Angiography in Identifying Choroidal Flow Voids in 3 Patients With Birdshot Chorioretinopathy. *JAMA Ophthalmol* 2018; 136(11):1288-1292.
  33. Liu TY et al. Evaluation of Choriocapillaris Blood Flow in Patients with Birdshot Chorioretinitis (BSCR) using Swept Source Optical Coherence Tomography Angiography (SS-OCTA). *ARVO Annual Meeting Abstract 2020; Investigative Ophthalmology & Visual Science 2020, Vol.61, 2088.*
  34. Aggarwal K, Agarwal A, Mahajan S, Invernizzi A, Mandadi SKR, Singh R, Bansal R, Dogra MR, Gupta V; OCTA Study Group. The Role of Optical Coherence Tomography Angiography in the Diagnosis and Management of Acute Vogt-Koyanagi-Harada Disease. *Ocul Immunol Inflamm.* 2018;26(1):142-153.
  35. Fan S, Lin D, Hu J et al. Evaluation of microvasculature alterations in convalescent Vogt-Koyanagi-Harada disease using optical coherence tomography angiography. *Eye* 2020. doi: 10.1038/s41433-020-01210-5.
  36. Brar M, Sharma M, Grewal SPS et al. Treatment Response in Sympathetic Ophthalmia as Assessed by Widefield OCT Angiography. *Ophthalmic Surg Lasers Imaging Retina* 2018; 49(9):726-730.



# 18.

# OCULAR TUMORS

Filomena Pinto<sup>1,2</sup>, Susana Henriques<sup>3</sup>

1- Centro Hospitalar Universitário Lisboa Norte- HSM

2- Faculdade de Medicina da Universidade de Lisboa

3 - Hospital Professor Doutor Fernando da Fonseca

Although rare, intraocular tumors (IOT) put some important diagnostic issues, particularly those less than 3 mm. This group comprises several small tumors of the retina and choroid, as well as other non-neoplastic lesions. Most of them appear clinically as a small dome shaped solid mass with variable pigmentation, from orange-yellow to dark brown, localized at the posterior pole or mid periphery. Clinically, the main concern about IOT is the differential diagnosis between choroidal malignant melanoma (CMM) and *pseudomelanomas*<sup>1</sup> especially choroidal nevus (CN), circumscribed choroidal hemangioma (CCH), optic disc melanocytoma (ODM) and choroidal metastasis (CM). Although the documented growth of small melanocytic lesions has been considered the most important signal of evolution for melanoma<sup>2</sup>, increased vascularity with complex patterns is a hallmark of malignancy or malignant transformation.

Multimodal imaging for evaluation of IOT include ultrasonography (US), fundus autofluorescence (FAF), angiography (fluorescein and indocyanine green) and optical coherence tomography (OCT). Recently, OCT angiography (OCTA) has been applied to the study of retinal and choroidal vasculature in several macular diseases including choroidal tumors<sup>3-9</sup>. OCTA has the ability to separately evaluate superficial and deep retinal vascular plexus, choriocapillaris (CC), and choroid, with no need for dye injection<sup>10,11</sup>. With this technique it is possible to identify normal and abnormal vascular features within the tumor and the effects over the surrounding tissues, as well as to monitor response to treatment<sup>7</sup>. More recently, Swept Source OCTA (SSOCTA), has shown the capacity to non-invasively visualize deeper choroidal vessels with significant detail<sup>12,13</sup>. Although imaging IOT with OCTA is technically difficult due to large/peripheral tumors and segmentation/projections artifacts, some good quality images can be obtained in tumors located in the posterior pole with a thickness less than 3mm.

## CHOROIDAL NEVUS

Choroidal nevus is defined by the Collaborative Ocular Melanoma Study (COMS) as a benign melanocytic tumor less than 1 mm in height<sup>14</sup>. However, Shields and al. in a large study with 3422 nevi showed an increased

mean thickness of 1,5 mm<sup>15</sup>. The typical choroidal nevus appears as a small gray to brown choroidal tumor with bland surface, often associated with drusen and RPE alterations. Most choroidal nevi are asymptomatic, however, when located in the macular region they may cause visual loss due to photoreceptor/RPE disruption, intra or subretinal fluid (SRF) and pigment epithelium detachment (PED). Although these features are secondary to chronic retinal and RPE degeneration or choroidal neovascularization (CNV), they may be confused with malignant signs<sup>15</sup>. The microcirculation of benign nevi is similar to the surrounding choroidal plexus and is defined as “normal vessels”, but they can also show avascular areas, straight vessels, and parallel vessels.

**Structural OCT features** may include<sup>16-18</sup>: domed shaped hyperreflective choroidal mass with choroidal shadowing; CC compression; PED; RPE irregularity, nodularity or atrophy; and chronic retinal degenerative signs.

**OCTA features**<sup>3-9</sup> may include: well defined margins; normal retinal plexus and avascular retina; iso or hyperreflectivity at the level of the CC over the lesion; variable intralesional signal, from hyporeflectivity to hyperreflectivity (Fig.1), depending on pigmentation, thickness and intrinsic vascularity, which usually appears homogeneous with or without straight radial vessels at the periphery (Fig.2); and signs of vascular complications such as CNV<sup>4,6,8,19</sup> (Fig.3) and polypoidal choroidal vasculopathy (PCV)<sup>6,19</sup> (Fig.4). Branch vascular networks (BVN) show different morphologic patterns like sea-fan, tangle and Medusa head and the polyps are mostly identified as hypoflow round structures or as hyperflow lesions with a surrounding hypointense halo<sup>20</sup>.

## INDETERMINATE MELANOCYTIC LESIONS AND SMALL CHOROIDAL MELANOMA

Uveal melanoma<sup>1,14</sup> is the most common primary intraocular malignant tumor, 90% arising in the posterior uvea. In contrast to medium and large sized melanomas that can be diagnosed based on ophthalmoscopy and ultrasonic features, indeterminate melanocytic lesions (IML) and small choroidal melanoma (SCM) can present a diagnostic challenge.

**Structural OCT features**<sup>16,18,21</sup> may include: domed-

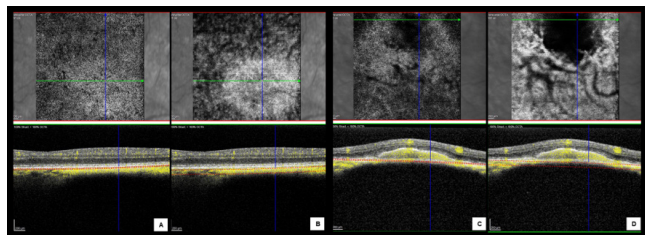


**Figure 1.** Choroidal nevus reflectivity on OCTA (en face and B-scan flow images). The two images on the left demonstrate a lesion isoreflective at the level of the CC (A) and hyperreflective at the level of the choroid (B) demonstrating homogeneous vascularity. The two images on the right demonstrate a lesion with central void at both levels, choriocapillaris (C) and choroid (D), possibly related to shadowing from overlying PED.

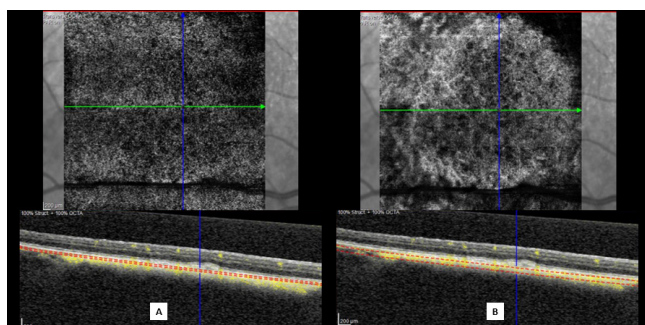


**Figure 2.** Choroidal flat nevus reflectivity on OCTA (en face and B-scan flow images): At the level of the choriocapillaris (A) the OCTA image demonstrates iso reflectivity; at the level of the choroid (B), the tumor demonstrates intrinsic vascularity with straight radial vessels at the periphery.

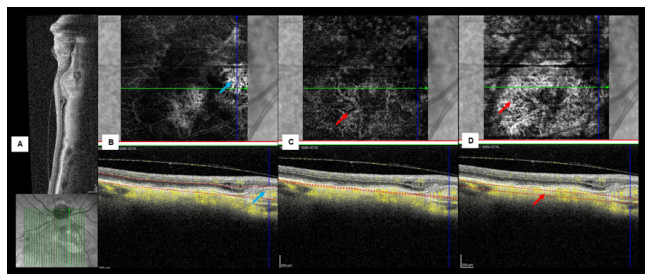


**Figure 3.** Multimodal imaging of a left choroidal nevus nasal to the optic disc complicated by type 1 CNV. (A) Structural OCT showing the nevus as a choroidal hyperreflective band with compression of CC, posterior shadowing, intraretinal fluid and a fusiform lesion with heterogeneous reflectivity over the nevus. (B) En face images and B-scan OCTA of OR displaying a juxta-papillary type 1 CNV (blue arrow). Customized slabs passing through the choriocapillaris (C) and the choroid (D) showing intrinsic vasculature (red arrow).

shaped smooth-surface topography, deep optical shadowing and overlying CC compression; abnormalities of OR; SRF; subretinal material compatible with lipofuscin; and *shaggy* photoreceptors.

**OCTA features**<sup>3–5,8,9,12,22–24</sup> may include: imprecise margins; iso or hyporeflective CC and decreased flow rate of superficial microvasculature (SMV); intratumoral complex and heterogeneous vascular patterns such as

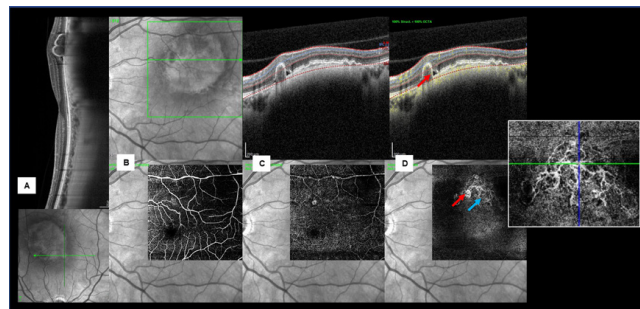


**Figure 4.** Multimodal imaging of a patient with a left macular nevus, PCV and SRF. (A) Structural OCT showing the nevus as a choroidal hyperreflective band with compression of CC; posterior shadowing and a large notched PED with heterogeneous reflectivity. B-scan OCTA and en face images, showing normal superficial (B) and deep (C) retinal plexus. (D) At the level of OR a thumb-like polypoidal lesion demonstrating intrinsic flow on fusion image (red arrow) and a BVN on en face OCTA (blue arrow).

vascular loops and vascular networks, but also avascular zones; OR involvement; enlargement of the deep foveal avascular zone (FAZ) and reduction in superficial and deep capillary vascular density (CVD).

Altered parafoveal microvasculature seems to be correlated with the presence of SRF, increasing tumor thickness and microvascular ischemia<sup>24</sup>. Also, the presence of a hyporeflective plexus or a hyperreflective ring surrounding the tumor (fig. 5), seems to be associated with higher risk of malignancy<sup>8</sup>.

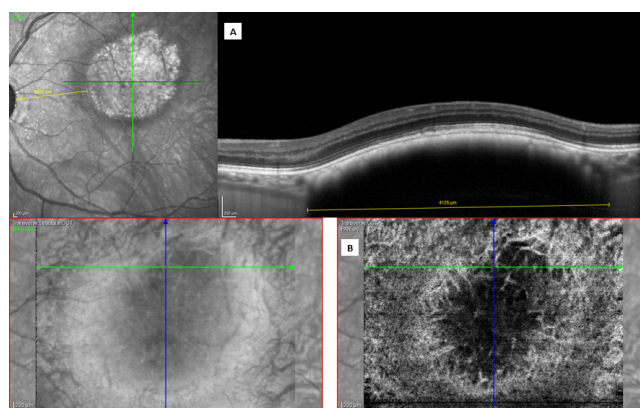


**Figure 5.** Multimodal imaging of a patient with a left IML. (A) Structural OCT showing a well delimited domed-shaped smooth-surface choroidal lesion with OR involvement, compression of CC and deep posterior shadowing. (B) En face images showing intratumoral vasculature with peripheral feeding vessels.

## CHOROIDAL HEMANGIOMA

Circumscribed choroidal hemangioma<sup>14,25</sup>, is a benign vascular tumor of the choroid, usually present as an isolated orange solid mass, typically located in the macular area. These lesions are often diagnosed when they impair

vision due to hyperopic shift, SRF or degenerative changes in the macular retina and RPE.

**Structural OCT features**<sup>16,18</sup> may include: medium hyperreflective tumor with a smooth anterior contour, without CC compression; partial optical shadowing; inner and OR usually appear normal (fig. 6). Long standing tumors may complicate with cystoid retinal edema, retinoschisis, OR abnormalities, SRF and *shaggy* photoreceptors

**OCTA features**<sup>7,8,12,13,26</sup> are variable and may include (fig. 6): well defined borders; regular sponge-like pattern<sup>13</sup>; irregularly organized hyperreflective internal structure with multiple dilated interconnected tumor vessels, intermixed with signal void areas<sup>12</sup>.

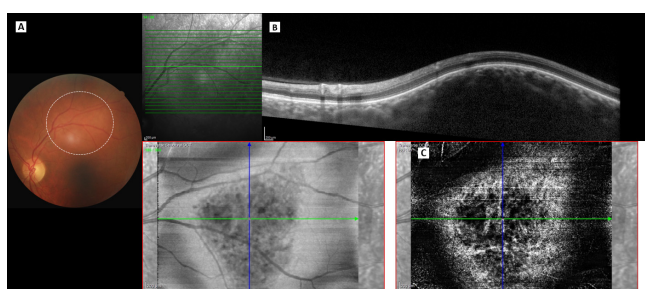


**Figure 6.** Multimodal imaging of a patient with a left macular choroidal hemangioma. (A) retinography showing a subretinal paramacular orange tumor. (B) Structural OCT showing a well delimited domed-shaped smooth-surface choroidal lesion, normal inner/outer retina and RPE and partial posterior shadowing. (C) En face images showing a lesion with well-defined borders and sponge-like pattern, visible intrinsic vessels intermixed with void area.

## CHOROIDAL METASTASIS

Choroidal metastasis<sup>14,27</sup> are the most common intraocular tumor. Clinically they appear as a small-to-medium size solid lesion, with a mean thickness of 3 mm located in the macular or paramacular region. They may affect both eyes and they often present as isolated or multiple yellow masses, with dome-shaped / plateau configuration and associated SRF.

**Structural OCT features**<sup>16,18</sup> may include: hyperreflective tumor with irregular (*lumpy bumpy*) anterior contour, CC compression and posterior shadowing; overlying RPE and OR abnormalities; *shaggy* photoreceptors; and SRF.

**OCTA features**<sup>3,7,8,28</sup> are scarce and contradictory and may include: signal void and hypovascularity at the level of the lesion and OR<sup>3,28</sup>; thick anastomotic vessels alongside thinner vasculature and hyporeflexive avascular regions<sup>8</sup>.

## OPTIC DISC MELANOCYTOMA

Optic disc melanocytoma<sup>14,29</sup>, which develops from uveal melanocytes, is a hamartoma with malignant potential, sometimes difficult to distinguish from MCM. Clinically

it appears as a dark brown or black, flat, or slightly elevated mass overlying the optic disc. Visual impairment is associated with optic disc/retinal edema, SRF, retinal hemorrhage and retinal vein occlusion.

**Structural OCT features**<sup>16,18</sup> may include (fig. 7): hyperreflective nodular tumor with dense posterior shadowing; disorganization of the retina overlying the tumor; and compressive or infiltrative changes in the optic nerve, peripapillary choroid, and retina.

**OCT-A features**<sup>12,30-32</sup> may include (fig. 7): surface vascularization in radial peripapillary plexus; intrinsic vascularity as tortuous blood vessels heterogeneously distributed within the tumor, intermixed with areas of void signal.

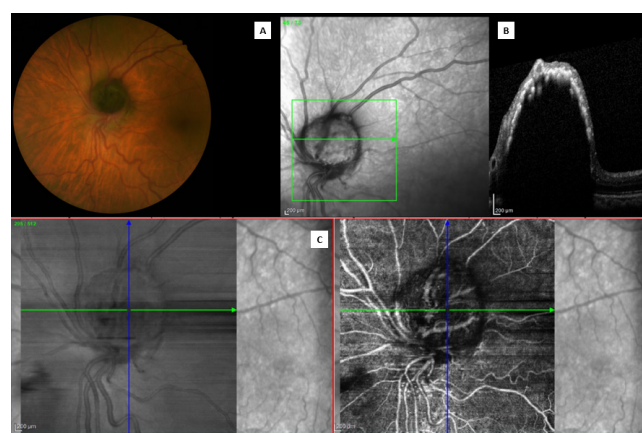


**Figure 7.** Multimodal imaging of a patient with a left optic disc melanocytoma. (A) Retinography showing an elevated brownish-black mass within the optic disc. (B) Structural OCT showing a hyperreflective lesion with posterior shadowing and absent optic cup. (C) OCTA en face images showing superficial telangiectatic vessels and intrinsic flow. (Courtesy of Inês Coutinho, HFF)

## RETINAL CAPILARY HEMANGIOMA (Retina hemangioblastoma)

Retinal capillary hemangioma<sup>18,33</sup> is a benign vascular tumor that arises from the retina or optic disc. It may be uni or bilateral and usually enlarges progressively, leading to exudative or tractional retinal detachment that impairs vision. It generally presents as a red spherical lesion, fed and drained by dilated tortuous retinal blood vessels. When hemangiomas develop from the optic disc, they may appear less well defined and without obvious feeding vessels. Commonly, there is intraretinal and subretinal exudation, particularly when the tumor is greater than 2-3 mm in diameter.

**Structural OCT features**<sup>18,34</sup> may include (fig. 8): hyperreflective full thickness retinal mass with domed shaped surface and deep optical shadowing; vitreoretinal traction; retinal disorganization; intraretinal edema; and surrounding SRF.

**OCTA features**<sup>35-37</sup> may include (fig. 8): bright, well-defined vascularized lesion in the superficial retina, better defined in en face images; signal void areas in the deeper



retina around the tumor; and identification of feeder and draining vessels.

In small tumors and optic disc tumors, the feeder and the draining vessels may be better identified in OCTA, than on retinography or fluorescein angiography<sup>36</sup>.

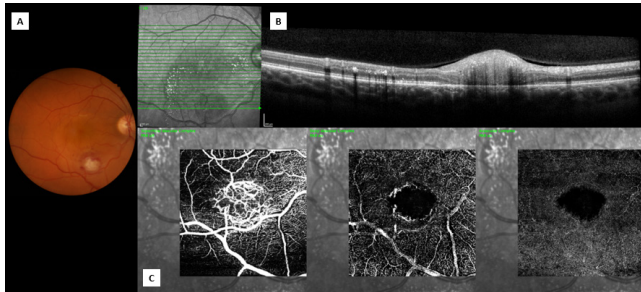


**Figure 8.** Multimodal imaging of a patient with a right capillary hemangioma. (A) Retinography showing a spherical retinal lesion with SRF. (B) Structural OCT showing hyperreflective full thickness retinal mass with dome shaped surface, retinal disorganization and surrounding hard exudates. (C) OCTA en face images showing a well-defined vascularized lesion in the superficial retina with feeder and draining vessels and void signal in deep plexus and avascular retina. (Courtesy of Inês Coutinho, HFF)

## CHOROIDAL OSTEOMA

Choroidal osteoma<sup>14</sup> is a rare, benign, ossifying tumor of the choroid, that usually occurs in healthy young females. Its natural course may include tumor growth, calcification, and decalcification. Impairment of visual acuity depends on retinal changes associated to decalcification or CNV.

**Structural OCT features**<sup>16,38,39</sup> may include (fig. 9): dome or undulating surface; intralesional horizontal lamellar lines; horizontal and vertical tubules with “spongy” flecks; and photoreceptor loss due to deossification.

**OCTA features**<sup>3,8,39,40</sup> may include (fig. 9): variable intralesional vascularity from absence to fine vascular network; dark background in decalcified areas; presence of a CNV.

The major application of OCTA in choroidal osteoma is assistance in the diagnosis of associated CNV (fig. 9)

## CONCLUSION

The use of OCTA to visualize IOT has some limitations, related to the depth of the tissues involved, the patient cooperation, fixation stability and media opacity. Despite these limitations, OCTA is a useful, safe and reproducible high-resolution imaging technique to monitor the vascularity of tumors located at the posterior pole, with thickness less than 3 mm. Recognition of the vascular features typical of neovascularization (CNV or PCV) is also important as this can be easily misinterpreted as a sign of malignancy. With optimization of OCTA in imaging of peripheral retina and deeper structures (wide-field OCTA and SSOCTA), the applicability of this modality will expand in ocular oncology.

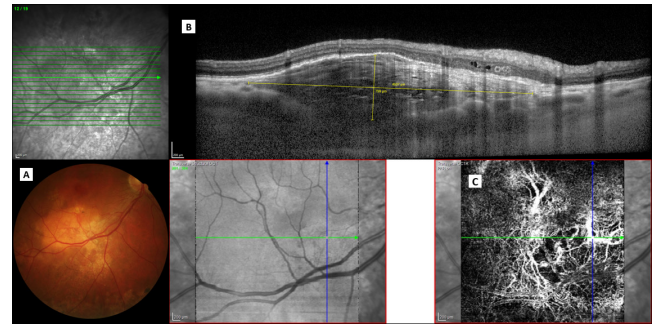


**Figure 9.** Multimodal imaging of a patient with a right paramacular choroidal osteoma. (A) Retinography showing an ill-defined amelanotic subretinal lesion. (B) Structural OCT showing a choroidal lesion with undulating surface, OR involvement, compression of CC and intralesional horizontal lamellar lines. (C) OCTA en face images showing intralesional void areas and quiescent choroidal neovascularization.

## REFERENCES

- Shields CL, Manalac J, Das C, Ferguson K, Shields JA. Choroidal melanoma: Clinical features, classification, and top 10 pseudomelanomas. *Curr Opin Ophthalmol.* 2014;25(3):177-185.
- Singh AD, Mokashi AA, Bena JF, Jacques R, Rundle PA, Rennie IG. Small Choroidal Melanocytic Lesions. Features Predictive of Growth. *Ophthalmology.* 2006;113(6):1032-1039.
- Cennamo G, Romano MR, Breve MA, et al. Evaluation of choroidal tumors with optical coherence tomography: Enhanced depth imaging and OCT-angiography features. *Eye.* 2017;31(6):906-915.
- Garcia-Arumi Fuste C, Peralta Iturburu F, Garcia-Arumi J. Is optical coherence tomography angiography helpful in the differential diagnosis of choroidal nevus versus melanoma? *Eur J Ophthalmol.* 2020;30(4):723-729.
- Ghassemi F, Mirshahi R, Fadakar K, Sabour S. Optical coherence tomography angiography in choroidal melanoma and nevus. *Clin Ophthalmol.* 2018;12:207-214.
- Henriques SP, Basto R, Roque J, et al. Optical coherence tomography angiography features of choroidal nevi. *Rev Soc Port Oftalmol.* 2020;44(3).
- Naseripour M, Ghasemi Falavarjani K, Mirshahi R, Sedaghat A. Optical coherence tomography angiography (OCTA) applications in ocular oncology. *Eye.* 2020;34(9):1535-1545.
- Toledo JJ, Asencio M, García JR, Morales LA, Tomkinson C, Cajigal C. OCT Angiography: Imaging of Choroidal and Retinal Tumors. *Ophthalmol Retin.* 2018;2(6):613-622.
- Toledo JJ, Asencio-Duran M, García-Martínez JR, López-Gaona A. Use of OCT Angiography in Choroidal Melanocytic Tumors. In: *Journal of Ophthalmology.* Vol 2017. Hindawi Limited; 2017.
- Spaide RF, Klancnik JM, Cooney MJ. Retinal vascular layers imaged by fluorescein angiography and optical coherence tomography angiography. *JAMA Ophthalmol.* 2015;133(1):45-50.
- Laíns I, Wang JC, Cui Y, et al. Retinal applications of swept source optical coherence tomography (OCT) and optical coherence tomography angiography (OCTA). *Prog Retin Eye Res.* 2021.
- Gündüz AK, Mirzayev I, Kasimoglu R, Özalp Ateş FS. Swept-

- source optical coherence tomography angiography findings in choroidal and retinal tumors. *Eye*. 2021;35(1):4-16.
13. Filloy A, Caminal JM, Arias L, Jordán S, Català J. Swept source optical coherence tomography imaging of a series of choroidal tumours. *Can J Ophthalmol*. 2015;50(3):242-248.
  14. Damato B, Singh A. *Clinical Ophthalmic Oncology. Uveal Tumors*. second. (Singh A, Damato B, eds.). Springer; 2014.
  15. Shields CL, Furuta M, Mashayekhi A, et al. Visual acuity in 3422 consecutive eyes with choroidal nevus. *Arch Ophthalmol*. 2007;125(11):1501-1507.
  16. Shields CL, Manalac J, Das C, Saktanasate J, Shields JA. Review of spectral domain enhanced depth imaging optical coherence tomography of tumors of the choroid. In: *Indian Journal of Ophthalmology*. Vol 63. Medknow Publications; 2015:117-121.
  17. Shah SU, Kaliki S, Shields CL, Ferenczy SR, Harmon SA, Shields JA. Enhanced depth imaging optical coherence tomography of choroidal nevus in 104 cases. *Ophthalmology*. 2012;119(5):1066-1072.
  18. Pinto F, Leal I. Pigmented lesions of the retina and choroid accessible to OCT. In: Henriques J, Duarte A, Quintão T, eds. *LASER Manual in Ophthalmology-Fundamentals and Laser Clinical Practice*. 1st ed. Lisbon: SPIILM Portuguese Medical Laser Society Publishing; 2017:329-334.
  19. Pellegrini M, Corvi F, Say EAT, Shields CL, Staurengi G. Optical coherence tomography angiography features of choroidal neovascularization associated with choroidal nevus. *Retina*. 2018;38(7):1338-1346.
  20. Chan SY, Wang Q, Wang YX, Shi XH, Jonas JB, Wei W Bin. Polypoidal choroidal vasculopathy upon optical coherence tomographic angiography. *Retina*. 2018;38(6):1187-1194.
  21. Shields CL, Kaliki S, Rojanaporn D, Ferenczy SR, Shields JA. Enhanced depth imaging optical coherence tomography of small choroidal melanoma: Comparison with choroidal nevus. *Arch Ophthalmol*. 2012;130(7):850-856.
  22. Zhou N, Xu X, Wei W. Optical coherence tomography angiography characteristics of choroidal melanoma. *Eye*. 2020.
  23. Valverde-Megias A, Say EAT, Ferenczy SR, Shields CL. Differential macular features on optical coherence tomography angiography in eyes with choroidal nevus and melanoma. *Retina*. 2017;37(4):731-740.
  24. Li Y, Say EAT, Ferenczy S, Agni M, Shields CL. Altered parafoveal microvasculature in treatment-naïve choroidal melanoma eyes detected by optical coherence tomography angiography. *Retina*. 2017;37(1):32-40.
  25. Sen M, Honavar SG. Circumscribed choroidal hemangioma: An overview of clinical manifestation, diagnosis and management. *Indian J Ophthalmol*. 2019;67(12):1965-1973.
  26. Konana V, Shanmugam P, Ramanjulu R, Mishra KC, Sagar P. Optical coherence tomography angiography features of choroidal hemangioma. *Indian J Ophthalmol*. 2018;66(4):581-583.
  27. Arepalli S, Kaliki S, Shields CL. Choroidal metastases: Origin, features, and therapy. In: *Indian Journal of Ophthalmology*. Vol 63. Medknow Publications; 2015:122-127.
  28. Cennamo G, Montorio D, Carosielli M, Romano MR, Cennamo G. Multimodal Imaging in Choroidal Metastasis. *Ophthalmic Res*. 2021;64(3):411-416.
  29. Shields JA, Demirci H, Mashayekhi A, Eagle RC, Shields CL. Melanocytoma of the optic disk: A review. *Indian J Ophthalmol*. 2019;67(12):1949-1958.
  30. Raval V, Reddy R, Kaliki S, Das T, Singh AD. Optic nerve head melanocytoma: Optical coherence tomography/angiography features. *Indian J Ophthalmol*. 2021;69(2):332-336.
  31. Carnevali A, Querques L, Zucchiatti I, Scordia V, Bandello F, Querques G. Optical coherence tomography angiography features in melanocytoma of the optic nerve. *Ophthalmic Surg Lasers Imaging Retin*. 2017;48(4):364-366.
  32. Zhou N, Xu X, Wei W. Optical coherence tomography angiography characteristics of optic disc melanocytoma. *BMC Ophthalmol*. 2020;20(1).
  33. Singh A, Damato B, eds. *Clinical Ophthalmology Oncology. Retinal Tumors*. second. Springer; 2014.
  34. Heimann H, Jmor F, Damato B. Imaging of retinal and choroidal vascular tumours. In: *Eye (Basingstoke)*. Vol 27. Nature Publishing Group; 2013:208-216.
  35. Sagar P, Shanmugam P, Konana V, Ramanjulu R, Mishra K, Simakurthy S. Optical coherence tomography angiography in assessment of response to therapy in retinal capillary hemangioblastoma and diffuse choroidal hemangioma. *Indian J Ophthalmol*. 2019;67(5):701-703.
  36. Sagar P, Rajesh R, Shanmugam M, Konana VK, Mishra D. Comparison of optical coherence tomography angiography and fundus fluorescein angiography features of retinal capillary hemangioblastoma. *Indian J Ophthalmol*. 2018;66(6):872-876.
  37. Custo Greig EP, Duker JS. Retinal hemangioblastoma vascular detail elucidated on swept source optical coherence tomography angiography. *Am J Ophthalmol Case Reports*. 2021;21.
  38. Shields CL, Arepalli S, Atalay HT, Ferenczy SR, Fulco E, Shields JA. Choroidal osteoma shows bone lamella and vascular channels on enhanced depth imaging optical coherence tomography in 15 eyes. *Retina*. 2015;35(4):750-757.
  39. Francisco Olguin-Manríquez, Ana Bety Enríquez, Nicolás Crim, Miroslava Meraz-Gutierrez, Vidal Soberón-Ventura, Ismael Ávila, Virgilio Morales-Canton, Juan Manuel Jimenez-Sierra Francisco Olguin-Manríquez, Ana Bety Enríquez, Nicolás Crim, Miroslava Meraz-Gu JMJ-S. Multimodal imaging in choroidal osteoma. *Int J Retin Vitre*. 2018.
  40. Shen C, Yan S, Du M, Zhao H, Shao L, Hu Y. Assessment of choroidal osteoma complicating choroidal neovascularization by optical coherence tomography angiography. *Int Ophthalmol*. 2018;38(2):787-792.



Catarina Rodrigues, Sandra Barrão  
 Instituto de Oftalmologia Dr. Gama Pinto

OCT-Angiography (OCT-A) is a revolutionary and promising image modality that allows depth-resolved visualization of the retinal and choroidal microvasculature in an easy, fast, and non-invasive way.

The vascular image is generated by calculating the decorrelation between consecutive B-scans on the same section and is based on the concept that in the static retinal tissue the only moving cells are blood cells in the vasculature. As so OCT-A enables repeated analyses of blood circulation without the need for intravenous dye injections and in a faster manner, making more accessible longitudinal analyses, providing new insights into retinal diseases, and changing the approach of clinicians daily-basis.

Fluorescein angiography (FA) retains some major advantage in analyzing the perfusion dynamics (perfusion delay or perfusion absence) and the vessel integrity and permeability (displayed by the dyeing of leakage along the vessels). However, in the past few years, interest in OCT-A has grown dramatically and is resulting in rapid developments of tools useful to the clinicians in therapeutic decisions and post treatment follow-up.

Besides the non-need for intravenous dye injections and the time-saving procedure, OCT-A has other specific advantages over traditional angiography:

- Visualize both the retinal and the choroidal microvasculature: while FA is more suitable for retinal vessels and Indocyanine green angiography (ICGA) is ideally for the choroid.
- Provides a three-dimensional image on retinal vascular: as it is acquired in volumetric scans that can be segmented to specific depths, allowing individual visualization on superficial and deep macular capillary plexus.
- Enables a functional analysis on blood flow in the vessels: as it is simultaneously achieved with structural B scans, it allows a comprehensive assessment of functional flow information on the structural details in each scan.
- It is suitable for patients where the contrast material is contraindicated or discouraged (allergy to iodine, previous adverse reactions, hepatic or renal failure, pregnant women)

In OCT-A, vascular disturbances can manifest as abnormal presence of flow, absence of flow or

anomalous vessel conformation. This allows us to detect neovascularization, aneurysms, areas of non-perfusion and shunts, and so OCT-A can highlight several signs of the most common retinal and choroidal diseases.

In this chapter we will explore the potential of OCT-A in daily-practice and enhance the benefits and disadvantages of the image modality.

## DEGENERATIVE DISEASES

Among retinal degenerative diseases, Age-Related Macular Degeneration (AMD) is the most common and explored clinical application of OCT-A.

In the past years, OCT-A had a huge clinical impact in AMD management, as it made fast and non-invasive the diagnosis of Macular Neovascularization (MNV), raising the detection rates of clinical active and subclinical MNV and shortening the time until anti-vascular endothelial growth factor (anti-VEGF) treatment establishment.

OCT-A can display all three types of MNV, taking particularly advantage in type 1 MNV, that is poorly visualized on FA. Furthermore, OCT-A can identify nonexudative MNV, which neither leak on FA nor have intraretinal or subretinal fluid on structural OCT.

Establishing the correlation between the MNV morphological characteristics on OCT-A and its exudative behavior<sup>1</sup> and understanding the significance of the nonexudative MNV displayed by OCT-A<sup>2</sup> are still hot topics in retinal imaging investigation.

OCT-A has also the benefit of systematic evaluations and as the image acquisition is simultaneous with the structural scans, it follows the remodeling of vessels during anti-VEGF injections and guides the therapeutic decisions on the regimen that is best suited to each patient

Regarding the Pachychoroid spectrum diseases, OCT-A can more reliably determine the presence of neovascularization<sup>3,4</sup>, that can be difficult to assess with FA as it may occur overlapping areas of extensive hyperfluorescence due to pooling effect. This OCT-A advantage is crucial for early recognition of patients who would benefit from anti-VEGF therapy.

## VASCULAR DISEASES

In retinal vascular diseases is essential to assess the

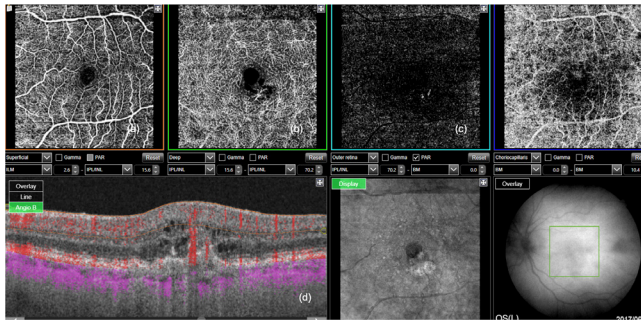


**Figure 1.** Retinal Angiomatous Proliferation  
(a) OCTA at the level of the superficial capillary plexus (SCP). (b) OCTA at the level of the deep capillary plexus (DCP) showing proliferation of intraretinal capillaries in the foveal area that penetrate towards the outer retina. (c) horizontal cross-sectional B-scan OCT with perfusion overlay identifying the retinal-choroidal anastomosis.

vascular flow dynamics. Leakage, pooling and staining are well described FA features used for qualitative evaluation of the vascular network. OCT-A lacks the ability to appreciate these dynamic phenomena and so it still hasn't replaced FA as the gold-standard image modality in vascular disease. As an easy access and non-dye image modality, an effort is being made to establish OCT-A biomarkers in most common retinal vascular diseases as diabetic retinopathy (DR) and retinal vein occlusion (RVO).

OCT-A can be useful to document microvascular alterations such as microaneurysms, shunts, neovascularization or areas of capillary non-perfusion. The OCT-A morphologic features of retinal neovascularization can be similar and indistinguishable from other vascular anomalies, and to differentiate it, one must correspond the suspect OCT-A finding with structural B scan, as in retinal neovascularization the vascular structure will protrude above the ILM.

One of the major advantages of FA was the periphery visualization, since in the primal OCT-A devices the scanning was limited to the posterior pole. Advances in OCT-A imaging technology made possible to image areas of 12x12mm in a single acquisition and to merge multiple scans to cover a wide-field area. This raised the interest in OCT-A pinpointing areas of ischemia, enabling the peripheral identification of capillary rarefaction and allowing targeted laser therapies.

OCT-A give an excellent *En face* view of the foveal avascular zone (FAZ). FAZ modification reflects the microvascular network alterations and is sequentially enlarged in each stage of Diabetic Retinopathy. FAZ and density of capillaries within the macula are both OCTA biomarkers known to have prognostic value in DR, denoting capillary nonperfusion and eventually macular ischemia<sup>5</sup>.

In RVO the usage of OCTA can be particularly important in the acute phase, when the extensive superficial flame hemorrhages create a masking effect, making determination of non-perfusion areas less precise with FA. Some authors found OCTA to be more precise in defining the extent and location of maximum ischemic insult following RVO<sup>6</sup>.

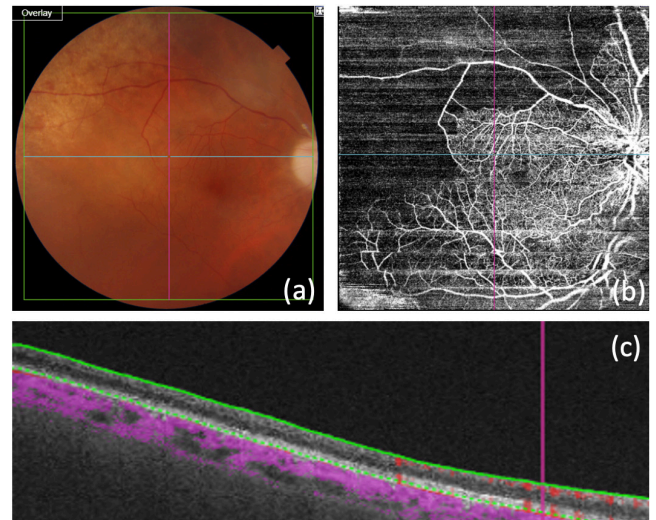


**Figure 2.** Arterial Occlusion  
(a) Fundus retinography showing pale areas corresponding to compromised circulation. (b) OCTA (12x12 mm) showing large areas of non-perfusion. (c) B-scan OCT, above the fovea, with perfusion overlay and segmentation lines, showing neuroretinal atrophy and lack of vessels (red dots) in the left zone of the scan corresponding to ischemic areas in the OCTA

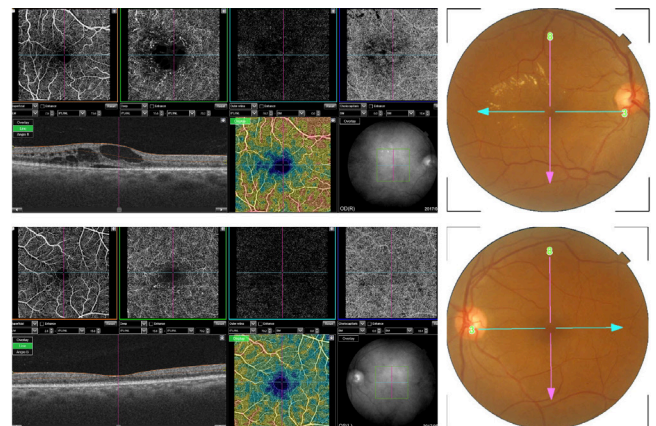


**Figure 3.** Diabetic retinopathy  
Vascular density map reveals abnormal FAZ. Note the presence of cystoid macular edema in the affected area that may cause misinterpretation considering automatic layers segmentation.

## INFLAMMATORY DISEASES

In Uveitis, OCTA is not able to detect signs of active vascular inflammation and so has a complementary role to traditional angiography, being mainly useful to display disruption of normal vascular flow, retinal neovascularization and inflammatory choroidal neovascularization (iCNV).

When evaluating the vascular architecture abnormalities, OCTA display all the vascular details that are missed in FA due to the mask effect from dye leakage. OCTA has also the major advantage of individual visualization of superficial capillary plexus, deep capillary and

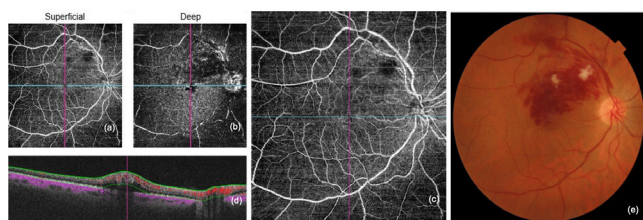


**Figure 4.** Superior BRVO

(a) OCTA (12x12 mm) at the level of the superficial capillary plexus (SCP). (b) OCTA at the level of the deep capillary plexus (DCP) showing areas of non-perfusion/no flow detected areas. (c) OCTA full macula showing mask effect of exudates but vascular visualization although the presence of retinal hemorrhages. (d) cross-sectional B-scan OCT with perfusion overlay and segmentation lines identifying macular edema with no significant alteration of SCP. (e) color retinography

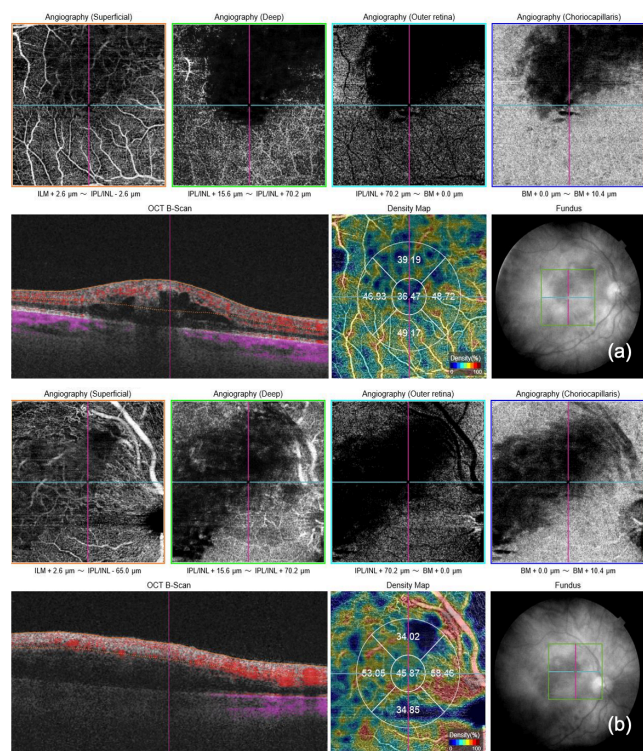


**Figure 5.** BRVO (same case)

(a) OCTA (4,5x4,5 mm) centered in the fovea, macular edema with cystic spaces, without vessels (b) centered in hemorrhagic area

choriocapillaris. This can be particularly important in the diagnosis since some diseases affect mainly one of the plexuses. OCTA also takes significance in the follow-up of the patients, for there is a good correspondence between areas of vascular disruption on OCTA and the findings in conventional angiography. One can dismiss the dye and monitor the treatment response and the disease relapse using longitudinal OCTA follow-up.

Regarding the uveitis commonly complicated by iCNV, the early diagnosis may not be apparent using FA since focal diffusion or accumulation of dye may mask the leakage of the iCNV. In these cases, where iCNV location is

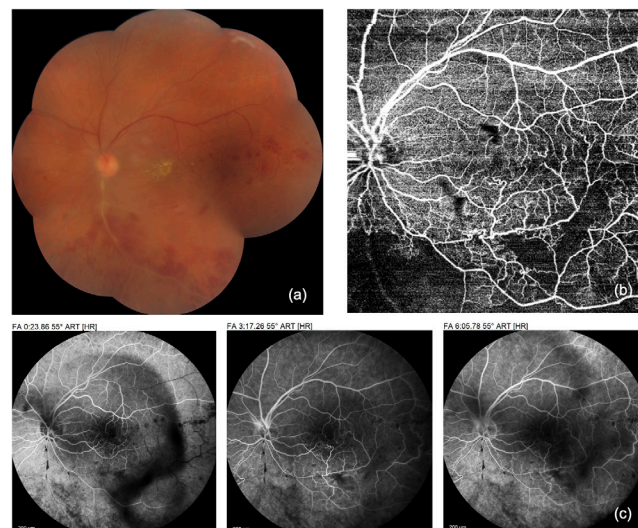


**Figure 6.** Occlusive vasculitis

(a) Composite retinography showing deep compromise of inferior retinal vascularization and dispersed areas of hemorrhages. (b) OCTA (12x12 mm) OCTA full macula showing vascular tortuosity, dilation and telangiectasia along with well defined non-perfusion areas. (c) Fluorescein angiography (FA).

overlapping an area of chorioretinitis or an area of retinal serous detachment, the signs of iCNV activity may also not be distinct on structural OCT and so, only the OCTA will clearly demonstrate the neovascular network forming.

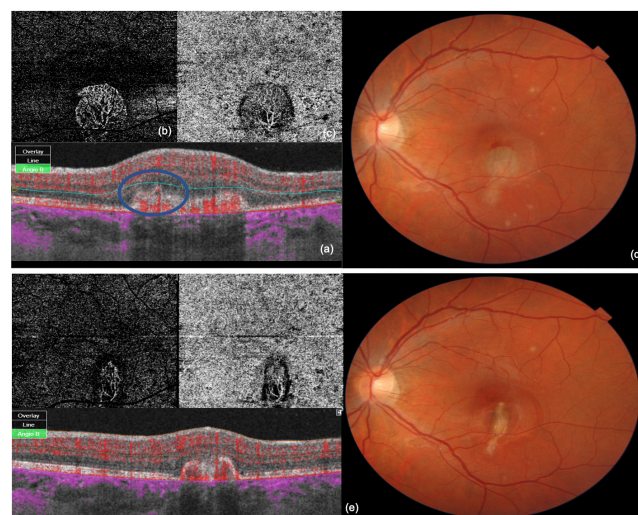


**Figure 7.** Inflammatory choroidal neovascularization (iCNV)

(a) cross-sectional B-scan showing a perifoveal subretinal hyper-reflective structure. The pitchfork sign (blue circle) raise suspicion on a iCNV that could be initially missed as an inflammatory lesion. (b) OCTA (4,5x4,5 mm) at the level of outer retina and (c) OCTA at the choriocapillaris displaying the iCNV. (d) Color retinography revealing multiple, small, yellowish choroiditis lesions and a larger grayish subfoveal lesion. (e) Composite image portraying the 6 months follow treatment with prednisolone, azathioprine and anti-VEGF. There is a significant decrease in iCNV area and in the number and size of choroiditis lesions

## CONCLUSION

OCTA has changed the approach of clinicians and scientists to retinal vascular analysis. The high resolution on vascular structure, the non-dye needs, and the easy access raise the diagnosis of major vascular complications, help the therapeutic institution without any delay and guide the longitudinal pos-treatment monitoring.

The future challenges for the image modality are concerning to:

- Improve OCTA technology: faster scanning speeds will be crucial to obtain larger fields of view with higher axial resolution.
- Improve clinical setting of OCTA: develop an OCTA nomenclature standardization and raise consensus on reported findings for each pathology.
- Apply the knowledge to deep learning and create diagnostic algorithms using OCTA.

## REFERENCES

1. Cabral D, Coscas F, Pereira T et al. Quantitative Optical Coherence Tomography Angiography Biomarkers in a Treat-and-Extend Dosing Regimen in Neovascular Age-Related Macular Degeneration. *Transl Vis Sci Technol.* 2020. 9(3):18
2. Laiginhas R, Yang J, Rosenfeld P, Falcão M. Nonexudative Macular Neovascularization - A Systematic Review of Prevalence, Natural History, and Recent Insights from OCT Angiography. *Ophthalmol Retina.* 2020;4(7):651-661
3. Bousquet E, Bonnin S, Mrejen S, Krivosic V, Tadayoni R, Gaudric A. Optical coherence tomography angiography of flat irregular pigment epithelium detachment in chronic central serous chorioretinopathy. *Retina.* 2017; 0: 1–10
4. Carlo T, Rosenblatt A, Goldstein M et al. Vascularization of Irregular Retinal Pigment Epithelial Detachments in Chronic Central Serous Chorioretinopathy Evaluated With OCT Angiography. *Ophthalmic Surg Lasers Imaging Retina.* 2016;47(2):128-33.
5. Chua J, Sim R, Tan B et al. Optical Coherence Tomography Angiography in Diabetes and Diabetic Retinopathy. *J Clin Med.* 2020 3;9(6):1723.
6. Moussa M, Leila M, Bessa A et al. Grading of macular perfusion in retinal vein occlusion using en-face swept-source optical coherence tomography angiography: a retrospective observational case series. *BMC Ophthalmol.* 2019 10;19(1):127.

# UNMET NEEDS

Rosa Dolz Marco, MD, PhD, FEBO  
Unit of Macula, Ophthalmic Clinic, Valencia, Spain

Optical coherence tomography angiography (OCTA) is a non-invasive technique allowing for the simultaneous visualization of the structural and vascular architecture of the eye.<sup>1</sup> The benefits of this relatively novel technique for a variety of eye conditions have been detailed in previous chapters, as well as the technical aspects, and the presence of different devices. In the present chapter, we will review the limitations we face while using OCTA as well as the direction of this promising technique currently still in development.

## Speed and field of view

For the detection of motion contrast, OCTA protocols re-scan the same retina region multiple times.<sup>1</sup> In order to maintain appropriate acquisition times, faster devices with higher A-scan rates are required compared with structural OCT images. In the last few years there is a trend to increase speed in these devices, however there is a limitation in the field of view that commercially available devices provide. Some papers and research prototypes already provide information on wide field OCTA images, with great value on vascular conditions such as diabetic retinopathy.<sup>3,4</sup> We should appreciate that wide field images also associate a decrease in scan density and resolution, thus balancing the A-scan rate, scan density and field of view of the different imaging patterns is important and there is still work in progress in this field.<sup>2,5</sup>

Another important factor in OCTA is the interscan rate. Longer interscan times are more sensitive to motion, but also to bulk motion. There are different projects using different interscan rates as a surrogate for flow velocity,<sup>2,6</sup> but this is still under evaluation.

## Resolution

Axial resolution is variable between devices, but also, the different OCTA algorithms may affect axial resolution differently. Those protocols splitting the spectrum improve signal to noise ratio, but also decrease axial resolution and may affect the visualization and differentiation of intermediate and deep vascular layers.<sup>7</sup> Lateral resolution is another variable that might be different between devices. As discussed earlier, the

density of the scan needs adjustment when trying to achieve wider fields of view in order to maintain suitable acquisition timings. In the macular analysis, current devices provide detailed information with similar appearance to histology.<sup>8</sup> While current OCTA devices achieve a lateral resolution of up to 6 micrometers, the increase in lateral resolution in adaptive optics OCTA devices provide a better visualization of the size of capillaries, diminishing its overestimation.<sup>9</sup> This promising technology is though still under development limiting its presence in daily practice.

## Artifacts

One of the main limitations of OCTA is the presence of a greater number of artifacts compared with other imaging techniques, mainly structural OCT.<sup>1,10</sup> Understanding how OCTA images are generated will help understanding how to interpret OCTA images and avoiding errors in the evaluation of artifacts. One of the current unmet aims on OCTA imaging is the lack of standard segmentation algorithms across platforms. Since OCTA images are based on *en face* or transversal analysis of the structure of interest, it is important to know segmentation boundaries when applying automated segmentation, as well as know the limitations when comparing the information from different devices.<sup>11</sup>

It is also important to highlight that despite the efforts removing projection artifacts, with different algorithms working both on *en face* reconstructions and B-scan images (2D-3D Projection Artifact Removal -PAR), training on this specific artifact is mandatory. Being aware of this artifact and knowing how to interpret images with and without PAR will contribute to a correct analysis of the scan.

## Review process

Despite technical complexity of OCTA, the enormous amount of data that a single scan provides might be difficult to analyze. An optimized image review protocol might be needed for a correct interpretation in an optimal workflow.<sup>12</sup>

## Standardization and analysis of data

As mentioned before, there is a broad variety of devices



in the market, using spectral domain or swept source technology, each of them with different pros and cons, and each of them using its own proprietary imaging processing algorithm. In addition, as stated earlier, algorithms used for segmentation, artifact removal, or image processing also differ across platforms. All this variability aims for the optimal use of each individual device, however, represents a major limitation for clinicians and researchers since we lack standards and ground truth information regarding OCTA images. This lack of standardization is even more significant when quantifying data using OCTA scans, and comparison between platforms should be avoided.<sup>9</sup>

For future implementation of OCTA data in clinical trials, consensus definition of OCTA parameters would be necessary, and normative databases mandatory for a correct implementation of data in such structured studies.<sup>13</sup> Also, in the era of artificial intelligence and big data, OCTA volumetric scans are of great interest due to the great amount of data that they provide, and 3D analysis will certainly provide new and valuable information.

## CONCLUSIONS

In the last years we have witnessed a rapid advance in OCTA hardware, with a parallel software sophistication, providing automated correction of artifacts, improvement of image quality, and quantification of data. These changes have positioned OCTA as a promising technology in our clinics. While all these technical developments are necessary and extremely useful, training of ophthalmologist on this imaging technique is required in order to provide a correct interpretation of the data. On the other hand, standardization of the data, with creation of normative databases is required for the correct use of quantitative OCTA data, as well as the introduction of OCTA images in clinical trials with future use of new biomarkers.

## REFERENCES

1. Ang M, Tan ACS, Cheung CMG, Keane PA, Dolz-Marco R, Sng CCA, Schmetterer L. Optical coherence tomography angiography: a review of current and future clinical applications. *Graefes Arch Clin Exp Ophthalmol*. 2018;256(2):237-245.
2. Spaide RF, Fujimoto JG, Waheed NK, Sadda SR, Staurengi G. Optical coherence tomography angiography. *Prog Retin Eye Res*. 2018;64:1-55.
3. Zhang Q, Rezaei KA, Saraf SS, Chu Z, Wang F, Wang RK. Ultra-wide optical coherence tomography angiography in diabetic retinopathy. *Quant Imaging Med Surg*. 2018;8(8):743-753.
4. Kalra G, Pichi F, Kumar Menia N, Shroff D, Phasukkijwatana N, Aggarwal K, Agarwal A. Recent advances in wide field and ultrawide field optical coherence tomography angiography in retinochoroidal pathologies. *Expert Rev Med Devices*. 2021;18(4):375-386.
5. Greig EC, Duker JS, Waheed NK. A practical guide to optical coherence tomography angiography interpretation. *Int J Retina Vitreous*. 2020;6(1):55.
6. Choi, W, Moulton, E.M., Waheed, N.K., Adhi, M., Lee, B., Lu, C.D., de Carlo, TE, Jayaraman V, Rosenfeld PJ, Duker JS, Fujimoto JG. Ultrahigh-speed, swept-source optical coherence tomography angiography in nonexudative age-related macular degeneration with geographic atrophy. *Ophthalmology* 2015; 122, 2532–2544
7. Hirano T, Chanwimol K, Weichsel J, Tepelus T, Sadda S. Distinct Retinal Capillary Plexuses in Normal Eyes as Observed in Optical Coherence Tomography Angiography Axial Profile Analysis. *Sci Rep*. 2018 20;8(1):9380.
8. Balaratnasingam C, An D, Freund KB, Francke A, Yu DY. Correlation between Histologic and OCT Angiography Analysis of Macular Circulation. *Ophthalmology*. 2019;126(11):1588-1589.
9. *Biomed Opt Express*. 2016;8(1):207-222. Salas M, Augustin M, Ginner L, Kumar A, Baumann B, Leitgeb R, Drexler W, Prager S, Hafner J, Schmidt-Erfurth U, Pircher M. Visualization of micro-capillaries using optical coherence tomography angiography with and without adaptive optics
10. Spaide RF, Fujimoto JG, Waheed NK. Image artifacts in optical coherence tomography angiography. *Retina*. 2015;35(11):2163-80.
11. Corvi F, Cozzi M, Barbolini E, Nizza D, Belotti M, Staurengi G, Giani A. Comparison between several optical coherence tomography angiography devices and indocyanine green angiography of choroidal neovascularization. *Retina*. 2020;40(5):873-880.
12. Ehlers JP. The OCT Angiography Revolution: Five Emerging Themes. *Ophthalmol Retina*. 2017;1(6):457-460.
13. Agarwal A, Grewal DS, Jaffe GJ, Stewart MW, Srivastava S, Gupta V. Current role of optical coherence tomography angiography: Expert panel discussion. *Indian J Ophthalmol*. 2018;66(12):1696-1699.





# Publication

Published by:  
Laboratoires Théa  
12 Rue Louis Blériot - ZI du Brézet  
63017 Clermont-Ferrand cedex 2 - France  
Tél. +33 (0)4 73 98 14 36



## Collection Librairie Médicale Théa



12 Rue Louis Blériot - ZI du Brézet  
63017 Clermont-Ferrand cedex 2 - France  
Tel. +33 (0)4 73 98 14 36 - Fax +33 (0)4 73 98 14 38  
[www.laboratoires-thea.com](http://www.laboratoires-thea.com)